11-9-2017 2:30 PM

Nicotinamide Phosphoribosyltransferase In Smooth Muscle Cells And Aortic Integrity

Alanna R. Watson
The University of Western Ontario

Supervisor
Dr. Geoffrey Pickering
The University of Western Ontario

Graduate Program in Biochemistry
A thesis submitted in partial fulfillment of the requirements for the degree in Doctor of Philosophy

ABSTRACT

The thoracic aortic wall can degenerate over time with catastrophic consequences. Vascular smooth muscle cells (SMCs) can resist and repair artery damage but their capacities decline with age and stress. Recently, cellular production of NAD^+ via nicotinamide phosphoribosyltransferase (Nampt) has emerged as a mediator of cell vitality. However, a role for Nampt in aortic SMCs in vivo is unknown. The purpose of this thesis was to determine if a Nampt-NAD^+ control system exists within the aortic media and to investigate the biological and clinical importance of such a system. An additional aim was to determine if there was a requisite necessity for Nampt for adult mouse survival.

To study the role of Nampt in SMCs, mice with Nampt-deficient SMCs were generated. SMC-*Nampt* knockout mice were viable but had mildly dilated aortas. Infusion of angiotensin II led to aortic medial hemorrhage and dissection. SMCs were not apoptotic but had indicators of premature senescence. Furthermore, there was evidence for oxidized DNA lesions and DNA breaks. This was linked to suppressed poly(ADP-ribose) polymerase-1 activity and was reversible upon re-supplying NAD^+ with nicotinamide riboside (NR). Evaluating ascending aortas from patients with dilated aortopathy revealed an inverse relationship between SMC NAMPT content and aortic diameter. Remarkably, I discovered unrepaired DNA strand breaks in SMCs within the human ascending aorta, which were specifically enriched in SMCs with low NAMPT. *NAMPT* promoter analysis revealed CpG hypermethylation within the dilated human aorta and in SMCs cultured from these tissues, which inversely correlated with *NAMPT* expression.

Global transcriptome analysis of *Nampt* knockout SMCs revealed a shift in gene transcription. Transcripts associated with the production and assembly of collagens were decreased, and transcripts associated with selected proteoglycans were increased. This was

associated with corresponding changes in extracellular matrix content in SMC-*Nampt* knockout mouse aortas, which may be an additional reason for aortic wall vulnerability.

Finally, by generating a global inducible *Nampt* knockout mouse, I determined that ablation of *Nampt* in the adult was lethal within 20 days. Interestingly, this early death was not due to vascular SMC abnormalities but was associated with rapid degeneration of the exocrine pancreas, gut epithelial abnormalities, and halted gastrointestinal transit of undigested food. Remarkably, supplementing *Nampt* knockout mice with NR was able to double their lifespan.

Collectively, my findings reveal new processes by which SMCs stay healthy and functional, with important implications for mitigating the consequences of the accumulation of the stresses that push blood vessels, and other organs, to catastrophic failure.

Keywords:

Vascular smooth muscle cells, Aortic disease, Nampt, DNA damage, Cell senescence, Extracellular matrix, Nicotinamide riboside

CO-AUTHORSHIP

Portions of this thesis have been published. The initial draft of all manuscripts were written by myself and further revised with recommendations from Dr. J. G. Pickering. The contributions of the authors of these articles are as follows:

Chapters 2 and 3:

Watson A, Nong Z, Yin H, O'Neil C, Fox S, Balint B, Guo L, Leo O, Chu MWA, Gros R, Pickering JG (2017) *Circ Res* **120**, 1889-1902. The design and implementation of the knockout mouse models were my work, along with all other experimentation with the exceptions that follow. Zengxuan Nong, with my assistance, performed mouse surgeries and tissue harvesting, processing and immunostaining was done in concert. Caroline O'Neil provided technical help with mouse cell isolation, and Hao Yin handled the harvesting and initial culturing of human cells and tissues. Britany Balint assisted in obtaining confocal micrograph images. Doctors L Guo and MWA Chu, assisted by Stephanie Fox, provided the human samples for my research that were obtained in their surgical practices. Dr O Leo provided us with the *Nampt*$^{flox/flox}$ mice. Dr. R Gros helped with the design and execution of the Ang II infusion and subsequent blood pressure studies.

Chapter 4: Microarray analysis was done with the assistance of David Carter and the London Regional Genomics Centre, at the Robarts Research Institute. All other experimental work was my own.

Chapter 5: Initial assessment of the *Nampt* KO phenotype was helped with services performed at the CMHD Pathology Core, Toronto Centre for Phenogenomics. Serum insulin measurements were performed by Cynthia Sawyez of Dr. Huff's laboratory. The Clinical Pathology Department of Charles River Laboratories measured all other serum parameters. All other experimental work was my own.

ACKNOWLEDGEMENTS

I would like to first acknowledge the support and guidance of Dr. Geoffrey Pickering. I am overwhelmingly grateful to have had the opportunity to study with a scientist of such high caliber. From his example I have learned the importance of meticulous attention to detail and precision, in addition to the importance of keeping a keen sense of how all this works ties and hangs together with a bigger vision. His mentorship has allowed me to develop skills and perspectives that would've remained outside of my natural inclinations, and for that I am deeply indebted.

This thesis would not have been possible without the support of lab members, past and present. Hao Yin, your infectious enthusiasm for our work and your wealth of knowledge have been invaluable. John Michael, Britney, and Jason, thanks for making this journey so much better with your friendship. Our previous masters students, Krista, Sina, Sharon, have been a joy to be around. I am grateful for the highly skilled Zengxuan Nong, without whom the animal work would have been much less comprehensive. Finally, the constant help, guidance, and friendship of Caroline O'Neil has made this endeavor possible. You will always have my deepest gratitude.

I am grateful to Dr. Rob Gros for the time he took to teach me many practical skills, for the many conversations and advice he provided, and for the resources that he allowed me to use. I learned much from him, and am confident this project would not have gone nearly as well without him. I have also valued the creative input from the members of my advisory committee: Dr. Gabe DiMattia and Dr. Frank Beier.

To my family, thank you for always supporting and encouraging me. I've been able to pursue this dream because of the safety of your love. Finally, to my husband, thank you for your unflagging encouragement, for your grace and patience, and for being my biggest fan.

TABLE OF CONTENTS

LIST OF TABLES

LIST OF FIGURES

LIST OF APPENDICES

LIST OF ABBREVIATIONS

8-oxodG	8-oxo-2'-deoxyguanosine
ADP	Adenosine diphosphate
AMP	Adenosine monophosphate
Ang II	Angiotensin II
ANOVA	Analysis of variance
ApoE	Apolipoprotein E
AR	Aortic regurgitation
ART	Adenosine diphosphate (ADP)–ribose transferase
AS	Aortic stenosis
ATP	Adenosine triphosphate
BAV	Bicuspid aortic valve
BER	Base excision repair
Bmal1	Aryl hydrocarbon receptor nuclear translocator-like protein 1
CAD	Coronary artery disease
cADPR	Cyclic ADP-ribose
CDK	Cyclin dependent kinase
Clock	Circadian locomotor output cycles kaput
DAB	3,3'-Diaminobenzidine
DAPI	4′,6′-diamidino-2-phenylindole
DAVID	Database for Annotation, Visualiation and Integrated Discovery
DMEM	Dulbecco's modified Eagle's medium
DNA	Deoxyribonucleic acid
DSB	Double strand break
ECM	Extracellular matrix
eGFP	Enhanced green fluorescent protein
Eln	Elastin
Emilin	Elastin microfibril interfacer protein 1
FACIT	Fibril associated collagens with interrupted triple helices
Fbn	Fibrillin
FBS	Fetal bovine serum
Flox	Flanking/flanked by LoxP
GAG	Glycosaminoglycan
GO	Gene ontology
H_2O_2	Hydrogen peroxide
Has	Hyaluronan synthase
HDAC	Histone deacetylase
HITC6	Human internal thoracic cells
HTAD	Heritable thoracic aortic disease
IPA	Ingenuity Pathway Analysis®
KEGG	Kyoto Encyclopedia of Genes and Genomes
KO	Knockout
loxP	Locus of X-over P1
Magp	Microfibril-associated glycoproteins
MAPK	Mitogen-activated protein kinase

MEM	Modified Eagle's medium
MMP	Matrix metalloproteinase
MMS	Methyl methanesulfonate
NA	Nicotinic acid
NAAD	NA adenine dinucleotide
NAD^+	Nicotinamide adenine dinucleotide (oxidized form)
NADH	Nicotinamide adenine dinucleotide (reduced form)
NADP	Nicotinamide adenine dinucleotide phosphate
NADPH	Nicotinamide adenine dinucleotide phosphate (reduced form)
Nadsyn	NAD^+ synthetase
NAM	Nicotinamide
NAMN	NA mononucleotide
Nampt	Nicotinamide phosphoribosyltransferase
NDH	Nudix homoly domains
NF-κB	Nuclear factor kappa-light-chain-enhancer of activated B cells
NMN	Nicotinamide mononucleotide
Nmnat	Nicotinamide mononucleotide adenylyltransferase
NR	Nicotinamide riboside
Nrk	Nicotinamide riboside kinase
OCT	Optimal cutting temperature compound
PAR	Poly(ADP-ribose)
Parp	Poly(ADP-ribose) polymerase
Pbef	Pre-B cell colony enhancing factor
PBS	Phosphate-buffered solution
PRPP	Phosphoribosyl pyrophosphate
PSR	Picrosirius red
RNA	Ribonucleic acid
ROS	Reactive oxygen species
RT-PCR	Real time polymerase chain reaction
SA β–gal	Senescence associated β-galatosidase
SASP	Senescence-associated secretory phenotype
Sirt	Sirtuin
SLRP	Small leucine-rich repeat proteoglycan
SMC	Smooth muscle cell
smMHC	Smooth muscle myosin heavy chain
SSB	Single strand break
TAA	Thoracic aortic aneurysm
TAAD	Thoracic aortic aneurysms and dissection
TCA	Tricarboxylic acid cycle (or, citric acid cycle, Krebs cycle)
TGF-β	Transforming growth factor-beta
TIMP	Tissue inhibitor of metalloproteinase
Tmx	Tamoxifen
TUNEL	Terminal deoxynucleotidyl transferase dUTP nick-end labeling
WT	Wild type
X-Gal	5-Bromo-4-Chloro-3-Indolyl β-D-Galactopyranoside
γ-H2AX	Phosphorylated H2A histone family, member X

CHAPTER 1 - GENERAL INTRODUCTION

Vascular smooth muscle cells (SMCs) are vital for regulating arterial tone and are also major reparative cells of the artery wall. However, the ability of adult SMCs to function with high fidelity declines with age and with environmental stress. This can lead to vascular disease, including a predisposition to aortic aneurysms and dissections. Accordingly, it is important to understand pathways that regulate the ability of human SMCs to maintain a stress- and aging-resistant state in vivo.

The broad goal of my research was to elucidate the in vivo role of nicotinamide phosphoribosyltransferase (Nampt), an NAD^+ regenerating enzyme that increases intracellular NAD^+, with a particular emphasis on the aorta. In order to address this goal I undertook four main aims:

1) To determine if Nampt-mediated NAD^+ biosynthesis in smooth muscle cells was required to maintain vascular stability in the mouse.
2) To determine if there is an association in humans between NAMPT expression and aortopathy.
3) To determine the role of Nampt-mediated NAD^+ regeneration in smooth muscle cells in the context of the integrity of extracellular components of the aorta.
4) To determine the consequences of global loss of Nampt in the adult mouse and the ability of nicotinamide riboside (NR) supplementation to mitigate the consequences.

1.1 Vascular system in health and disease

1.1.1 Importance of vascular health

At the core of the human body is a system of blood-flowing conduits. It is through this system that the heart pumps blood rich with oxygen and nutrients to every tissue in the

body. Arteries transport blood away from the heart. Veins capture and return the blood to the heart once oxygen and other nutrients have been delivered to the tissues and waste products have been collected. The entirety of this network is the vascular system – "vascular" being from the Latin meaning hollow container.

Diseases of the vascular system are a major factor contributing to global population morbidity and mortality (Lloyd-Jones, D et al. 2010). The term "vascular disease" broadly encompasses a great number of pathologies, and examples include: diseases relating to the narrowing of cardiac or peripheral vessels (i.e. by the build-up of plaque in atherosclerotic lesions or spontaneous spasm); the formation of blood clots; the disordered function of veins or the valves therein (e.g. chronic venous insufficiency); and aortic aneurysms, either thoracic or abdominal. Aneurysms can form in any blood vessel, but they occur most commonly in the aorta which is the main blood vessel leaving the heart. The importance of maintaining the integrity and proper functioning of the vascular system is underscored by the reality that every tissue and organ is dependent on this network for delivery of oxygen and nutrients and the removal of waste products generated by the normal function of each terminal cell (Topol and Califf 2007).

1.1.2 Vessel morphology

The arterial side of the vascular system is a dynamic network that is able to control the systemic delivery of blood oxygen and nutrients, and to respond to changes, even sudden changes, in hemodynamic stresses. The healthy artery is comprised of 3 layers: the outer tunica adventitia, the middle tunica media, and the inner (lumen-facing) tunica intima. These layers are discrete, and are identifiable by their cellular components and morphology. The outermost layer, the adventitia, is a loosely formed layer comprised of fibroblasts, progenitor cells, and connective tissue, including collagen. The medial layer is comprised mainly of layers of SMCs arranged in a mostly end-to-end fashion, interleaved

with layers of elastin. SMCs regulate vessel tone through contraction. They also provide structural integrity to the vessel wall through the synthesis and assembly of elastin and collagen. The innermost layer, the intima, is a thin layer of endothelial cells, on top of a specialized basement membrane composed of laminin, type IV collagen, and nidogen. The intima is separated from the media by the internal elastic lamina, providing elasticity to the arteries and allowing them to accommodate changes in blood pressure and flow. The media is separated from the adventitia by the external elastic lamina (Fig. 1.1).

Vessels on the venous side of the vascular system function mainly as a collection system for de-oxygenated blood and the waste products of cellular metabolism. The cellular layers that make up a vein are similar to those that form an artery, however the medial layer of SMCs is much thinner with fewer layers. As such, veins are less muscular, contain less elastin, and have relatively larger lumen sizes.

Between the arterial system and venous system is an extensive bed of tiny vessels, the thickness of one-to-two cell layers. This is where the delivery of oxygen and nutrients to the tissues and organs occurs.

1.1.3 The aorta

The aorta is the largest blood vessel of the body, emerging directly from the heart and serving as a conduit the rest of the vascular tree. The aorta begins at the aortic valve, the most commonly replaced heart valve (Nishimura et al. 2014). The reasons for this include congenital malformations (bicuspid) or age-related degeneration. The capacity of the aorta to withstand a large and dynamic volume and pressure of blood that is pulsatile by nature is upheld by the stretch-resistant capacity of SMCs and the elasticity of the internal elastic lamina.

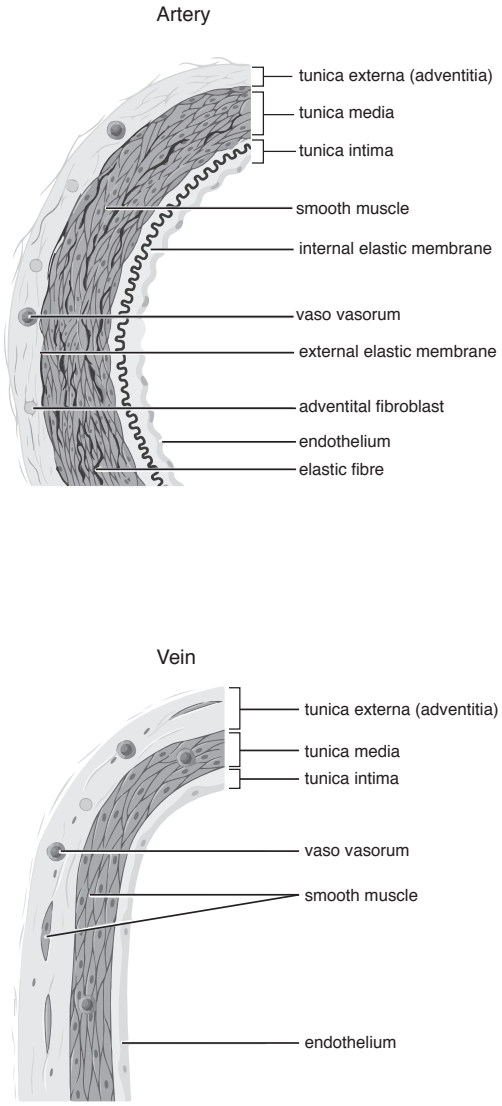

Figure 1.1 Architecture of the vessel wall

Cross-sectional views of the arterial vessel (Top) and venous vessel (Bottom) walls. Vessel walls are organized into three concentric layers, named: tunica externa (adventitia), tunica media, and tunica intima. The tunica externa is mainly comprised of collagen fibres, fibroblasts, and the occasional small blood vessel (vaso vasorum). The tunica media is comprised of smooth muscle cells, elastic fibres, and interstitial matrix – predominantly collagen. The tunica intima is a thin layer of endothelial cells lining the lumen of the blood vessel. Image adapted from "Types of Arteries and Arterioles" by Phil Schatz, Anatomy & Physiology. OpenStax CNX. 2016 http://cnx.org/contents/14fb4ad7-39a1-4eee-ab6e-3ef2482e3e22@8.24

1.1.4 Aortic diseases

The term “aortic disease” comprises a group of different pathologies of high prevalence. Acute aortic dissection typically occurs when a small tear in the intimal layer allows blood to enter into the medial space, which itself is often diseased and contains degraded elastin and reduced SMC content. The pulsatile hemodynamic pressure forces blood to travel along the medial layers, separating them to create a “false” lumen. Acute aortic dissections are relatively uncommon in the broad population (approximately 3.5-6.0 per 100,000 patient-years) but have a high mortality rate (Mussa et al. 2016). Moreover, dissections are much more prevalent in predisposed subpopulations with thoracic aortic disease. Thoracic aortic disease comprises rare syndromic forms and common nonsyndromic forms of thoracic aortic aneurysms (TAAs) and dissections (TAADs). Mechanisms of TAA formation overlap those of aortic dissection and largely involve the process that has historically been termed “cystic medial necrosis”, with focal degeneration of the elastic and muscle tissue within the medial layer of the aortic wall. The aortic wall subsequently weakens and dilates as a result of the high pressure of intraluminal blood flow. Acquired and hereditary conditions can exacerbate the process of degeneration.

Chronic arterial hypertension is widely accepted as the most common acquired condition that leads to aneurysm and dissection of the aorta. Nearly 75% of patients with acute aortic dissection have a history of hypertension (Meszaros et al. 2000, Ramanath et al. 2009). In a large series from the Mayo Clinic, hypertension was present in ~ 60% of patients with a surgically resected thoracic aneurysm due to noninflammatory aortic disease (Homme et al. 2006).

Heritable thoracic aortic disease (HTAD) refers to thoracic aortic disease caused by mutation of a gene that confers a high risk for thoracic aortic disease. The most common genetically inherited conditions that are associated HTAD include Marfan syndrome,

vascular Ehlers-Danlos syndrome (or Ehlers-Danlos syndrome type IV), and Loeys-Dietz syndrome (Ramanath et al. 2009). Moreover, up to 20% of individuals with thoracic aortic disease who do not have features of Marfan syndrome, vEDS or Loeys-Dietz syndrome have a family history, thus indicating that their disease is heritable (Biddinger et al. 1997). Approximately 30% families with HTAD who do not have a clinical diagnosis of Marfan syndrome or another syndrome have a causative pathogenic variant in one of the known HTAD-related genes (Milewicz and Regalado 1993) (see Table 1).

Marfan syndrome may be the most prevalent amongst the etiologies, with an incidence of approximately 1 in 10,000. The most common form of Marfan syndrome is caused by a sequence variation of the fibrillin gene. The aortic pathology is characterized at the histologic level by medial degeneration, abnormal extracellular matrix accumulation, SMC loss, and elastin fragmentation (Halushka et al. 2016). Vascular Ehlers-Danlos syndrome is a connective tissue disorder associated with a defect of either the expression or assembly of type III procollagen, one of the collagen moieties present in high amounts in the aortic media (Eagleton 2016). This syndrome is characterized by thin, translucent skin, easy bruising, characteristic facial appearance, and arterial, intestinal, and/or uterine fragility, and affected individuals are at risk for arterial rupture, aneurysm, and/or dissection (Pepin et al. 1993). Loeys-Dietz syndrome, is associated with pathogenic genetic variants of transforming growth factor beta receptors 1 and 2, Smad3, and the ligand TGFβ-2 (Loeys and Dietz 1993). Patients with Loeys-Dietz syndrome manifest TAAs and dissections in an autosomal dominant pattern of inheritance and at an early age of onset (Loeys et al. 2006).

Table 1-1 HTAD-related genes and syndromes

Syndrome/Disorder	Associated genes
Marfan	FBN-1; fibrillin-1
Loeys-Dietz	TGFBR1; TGF-β receptor 1 TGFBR2; TGF-β receptor 2 SMAD3; SMAD family member 3 TGFB2; TGF-β 2 ligand TGFB3; TGF-β 3 ligand
Vascular Ehlers-Danlos	COL3A1; type III procollagen
Other	ACTA2; smooth muscle alpha-2-actin MYH11; smooth muscle myosin heavy chain MYLK; myosin light chain kinase PRKG1; type I cGMP-dependent protein kinase regulating smooth muscle cell relaxation MFAP5; microfibril associated protein 5

(Milewicz and Regalado 1993, Goyal et al. 2017).

Other congenital disorders can also result in susceptibility to aortic aneurysms (Halushka et al. 2016). This includes: bicuspid aortic valve (BAV) disease (Edwards et al. 1978), coarctation of the aorta (Rosenthal 2005), tetralogy of Fallot (Rosenthal 2005), and diverticulum of Kommerell (Kim et al. 2014). BAVs are among the most common congenital heart abnormalities, occurring in approximately 2% of the population. It has been established that there is an association between congenital BAVs, and proximal aortic dilatation and aortic aneurysm/dissection (Ramanath et al. 2009). Patients with BAVs may inherit a predisposition to medial degeneration of the aorta (McKusick 1972). Some studies report that as many as half of all patients with a congenital BAV have or will develop dilatation of the ascending aorta (Nistri et al. 1999, Kim et al. 2014).

Recent classification of degenerative pathology of the aorta by the Society for Cardiovascular Pathology and the Association For European Cardiovascular Pathology has also identified age as a risk factor for aortic disease (Halushka et al. 2016). In the aging aorta the elastin, SMCs, and extracellular matrix are all altered in progressive and negative ways. These changes can be exacerbated by the associated risk factors of smoking, hypertension, and hypercholesterolemia.

1.2 Smooth muscle cell biology, dysfunction, and aging

1.2.1 SMC embryological origins

Vascular smooth muscle cells (SMCs) arise from multiple origins during the development of the vascular system and constitutes an early event during embryogenesis. The organization of endothelial cells into the primary vascular plexus is initiated shortly after gastrulation (the period of formation of the three germ layers; ectoderm, mesoderm, and endoderm) and marks the onset of vascular development. The endothelial vasculature is subsequently remodeled by recruitment of SMCs and pericytes to form a complex vascular system (Carmeliet 2000, Jain 2003). The origin of aortic SMCs is complex with

contributions from several independent cell lineages (Gittenberger-de Groot et al. 1999, Majesky 2007). SMCs of the basal aortic root is derived from the secondary heart field (Waldo et al. 2005), whereas SMCs of the ascending aorta and the arch are neural crest derived (Jiang et al. 2000). Descending aortic SMCs originate from paraxial (somitic) mesoderm (Wasteson et al. 2008).

Recruitment of aortic SMCs to the primordial endothelial structure occurs in a ventral to dorsal manner as well as in a radial pattern emanating from the layer of cells most adjacent to the endothelium (Hungerford et al. 1996). Embryonic differentiating SMCs exhibit high rates of cell proliferation and migration. They also produce a large amount of extracellular matrix molecules, including collagens, elastin, and proteoglycans that comprise a major portion of the blood vessel mass (Hungerford and Little 1999).

A major challenge in understanding differentiation of the SMC is that it can exhibit a wide range of phenotypes at different stages of development. Even in adult organisms SMCs are not terminally differentiated and are capable of major changes in their phenotype, in response to changes in its local environment. This phenotypic plasticity is often considered in terms of two functional phenotypes: “contractile” and “synthetic” (Fig. 1.2). Adult, differentiated SMCs are generally thought to be contractile SMCs; expressing a repertoire of appropriate receptors, ion channels, signal transduction molecules, calcium regulatory proteins, and contractile proteins necessary for the unique contractile properties of the SMC (Owens 1995). A number of these genes are often used as signifiers of SMC differentiation. Upon vascular injury these contractile SMCs have the ability to undergo a phenotypic switch to a synthetic phenotype that plays a role in repair. This switch is associated with a downregulation of many of the genes associated with a contractile phenotype, and an upregulation of many of the factors that were being produced during

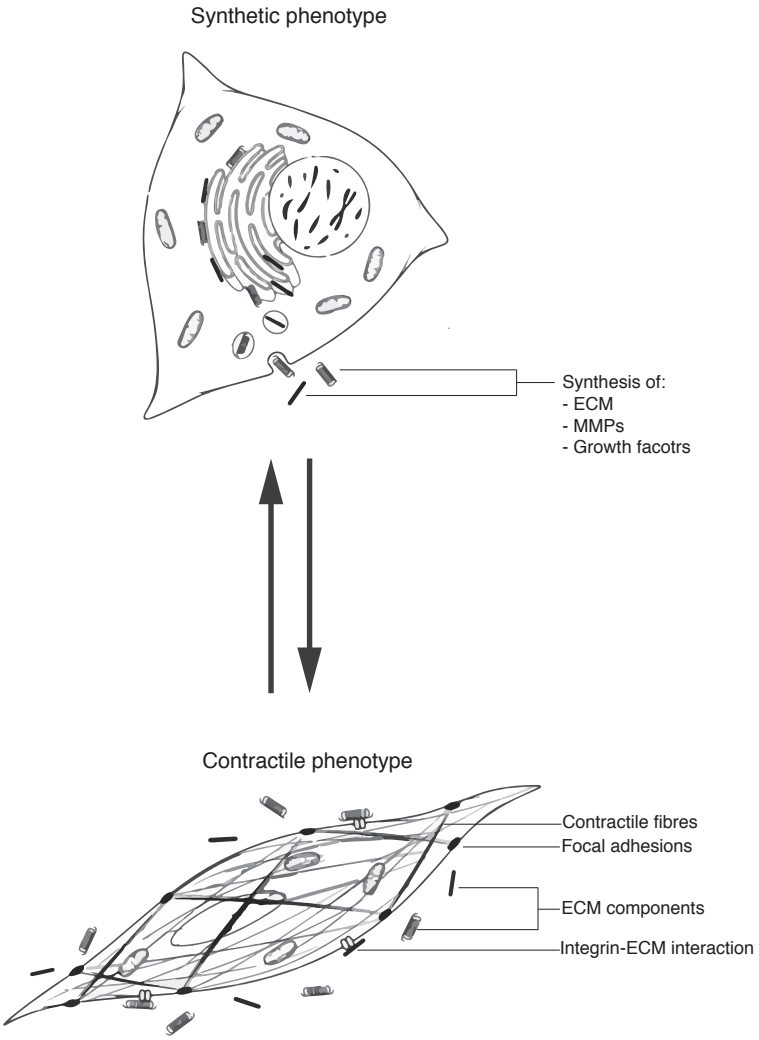

Figure 1.2 Smooth muscle phenotypes

SMCs have been considered to have two distinct phenotypes: synthetic (Top) and contractile (Bottom). The synthetic state is characterized by spread, flattened morphology in culture, where the cells are non-contractile. These synthetic SMCs are proliferative and migratory. As well, they actively secrete ECM proteins, including collagen and elastin, as well as MMPs and growth factors. The contractile state is characterized by an elongated morphology in culture, owing to the accumulation of contractile-proteins. Contractile SMCs are relatively non-proliferative and migratory, and they have low secretory activity. SMCs can readily switch between synthetic and contractile phenotypes.

development that led to the formation of the vessel wall. Whether the synthetic SMCs active in the repair process are local contractile SMCs that have de-differentiated, or are derived from infiltrating precursors to SMCs, is not always clear. In either case however the production of various components that make up the artery wall is a necessity. The ability to withstand the dynamic hemodynamic stress to which an artery is exposed is conferred not only by the contractile apparatus of a differentiated vascular SMC, but also by the components of the extracellular milieu that the synthetic SMC has produced (and continues to produce even in the differentiated state, albeit at a lower level) (Humphrey et al. 2015).

1.2.2 Extracellular components of the aorta

1.2.2.1 Elastic fibres

Elastin is the primary ECM molecule in large conduit vessels. In humans, the aortic media is composed of over 50 alternating layers of elastic fibres and SMCs. The elastic fibres are organized in concentric laminae. The core of elastin (Eln) is surrounded by microfibrils. These microfibrils are 10 – 15 nm filaments composed primarily of a large glycoprotein called fibrillin (Fbn1, Fbn2 and Fbn3). There are additional microfibril-associated glycoproteins (Magps), including Magp-1 and Magp -2 (Mfap2 and Mfap5), and elastin microfibril interfacer protein 1 (Emilin1). These microfibril extensions are organized in an oblique orientation to the elastic fibres, and are attached to dense plaques in the SMC cell membrane (Karimi and Milewicz 2016).

1.2.2.2 Collagen

Other than elastin, collagen is the most abundant matrix protein in the aorta. There are 17 different collagen types expressed in the mouse aorta, with α chains for collagens I, III, IV, V, and VI having the highest expression levels (Kelleher et al. 2004, Wagenseil and Mecham 2009). Present in lesser amounts are collagens VII, VIII, IX, X, XI, XIV, XV,

XVIII, and XIX. Collagens II, XII, XIII, and XVII have little to no expression. Collagen types I, III, and V are fibril-forming collagens, with types I and III being mainly responsible for imparting strength to the vessel wall (Wagenseil and Mecham 2009). Type V collagen plays a critical role in collagen fibril nucleation (Wenstrup et al. 2004). Expression of type VI collagen chains in the mouse aorta is similar in abundance to elastin and collagen type I, but while it is a fibril-forming collagen, it does not colocalize in large collagen bundles with collagens I and III. Instead, collagen VI is frequently associated with fibrillin-1 and may serve to connect elastic lamellae to the basement membrane of SMCs, or connect SMCs to other ECM structures (Dingemans et al. 2000). Collagens IV, VIII, and X are members of the network-forming collagen family and create basket weave-like structures through associations between their helical and non-helical domains. Type IV collagen is the major structural protein of basement membranes. Collagens IX, XIV, and XIX are FACIT (fibril associated collagens with interrupted triple helices) collagens that attach to the surface of fibril-forming collagens but do not form fibers themselves. Collagen XIII is a collagen with a transmembrane domain that resides in adhesive structures of cells and has been implicated in cell adhesion. Collagens XV and XVIII are closely related non-fibrillar collagens that are associated with basement membranes.

1.2.2.3 Proteoglycans

The proteoglycans constitute a number of genetically unrelated families of multidomain proteins that have covalently attached glycosaminoglycan (GAG) chains. Proteoglycans are categorized based on the type of attached GAGs: 1) chondroitin sulfate and dermatan sulfate, 2) heparin and heparan sulfate, and 3) keratan sulphate. The proteoglycans found in greatest abundance in the vessel wall can be categorized into two classes: large proteoglycans that form large aggregates by interaction with hyaluronan, and small leucine-rich proteoglycans (Wagenseil and Mecham 2009). The large proteoglycans interact with hyaluronic acid to form an extensive, interconnected polymeric network in the

extracellular space. Hyaluronan is a linear polymer composed of repeating disaccharides of glucuronic acid and N-acetylglucosamine. It is synthesized at the plasma membrane by three different but related hyaluronan synthases: Has1, Has2, and Has3 (Weigel et al. 1997). Versican is the largest proteoglycan in the vessel wall and has been localized to the aortic media and endothelial layers (Yao et al. 1994). Interestingly, in vascular injury models, high versican levels correlate with low elastin content, most likely due to inhibition of elastic fibre assembly by the chondroitin sulfate GAGs on versican (Huang et al. 2006, Wagenseil and Mecham 2009).

The small leucine-rich proteoglycans (SLRPs) are a family of secreted proteoglycans that do not interact with hyaluronic acid but, instead, bind ECM molecules such as collagen, tropoelastin, fibronectin, and fibrillin-containing microfibrils, among others (Reinboth et al. 2002). The SLRP family includes decorin, biglycan, fibromodulin, osteoglycin, and lumican (Wagenseil and Mecham 2009). Both biglycan and decorin bind to and regulate collagen fibrillogenesis (Hocking et al. 1998). Biglycan localizes to all layers of the human aorta, whereas decorin is found only in the adventitia (Theocharis and Karamanos 2002).

1.2.2.4 MMPs/TIMPs

ECM proteins, including collagens and elastin, can be cleaved by matrix metalloproteinases (MMPs), a family of endopeptidases. MMPs are usually grouped according to substrate specificity as collagenases (Mmp-1, Mmp-8, Mmp-13 and Mmp-18), gelatinases (Mmp-2 and Mmp-9), stromelysins (Mmp-3, Mmp-10 and Mmp-11), matrilysins (Mmp-7 and Mmp-26), membrane type (Mmp-14-17, Mmp-24 and Mmp-25), and others (Mmp-12, Mmp-19-21, Mmp-23, Mmp-27 and Mmp-28) (Visse and Nagase 2003). In the arterial wall, contractile medial SMCs express Mmp-2 and minor amounts of Mmp-14, a membrane-type Mmp-1 (Wang and Keiser 1998). However,

activated SMCs, such as cells in atherosclerotic plaque, express large amounts of Mmp-1, -3, -9, and -14, and activated Mmp-2 (Galis et al. 1994, Wang and Keiser 1998). MMPs are normally inhibited by endogenous inhibitors called TIMPs (tissue inhibitor of metalloproteinases), of which there four isoforms (Timp1-4). Alterations in the balance between ECM MMPs and TIMPs may contribute to the profibrotic phenotype in aging and hypertension (Wang et al. 2006, Giannandrea and Parks 2014, Harvey et al. 2016).

1.2.3 SMC senescence

As outlined above, aortic SMCs are the main cellular mediators that give the aorta its resilience against hemodynamic forces and other environmental stress. As such, a dysfunctional SMC can lead to a vulnerable aortic wall. SMC dysfunction may be caused by a mutation or a polymorphism that affects the expression of a gene associated with the contractile or synthetic functions of the cell. Additionally, one process that has emerged as a potential contributor to cellular dysfunction in the vasculature is cellular senescence.

Cellular senescence is a process typically induced by severe insult, whereby the affected cell enters a state of essentially permanent cell cycle arrest (Childs et al. 2015). This process is often explored in the context of tumor protection, where proliferative arrest occurs in response to severe or unrepairable DNA damage, typically a double strand DNA break, that could otherwise lead to oncogenic transformation. Thus, serves a vital protective mechanism to safeguard against cancer (Campisi 2013). However, the first description of cellular senescence was the observed proliferative arrest that occurs after long-term culture of human fibroblasts (Hayflick and Moorhead 1961). This form of senescence is termed replicative senescence and has been linked to progressive shortening of telomeres. This concept can be congruent with what happens in replicating tumor cells, but is also applied to aging cells both in culture and in vivo (van Deursen 2014).

Senescence can also occur independent of continuous cell replication and critically short telomeres. Some stresses such as oxidative stress and DNA damage elicit quite similar cell growth arrest within just a few days (Collado et al. 2007). This circumstance has been referred to as stress-induced premature senescence. Regardless of the cause, senescent cells of all tissue types (including those undergoing replicative and stress-induced premature senescence) look alike and show similar characteristics (Bernadotte et al. 2016). Senescent cells are defined not only by proliferative arrest but also by the secretion of a set of proteins - a host of inflammatory cytokines and chemokines, growth factors, and proteases, that can affect the senescent cell and also the local tissue (Coppe et al. 2008, Tchkonia et al. 2013). This phenomenon is referred to as the senescence-associated secretory phenotype (SASP) (Yin and Pickering 2016).

1.2.3.1 Mechanisms of cellular senescence

As noted, progressive shortening of telomeres upon repeated cell replication is an established route to cellular senescence (Hayflick and Moorhead 1961). However, stress-induced senescence can be mediated by different stimuli that are beginning to be understood more fully (Yin and Pickering 2016). These stimuli are signalled through various pathways, many of which activate p53 (encoded by *TP53* in humans and by *Trp53* in mice), and essentially all of them converge in the activation of the cyclin-dependent kinase (CDK) inhibitors p16 (also known as Ink4a; encoded by Cdkn2a), p15 (also known as Ink4b; encoded by Cdkn2b), p21 (also known as Waf1; encoded by Cdkn1a) and p27 (encoded by Cdkn1b). The inhibition of CDK–cyclin complexes results in proliferative arrest, and the crucial component responsible for the implementation of senescence is the hypo-phosphorylated form of Rb (Chicas et al. 2010). (Fig. 1.3)

DNA damage is a potent driver of cellular senescence. The main mediators of the DNA damage response are the DNA damage kinases ATM, ATR, CHK1 and CHK2,

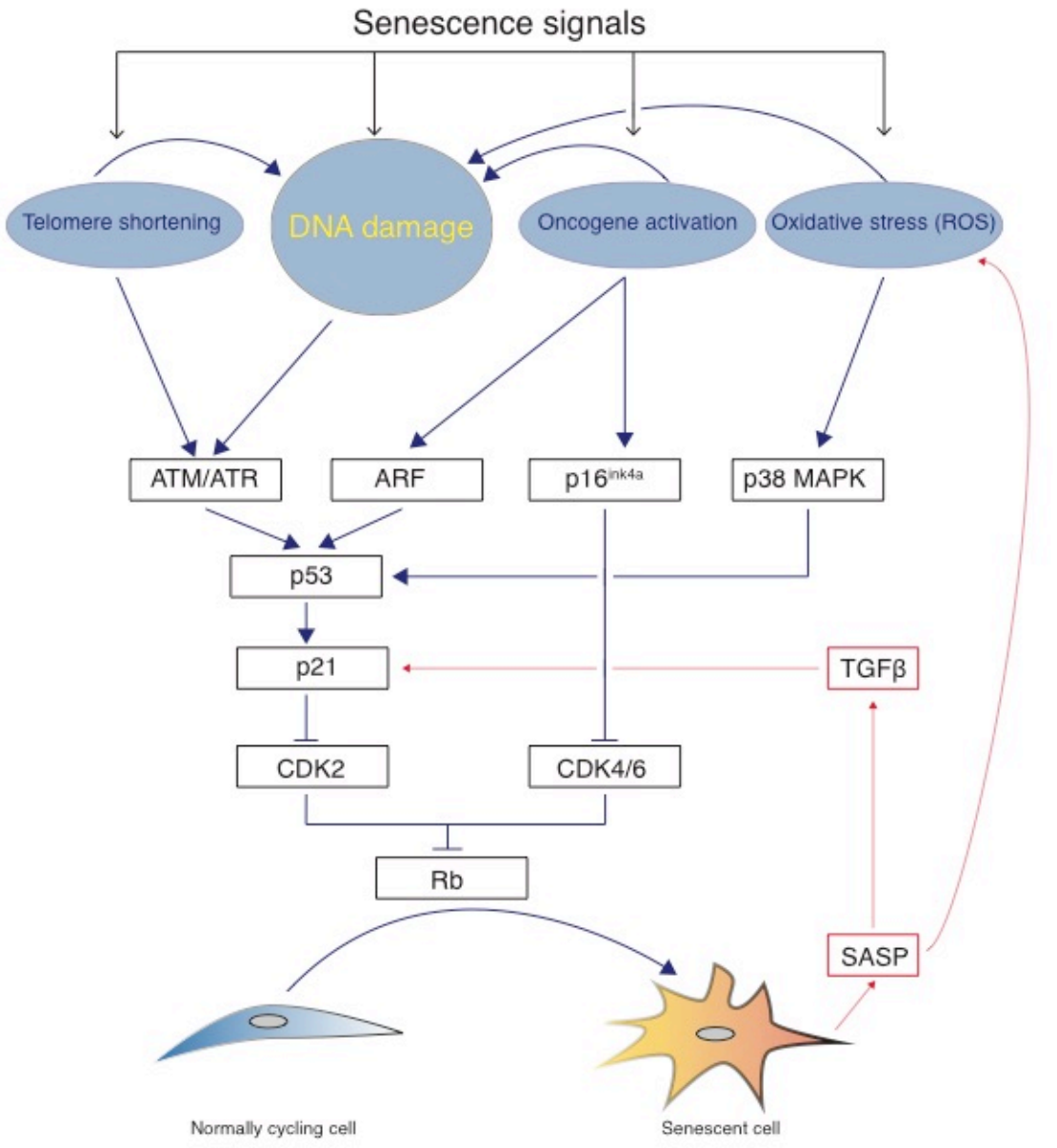

Figure 1.3 Molecular mechanisms leading to cell senescence

A range of stressors can trigger cell senescence. These include DNA damage, including critical telomere shortening, as well as oncogene activation, oxidative stresses, and TGF-β produced either during normal developmental remodeling or from senescent cells themselves. These stressors engage different signaling cascades that induce expression of p16 and/or p21. The resulting inhibition of cyclin-dependent kinase activity prevents Rb inactivation, leading to cellular senescence. ARF, alternative reading frame; ATM, ataxia telangiectasia mutated kinase; ATR, ataxia telangiectasia and Rad3- related kinase; CDK, cyclin-dependent kinase; ECM, extracellular matrix; Rb, retinoblastoma protein; SASP, senescence-associated secretory phenotype; TGF, transforming growth factor.

which phosphorylate and activate several cell cycle proteins, including p53 (Campisi and d'Adda di Fagagna 2007).. In turn, phosphorylated p53 protein activates the expression of p21, which binds to and inhibits certain CDK–cyclin complexes (Munoz-Espin and Serrano 2014).

Reactive oxygen species (ROS) also play an important role in the senescence of vascular cells (Chen et al. 1995). Levels of ROS increase after many different types of stresses, including chemotherapeutic drugs, loss of telomeric protective functions (Lee et al. 2009), and oncogene activation. Additionally, angiotensin II (Ang II), which has been widely implicated in the pathogenesis of cardiovascular disease, induces ROS production in SMCs (Herbert et al. 2008). A persistent ROS burden has been associated with an increase of oxidized DNA lesions (Chen et al. 1995) as well as an increase in senescence through several mechanisms, including lipid oxidation and interference with cellular metabolism (Yin and Pickering 2016). In addition, oxidized DNA lesions themselves have been found to be pathological and their continuous clearance is required to prevent the cell from entering a senescent cascade (Rai et al. 2009). ROS also introduces DNA base or sugar damage leading to single-strand break (SSB) formation (Lindahl 1993). Single-strand DNA breaks are linked to cellular senescence, either directly or by predisposing to double-strand DNA breakage (Kuzminov 2001, Nassour et al. 2016). As noted above, double-strand DNA breakage in turn is a well established driver of cellular senescence (d'Adda di Fagagna 2008). ROS can also induce senescence in a DNA damage-independent fashion by activating p38 mitogen-activated protein kinase (MAPK). This stress-activated kinase drives p21 transcription and also that of another cyclin- dependent kinase inhibitor, p16Ink4a (Munoz-Espin and Serrano 2014).

Normal cells can respond to the activation of many oncogenes by undergoing cellular senescence. A general feature of oncogene-induced senescence is the derepression of the Cdkn2a locus. This type of senescence may also induce a robust DNA damage

response owing to the DNA damage that is caused by aberrant DNA replication and/or ROS (Munoz-Espin and Serrano 2014).

There is also a role that senescent cells themselves play in potentiating the spread of senescence to other cells. The secretion of SASP factors, including pro-inflammatory cytokines (interleukin-6 (IL-6) and IL-8), chemokines (monocyte chemoattractant proteins (MCPs) and macrophage inflammatory proteins (MIPs)), growth factors (transforming growth factor-β (TGF-β) and granulocyte–macrophage colony-stimulating factor (GM-CSF)), and proteases causes inflammation. In some cases this response may be important for the clearance of senescent cells by phagocytosis (Hoenicke and Zender 2012, Munoz-Espin and Serrano 2014). However, SASP components, most notably TGF-β, can also trigger senescence in neighbouring cells in a paracrine manner, through a mechanism that generates ROS and DNA damage (Nelson et al. 2012, Acosta et al. 2013).

1.2.3.2 Markers of senescence

There is no one marker that can identify a senescent cell. However, it is possible to identify a senescent cell using a set of indicators taken together. Identifying cells in culture that have ceased to replicate even under mitogenic conditions is a good indication that senescence is occurring. These cells often become more flattened and spread in appearance. Also, a powerful biomarker is the presence of senescence-associated β-galactosidase (SA-β Gal) activity. In senescent cells, lysosomal β galactosidase activity can be detected at an otherwise sub-optimal pH (pH 6), (Dimri et al. 1995) as a result of marked expansion of the lysosomal compartment (Lee et al. 2006). Other molecular markers are on the basis of the signaling hallmarks of cellular senescence, including high levels of p16Ink4a, p21, phosphorylated p38, and the presence of double-stranded DNA breaks as denoted by the modified histone, γ-H2AX (Yin and Pickering 2016).

1.2.3.3 Vascular cell senescence

Senescent endothelial cells and SMCs have been identified in culture, and senescence of these cells is mainly driven by culture conditions (van der Veer et al. 2007, Borradaile and Pickering 2009). Senescent vascular cells have also been identified in vivo, although at a low prevalence. This may be because senescence develops at a very low rate, or because immune cells clear the senescent cells (Hoenicke and Zender 2012, Munoz-Espin and Serrano 2014). Regardless, there is good evidence that senescent cells are associated with vascular disease and dysfunction. Senescent SMCs and endothelial cells have been identified in human atherosclerotic samples (Minamino et al. 2002, Minamino et al. 2003, Matthews et al. 2006). Senescent aortic SMCs have also been identified in mouse models of hypertension (Boe et al. 2013, Vafaie et al. 2014) and aging (Yepuri et al. 2012, Wang and Shah 2015).

1.2.3.4 Benefits of cellular senescence

Cellular senescence can be beneficial and, in fact, proceeds as part of normal embryonic development. For example: the mesonephric tubules during mesonephros involution; the endolymphatic sac of the inner ear, the apical ectodermal ridge of the limbs; the regressing interdigital webs and the closing neural tube (Munoz-Espin et al. 2013, Storer et al. 2013). In addition to embryonic development, senescence also occurs in a physiologically programmed manner in adult organisms. Normal megakaryocytes and placental syncytiotrophoblasts undergo senescence as part of their natural maturation programmes (Besancenot et al. 2010, Chuprin et al. 2013). Senescence can also protect against a damaging fibrotic response to injury. For example, senescent fibroblasts display a collagen suppressive phenotype, with upregulation of matrix metalloproteinases and downregulation of fibrillar collagen (Yin and Pickering 2016). The development of senescent fibroblasts has been reported to be a mechanism for limiting fibrosis in the heart, as well as in other organs (Krizhanovsky et al. 2008, Jun and Lau 2010, Zhu et al. 2013).

However, as extensively reviewed in Munoz-Espin and Serrano (Munoz-Espin and Serrano 2014), there are a number of pathologies associated with cell senescence that illustrate the detrimental effect senescence can have, including the aggravation of pulmonary fibrosis and sarcopenia, and contributing to type II diabetes, cataracts, obesity, and radiation-induced oral mucositis. Senescence has been associated with human aneurysms in the brain and the heart.

1.3 NAD^+

Nicotinamide adenine dinucleotide (NAD^+) is an essential dinucleotide that has emerged as a multi-role determinant of cell health. NAD^+ has classically been known as a cofactor for the oxidation-reduction events of cellular nutrient metabolism. Importantly, recent studies have established that, in addition to its redox carrier role, NAD^+ can serve as a signalling nucleotide that regulates gene expression, genome integrity, and mitochondrial function.

1.3.1 NAD^+ in redox reactions

NAD^+ and its phosphorylated derivative, nicotinamide adenine dinucleotide phosphate (NADP), serve as essential coenzymes for hydride-transfer enzymes. They participate in redox reactions as hydride acceptors (NAD^+ and $NADP^+$) or donors [NADH or NADPH (reduced forms)]. These two redox pairs are kept in chemical opposition: NAD^+ is mostly maintained in its oxidized form; NADP is mostly in its reduced form, NADPH. As a cosubstrate, NAD^+ is essential for energy generation by transferring reducing equivalents from glycolysis (from the activity of glyceraldehyde-3-phosphate dehydrogenase) and from the TCA cycle under the form of NADH. When oxygen is limiting, NADH is converted to NAD^+ by reduction of pyruvate into lactate. With oxygen, cytoplasmic NADH transfers its reducing equivalent through the malate-aspartate shuttle or the glycerol-3-3-phosphate shuttle to the mitochondrial matrix. These reducing equivalents

are oxidized by complex I of the electron-transport chain, thereby coupling glycolysis and the TCA cycle to ATP synthesis via oxidative phosphorylation. NADP is critical in several pathways, including fatty acid oxidation and cholesterol synthesis, as well as in redox protection. In these reactions, NAD^+ and NADH (or NADP and NADPH) interconvert but are not consumed. (Fig 1.4)

1.3.2 NAD^+ in signaling.

Beyond its role as a coenzyme in redox reactions, NAD^+ is an important cosubstrate for three classes of enzymes: (i) the sirtuins (Sirts), (ii) the adenosine diphosphate (ADP)–ribose transferases (ARTs) and poly(ADP-ribose) polymerases (Parps), and (iii) the cyclic ADP-ribose (cADPR) synthases (CD38 and CD157). NAD^+ is consumed by these enzymes and continuously degraded.

1.3.2.1 Sirtuins

Silent information regulator 2 (Sir2) proteins, or sirtuins (Sirts), are NAD^+-dependent protein deacetylases/mono-ADP-ribosyltransferases found in organisms ranging from bacteria to humans (Schwer and Verdin 2008, Soppa 2010). In mammals the sirtuin family comprises seven proteins (Sirt1–Sirt7), which vary in tissue specificity, subcellular localization, enzymatic activity and targets. Sirt1 is mainly localized in the nucleus but is also present in the cytosol (Tanno et al. 2007). Sirt2 is considered to be cytosolic but is also present in the nucleus in the G2 phase to M phase transition of the cell cycle (Vaquero et al. 2006). Sirt3, Sirt4 and Sirt5 have a mitochondrial targeting sequence, and their localization to this organelle has been confirmed experimentally (Huang et al. 2010). Sirt6 is predominantly nuclear (Mostoslavsky et al. 2006) and Sirt7 was reported to reside in the nucleolus, (Ford et al. 2006) although recent reports identify a cytosolic pool and a presence in the nucleus (Kiran et al. 2013). Sequence-based phylogenetic analysis revealed

that mammalian sirtuins can be divided into four classes: Sirt1–Sirt3 belong to class I, Sirt4 to class II, Sirt5 to class III, and Sirt6 and Sirt7 to class IV (Frye 2000).

Sirtuins were originally described as NAD^+-dependent type III HDACs, as the founding member, Sir2 in yeast, silenced specific genomic loci by deacetylating histones H3 and H4 (Braunstein et al. 1996). Not only do Sirts deacetylate histones, but they also deacetylate a wide range of proteins in different subcellular compartments (Houtkooper et al. 2010). In addition, Sirt4 and Sirt6 were reported to function as ADP-ribosyltransferases,(Liszt et al. 2005, Haigis et al. 2006) even though Sirt6 also can act as a deacetylase (Zhong et al. 2010). Sirt5 was initially reported to be a deacetylase, but has been shown to primarily demalonylate and desuccinylate proteins(Du et al. 2011).

Of the sirtuin family, Sirt1 has been studied the most extensively. The protein deacetylase of Sirt1 functions as an epigenetic regulator by targeting specific histone-acetylated residues (e.g., H3K9, H3K14, and H4K16) but also regulates transcription by deacetylating transcription factors (such as TP53, NF-κB, PGC-1α, and FOXO3a) (Verdin 2015). Sirtuin 3 is the major mitochondrial protein deacetylase, and several of its targets have been identified, many of which have important roles in metabolic homeostasis (Verdin 2015). Additionally, Sirt3 also affects oxidative stress defence by protecting cells from ROS (Qiu et al. 2010).

The enzymatic reaction catalysed by sirtuins requires NAD^+ as a substrate, the concentration of which is determined by the nutritional state of the cell. Consequently, NAD^+ controls adaptive responses to energy stress by modulating the activity of sirtuins and their downstream effectors. Sirtuins convert NAD^+ to nicotinamide, which at higher concentrations can non-competitively bind and thereby feedback-inhibit sirtuin activity (Bitterman et al. 2002).

1.3.2.2 Parps

The most potent NAD^+-consuming reaction is believed to be one catalyzed by poly(ADP-ribose) polymerase (Parp). Poly(ADP-ribosyl)ation (PARylation) is a posttranslational protein modification catalyzed by members of the Parp enzyme family. The best-characterized Parp is Parp-1. Parp-1 is a 116 kDa protein that contains a "Parp signature" sequence required for the catalysis of PAR synthesis (Luo and Kraus 2012). Parp-1 belongs to a family of 17 proteins with confirmed or putative mono(ADP-ribosyl) and poly(ADP-ribosyl) transferase activity, which share the "Parp signature motif" in the homologous catalytic domain (Kraus 2015). Some of the family members (e.g., Parp-1 and Parp-2) catalyze the synthesis of PAR on target proteins using NAD^+ as a donor of ADP-ribose units. However, other family members—the mono(ADP-ribosyl) transferases (e.g., Parp-3 and Parp-16), which comprise most of the family—use NAD^+ to catalyze the covalent attachment of mono-ADP-ribose (MAR) on target proteins. Finally, three remaining family members lack any apparent catalytic activity (Hottiger et al. 2010, Hottiger 2015).

Parp-1 catalyzes the covalent attachment of PAR polymers on itself and other acceptor proteins, including histones, DNA repair proteins, transcription factors, and chromatin modulators, using NAD^+ as a donor of ADP-ribose units (D'Amours et al. 1999, Hassa and Hottiger 2008). Parps are best characterized for their role in DNA damage pathways, but more generally Parps regulate adaptive stress responses, including inflammatory, oxidative, proteotoxic, and genotoxic stresses (Luo and Kraus 2012).

1.3.2.2.1 Parp-1 and DNA damage response

Parp1 is the most abundant Parp and is expressed ubiquitously. Parp1 is strongly activated by DNA damage, leading to consumption of a large amount of cellular NAD^+. In fact, DNA damage leads to a decrease (up to 80% in acute situations) in cellular

NAD^+ concentrations. Parp1 has been reported to bind to a variety of aberrant DNA structures, including cyclobutane pyrimidine dimers, 6,4-photoproducts, apurinic and apyrimidinic sites, SSBs and double-strand breaks (DSBs) (Lonskaya et al. 2005, Khodyreva et al. 2010). In fact, Parp1 is one of the first proteins to recognize damaged DNA and its interaction with DNA lesions triggers the PARylation of a variety of proteins, with Parp1 itself being the main PAR acceptor (Haince et al. 2007). Parp1 activation immediately creates long negatively charged PAR polymers attached to Parp1 at DNA lesion sites (D'Amours et al. 1999). Although none of the Parp family members have any known DNA repair enzymatic activity, Parp activity has been linked to DNA repair (Woodhouse et al. 2008). The evidence for this relationship: (i) DNA damage is the main activator of PAR synthesis, (ii) the depletion or inhibition of Parps 1–3 sensitizes cells to DNA-damaging agents and (iii) Parps 1–3 have been reported to interact physically and/or functionally with diverse DNA repair proteins (Sousa et al. 2012). Parp1 has been reported to be involved in different DNA repair systems, including BER, single-strand break repair and double-strand break repair (Yelamos et al. 2011). Parp1 plays an important role in the early steps of DNA repair targeting and in modulating the DNA repair proteins at the sites of DNA lesions, with the formation of long PAR chains that possibly act as scaffolds on which DNA damage repair proteins can assemble. Furthermore, Parp1-dependent chromatin remodeling was shown to facilitate the access of DNA repair proteins to DNA damage (Escargueil et al. 2008).

1.3.2.2.2 PAR-dependent cell death induction—parthanatos

When the levels of DNA damage are beyond the cellular repair capacity, programmed cell death is activated to prevent cells from accumulating mutations that may lead to carcinogenesis (Sousa et al. 2012). Because PARylation is a DNA damage-dependent enzymatic activity, extensive DNA damage is accompanied by large-scale PAR polymer synthesis (Herceg and Wang 2001). However, excessive PAR production may

leads to a unique form of caspase-independent cell death, termed parthanatos (Andrabi et al. 2008). This type of cell death is associated with rapid Parp1 activation, early PAR accumulation, mitochondrial depolarization, early AIF translocation, loss of cellular NAD^+ and ATP and late caspase activation (Yu et al. 2002, Andrabi et al. 2006, Yu et al. 2006).

1.3.2.3 cyclic ADP-ribose synthases

$NAD(P)^+$-derived molecules are key elements of intracellular calcium signaling (Verdin 2015). Several of these derivatives, namely, nicotinic acid adenine dinucleotide phosphate (NAADP), cyclic ADP-ribose (cADPR) and ADPR have been characterized as potent calcium-mobilizing agents. All three molecules, ADPR, cADPR and NAADP are synthesized by multifunctional NAD^+ glycohydrolases, in humans represented by the ADP-ribosyl cyclase CD38 and its structural and functional homolog, CD157 (Malavasi et al. 2008). CD38 and CD157 are membrane-bound ectoenzymes. Mice deficient in CD38 show significantly elevated levels of NAD^+ (10- to 30-fold) in tissues such as liver, muscle, brain, and heart, (Aksoy et al. 2006, Barbosa et al. 2007) confirming the role of CD38 as a major NAD^+ consumer. Conversely, cells overexpressing CD38 showed reductions in NAD^+ levels and in the expression of proteins related to energy metabolism and antioxidant defense (Hu et al. 2014).

An additional ectoenzyme has recently been shown to have NAD^+ degrading activity. CD73, mostly known as the ectoenzyme dephosphorylating extracellular AMP to adenosine, is in fact also capable of degrading both NAD^+ and NMN: specifically, CD73 degrades NAD^+ to NMN, which is subsequently dephosphorylated by the same enzyme to nicotinamide riboside (NR) (Garavaglia et al. 2012, Grozio et al. 2013).

1.3.3 NAD^+ as a neurotransmitter

NAD^+ is most widely considered in the paradigms outlined above: either as a coenzyme in redox reactions or a cosubstrate for the activities of Sirts, Parps, and cADPR-

synthases. However, there is evidence that NAD^+ may also be an inhibitory neurotransmitter candidate. NAD^+ (referred to as ß-NAD in this field) is a purine substance released by nerve stimulation in vascular and visceral smooth muscles and neuro-secretory cells (Smyth et al. 2004, Smyth et al. 2006, Mutafova-Yambolieva et al. 2007). Purines can be released from intrinsic enteric nerves, sympathetic nerves or sensory motor nerves during axon reflexes, to act directly on smooth muscle purinoceptors mediating relaxation or contraction or on epithelial cell receptors. They act on prejunctional nerve terminals to modify transmitter release from motor and inhibitory neural control pathways (Burnstock 2014). They participate in synaptic transmission in myenteric and submucosal ganglia that are involved in the control of gastrointestinal motility, mucosal secretion and absorption. They act on blood vessels or interstitial cells of Cajal (ICC) thereby indirectly modulating motility patterns. Purines also can act on sensory nerve endings in the gut wall after release from epithelial cells to initiate local and/or central reflex activity that alters gastrointestinal motility and secretory patterns and initiate nociception (Burnstock 2008, Burnstock 2014).

To date the role of NAD^+ as an enteric neurotransmitter is controversial as ATP has been assumed to be the known purine neurotransmitter (Xue et al. 1999), however experiments on mouse (Mutafova-Yambolieva et al. 2007) and primate colons (Hwang et al. 2011) showed that NAD^+ and its bioactive metabolite, ADP-ribose (Durnin et al. 2013), mimic the endogenous purine neurotransmitter better than ATP. To date, experiments have shown both ATP and NAD^+ and their metabolites, ADP and ADP-ribose, produced relaxation of murine colonic smooth muscle, and it was suggested that they might be involved in motility disorders (Durnin et al. 2012, Gallego et al. 2016).

1.3.4 NAD^+ biosynthetic pathways

NAD^+ can be synthesized from diverse dietary sources, including nicotinic acid (NA) and nicotinamide (NAM), tryptophan, and nicotinamide riboside (NR). (Fig. 1.4)

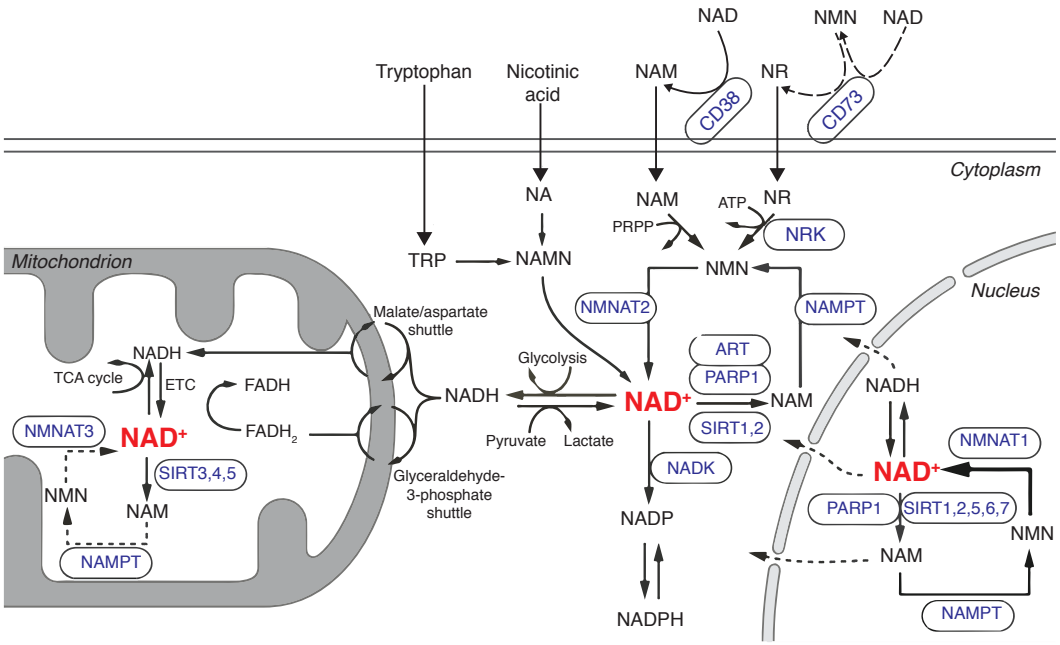

Figure 1.4 NAD^+ metabolism

The different precursors to intracellular NAD metabolism—tryptophan, nicotinic acid (NA), nicotinamide, NR, and NMN—are shown. The cytoplasmic and nuclear NAD^+ pools probably equilibrate by diffusion through the nuclear pore. However, the mitochondrial membrane is impermeable to both NAD^+ and NADH. Reducing equivalents generated by glycolysis are transferred to the mitochondrial matrix via the malate/aspartate shuttle and the glyceraldehyde-3-phosphate shuttle. The resulting mitochondrial NADH (malate/aspartate shuttle) is oxidized by complex I in the respiratory chain (ETC), whereas the resulting $FADH_2$ (glyceraldehyde-3-phosphate shuttle) is oxidized by complex II. In each of the three compartments, different NAD^+-consuming enzymes lead to the generation of nicotinamide, which is recycled via the NAD^+ salvage pathway. Different forms of the NMNAT enzyme and sirtuins are localized in different compartments.

The primary biosynthesis of NAD^+ starts with the essential amino acid L-tryptophan, which is taken up from the diet (Bender 1983), and serves as the precursor for NAD^+ through the multi-step de novo kynurenine pathway. The first step in this pathway is the rate-limiting conversion of tryptophan to N-formylkinurenine by either IDO or TDO. Formylkinurenine is transformed into L-kinurenine, 3-hydroxykinurenine, and 3-hydroxyanthranilic acid and finally to ACMS. This compound can spontaneously condense and rearrange into quinolinic acid, which is transformed into NAMN, at which point it converges with the Preiss-Handler pathway.

NAD^+ synthesis from NA, also known as the Preiss-Handler pathway, is initiated by the NA phosphoribosyltransferase (Naprt) which forms NA mononucleotide (NAMN) from NA. Together with ATP, NAMN is then converted into NA adenine dinucleotide (NAAD) by the nicotinamide mononucleotide adenylyltransferase (Nmnat1–3) enzymes. Finally, NAAD is transformed to NAD^+ through an amidation reaction catalyzed by the NAD^+ synthetase (Nadsyn) enzyme.

The synthesis of NAD^+ from NAM or NR is more direct and relies on only two steps each. NAM is converted by the rate-limiting Nampt to form nicotinamide mononucleotide (NMN). NMN is also the product of phosphorylation of NR by the NR kinases (Nrk1 and Nrk2). The subsequent conversion of NMN to NAD^+ is catalyzed by the Nmnat1-3 enzymes.

The formation of NAD^+ from NR can be considered a de novo pathway in some respects as there have been nutritional sources of NR identified, i.e. milk (Bieganowski and Brenner 2004). The salvage pathway uses NAM or NA (together called niacin or B3) to make NAD^+ (Bogan and Brenner 2008). While dietary maintenance may meet baseline requirements for NAD^+, the local salvage pathways that supply or regenerate NAD^+ are critical determinants of cell health and survival (Sauve 2008).

1.4 Nampt

1.4.1 Biochemical function of Nampt

Nicotinamide phosphoribosyltransferase (Nampt) was originally identified as a putative cytokine, pre-B enhancing colony factor (Pbef) (Samal et al. 1994, Rongvaux et al. 2002), and subsequently as a putative insulin-mimetic hormone, Visfatin (Fukuhara et al. 2005). Evidence for the former is inconclusive, and the index report for the latter has since been retracted (Fukuhara et al. 2007). Bacterial and murine homologues of Nampt were later identified as enzymes involved in NAD^+ biosynthesis (Martin et al. 2001, Rongvaux et al. 2002), and this was enzymatic activity was first confirmed in humans cells in aortic SMCs (van der Veer et al. 2005). Nampt is known to catalyze NAD^+ synthesis by transferring the phosphoribosyl group of 5-phosporibosyl-1-pyrophosphate to NAM, forming NMN. NAD^+ synthesis is completed by Nmnat, which converts NMN into NAD^+ (Fig. 1.5) (Rongvaux et al. 2002). Nampt's catalytic activity is ~46-fold lower than Nmnat activity, and thus Nampt catalyzes the rate-limiting step in this two-step pathway of NAD^+ synthesis from NAM. Thus, even very small changes in Nampt activity levels, but not Nmnat levels, can have a profound effect on NAD^+ metabolism (Rongvaux et al. 2002, Revollo et al. 2004).

1.4.2 Cellular localization of Nampt

Nampt is a ubiquitously expressed protein, and expression is variable across tissue and cell types. Nampt is localized intracellularly (mainly in the cytoplasm and nucleus) (Kitani et al. 2003), but also has been found extracellularly (Revollo et al. 2007), in which case it is generally referred to as eNampt. eNampt has been found in human circulation (Korner et al. 2007) and mouse circulation (Revollo et al. 2007), as well as in the supernatant of certain cell types including differentiated adipocytes (Revollo et al. 2007, Tanaka et al. 2007, Yoon et al. 2015),

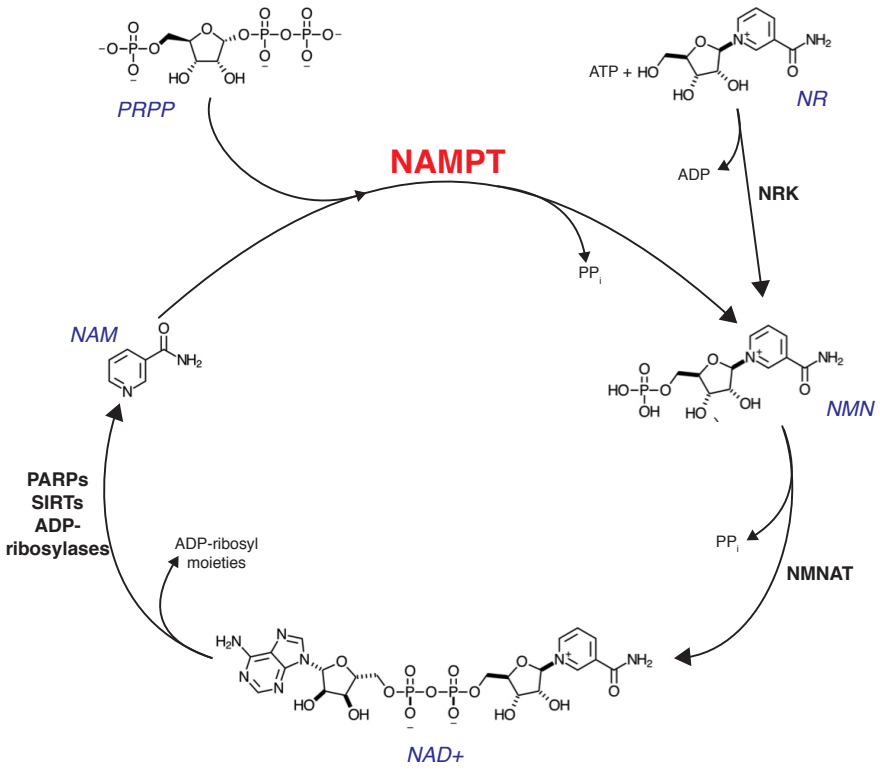

Figure 1.5 NAD$^+$ salvage by Nampt

NAD$^+$ is consumed by Parps, Sirts and ADP-ribosylases, releasing the NAM moiety. Nampt catalyzes the addition of a phosphoribosyl group in the first step of salvage. The resulting NMN product then gains a phosphor-adenine group from ATP to form NAD$^+$, catalyzed by the Nmnat family of enzymes. NR enters this two-step salvage pathway by receiving a phosphate group from ATP to form NMN, catalyzed by Nrk1.

hepatocytes (Garten et al. 2010, Schuster et al. 2014), leucocytes (Friebe et al. 2011), cardiomyocytes (Pillai et al. 2013), and neurons (Zhao et al. 2013, Jing et al. 2014). However, a secretory pathway for eNampt has not been identified. Some reports claim that eNampt is released via a "non-classical secretory pathway", but these reports cannot preclude that intracellular Nampt is simply being released upon cell death (Revollo et al. 2007, Tanaka et al. 2007, Garten et al. 2010). As well, a cell-surface role for eNampt has yet to be identified and the role of eNampt in the extracellular space is still a matter of debate. Several studies have measured enzymatic activity of eNampt (Revollo et al. 2007, Garten et al. 2010, Friebe et al. 2011, Kover et al. 2013, Zamporlini et al. 2014). However, it has been reported that eNampt is not enzymatically active in mouse plasma owing to the low concentrations of PRPP and ATP (Hara et al. 2011).

1.4.3 Regulation of Nampt expression

Because Nampt is the rate-limiting enzyme in the regeneration of NAD^+, Nampt is a key regulator of the intracellular NAD^+ pool (Rongvaux et al. 2002, Revollo et al. 2004). Through its NAD^+-biosynthetic activity, Nampt influences the activity of NAD^+-dependent enzymes, such as Sirts (Revollo et al. 2004, van der Veer et al. 2007, Yang et al. 2007, Borradaile and Pickering 2009, Bruzzone et al. 2009, Ho et al. 2009, Van Gool et al. 2009, Koltai et al. 2010, Bowlby et al. 2012) and Parps, (Pillai et al. 2013) and thereby regulates cellular metabolism, mitochondrial biogenesis (van der Horst et al. 2004, Bordone et al. 2006, Rodgers et al. 2008) and adaptive responses to inflammatory, oxidative, proteotoxic and genotoxic stress (Luo and Kraus 2012).

Nampt itself seems to be regulated in a circadian fashion. Levels of *Nampt* RNA display a diurnal oscillation in the liver and white adipose tissue, with a peak around the beginning of the dark period (Ramsey et al. 2009), a phenomenon also observed in serum-entrained mouse embryonic fibroblasts (Nakahata et al. 2009). These robust diurnal and

circadian oscillation patterns of *Nampt* RNA and protein are completely abolished in tissues from the circadian rhythm-deficient *Clock*Δ19 mutant mice, or mice deficient in Bmal1, the binding partner of Clock (Ramsey et al. 2009). The *Nampt* promoter region contains putative E-box sequences (CACGTG sequences - DNA response elements acting as protein-binding sites that have been found to impact the regulation of transcription). Nakahata et al (Nakahata et al. 2009) demonstrated that the *Nampt* promoter is readily activated by Clock:Bmal1 through the E-boxes in a time-dependent manner. Interestingly, dual cross-linking ChIP assays showed that Sirt1 binds to the E-boxes in a time-dependent manner, following the circadian timing of Clock:Bmal1 recruitment. In addition, Sirt1 negatively regulates the transcriptional activation of clock genes. Thus, Clock and Sirt1 contribute to circadian chromatin remodeling at the *Nampt* promoter. As NAD^+ intracellular levels directly influence the histone deacetylase activity of Sirt1, an enzymatic- transcription feedback loop seems to operate in which NAD^+ levels determine the oscillatory synthesis of Nampt.

1.4.4 Biological expression and importance of Nampt

Several studies have reported Nampt to be highly expressed in lung, liver, kidney, heart, and skeletal muscle, with much lower expression in brain and pancreas (Samal et al. 1994, Revollo et al. 2007). The expression of Nampt was found to be upregulated in immune cells upon activation (Samal et al. 1994, Rongvaux et al. 2002, Jia et al. 2004) whereas another report identified this protein as a gene strongly expressed in adipocytes (Revollo et al. 2007).

Within vascular tissue we have identified that Nampt is expressed in endothelial cells and SMCs, with relatively higher expression in the former (Ho et al. 2009). We have also shown that expression in smooth muscle cells is dynamic: Nampt expression is decreased in aging and senescent primary human smooth muscle cells, and in HITC6 cells,

and an increase in Nampt expression has been correlated with a shift of the SMC phenotype from a contractile to a synthetic phenotype (van der Veer et al. 2007).

Overexpressing Nampt in SMCs and endothelial cells in culture enhances cell life span via enhancing Sirt1 activity and p53 degradation (van der Veer et al. 2007). Nampt overexpression leads to an increase of NAD^+ in the cells, associated with prolonged cell survival and resistance to oxidative stress (van der Veer et al. 2007, Borradaile and Pickering 2009, Ho et al. 2009). Exposure of cells with an inhibitor of Nampt, FK866, results in the decreased ability of the cell to withstand genotoxic stress (Rongvaux et al. 2008). Incubation with FK866 also aggravated brain infarction in a model of mouse cerebral ischemia and activated T cells were found to undergo massive NAD^+ depletion upon treatment with FK866 (Bruzzone et al. 2009, Wang et al. 2011).

Gene-targeting strategies in mice have revealed a pattern of degenerative or aging-related tissue dysfunction when Nampt is perturbed in skeletal muscle, adipose tissue, and brain (Stein and Imai 2014, Frederick et al. 2016, Stromsdorfer et al. 2016, Zhou et al. 2016). Mice lacking *Nampt* in forebrain excitatory neurons showed hippocampal and cortical atrophy, astrogliosis, microgliosis, and abnormal CA1 dendritic morphology by 2–3 months of age (Stein et al. 2014). Ablation of *Nampt* in adult neural stem cells also causes signs of accelerated aging in this neural cell population (Stein and Imai 2014). Knockout of *Nampt* in skeletal muscle contributed to an aging phenotype-related loss mass and contractile function (Frederick et al. 2016). Adipocyte-specific *Nampt* knockout mice had severe insulin resistance in adipose tissue, liver, and skeletal muscle, and adipose tissue dysfunction. This dysfunction was manifested by increased plasma free fatty acid concentrations and decreased plasma concentrations of a major insulin-sensitizing adipokine, adiponectin (Stromsdorfer et al. 2016). Additionally, Nampt is critically required for the development of both T and B lymphocytes (Rongvaux et al. 2008).

In contrast, there has been some evidence that a decrease in Nampt expression in certain tissue may have a limited protective effect. shRNA-mediated knockdown of *Nampt* in mouse liver increased plasma HDL-C levels, reduced the plaque area of the total aorta en face and the cross-sectional aortic sinus, decreased macrophage number and apoptosis, and promoted reverse cholesterol transport in high fat diet-fed ApoE KO mice (Li et al. 2016). Heterozygous *Nampt*$^{+/-}$ mice were significantly protected when exposed to a model of sepsis-induced acute lung injury (Hong et al. 2008), and also were protected from Ang II-induced cardiac hypertrophy (Pillai et al. 2013). Overexpression of Nampt in cardiomyocytes exacerbated Ang II-induced cardiac hypertrophy (Pillai et al. 2013), however in another model of cardiomyocyte-specifc overexpression of Nampt, Nampt was protective against ischemia-reperfusion injury (Hsu et al. 2009). In addition, female *Nampt*$^{+/-}$ mice show moderately impaired glucose tolerance and reduced glucose-stimulated insulin secretion, consistent with significant decreases in NAD^+ biosynthesis and insulin secretion in response to glucose in primary islets isolated from *Nampt*$^{+/-}$ mice (Revollo et al. 2007).

A very recent report of global *Nampt* knockout in the adult mouse has shown that *Nampt* is an essential gene, as mice in which *Nampt* has been ablated do not survive longer than 10 days (Zhang et al. 2017). However, the reasons for poor survival were not elaborated on beyond an indication that the endothelial cells of the gastrointestinal tract were disturbed and death occurred due to a deficiency in gastrointestinal ion transport.

Taken together, the role of Nampt in vivo has not been clearly defined. The evidence presented above speaks to the importance of Nampt with respect to maintaining a healthy cell in vitro, and also resistant to the normal physiological stresses in vivo; however, not much is know about the role that Nampt plays in normal cell and tissue development. It has been reported that Nampt expression begins in the embryo around e8.5 and that knockout mice are embryonically lethal before e10.5 (Revollo et al. 2007, Zhang

et al. 2017). Additionally, male *Nampt* heterozygous mice are ostensibly normal (Revollo et al. 2007). The extent to which Nampt is required for SMC and endothelial cell development and function is, to this point, unknown.

1.5 Therapeutic augmentation of the NAD^+ biosynthesis pathway

NAD^+ levels in the cells depend on several variables, including the cellular redox state (NAD^+/NADH ratio) and the rates of NAD^+ synthesis and NAD^+ consumption. As noted in previous sections, they can also fluctuate in a circadian manner, through activation of the NAD^+ salvage pathway (i.e. through Nampt activity) (Nakahata et al. 2009). In addition, NAD^+ concentrations increase in response to conditions associated with lower energy loads, such as fasting, glucose deprivation, calorie restriction, and exercise (Rodgers et al. 2005, Chen et al. 2008, Fulco et al. 2008, Canto et al. 2009, Nakahata et al. 2009, Ramsey et al. 2009, Costford et al. 2010). In contrast, NAD^+ concentrations decrease in animals on high-fat diets (Bai et al. 2011, Yoshino et al. 2011, Canto et al. 2012, Kraus et al. 2014, Pirinen et al. 2014, Yang et al. 2014), and during aging and senescence (Ramsey et al. 2008, Braidy et al. 2011, Yoshino et al. 2011, Massudi et al. 2012, Gomes et al. 2013, Mouchiroud et al. 2013, Pugh et al. 2013, Cerutti et al. 2014).

It is interesting to note the conditions in which NAD^+ is upregulated are conditions associated with longevity. These data support the idea that decreased NAD^+ levels contribute to the aging process and that NAD^+ supplementation might exert protective effects during aging. Indeed, NAD^+ supplementation increases life span in yeast and worms (Belenky et al. 2007, Mouchiroud et al. 2013).

Lower overall NAD^+ levels have been reported in various aged rat and human tissue (Braidy et al. 2011, Massudi et al. 2012). Declining levels can be explained by increased NAD^+ consumption through hyperstimulation of NAD^+-consuming enzymes, particularly Parp1, the activity of which increases during aging as DNA damage accumulates (Braidy et

al. 2011, Mouchiroud et al. 2013). Additionally, defective circadian rhythm regulation by Clock and Bmal1 has been reported to lower levels of Nampt as well as NAD^+ (Nakahata et al. 2009). Reports of decreased Nampt expression levels in aged mice were associated with chronic inflammation and oxidative stress; both lowering Nampt and NAD^+ in primary hepatocytes (Cavadini et al. 2007, Yoshino et al. 2011). Also, mitochondrial homeostasis can be impacted by declining NAD^+ levels, requiring more resource input to generate ATP in less functional mitochondria in aged tissue (Gomes et al. 2013). Taken together, increased consumption, decreased biosynthetic capacity and lower energy production efficiency contribute to an NAD^+-deficient system in aged models.

In the face of declining NAD^+ levels in pathology, there may be an opportunity for augmentation of NAD^+ levels either by upregulating Nampt expression or with the delivery of NAD^+ precursors. Historically, niacin (consisting of NAD^+ precursors NAM and NA) has been used therapeutically to treat dyslipidemia by lowering triglycerides circulating in the blood stream and raising HDL levels (Creider et al. 2012). However, two clinical trials have reported that niacin did not reduce cardiac events in high-risk patients (Ginsberg and Reyes-Soffer 2013). Additional studies suggest that niacin's benefits on vascular health act independently of its lipid-lowering effects (Wu et al. 2010, Huang et al. 2012, Lavigne and Karas 2013). Instead, recent work suggests that niacin can improve endothelial function and reduce oxidative stress (Kaplon et al. 2014), thereby enabling stress management in models of ischemia & reperfusion injury or stroke (Chen et al. 2007).

NMN supplementation has been reported to protect the heart from ischemia & reperfusion injury (Yamamoto et al. 2014) and to treat diabetes in aged mice (Yoshino et al. 2011). Endogenous Nampt is decreased in response to cardiac ischemia and reperfusion (Hsu et al. 2009). Augmenting NAD^+ levels by NMN supplementation mitigates the effects of the ischemia and reperfusion injury in a Sirt1-dependent fashion (Yamamoto et al. 2014). In diabetic mice induced by a high-fat diet, Nampt-mediated NAD^+ biosynthesis is

compromised in liver and adipose tissue. NMN administration successfully restored NAD^+ levels in the liver and adipose of diabetic mice, and even in diabetic skeletal muscle, a moderate but significant increase in NAD^+ was detected (Yoshino et al. 2011). NMN supplementation was also beneficial in models of age-induced type II diabetes (Yoshino et al. 2011). In two additional studies, NMN was found to overcome NAD^+ decline in skeletal muscle induced by age-associated increases in Parp activation (Gomes et al. 2013, Mouchiroud et al. 2013). The mechanisms by which extracellular NMN is converted to cellular NAD^+ also remain elusive. On the one hand, it was claimed that NMN is transported intact to hepatocytes (Yoshino et al. 2011). On the other hand, it has been proposed that extracellular dephosphorylation of NMN to nicotinamide riboside (NR) is required to elevate cellular NAD^+ metabolism (Belenky et al. 2007, Nikiforov et al. 2011, Grozio et al. 2013, Sociali et al. 2016).

NR metabolism constitutes an additional path for NAD^+ biosynthesis. NR has been identified as a nutrient naturally present in the human diet including milk. NR offers a favourable mechanism of absorption into the cell. NR is transported into cells by nucleoside transporters (Nikiforov et al. 2011) and is then phosphorylated by the NR kinases 1 and 2 (Nrks) (Bieganowski and Brenner 2004), generating NMN. NR has been observed to stably elevate NAD^+ levels and increase NAD^+ bioavailability in HEK293, Neuro2a, AB1, C2C 12 and Hepa1.6 mammalian cell lines (Yang et al. 2007, Canto et al. 2012). In addition, NR has potential therapeutic benefits over NAM. NAM has been reported to negatively affecting Sirt activity, whereas NR increases Sirt activities (Canto et al. 2012, Brown et al. 2014). Further, niacin (consisting of NA and NAM) has been known to induce painful flushing; these side effects may be avoided by instead administering NR (Creider et al. 2012).

1.6 Aims of thesis

In summary, maintaining a pool of bioavailable NAD^+ involves the metabolism of different precursors, and the regenerative activity of Nampt. In short, it is a complex process of biosynthesis that is of vital importance to the health and vitality of a cell. As the rate-limiting enzyme in the regeneration of cellular NAD^+, Nampt is a point of vulnerability in maintaining an equilibrium of NAD^+ levels. Work done by Dr. Pickering's research group had previously identified that Nampt is expressed in endothelial cells and SMCs (Ho et al. 2009). We have also shown that expression in smooth muscle cells is dynamic: Nampt expression is decreased in aging and senescent primary human smooth muscle cells, and in HITC6 cells, and an increase in Nampt expression has been correlated with a shift of the SMC phenotype from a contractile to a synthetic phenotype (van der Veer et al. 2007). Overexpressing Nampt in SMCs and endothelial cells in culture enhances cell life span via enhancing Sirt1 activity and p53 degradation (van der Veer et al. 2007). Nampt overexpression leads to an increase of NAD^+ in the cells, associated with prolonged cell survival and resistance to oxidative stress (van der Veer et al. 2007, Borradaile and Pickering 2009, Ho et al. 2009). It has also been established that increases in oxidative stress and SMC senescence in vivo has been associated with vascular disease and dysfunction. Senescent SMCs and endothelial cells have been identified in human atherosclerotic samples (Minamino et al. 2002, Minamino et al. 2003, Matthews et al. 2006). Senescent aortic SMCs have also been identified in mouse models of hypertension (Boe et al. 2013, Vafaie et al. 2014) and aging (Yepuri et al. 2012, Wang and Shah 2015). However, the role of Nampt in SMCs in vivo is unknown. Additionally, although there is very recent evidence that Nampt is globally important to the adult mouse, the tissue-specific vulnerabilities of global *Nampt* ablation are unclear and it is also unclear if a global Nampt deficiency could be overcome by augmenting an NAD^+ generation pathway.

Therefore, the broad aims of my research were two-fold: 1) to the elucidate the role that Nampt plays in maintaining the integrity of the vascular tissue; and 2) to determine the role that Nampt plays globally and if a global Nampt deficiency is able to be overcome. To address these 2 broad goals I generated two new mouse models of *Nampt* knockout in order to characterize the ensuing deficiencies: a smooth muscle-specific *Nampt* knockout mouse and a mouse model in which *Nampt* could be deleted in the whole body in an inducible fashion.

In order to address the broad aims of my research I had four specific aims:

1. To determine if Nampt in smooth muscle cells is required to maintain vascular stability in the mouse.
2. To determine if there is a relationship between Nampt biology and life-threatening ascending aortic dysfunction in humans.
3. To determine if Nampt in smooth muscle cells regulates the mechanical structure of the aorta.
4. To determine if there are fundamental Nampt requirements in organs in addition to the aorta in the adult mouse.

1.7 References

Acosta, J. C., Banito, A., Wuestefeld, T., Georgilis, A., Janich, P., Morton, J. P., Athineos, D., Kang, T. W., Lasitschka, F., Andrulis, M., Pascual, G., Morris, K. J., Khan, S., Jin, H., Dharmalingam, G., Snijders, A. P., Carroll, T., Capper, D., Pritchard, C., Inman, G. J., Longerich, T., Sansom, O. J., Benitah, S. A., Zender, L., & Gil, J. (2013). A complex secretory program orchestrated by the inflammasome controls paracrine senescence. *Nat Cell Biol, 15*(8), 978-990

Aksoy, P., White, T. A., Thompson, M., & Chini, E. N. (2006). Regulation of intracellular levels of NAD: a novel role for CD38. *Biochem Biophys Res Commun, 345*(4), 1386-1392

Andrabi, S. A., Dawson, T. M., & Dawson, V. L. (2008). Mitochondrial and nuclear cross talk in cell death: parthanatos. *Ann N Y Acad Sci, 1147*, 233-241

Andrabi, S. A., Kim, N. S., Yu, S. W., Wang, H., Koh, D. W., Sasaki, M., Klaus, J. A., Otsuka, T., Zhang, Z., Koehler, R. C., Hurn, P. D., Poirier, G. G., Dawson, V. L., & Dawson, T. M. (2006). Poly(ADP-ribose) (PAR) polymer is a death signal. *Proc Natl Acad Sci U S A, 103*(48), 18308-18313

Bai, P., Canto, C., Oudart, H., Brunyanszki, A., Cen, Y., Thomas, C., Yamamoto, H., Huber, A., Kiss, B., Houtkooper, R. H., Schoonjans, K., Schreiber, V., Sauve, A. A., Menissier-de Murcia, J., & Auwerx, J. (2011). PARP-1 inhibition increases mitochondrial metabolism through SIRT1 activation. *Cell Metab, 13*(4), 461-468

Barbosa, M. T., Soares, S. M., Novak, C. M., Sinclair, D., Levine, J. A., Aksoy, P., & Chini, E. N. (2007). The enzyme CD38 (a NAD glycohydrolase, EC 3.2.2.5) is necessary for the development of diet-induced obesity. *FASEB J, 21*(13), 3629-3639

Belenky, P., Bogan, K. L., & Brenner, C. (2007). NAD+ metabolism in health and disease. *Trends Biochem Sci, 32*(1), 12-19

Bender, D. A. (1983). Biochemistry of tryptophan in health and disease. *Mol Aspects Med, 6*(2), 101-197

Bernadotte, A., Mikhelson, V. M., & Spivak, I. M. (2016). Markers of cellular senescence. Telomere shortening as a marker of cellular senescence. *Aging (Albany NY), 8*(1), 3-11

Besancenot, R., Chaligne, R., Tonetti, C., Pasquier, F., Marty, C., Lecluse, Y., Vainchenker, W., Constantinescu, S. N., & Giraudier, S. (2010). A senescence-like cell-cycle arrest occurs during megakaryocytic maturation: implications for physiological and pathological megakaryocytic proliferation. *PLoS Biol, 8*(9)

Biddinger, A., Rocklin, M., Coselli, J., & Milewicz, D. M. (1997). Familial thoracic aortic dilatations and dissections: a case control study. *J Vasc Surg, 25*(3), 506-511

Bieganowski, P., & Brenner, C. (2004). Discoveries of nicotinamide riboside as a nutrient and conserved NRK genes establish a Preiss-Handler independent route to NAD+ in fungi and humans. *Cell, 117*(4), 495-502

Bitterman, K. J., Anderson, R. M., Cohen, H. Y., Latorre-Esteves, M., & Sinclair, D. A. (2002). Inhibition of silencing and accelerated aging by nicotinamide, a putative negative regulator of yeast sir2 and human SIRT1. *J Biol Chem, 277*(47), 45099-45107

Boe, A. E., Eren, M., Murphy, S. B., Kamide, C. E., Ichimura, A., Terry, D., McAnally, D., Smith, L. H., Miyata, T., & Vaughan, D. E. (2013). Plasminogen activator inhibitor-1 antagonist TM5441 attenuates Nomega-nitro-L-arginine methyl ester-induced hypertension and vascular senescence. *Circulation, 128*(21), 2318-2324

Bogan, K. L., & Brenner, C. (2008). Nicotinic acid, nicotinamide, and nicotinamide riboside: a molecular evaluation of NAD+ precursor vitamins in human nutrition. *Annu Rev Nutr, 28*, 115-130

Bordone, L., Motta, M. C., Picard, F., Robinson, A., Jhala, U. S., Apfeld, J., McDonagh, T., Lemieux, M., McBurney, M., Szilvasi, A., Easlon, E. J., Lin, S. J., & Guarente, L. (2006). Sirt1 regulates insulin secretion by repressing UCP2 in pancreatic beta cells. *PLoS Biol, 4*(2), e31

Borradaile, N. M., & Pickering, J. G. (2009). Nicotinamide phosphoribosyltransferase imparts human endothelial cells with extended replicative lifespan and enhanced angiogenic capacity in a high glucose environment. *Aging Cell, 8*(2), 100-112

Bowlby, S. C., Thomas, M. J., D'Agostino, R. B., Jr., & Kridel, S. J. (2012). Nicotinamide phosphoribosyl transferase (Nampt) is required for de novo lipogenesis in tumor cells. *PLOS ONE, 7*(6), e40195

Braidy, N., Guillemin, G. J., Mansour, H., Chan-Ling, T., Poljak, A., & Grant, R. (2011). Age related changes in NAD+ metabolism oxidative stress and Sirt1 activity in wistar rats. *PLOS ONE, 6*(4), e19194

Braunstein, M., Sobel, R. E., Allis, C. D., Turner, B. M., & Broach, J. R. (1996). Efficient transcriptional silencing in Saccharomyces cerevisiae requires a heterochromatin histone acetylation pattern. *Mol Cell Biol, 16*(8), 4349-4356

Brown, K. D., Maqsood, S., Huang, J. Y., Pan, Y., Harkcom, W., Li, W., Sauve, A., Verdin, E., & Jaffrey, S. R. (2014). Activation of SIRT3 by the NAD(+) precursor nicotinamide riboside protects from noise-induced hearing loss. *Cell Metab, 20*(6), 1059-1068

Bruzzone, S., Fruscione, F., Morando, S., Ferrando, T., Poggi, A., Garuti, A., D'Urso, A., Selmo, M., Benvenuto, F., Cea, M., Zoppoli, G., Moran, E., Soncini, D., Ballestrero, A., Sordat, B., Patrone, F., Mostoslavsky, R., Uccelli, A., & Nencioni, A. (2009). Catastrophic NAD+ depletion in activated T lymphocytes through Nampt inhibition reduces demyelination and disability in EAE. *PLOS ONE, 4*(11), e7897

Burnstock, G. (2008). Purinergic receptors as future targets for treatment of functional GI disorders. *Gut, 57*(9), 1193-1194

Burnstock, G. (2014). Purinergic signalling in the gastrointestinal tract and related organs in health and disease. *Purinergic Signal, 10*(1), 3-50

Campisi, J. (2013). Aging, cellular senescence, and cancer. *Annu Rev Physiol, 75*, 685-705

Campisi, J., & d'Adda di Fagagna, F. (2007). Cellular senescence: when bad things happen to good cells. *Nat Rev Mol Cell Biol, 8*(9), 729-740

Canto, C., Gerhart-Hines, Z., Feige, J. N., Lagouge, M., Noriega, L., Milne, J. C., Elliott, P. J., Puigserver, P., & Auwerx, J. (2009). AMPK regulates energy expenditure by modulating NAD+ metabolism and SIRT1 activity. *Nature, 458*(7241), 1056-1060

Canto, C., Houtkooper, R. H., Pirinen, E., Youn, D. Y., Oosterveer, M. H., Cen, Y., Fernandez-Marcos, P. J., Yamamoto, H., Andreux, P. A., Cettour-Rose, P.,

Gademann, K., Rinsch, C., Schoonjans, K., Sauve, A. A., & Auwerx, J. (2012). The NAD(+) precursor nicotinamide riboside enhances oxidative metabolism and protects against high-fat diet-induced obesity. *Cell Metab, 15*(6), 838-847

Carmeliet, P. (2000). Mechanisms of angiogenesis and arteriogenesis. *Nat Med, 6*(4), 389-395

Cavadini, G., Petrzilka, S., Kohler, P., Jud, C., Tobler, I., Birchler, T., & Fontana, A. (2007). TNF-alpha suppresses the expression of clock genes by interfering with E-box-mediated transcription. *Proc Natl Acad Sci U S A, 104*(31), 12843-12848

Cerutti, R., Pirinen, E., Lamperti, C., Marchet, S., Sauve, A. A., Li, W., Leoni, V., Schon, E. A., Dantzer, F., Auwerx, J., Viscomi, C., & Zeviani, M. (2014). NAD(+)-dependent activation of Sirt1 corrects the phenotype in a mouse model of mitochondrial disease. *Cell Metab, 19*(6), 1042-1049

Chen, D., Bruno, J., Easlon, E., Lin, S. J., Cheng, H. L., Alt, F. W., & Guarente, L. (2008). Tissue-specific regulation of SIRT1 by calorie restriction. *Genes Dev, 22*(13), 1753-1757

Chen, J., Cui, X., Zacharek, A., Jiang, H., Roberts, C., Zhang, C., Lu, M., Kapke, A., Feldkamp, C. S., & Chopp, M. (2007). Niaspan increases angiogenesis and improves functional recovery after stroke. *Ann Neurol, 62*(1), 49-58

Chen, Q., Fischer, A., Reagan, J. D., Yan, L. J., & Ames, B. N. (1995). Oxidative DNA damage and senescence of human diploid fibroblast cells. *Proc Natl Acad Sci U S A, 92*(10), 4337-4341

Chicas, A., Wang, X., Zhang, C., McCurrach, M., Zhao, Z., Mert, O., Dickins, R. A., Narita, M., Zhang, M., & Lowe, S. W. (2010). Dissecting the unique role of the retinoblastoma tumor suppressor during cellular senescence. *Cancer Cell, 17*(4), 376-387

Childs, B. G., Durik, M., Baker, D. J., & van Deursen, J. M. (2015). Cellular senescence in aging and age-related disease: from mechanisms to therapy. *Nat Med, 21*(12), 1424-1435

Chuprin, A., Gal, H., Biron-Shental, T., Biran, A., Amiel, A., Rozenblatt, S., & Krizhanovsky, V. (2013). Cell fusion induced by ERVWE1 or measles virus causes cellular senescence. *Genes Dev, 27*(21), 2356-2366

Collado, M., Blasco, M. A., & Serrano, M. (2007). Cellular senescence in cancer and aging. *Cell, 130*(2), 223-233

Coppe, J. P., Patil, C. K., Rodier, F., Sun, Y., Munoz, D. P., Goldstein, J., Nelson, P. S., Desprez, P. Y., & Campisi, J. (2008). Senescence-associated secretory phenotypes reveal cell-nonautonomous functions of oncogenic RAS and the p53 tumor suppressor. *PLoS Biol, 6*(12), 2853-2868

Costford, S. R., Bajpeyi, S., Pasarica, M., Albarado, D. C., Thomas, S. C., Xie, H., Church, T. S., Jubrias, S. A., Conley, K. E., & Smith, S. R. (2010). Skeletal muscle NAMPT is induced by exercise in humans. *Am J Physiol Endocrinol Metab, 298*(1), E117-126

Creider, J. C., Hegele, R. A., & Joy, T. R. (2012). Niacin: another look at an underutilized lipid-lowering medication. *Nat Rev Endocrinol, 8*(9), 517-528

d'Adda di Fagagna, F. (2008). Living on a break: cellular senescence as a DNA-damage response. *Nat Rev Cancer, 8*(7), 512-522

D'Amours, D., Desnoyers, S., D'Silva, I., & Poirier, G. G. (1999). Poly(ADP-ribosyl)ation reactions in the regulation of nuclear functions. *Biochem J, 342 (Pt 2)*, 249-268

Dimri, G. P., Lee, X., Basile, G., Acosta, M., Scott, G., Roskelley, C., Medrano, E. E., Linskens, M., Rubelj, I., Pereira-Smith, O., & et al. (1995). A biomarker that identifies senescent human cells in culture and in aging skin in vivo. *Proc Natl Acad Sci U S A, 92*(20), 9363-9367

Dingemans, K. P., Teeling, P., Lagendijk, J. H., & Becker, A. E. (2000). Extracellular matrix of the human aortic media: an ultrastructural histochemical and immunohistochemical study of the adult aortic media. *Anat Rec, 258*(1), 1-14

Du, J., Zhou, Y., Su, X., Yu, J. J., Khan, S., Jiang, H., Kim, J., Woo, J., Kim, J. H., Choi, B. H., He, B., Chen, W., Zhang, S., Cerione, R. A., Auwerx, J., Hao, Q., & Lin, H. (2011). Sirt5 is a NAD-dependent protein lysine demalonylase and desuccinylase. *Science, 334*(6057), 806-809

Durnin, L., Hwang, S. J., Ward, S. M., Sanders, K. M., & Mutafova-Yambolieva, V. N. (2012). Adenosine 5-diphosphate-ribose is a neural regulator in primate and murine large intestine along with beta-NAD(+). *J Physiol, 590*(8), 1921-1941

Durnin, L., Sanders, K. M., & Mutafova-Yambolieva, V. N. (2013). Differential release of beta-NAD(+) and ATP upon activation of enteric motor neurons in primate and murine colons. *Neurogastroenterol Motil, 25*(3), e194-204

Eagleton, M. J. (2016). Arterial complications of vascular Ehlers-Danlos syndrome. *J Vasc Surg, 64*(6), 1869-1880

Edwards, W. D., Leaf, D. S., & Edwards, J. E. (1978). Dissecting aortic aneurysm associated with congenital bicuspid aortic valve. *Circulation, 57*(5), 1022-1025

Escargueil, A. E., Soares, D. G., Salvador, M., Larsen, A. K., & Henriques, J. A. (2008). What histone code for DNA repair? *Mutat Res, 658*(3), 259-270

Ford, E., Voit, R., Liszt, G., Magin, C., Grummt, I., & Guarente, L. (2006). Mammalian Sir2 homolog SIRT7 is an activator of RNA polymerase I transcription. *Genes Dev, 20*(9), 1075-1080

Frederick, D. W., Loro, E., Liu, L., Davila, A., Jr., Chellappa, K., Silverman, I. M., Quinn, W. J., 3rd, Gosai, S. J., Tichy, E. D., Davis, J. G., Mourkioti, F., Gregory, B. D., Dellinger, R. W., Redpath, P., Migaud, M. E., Nakamaru-Ogiso, E., Rabinowitz, J. D., Khurana, T. S., & Baur, J. A. (2016). Loss of NAD Homeostasis Leads to Progressive and Reversible Degeneration of Skeletal Muscle. *Cell Metab, 24*(2), 269-282

Friebe, D., Neef, M., Kratzsch, J., Erbs, S., Dittrich, K., Garten, A., Petzold-Quinque, S., Bluher, S., Reinehr, T., Stumvoll, M., Bluher, M., Kiess, W., & Korner, A. (2011). Leucocytes are a major source of circulating nicotinamide phosphoribosyltransferase (NAMPT)/pre-B cell colony (PBEF)/visfatin linking obesity and inflammation in humans. *Diabetologia, 54*(5), 1200-1211

Frye, R. A. (2000). Phylogenetic classification of prokaryotic and eukaryotic Sir2-like proteins. *Biochem Biophys Res Commun, 273*(2), 793-798

Fukuhara, A., Matsuda, M., Nishizawa, M., Segawa, K., Tanaka, M., Kishimoto, K., Matsuki, Y., Murakami, M., Ichisaka, T., Murakami, H., Watanabe, E., Takagi, T., Akiyoshi, M., Ohtsubo, T., Kihara, S., Yamashita, S., Makishima, M., Funahashi, T., Yamanaka, S., Hiramatsu, R., Matsuzawa, Y., & Shimomura, I. (2005). Visfatin: a protein secreted by visceral fat that mimics the effects of insulin. *Science, 307*(5708), 426-430

Fukuhara, A., Matsuda, M., Nishizawa, M., Segawa, K., Tanaka, M., Kishimoto, K., Matsuki, Y., Murakami, M., Ichisaka, T., Murakami, H., Watanabe, E., Takagi, T., Akiyoshi, M., Ohtsubo, T., Kihara, S., Yamashita, S., Makishima, M., Funahashi, T., Yamanaka, S., Hiramatsu, R., Matsuzawa, Y., & Shimomura, I. (2007). Retraction. *Science, 318*(5850), 565

Fulco, M., Cen, Y., Zhao, P., Hoffman, E. P., McBurney, M. W., Sauve, A. A., & Sartorelli, V. (2008). Glucose restriction inhibits skeletal myoblast differentiation by activating SIRT1 through AMPK-mediated regulation of Nampt. *Dev Cell, 14*(5), 661-673

Galis, Z. S., Sukhova, G. K., Lark, M. W., & Libby, P. (1994). Increased expression of matrix metalloproteinases and matrix degrading activity in vulnerable regions of human atherosclerotic plaques. *J Clin Invest, 94*(6), 2493-2503

Gallego, D., Mane, N., Gil, V., Martinez-Cutillas, M., & Jimenez, M. (2016). Mechanisms responsible for neuromuscular relaxation in the gastrointestinal tract. *Rev Esp Enferm Dig, 108*(11), 721-731

Garavaglia, S., Bruzzone, S., Cassani, C., Canella, L., Allegrone, G., Sturla, L., Mannino, E., Millo, E., De Flora, A., & Rizzi, M. (2012). The high-resolution crystal structure of periplasmic Haemophilus influenzae NAD nucleotidase reveals a novel enzymatic function of human CD73 related to NAD metabolism. *Biochem J, 441*(1), 131-141

Garten, A., Petzold, S., Barnikol-Oettler, A., Korner, A., Thasler, W. E., Kratzsch, J., Kiess, W., & Gebhardt, R. (2010). Nicotinamide phosphoribosyltransferase (NAMPT/PBEF/visfatin) is constitutively released from human hepatocytes. *Biochem Biophys Res Commun, 391*(1), 376-381

Giannandrea, M., & Parks, W. C. (2014). Diverse functions of matrix metalloproteinases during fibrosis. *Dis Model Mech, 7*(2), 193-203

Ginsberg, H. N., & Reyes-Soffer, G. (2013). Niacin: a long history, but a questionable future. *Curr Opin Lipidol, 24*(6), 475-479

Gittenberger-de Groot, A. C., DeRuiter, M. C., Bergwerff, M., & Poelmann, R. E. (1999). Smooth muscle cell origin and its relation to heterogeneity in development and disease. *Arterioscler Thromb Vasc Biol, 19*(7), 1589-1594

Gomes, A. P., Price, N. L., Ling, A. J., Moslehi, J. J., Montgomery, M. K., Rajman, L., White, J. P., Teodoro, J. S., Wrann, C. D., Hubbard, B. P., Mercken, E. M., Palmeira, C. M., de Cabo, R., Rolo, A. P., Turner, N., Bell, E. L., & Sinclair, D. A. (2013). Declining NAD(+) induces a pseudohypoxic state disrupting nuclear-mitochondrial communication during aging. *Cell, 155*(7), 1624-1638

Grozio, A., Sociali, G., Sturla, L., Caffa, I., Soncini, D., Salis, A., Raffaelli, N., De Flora, A., Nencioni, A., & Bruzzone, S. (2013). CD73 protein as a source of extracellular precursors for sustained NAD+ biosynthesis in FK866-treated tumor cells. *J Biol Chem, 288*(36), 25938-25949

Haigis, M. C., Mostoslavsky, R., Haigis, K. M., Fahie, K., Christodoulou, D. C., Murphy, A. J., Valenzuela, D. M., Yancopoulos, G. D., Karow, M., Blander, G., Wolberger, C., Prolla, T. A., Weindruch, R., Alt, F. W., & Guarente, L. (2006). SIRT4 inhibits glutamate dehydrogenase and opposes the effects of calorie restriction in pancreatic beta cells. *Cell, 126*(5), 941-954

Haince, J. F., Kozlov, S., Dawson, V. L., Dawson, T. M., Hendzel, M. J., Lavin, M. F., & Poirier, G. G. (2007). Ataxia telangiectasia mutated (ATM) signaling network is modulated by a novel poly(ADP-ribose)-dependent pathway in the early response to DNA-damaging agents. *J Biol Chem, 282*(22), 16441-16453

Halushka, M. K., Angelini, A., Bartoloni, G., Basso, C., Batoroeva, L., Bruneval, P., Buja, L. M., Butany, J., d'Amati, G., Fallon, J. T., Gallagher, P. J., Gittenberger-de Groot, A. C., Gouveia, R. H., Kholova, I., Kelly, K. L., Leone, O., Litovsky, S. H., Maleszewski, J. J., Miller, D. V., Mitchell, R. N., Preston, S. D., Pucci, A., Radio, S. J., Rodriguez, E. R., Sheppard, M. N., Stone, J. R., Suvarna, S. K., Tan, C. D., Thiene, G., Veinot, J. P., & van der Wal, A. C. (2016). Consensus statement on surgical pathology of the aorta from the Society for Cardiovascular Pathology and the Association For European Cardiovascular Pathology: II. Noninflammatory degenerative diseases - nomenclature and diagnostic criteria. *Cardiovasc Pathol, 25*(3), 247-257

Hara, N., Yamada, K., Shibata, T., Osago, H., & Tsuchiya, M. (2011). Nicotinamide phosphoribosyltransferase/visfatin does not catalyze nicotinamide mononucleotide formation in blood plasma. *PLOS ONE, 6*(8), e22781

Harvey, A., Montezano, A. C., Lopes, R. A., Rios, F., & Touyz, R. M. (2016). Vascular Fibrosis in Aging and Hypertension: Molecular Mechanisms and Clinical Implications. *Can J Cardiol, 32*(5), 659-668

Hassa, P. O., & Hottiger, M. O. (2008). The diverse biological roles of mammalian PARPS, a small but powerful family of poly-ADP-ribose polymerases. *Front Biosci, 13*, 3046-3082

Hayflick, L., & Moorhead, P. S. (1961). The serial cultivation of human diploid cell strains. *Exp Cell Res, 25*, 585-621

Herbert, K. E., Mistry, Y., Hastings, R., Poolman, T., Niklason, L., & Williams, B. (2008). Angiotensin II-mediated oxidative DNA damage accelerates cellular senescence in cultured human vascular smooth muscle cells via telomere-dependent and independent pathways. *Circ Res, 102*(2), 201-208

Herceg, Z., & Wang, Z. Q. (2001). Functions of poly(ADP-ribose) polymerase (PARP) in DNA repair, genomic integrity and cell death. *Mutat Res, 477*(1-2), 97-110

Ho, C., van der Veer, E., Akawi, O., & Pickering, J. G. (2009). SIRT1 markedly extends replicative lifespan if the NAD+ salvage pathway is enhanced. *FEBS Lett, 583*(18), 3081-3085

Hocking, A. M., Shinomura, T., & McQuillan, D. J. (1998). Leucine-rich repeat glycoproteins of the extracellular matrix. *Matrix Biol, 17*(1), 1-19

Hoenicke, L., & Zender, L. (2012). Immune surveillance of senescent cells--biological significance in cancer- and non-cancer pathologies. *Carcinogenesis, 33*(6), 1123-1126

Homme, J. L., Aubry, M. C., Edwards, W. D., Bagniewski, S. M., Shane Pankratz, V., Kral, C. A., & Tazelaar, H. D. (2006). Surgical pathology of the ascending aorta: a clinicopathologic study of 513 cases. *Am J Surg Pathol, 30*(9), 1159-1168

Hong, S. B., Huang, Y., Moreno-Vinasco, L., Sammani, S., Moitra, J., Barnard, J. W., Ma, S. F., Mirzapoiazova, T., Evenoski, C., Reeves, R. R., Chiang, E. T., Lang, G. D., Husain, A. N., Dudek, S. M., Jacobson, J. R., Ye, S. Q., Lussier, Y. A., & Garcia, J. G. (2008). Essential role of pre-B-cell colony enhancing factor in ventilator-induced lung injury. *Am J Respir Crit Care Med, 178*(6), 605-617

Hottiger, M. O. (2015). SnapShot: ADP-Ribosylation Signaling. *Mol Cell, 58*(6), 1134-1134 e1131

Hottiger, M. O., Hassa, P. O., Luscher, B., Schuler, H., & Koch-Nolte, F. (2010). Toward a unified nomenclature for mammalian ADP-ribosyltransferases. *Trends Biochem Sci, 35*(4), 208-219

Houtkooper, R. H., Canto, C., Wanders, R. J., & Auwerx, J. (2010). The secret life of NAD+: an old metabolite controlling new metabolic signaling pathways. *Endocr Rev, 31*(2), 194-223

Hsu, C. P., Oka, S., Shao, D., Hariharan, N., & Sadoshima, J. (2009). Nicotinamide phosphoribosyltransferase regulates cell survival through NAD+ synthesis in cardiac myocytes. *Circ Res, 105*(5), 481-491

Hu, Y., Wang, H., Wang, Q., & Deng, H. (2014). Overexpression of CD38 decreases cellular NAD levels and alters the expression of proteins involved in energy metabolism and antioxidant defense. *J Proteome Res, 13*(2), 786-795

Huang, J. Y., Hirschey, M. D., Shimazu, T., Ho, L., & Verdin, E. (2010). Mitochondrial sirtuins. *Biochim Biophys Acta, 1804*(8), 1645-1651

Huang, P. H., Lin, C. P., Wang, C. H., Chiang, C. H., Tsai, H. Y., Chen, J. S., Lin, F. Y., Leu, H. B., Wu, T. C., Chen, J. W., & Lin, S. J. (2012). Niacin improves ischemia-induced neovascularization in diabetic mice by enhancement of endothelial progenitor cell functions independent of changes in plasma lipids. *Angiogenesis, 15*(3), 377-389

Huang, R., Merrilees, M. J., Braun, K., Beaumont, B., Lemire, J., Clowes, A. W., Hinek, A., & Wight, T. N. (2006). Inhibition of versican synthesis by antisense alters smooth muscle cell phenotype and induces elastic fiber formation in vitro and in neointima after vessel injury. *Circ Res, 98*(3), 370-377

Humphrey, J. D., Schwartz, M. A., Tellides, G., & Milewicz, D. M. (2015). Role of mechanotransduction in vascular biology: focus on thoracic aortic aneurysms and dissections. *Circ Res, 116*(8), 1448-1461

Hungerford, J. E., & Little, C. D. (1999). Developmental biology of the vascular smooth muscle cell: building a multilayered vessel wall. *J Vasc Res, 36*(1), 2-27

Hungerford, J. E., Owens, G. K., Argraves, W. S., & Little, C. D. (1996). Development of the aortic vessel wall as defined by vascular smooth muscle and extracellular matrix markers. *Dev Biol, 178*(2), 375-392

Hwang, S. J., Durnin, L., Dwyer, L., Rhee, P. L., Ward, S. M., Koh, S. D., Sanders, K. M., & Mutafova-Yambolieva, V. N. (2011). beta-nicotinamide adenine dinucleotide is an enteric inhibitory neurotransmitter in human and nonhuman primate colons. *Gastroenterology, 140*(2), 608-617 e606

Jain, R. K. (2003). Molecular regulation of vessel maturation. *Nat Med, 9*(6), 685-693

Jia, S. H., Li, Y., Parodo, J., Kapus, A., Fan, L., Rotstein, O. D., & Marshall, J. C. (2004). Pre-B cell colony-enhancing factor inhibits neutrophil apoptosis in experimental inflammation and clinical sepsis. *J Clin Invest, 113*(9), 1318-1327

Jiang, X., Rowitch, D. H., Soriano, P., McMahon, A. P., & Sucov, H. M. (2000). Fate of the mammalian cardiac neural crest. *Development, 127*(8), 1607-1616

Jing, Z., Xing, J., Chen, X., Stetler, R. A., Weng, Z., Gan, Y., Zhang, F., Gao, Y., Chen, J., Leak, R. K., & Cao, G. (2014). Neuronal NAMPT is released after cerebral ischemia and protects against white matter injury. *J Cereb Blood Flow Metab, 34*(10), 1613-1621

Jun, J. I., & Lau, L. F. (2010). The matricellular protein CCN1 induces fibroblast senescence and restricts fibrosis in cutaneous wound healing. *Nat Cell Biol, 12*(7), 676-685

Kaplon, R. E., Gano, L. B., & Seals, D. R. (2014). Vascular endothelial function and oxidative stress are related to dietary niacin intake among healthy middle-aged and older adults. *J Appl Physiol (1985), 116*(2), 156-163

Karimi, A., & Milewicz, D. M. (2016). Structure of the Elastin-Contractile Units in the Thoracic Aorta and How Genes That Cause Thoracic Aortic Aneurysms and Dissections Disrupt This Structure. *Can J Cardiol, 32*(1), 26-34

Kelleher, C. M., McLean, S. E., & Mecham, R. P. (2004). Vascular extracellular matrix and aortic development. *Curr Top Dev Biol, 62*, 153-188

Khodyreva, S. N., Prasad, R., Ilina, E. S., Sukhanova, M. V., Kutuzov, M. M., Liu, Y., Hou, E. W., Wilson, S. H., & Lavrik, O. I. (2010). Apurinic/apyrimidinic (AP) site

recognition by the 5'-dRP/AP lyase in poly(ADP-ribose) polymerase-1 (PARP-1). *Proc Natl Acad Sci U S A, 107*(51), 22090-22095

Kim, K. M., Cambria, R. P., Isselbacher, E. M., Baker, J. N., LaMuraglia, G. M., Stone, J. R., & MacGillivray, T. E. (2014). Contemporary surgical approaches and outcomes in adults with Kommerell diverticulum. *Ann Thorac Surg, 98*(4), 1347-1354

Kiran, S., Chatterjee, N., Singh, S., Kaul, S. C., Wadhwa, R., & Ramakrishna, G. (2013). Intracellular distribution of human SIRT7 and mapping of the nuclear/nucleolar localization signal. *FEBS J, 280*(14), 3451-3466

Kitani, T., Okuno, S., & Fujisawa, H. (2003). Growth phase-dependent changes in the subcellular localization of pre-B-cell colony-enhancing factor. *FEBS Lett, 544*(1-3), 74-78

Koltai, E., Szabo, Z., Atalay, M., Boldogh, I., Naito, H., Goto, S., Nyakas, C., & Radak, Z. (2010). Exercise alters SIRT1, SIRT6, NAD and NAMPT levels in skeletal muscle of aged rats. *Mech Ageing Dev, 131*(1), 21-28

Korner, A., Garten, A., Bluher, M., Tauscher, R., Kratzsch, J., & Kiess, W. (2007). Molecular characteristics of serum visfatin and differential detection by immunoassays. *J Clin Endocrinol Metab, 92*(12), 4783-4791

Kover, K., Tong, P. Y., Watkins, D., Clements, M., Stehno-Bittel, L., Novikova, L., Bittel, D., Kibiryeva, N., Stuhlsatz, J., Yan, Y., Ye, S. Q., & Moore, W. V. (2013). Expression and regulation of nampt in human islets. *PLOS ONE, 8*(3), e58767

Kraus, D., Yang, Q., Kong, D., Banks, A. S., Zhang, L., Rodgers, J. T., Pirinen, E., Pulinilkunnil, T. C., Gong, F., Wang, Y. C., Cen, Y., Sauve, A. A., Asara, J. M., Peroni, O. D., Monia, B. P., Bhanot, S., Alhonen, L., Puigserver, P., & Kahn, B. B. (2014). Nicotinamide N-methyltransferase knockdown protects against diet-induced obesity. *Nature, 508*(7495), 258-262

Kraus, W. L. (2015). PARPs and ADP-Ribosylation: 50 Years ... and Counting. *Mol Cell, 58*(6), 902-910

Krizhanovsky, V., Yon, M., Dickins, R. A., Hearn, S., Simon, J., Miething, C., Yee, H., Zender, L., & Lowe, S. W. (2008). Senescence of activated stellate cells limits liver fibrosis. *Cell, 134*(4), 657-667

Kuzminov, A. (2001). Single-strand interruptions in replicating chromosomes cause double-strand breaks. *Proc Natl Acad Sci U S A, 98*(15), 8241-8246

Lavigne, P. M., & Karas, R. H. (2013). The current state of niacin in cardiovascular disease prevention: a systematic review and meta-regression. *J Am Coll Cardiol, 61*(4), 440-446

Lee, B. Y., Han, J. A., Im, J. S., Morrone, A., Johung, K., Goodwin, E. C., Kleijer, W. J., DiMaio, D., & Hwang, E. S. (2006). Senescence-associated beta-galactosidase is lysosomal beta-galactosidase. *Aging Cell, 5*(2), 187-195

Lee, M. S., Yaar, M., Eller, M. S., Runger, T. M., Gao, Y., & Gilchrest, B. A. (2009). Telomeric DNA induces p53-dependent reactive oxygen species and protects against oxidative damage. *J Dermatol Sci, 56*(3), 154-162

Li, S., Wang, C., Li, K., Li, L., Tian, M., Xie, J., Yang, M., Jia, Y., He, J., Gao, L., Boden, G., Liu, H., & Yang, G. (2016). NAMPT knockdown attenuates atherosclerosis and promotes reverse cholesterol transport in ApoE KO mice with high-fat-induced insulin resistance. *Sci Rep, 6*, 26746

Lindahl, T. (1993). Instability and decay of the primary structure of DNA. *Nature, 362*(6422), 709-715

Liszt, G., Ford, E., Kurtev, M., & Guarente, L. (2005). Mouse Sir2 homolog SIRT6 is a nuclear ADP-ribosyltransferase. *J Biol Chem, 280*(22), 21313-21320

Lloyd-Jones, D. R. J. Adams, T. M. Brown, M. Carnethon, S. Dai, G. De Simone, T. B. Ferguson, E. Ford, K. Furie, C. Gillespie, A. Go, K. Greenlund, N. Haase, S. Hailpern, P. M. Ho, V. Howard, B. Kissela, S. Kittner, D. Lackland, L. Lisabeth, A. Marelli, M. M. McDermott, J. Meigs, D. Mozaffarian, M. Mussolino, G. Nichol, V. L. Roger, W. Rosamond, R. Sacco, P. Sorlie, V. L. Roger, T. Thom, S. Wasserthiel-Smoller, N. D. Wong, J. Wylie-Rosett, C. American Heart Association Statistics and S. Stroke Statistics (2010). "Heart disease and stroke statistics--2010 update: a report from the American Heart Association." Circulation **121**(7): e46-e215

Loeys, B. L., & Dietz, H. C. (1993). Loeys-Dietz Syndrome. In R. A. Pagon, M. P. Adam, H. H. Ardinger, S. E. Wallace, A. Amemiya, L. J. H. Bean, T. D. Bird, N.

Ledbetter, H. C. Mefford, R. J. H. Smith, & K. Stephens (Eds.), *GeneReviews(R)*. Seattle (WA).

Loeys, B. L., Schwarze, U., Holm, T., Callewaert, B. L., Thomas, G. H., Pannu, H., De Backer, J. F., Oswald, G. L., Symoens, S., Manouvrier, S., Roberts, A. E., Faravelli, F., Greco, M. A., Pyeritz, R. E., Milewicz, D. M., Coucke, P. J., Cameron, D. E., Braverman, A. C., Byers, P. H., De Paepe, A. M., & Dietz, H. C. (2006). Aneurysm syndromes caused by mutations in the TGF-beta receptor. *N Engl J Med, 355*(8), 788-798

Lonskaya, I., Potaman, V. N., Shlyakhtenko, L. S., Oussatcheva, E. A., Lyubchenko, Y. L., & Soldatenkov, V. A. (2005). Regulation of poly(ADP-ribose) polymerase-1 by DNA structure-specific binding. *J Biol Chem, 280*(17), 17076-17083

Luo, X., & Kraus, W. L. (2012). On PAR with PARP: cellular stress signaling through poly(ADP-ribose) and PARP-1. *Genes Dev, 26*(5), 417-432

Majesky, M. W. (2007). Developmental basis of vascular smooth muscle diversity. *Arterioscler Thromb Vasc Biol, 27*(6), 1248-1258

Malavasi, F., Deaglio, S., Funaro, A., Ferrero, E., Horenstein, A. L., Ortolan, E., Vaisitti, T., & Aydin, S. (2008). Evolution and function of the ADP ribosyl cyclase/CD38 gene family in physiology and pathology. *Physiol Rev, 88*(3), 841-886

Martin, P. R., Shea, R. J., & Mulks, M. H. (2001). Identification of a plasmid-encoded gene from Haemophilus ducreyi which confers NAD independence. *J Bacteriol, 183*(4), 1168-1174

Massudi, H., Grant, R., Braidy, N., Guest, J., Farnsworth, B., & Guillemin, G. J. (2012). Age-associated changes in oxidative stress and NAD+ metabolism in human tissue. *PLOS ONE, 7*(7), e42357

Matthews, C., Gorenne, I., Scott, S., Figg, N., Kirkpatrick, P., Ritchie, A., Goddard, M., & Bennett, M. (2006). Vascular smooth muscle cells undergo telomere-based senescence in human atherosclerosis: effects of telomerase and oxidative stress. *Circ Res, 99*(2), 156-164

McKusick, V. A. (1972). Association of congenital bicuspid aortic valve and erdheim's cystic medial necrosis. *Lancet, 1*(7758), 1026-1027

Meszaros, I., Morocz, J., Szlavi, J., Schmidt, J., Tornoci, L., Nagy, L., & Szep, L. (2000). Epidemiology and clinicopathology of aortic dissection. *Chest, 117*(5), 1271-1278

Milewicz, D. M., & Regalado, E. (1993). Heritable Thoracic Aortic Disease Overview. In R. A. Pagon, M. P. Adam, H. H. Ardinger, S. E. Wallace, A. Amemiya, L. J. H. Bean, T. D. Bird, N. Ledbetter, H. C. Mefford, R. J. H. Smith, & K. Stephens (Eds.), *GeneReviews(R)*. Seattle (WA).

Minamino, T., Miyauchi, H., Yoshida, T., Ishida, Y., Yoshida, H., & Komuro, I. (2002). Endothelial cell senescence in human atherosclerosis: role of telomere in endothelial dysfunction. *Circulation, 105*(13), 1541-1544

Minamino, T., Yoshida, T., Tateno, K., Miyauchi, H., Zou, Y., Toko, H., & Komuro, I. (2003). Ras induces vascular smooth muscle cell senescence and inflammation in human atherosclerosis. *Circulation, 108*(18), 2264-2269

Mostoslavsky, R., Chua, K. F., Lombard, D. B., Pang, W. W., Fischer, M. R., Gellon, L., Liu, P., Mostoslavsky, G., Franco, S., Murphy, M. M., Mills, K. D., Patel, P., Hsu, J. T., Hong, A. L., Ford, E., Cheng, H. L., Kennedy, C., Nunez, N., Bronson, R., Frendewey, D., Auerbach, W., Valenzuela, D., Karow, M., Hottiger, M. O., Hursting, S., Barrett, J. C., Guarente, L., Mulligan, R., Demple, B., Yancopoulos, G. D., & Alt, F. W. (2006). Genomic instability and aging-like phenotype in the absence of mammalian SIRT6. *Cell, 124*(2), 315-329

Mouchiroud, L., Houtkooper, R. H., Moullan, N., Katsyuba, E., Ryu, D., Canto, C., Mottis, A., Jo, Y. S., Viswanathan, M., Schoonjans, K., Guarente, L., & Auwerx, J. (2013). The NAD(+)/Sirtuin Pathway Modulates Longevity through Activation of Mitochondrial UPR and FOXO Signaling. *Cell, 154*(2), 430-441

Munoz-Espin, D., Canamero, M., Maraver, A., Gomez-Lopez, G., Contreras, J., Murillo-Cuesta, S., Rodriguez-Baeza, A., Varela-Nieto, I., Ruberte, J., Collado, M., & Serrano, M. (2013). Programmed cell senescence during mammalian embryonic development. *Cell, 155*(5), 1104-1118

Munoz-Espin, D., & Serrano, M. (2014). Cellular senescence: from physiology to pathology. *Nat Rev Mol Cell Biol, 15*(7), 482-496

Mussa, F. F., Horton, J. D., Moridzadeh, R., Nicholson, J., Trimarchi, S., & Eagle, K. A. (2016). Acute Aortic Dissection and Intramural Hematoma: A Systematic Review. *JAMA, 316*(7), 754-763

Mutafova-Yambolieva, V. N., Hwang, S. J., Hao, X., Chen, H., Zhu, M. X., Wood, J. D., Ward, S. M., & Sanders, K. M. (2007). Beta-nicotinamide adenine dinucleotide is an inhibitory neurotransmitter in visceral smooth muscle. *Proc Natl Acad Sci U S A, 104*(41), 16359-16364

Nakahata, Y., Sahar, S., Astarita, G., Kaluzova, M., & Sassone-Corsi, P. (2009). Circadian control of the NAD+ salvage pathway by CLOCK-SIRT1. *Science, 324*(5927), 654-657

Nassour, J., Martien, S., Martin, N., Deruy, E., Tomellini, E., Malaquin, N., Bouali, F., Sabatier, L., Wernert, N., Pinte, S., Gilson, E., Pourtier, A., Pluquet, O., & Abbadie, C. (2016). Defective DNA single-strand break repair is responsible for senescence and neoplastic escape of epithelial cells. *Nat Commun, 7*, 10399

Nelson, G., Wordsworth, J., Wang, C., Jurk, D., Lawless, C., Martin-Ruiz, C., & von Zglinicki, T. (2012). A senescent cell bystander effect: senescence-induced senescence. *Aging Cell, 11*(2), 345-349

Nikiforov, A., Dolle, C., Niere, M., & Ziegler, M. (2011). Pathways and subcellular compartmentation of NAD biosynthesis in human cells: from entry of extracellular precursors to mitochondrial NAD generation. *J Biol Chem, 286*(24), 21767-21778

Nishimura, R. A., Otto, C. M., Bonow, R. O., Carabello, B. A., Erwin, J. P., 3rd, Guyton, R. A., O'Gara, P. T., Ruiz, C. E., Skubas, N. J., Sorajja, P., Sundt, T. M., 3rd, Thomas, J. D., Anderson, J. L., Halperin, J. L., Albert, N. M., Bozkurt, B., Brindis, R. G., Creager, M. A., Curtis, L. H., DeMets, D., Guyton, R. A., Hochman, J. S., Kovacs, R. J., Ohman, E. M., Pressler, S. J., Sellke, F. W., Shen, W. K., Stevenson, W. G., Yancy, C. W., American College of, C., American College of Cardiology/American Heart, A., & American Heart, A. (2014). 2014 AHA/ACC guideline for the management of patients with valvular heart disease: a report of the American College of Cardiology/American Heart Association Task Force on Practice Guidelines. *J Thorac Cardiovasc Surg, 148*(1), e1-e132

Nistri, S., Sorbo, M. D., Marin, M., Palisi, M., Scognamiglio, R., & Thiene, G. (1999). Aortic root dilatation in young men with normally functioning bicuspid aortic valves. *Heart, 82*(1), 19-22

Owens, G. K. (1995). Regulation of differentiation of vascular smooth muscle cells. *Physiol Rev, 75*(3), 487-517

Pepin, M. G., Murray, M. L., & Byers, P. H. (1993). Vascular Ehlers-Danlos Syndrome. In R. A. Pagon, M. P. Adam, H. H. Ardinger, S. E. Wallace, A. Amemiya, L. J. H. Bean, T. D. Bird, N. Ledbetter, H. C. Mefford, R. J. H. Smith, & K. Stephens (Eds.), *GeneReviews(R)*. Seattle (WA).

Pillai, V. B., Sundaresan, N. R., Kim, G., Samant, S., Moreno-Vinasco, L., Garcia, J. G., & Gupta, M. P. (2013). Nampt secreted from cardiomyocytes promotes development of cardiac hypertrophy and adverse ventricular remodeling. *Am J Physiol Heart Circ Physiol, 304*(3), H415-426

Pirinen, E., Canto, C., Jo, Y. S., Morato, L., Zhang, H., Menzies, K. J., Williams, E. G., Mouchiroud, L., Moullan, N., Hagberg, C., Li, W., Timmers, S., Imhof, R., Verbeek, J., Pujol, A., van Loon, B., Viscomi, C., Zeviani, M., Schrauwen, P., Sauve, A. A., Schoonjans, K., & Auwerx, J. (2014). Pharmacological Inhibition of poly(ADP-ribose) polymerases improves fitness and mitochondrial function in skeletal muscle. *Cell Metab, 19*(6), 1034-1041

Pugh, T. D., Conklin, M. W., Evans, T. D., Polewski, M. A., Barbian, H. J., Pass, R., Anderson, B. D., Colman, R. J., Eliceiri, K. W., Keely, P. J., Weindruch, R., Beasley, T. M., & Anderson, R. M. (2013). A shift in energy metabolism anticipates the onset of sarcopenia in rhesus monkeys. *Aging Cell, 12*(4), 672-681

Qiu, X., Brown, K., Hirschey, M. D., Verdin, E., & Chen, D. (2010). Calorie restriction reduces oxidative stress by SIRT3-mediated SOD2 activation. *Cell Metab, 12*(6), 662-667

Rai, P., Onder, T. T., Young, J. J., McFaline, J. L., Pang, B., Dedon, P. C., & Weinberg, R. A. (2009). Continuous elimination of oxidized nucleotides is necessary to prevent rapid onset of cellular senescence. *Proc Natl Acad Sci U S A, 106*(1), 169-174

Ramanath, V. S., Oh, J. K., Sundt, T. M., 3rd, & Eagle, K. A. (2009). Acute aortic syndromes and thoracic aortic aneurysm. *Mayo Clin Proc, 84*(5), 465-481

Ramsey, K. M., Mills, K. F., Satoh, A., & Imai, S. (2008). Age-associated loss of Sirt1-mediated enhancement of glucose-stimulated insulin secretion in beta cell-specific Sirt1-overexpressing (BESTO) mice. *Aging Cell, 7*(1), 78-88

Ramsey, K. M., Yoshino, J., Brace, C. S., Abrassart, D., Kobayashi, Y., Marcheva, B., Hong, H. K., Chong, J. L., Buhr, E. D., Lee, C., Takahashi, J. S., Imai, S., & Bass, J. (2009). Circadian clock feedback cycle through NAMPT-mediated NAD+ biosynthesis. *Science, 324*(5927), 651-654

Reinboth, B., Hanssen, E., Cleary, E. G., & Gibson, M. A. (2002). Molecular interactions of biglycan and decorin with elastic fiber components: biglycan forms a ternary complex with tropoelastin and microfibril-associated glycoprotein 1. *J Biol Chem, 277*(6), 3950-3957

Revollo, J. R., Grimm, A. A., & Imai, S. (2004). The NAD biosynthesis pathway mediated by nicotinamide phosphoribosyltransferase regulates Sir2 activity in mammalian cells. *J Biol Chem, 279*(49), 50754-50763

Revollo, J. R., Korner, A., Mills, K. F., Satoh, A., Wang, T., Garten, A., Dasgupta, B., Sasaki, Y., Wolberger, C., Townsend, R. R., Milbrandt, J., Kiess, W., & Imai, S. (2007). Nampt/PBEF/Visfatin regulates insulin secretion in beta cells as a systemic NAD biosynthetic enzyme. *Cell Metab, 6*(5), 363-375

Rodgers, J. T., Lerin, C., Gerhart-Hines, Z., & Puigserver, P. (2008). Metabolic adaptations through the PGC-1 alpha and SIRT1 pathways. *FEBS Lett, 582*(1), 46-53

Rodgers, J. T., Lerin, C., Haas, W., Gygi, S. P., Spiegelman, B. M., & Puigserver, P. (2005). Nutrient control of glucose homeostasis through a complex of PGC-1alpha and SIRT1. *Nature, 434*(7029), 113-118

Rongvaux, A., Galli, M., Denanglaire, S., Van Gool, F., Dreze, P. L., Szpirer, C., Bureau, F., Andris, F., & Leo, O. (2008). Nicotinamide phosphoribosyl transferase/pre-B cell colony-enhancing factor/visfatin is required for lymphocyte development and cellular resistance to genotoxic stress. *J Immunol, 181*(7), 4685-4695

Rongvaux, A., Shea, R. J., Mulks, M. H., Gigot, D., Urbain, J., Leo, O., & Andris, F. (2002). Pre-B-cell colony-enhancing factor, whose expression is up-regulated in activated lymphocytes, is a nicotinamide phosphoribosyltransferase, a cytosolic enzyme involved in NAD biosynthesis. *Eur J Immunol, 32*(11), 3225-3234

Rosenthal, E. (2005). Coarctation of the aorta from fetus to adult: curable condition or life long disease process? *Heart, 91*(11), 1495-1502

Samal, B., Sun, Y., Stearns, G., Xie, C., Suggs, S., & McNiece, I. (1994). Cloning and characterization of the cDNA encoding a novel human pre-B-cell colony-enhancing factor. *Mol Cell Biol, 14*(2), 1431-1437

Sauve, A. A. (2008). NAD+ and vitamin B3: from metabolism to therapies. *J Pharmacol Exp Ther, 324*(3), 883-893

Schuster, S., Penke, M., Gorski, T., Petzold-Quinque, S., Damm, G., Gebhardt, R., Kiess, W., & Garten, A. (2014). Resveratrol differentially regulates NAMPT and SIRT1 in Hepatocarcinoma cells and primary human hepatocytes. *PLOS ONE, 9*(3), e91045

Schwer, B., & Verdin, E. (2008). Conserved metabolic regulatory functions of sirtuins. *Cell Metab, 7*(2), 104-112

Smyth, L. M., Bobalova, J., Mendoza, M. G., Lew, C., & Mutafova-Yambolieva, V. N. (2004). Release of beta-nicotinamide adenine dinucleotide upon stimulation of postganglionic nerve terminals in blood vessels and urinary bladder. *J Biol Chem, 279*(47), 48893-48903

Smyth, L. M., Breen, L. T., & Mutafova-Yambolieva, V. N. (2006). Nicotinamide adenine dinucleotide is released from sympathetic nerve terminals via a botulinum neurotoxin A-mediated mechanism in canine mesenteric artery. *Am J Physiol Heart Circ Physiol, 290*(5), H1818-1825

Sociali, G., Raffaghello, L., Magnone, M., Zamporlini, F., Emionite, L., Sturla, L., Bianchi, G., Vigliarolo, T., Nahimana, A., Nencioni, A., Raffaelli, N., & Bruzzone, S. (2016). Antitumor effect of combined NAMPT and CD73 inhibition in an ovarian cancer model. *Oncotarget, 7*(3), 2968-2984

Soppa, J. (2010). Protein acetylation in archaea, bacteria, and eukaryotes. *Archaea, 2010*

Sousa, F. G., Matuo, R., Soares, D. G., Escargueil, A. E., Henriques, J. A., Larsen, A. K., & Saffi, J. (2012). PARPs and the DNA damage response. *Carcinogenesis, 33*(8), 1433-1440

Stein, L. R., & Imai, S. (2014). Specific ablation of Nampt in adult neural stem cells recapitulates their functional defects during aging. *EMBO J, 33*(12), 1321-1340

Stein, L. R., Wozniak, D. F., Dearborn, J. T., Kubota, S., Apte, R. S., Izumi, Y., Zorumski, C. F., & Imai, S. (2014). Expression of Nampt in hippocampal and cortical excitatory neurons is critical for cognitive function. *J Neurosci, 34*(17), 5800-5815

Storer, M., Mas, A., Robert-Moreno, A., Pecoraro, M., Ortells, M. C., Di Giacomo, V., Yosef, R., Pilpel, N., Krizhanovsky, V., Sharpe, J., & Keyes, W. M. (2013). Senescence is a developmental mechanism that contributes to embryonic growth and patterning. *Cell, 155*(5), 1119-1130

Stromsdorfer, K. L., Yamaguchi, S., Yoon, M. J., Moseley, A. C., Franczyk, M. P., Kelly, S. C., Qi, N., Imai, S., & Yoshino, J. (2016). NAMPT-Mediated NAD(+) Biosynthesis in Adipocytes Regulates Adipose Tissue Function and Multi-organ Insulin Sensitivity in Mice. *Cell Rep, 16*(7), 1851-1860

Tanaka, M., Nozaki, M., Fukuhara, A., Segawa, K., Aoki, N., Matsuda, M., Komuro, R., & Shimomura, I. (2007). Visfatin is released from 3T3-L1 adipocytes via a non-classical pathway. *Biochem Biophys Res Commun, 359*(2), 194-201

Tanno, M., Sakamoto, J., Miura, T., Shimamoto, K., & Horio, Y. (2007). Nucleocytoplasmic shuttling of the NAD+-dependent histone deacetylase SIRT1. *J Biol Chem, 282*(9), 6823-6832

Tchkonia, T., Zhu, Y., van Deursen, J., Campisi, J., & Kirkland, J. L. (2013). Cellular senescence and the senescent secretory phenotype: therapeutic opportunities. *J Clin Invest, 123*(3), 966-972

Theocharis, A. D., & Karamanos, N. K. (2002). Decreased biglycan expression and differential decorin localization in human abdominal aortic aneurysms. *Atherosclerosis, 165*(2), 221-230

Topol, E. J. and R. M. Califf (2007). Textbook of Cardiovascular Medicine. Phildelphia, Lippincott Williams & Wilkins.

Vafaie, F., Yin, H., O'Neil, C., Nong, Z., Watson, A., Arpino, J. M., Chu, M. W., Wayne Holdsworth, D., Gros, R., & Pickering, J. G. (2014). Collagenase-resistant collagen promotes mouse aging and vascular cell senescence. *Aging Cell, 13*(1), 121-130

van der Horst, A., Tertoolen, L. G., de Vries-Smits, L. M., Frye, R. A., Medema, R. H., & Burgering, B. M. (2004). FOXO4 is acetylated upon peroxide stress and

deacetylated by the longevity protein hSir2(SIRT1). *J Biol Chem, 279*(28), 28873-28879

van der Veer, E., Ho, C., O'Neil, C., Barbosa, N., Scott, R., Cregan, S. P., & Pickering, J. G. (2007). Extension of human cell lifespan by nicotinamide phosphoribosyltransferase. *J Biol Chem, 282*(15), 10841-10845

van der Veer, E., Nong, Z., O'Neil, C., Urquhart, B., Freeman, D., & Pickering, J. G. (2005). Pre-B-cell colony-enhancing factor regulates NAD+-dependent protein deacetylase activity and promotes vascular smooth muscle cell maturation. *Circ Res, 97*(1), 25-34

van Deursen, J. M. (2014). The role of senescent cells in ageing. *Nature, 509*(7501), 439-446

Van Gool, F., Galli, M., Gueydan, C., Kruys, V., Prevot, P. P., Bedalov, A., Mostoslavsky, R., Alt, F. W., De Smedt, T., & Leo, O. (2009). Intracellular NAD levels regulate tumor necrosis factor protein synthesis in a sirtuin-dependent manner. *Nat Med, 15*(2), 206-210

Vaquero, A., Scher, M. B., Lee, D. H., Sutton, A., Cheng, H. L., Alt, F. W., Serrano, L., Sternglanz, R., & Reinberg, D. (2006). SirT2 is a histone deacetylase with preference for histone H4 Lys 16 during mitosis. *Genes Dev, 20*(10), 1256-1261

Verdin, E. (2015). NAD(+) in aging, metabolism, and neurodegeneration. *Science, 350*(6265), 1208-1213

Visse, R., & Nagase, H. (2003). Matrix metalloproteinases and tissue inhibitors of metalloproteinases: structure, function, and biochemistry. *Circ Res, 92*(8), 827-839

Wagenseil, J. E., & Mecham, R. P. (2009). Vascular extracellular matrix and arterial mechanics. *Physiol Rev, 89*(3), 957-989

Waldo, K. L., Hutson, M. R., Ward, C. C., Zdanowicz, M., Stadt, H. A., Kumiski, D., Abu-Issa, R., & Kirby, M. L. (2005). Secondary heart field contributes myocardium and smooth muscle to the arterial pole of the developing heart. *Dev Biol, 281*(1), 78-90

Wang, H., & Keiser, J. A. (1998). Expression of membrane-type matrix metalloproteinase in rabbit neointimal tissue and its correlation with matrix-metalloproteinase-2 activation. *J Vasc Res, 35*(1), 45-54

Wang, M., & Shah, A. M. (2015). Age-associated pro-inflammatory remodeling and functional phenotype in the heart and large arteries. *J Mol Cell Cardiol, 83*, 101-111

Wang, M., Zhao, D., Spinetti, G., Zhang, J., Jiang, L. Q., Pintus, G., Monticone, R., & Lakatta, E. G. (2006). Matrix metalloproteinase 2 activation of transforming growth factor-beta1 (TGF-beta1) and TGF-beta1-type II receptor signaling within the aged arterial wall. *Arterioscler Thromb Vasc Biol, 26*(7), 1503-1509

Wang, P., Xu, T.-Y., Guan, Y.-F., Tian, W.-W., Viollet, B., Rui, Y.-C., Zhai, Q.-W., Su, D.-F., & Miao, C.-Y. (2011). Nicotinamide phosphoribosyltransferase protects against ischemic stroke through SIRT1-dependent adenosine monophosphate-activated kinase pathway. *Annals of neurology*

Wasteson, P., Johansson, B. R., Jukkola, T., Breuer, S., Akyurek, L. M., Partanen, J., & Lindahl, P. (2008). Developmental origin of smooth muscle cells in the descending aorta in mice. *Development, 135*(10), 1823-1832

Weigel, P. H., Hascall, V. C., & Tammi, M. (1997). Hyaluronan synthases. *J Biol Chem, 272*(22), 13997-14000

Wenstrup, R. J., Florer, J. B., Brunskill, E. W., Bell, S. M., Chervoneva, I., & Birk, D. E. (2004). Type V collagen controls the initiation of collagen fibril assembly. *J Biol Chem, 279*(51), 53331-53337

Woodhouse, B. C., Dianova, II, Parsons, J. L., & Dianov, G. L. (2008). Poly(ADP-ribose) polymerase-1 modulates DNA repair capacity and prevents formation of DNA double strand breaks. *DNA Repair (Amst), 7*(6), 932-940

Wu, B. J., Yan, L., Charlton, F., Witting, P., Barter, P. J., & Rye, K. A. (2010). Evidence that niacin inhibits acute vascular inflammation and improves endothelial dysfunction independent of changes in plasma lipids. *Arterioscler Thromb Vasc Biol, 30*(5), 968-975

Xue, L., Farrugia, G., Sarr, M. G., & Szurszewski, J. H. (1999). ATP is a mediator of the fast inhibitory junction potential in human jejunal circular smooth muscle. *Am J Physiol, 276*(6 Pt 1), G1373-1379

Yamamoto, T., Byun, J., Zhai, P., Ikeda, Y., Oka, S., & Sadoshima, J. (2014). Nicotinamide mononucleotide, an intermediate of NAD+ synthesis, protects the heart from ischemia and reperfusion. *PLOS ONE, 9*(6), e98972

Yang, H., Yang, T., Baur, J. A., Perez, E., Matsui, T., Carmona, J. J., Lamming, D. W., Souza-Pinto, N. C., Bohr, V. A., Rosenzweig, A., de Cabo, R., Sauve, A. A., & Sinclair, D. A. (2007). Nutrient-sensitive mitochondrial NAD+ levels dictate cell survival. *Cell, 130*(6), 1095-1107

Yang, S. J., Choi, J. M., Kim, L., Park, S. E., Rhee, E. J., Lee, W. Y., Oh, K. W., Park, S. W., & Park, C. Y. (2014). Nicotinamide improves glucose metabolism and affects the hepatic NAD-sirtuin pathway in a rodent model of obesity and type 2 diabetes. *J Nutr Biochem, 25*(1), 66-72

Yang, T., Chan, N. Y., & Sauve, A. A. (2007). Syntheses of nicotinamide riboside and derivatives: effective agents for increasing nicotinamide adenine dinucleotide concentrations in mammalian cells. *J Med Chem, 50*(26), 6458-6461

Yao, L. Y., Moody, C., Schonherr, E., Wight, T. N., & Sandell, L. J. (1994). Identification of the proteoglycan versican in aorta and smooth muscle cells by DNA sequence analysis, in situ hybridization and immunohistochemistry. *Matrix Biol, 14*(3), 213-225

Yelamos, J., Farres, J., Llacuna, L., Ampurdanes, C., & Martin-Caballero, J. (2011). PARP-1 and PARP-2: New players in tumour development. *Am J Cancer Res, 1*(3), 328-346

Yepuri, G., Velagapudi, S., Xiong, Y., Rajapakse, A. G., Montani, J. P., Ming, X. F., & Yang, Z. (2012). Positive crosstalk between arginase-II and S6K1 in vascular endothelial inflammation and aging. *Aging Cell, 11*(6), 1005-1016

Yin, H., & Pickering, J. G. (2016). Cellular Senescence and Vascular Disease: Novel Routes to Better Understanding and Therapy. *Can J Cardiol, 32*(5), 612-623

Yoon, M. J., Yoshida, M., Johnson, S., Takikawa, A., Usui, I., Tobe, K., Nakagawa, T., Yoshino, J., & Imai, S. (2015). SIRT1-Mediated eNAMPT Secretion from Adipose Tissue Regulates Hypothalamic NAD+ and Function in Mice. *Cell Metab, 21*(5), 706-717

Yoshino, J., Mills, K. F., Yoon, M. J., & Imai, S. (2011). Nicotinamide mononucleotide, a key NAD(+) intermediate, treats the pathophysiology of diet- and age-induced diabetes in mice. *Cell Metab, 14*(4), 528-536

Yu, S. W., Andrabi, S. A., Wang, H., Kim, N. S., Poirier, G. G., Dawson, T. M., & Dawson, V. L. (2006). Apoptosis-inducing factor mediates poly(ADP-ribose) (PAR) polymer-induced cell death. *Proc Natl Acad Sci U S A, 103*(48), 18314-18319

Yu, S. W., Wang, H., Poitras, M. F., Coombs, C., Bowers, W. J., Federoff, H. J., Poirier, G. G., Dawson, T. M., & Dawson, V. L. (2002). Mediation of poly(ADP-ribose) polymerase-1-dependent cell death by apoptosis-inducing factor. *Science, 297*(5579), 259-263

Zamporlini, F., Ruggieri, S., Mazzola, F., Amici, A., Orsomando, G., & Raffaelli, N. (2014). Novel assay for simultaneous measurement of pyridine mononucleotides synthesizing activities allows dissection of the NAD(+) biosynthetic machinery in mammalian cells. *FEBS J, 281*(22), 5104-5119

Zhang, L. Q., Van Haandel, L., Xiong, M., Huang, P., Heruth, D. P., Bi, C., Gaedigk, R., Jiang, X., Li, D. Y., Wyckoff, G., Grigoryev, D. N., Gao, L., Li, L., Wu, M., Leeder, J. S., & Ye, S. Q. (2017). Metabolic and molecular insights into an essential role of nicotinamide phosphoribosyltransferase. *Cell Death Dis, 8*(3), e2705

Zhao, B., Zhang, M., Han, X., Zhang, X. Y., Xing, Q., Dong, X., Shi, Q. J., Huang, P., Lu, Y. B., Wei, E. Q., Xia, Q., Zhang, W. P., & Tang, C. (2013). Cerebral ischemia is exacerbated by extracellular nicotinamide phosphoribosyltransferase via a non-enzymatic mechanism. *PLOS ONE, 8*(12), e85403

Zhong, L., D'Urso, A., Toiber, D., Sebastian, C., Henry, R. E., Vadysirisack, D. D., Guimaraes, A., Marinelli, B., Wikstrom, J. D., Nir, T., Clish, C. B., Vaitheesvaran, B., Iliopoulos, O., Kurland, I., Dor, Y., Weissleder, R., Shirihai, O. S., Ellisen, L. W., Espinosa, J. M., & Mostoslavsky, R. (2010). The histone deacetylase Sirt6 regulates glucose homeostasis via Hif1alpha. *Cell, 140*(2), 280-293

Zhou, C. C., Yang, X., Hua, X., Liu, J., Fan, M. B., Li, G. Q., Song, J., Xu, T. Y., Li, Z. Y., Guan, Y. F., Wang, P., & Miao, C. Y. (2016). Hepatic NAD(+) deficiency as a

therapeutic target for non-alcoholic fatty liver disease in ageing. *Br J Pharmacol, 173*(15), 2352-2368

Zhu, F., Li, Y., Zhang, J., Piao, C., Liu, T., Li, H. H., & Du, J. (2013). Senescent cardiac fibroblast is critical for cardiac fibrosis after myocardial infarction. *PLOS ONE, 8*(9), e74535

CHAPTER 2 - NICOTINAMIDE PHOSPHORIBOSYLTRANSFERASE IN SMOOTH MUSCLE CELLS MAINTAINS GENOME INTEGRITY AND RESISTS AORTIC MEDIAL DEGENERATION

2.1 Introduction

The aortic wall is subjected to unrelenting hemodynamic stress. Although structurally designed to withstand this stress, the aorta can nonetheless degenerate over time, particularly when also subjected to hypertension, atherosclerosis, or the effects of genetic mutations (Schlatmann and Becker 1977, Howard et al. 2013). When the aorta degenerates it dilates and becomes vulnerable to dissection and rupture. Vascular SMCs are critical to maintaining aortic integrity, evidenced by the development of thoracic aneurysms in individuals with mutations in SMC-specific genes (Milewicz et al. 2008). SMCs have a range of functions relevant to aortic homeostasis including contraction, synthesis of extracellular matrix (ECM), and the assembly of ECM fibers in accordance with local mechanical forces (Li et al. 2003, Humphrey et al. 2014). However, the abundance and functionality of SMCs can decline with age and chronic diseases (Schlatmann and Becker 1977, Ruiz-Torres et al. 1999, van der Veer et al. 2007, Halushka et al. 2016). Understanding the molecular pathways that can be engaged by SMCs to survive and retain their repertoire of functions in the stressed environment of the aortic wall may be critical to advancing strategies for reducing aortic catastrophes.

Nicotinamide adenine dinucleotide (NAD^+) is an essential dinucleotide that serves as a cofactor for the oxidation-reduction events of cellular nutrient metabolism. NAD^+ can also serve as a signaling nucleotide that regulates gene expression, genome integrity, and mitochondrial function. When NAD^+ participates in signaling reactions, it does so as an enzyme substrate rather than a cofactor and is thus consumed in the process. The most potent NAD^+-consuming reaction is believed to be the assembly of poly(ADP-ribose) (PAR) on histones, an event triggered by DNA strand breakage and catalyzed by the

enzyme poly(ADP-ribose) polymerase-1 (PARP1) (Dantzer et al. 2006). Other NAD^+ consuming enzymes include those of the sirtuin family, which catalyze deacetylation and ADP-ribose transfer reactions, and CD38, which generates cADPR (Nikiforov et al. 2015).

The growing recognition of the importance of NAD^+-consuming reactions has heightened interest in understanding the pathways by which NAD^+ is generated and replenished. NAD^+ can be synthesized from dietary sources but the routes to NAD^+ production are proving to be complex and tissue-specific (Canto et al. 2015). Important to maintaining the NAD^+ pool is the salvage pathway, wherein nicotinamide liberated during NAD^+-consuming reactions is recycled back to NAD^+ (van der Veer et al. 2005, Revollo et al. 2007, Nikiforov et al. 2015). Nicotinamide phosphoribosyltransferase (Nampt) is the rate-limiting enzyme for this salvage pathway, converting nicotinamide to nicotinamide mononucleotide (van der Veer et al. 2005). Development of the mouse embryo cannot proceed without Nampt (Revollo et al. 2007). As well, gene targeting strategies in mice have revealed a pattern of degenerative or aging-related tissue dysfunction when Nampt is perturbed, including in the liver, skeletal muscle, and brain (Stein and Imai 2014, Frederick et al. 2016, Zhou et al. 2016).

A role for Nampt in SMC-based vascular health is less clear but the possibility has been raised. Nampt is expressed in cultured SMCs and its content and activity decline during advanced SMC aging (van der Veer et al. 2005, van der Veer et al. 2007). As well, Nampt has been found to regulate in vitro SMC longevity and migratory behaviour (van der Veer et al. 2007, Yin et al. 2012) There are also reports that exogenous delivery of Nampt impacts SMC contractile function, although with contradictory findings (Wang et al. 2016) Nampt is expressed in peri-aortic adipose tissue (Wang et al. 2009) and altering NAD^+ metabolism through the diet has been found to suppressed age-related aortic dysfunction (de Picciotto et al. 2016). However it remains unknown whether Nampt is

needed for aortic health or if a Nampt-based NAD^+ generation system exists within the aortic media.

I have investigated the role of Nampt in the aortic media by in vivo ablation of *Nampt* in SMCs in mice. My findings reveal the existence of an intrinsic NAD^+ fueling system in the aortic media and its necessity for maintaining aortic integrity. The findings also shed new insights into DNA repair and senescence resistance cascades in the aortic media that may underlie vulnerability in NAD^+ homeostasis in thoracic aortopathy.

2.2 Methods

2.2.1 Generation of Nampt-deficient mouse models

Mouse experiments followed protocols approved by the Western University Animal Use Committee. All mice were on a C57Bl/6 background. To generate mice with a SMC-specific knockout of *Nampt*, an initial cross was undertaken between female mice harbouring loxP sites flanking exons 5 and 6 of *Nampt* (*Nampt*$^{flox/flox}$)(Rongvaux et al. 2002) and male transgenic mice expressing Cre recombinase and eGFP under the control of the SMC-specific myosin heavy chain promoter (*smMHC*-Cre/eGFP, Jackson Laboratories, Bar Harbor, ME) (Xin et al. 2002). Expression of Cre in the aorta of the latter mice was verified by whole tissue epifluorescence microscopy (Zeiss SteREO Lumar V12 Microscope, Carl Zeiss Canada Ltd, Toronto, ON, Canada) and by immunostaining OCT-embedded frozen sections using an anti-eGFP antibody (Fig. S1). In a second round of breeding, the male SMC-targeted *Nampt* heterozygotes (*Nampt*$^{flox/+}$; *smMHC*-Cre+) were bred with female *Nampt*$^{flox/flox}$ mice. Because of transient expression of Cre in the sperm of male *smMHC*-Cre/eGFP mice (de Lange et al. 2008), the floxed allele transmitted from the Cre-expressing parent is recombined, yielding a global heterozygous null allele of *Nampt* (hereafter referred to as "-"). Genotyping using PCR primers to amplify floxed, wildtype, exon 5/6-deleted *Nampt*, and the Cre transgene (Rongvaux et al. 2002, Xin et al. 2002)

confirmed the four possible genotypes of the offspring: *Nampt*$^{flox/+}$; *smMHC-Cre-* (wild-type), *Nampt*$^{flox/+}$; smMHC-Cre+ (SMC-specific *Nampt* heterozygous), *Nampt*$^{flox/-}$; *smMHC-Cre-* (global *Nampt* heterozygous), and *Nampt*$^{flox/-}$; smMHC-Cre+ (SMC-specific knockout with a global heterozygous *Nampt* background, "SMC-*Nampt* KO"). We used the wild-type mice as control and global *Nampt* heterozygous as an additional control for key endpoints. Importantly, prior studies have shown that global *Nampt* heterozygous mice are not overtly different from wild-type mice (Revollo et al. 2007). SMC-*Nampt* KO mice in the upper size tertile at 10-12 weeks of age were used for all studies.

We also generated mice in which *Nampt* could be globally and inducibly deleted. *Nampt*$^{flox/flox}$ mice were bred with mice expressing Cre recombinase fused to the mutated ligand binding domain of the human estrogen receptor (ER) under the control of a chimeric cytomegalovirus immediate-early enhancer/chicken ß-actin promoter (B6.Cg-Tg(CAG-Cre/Esr1)5Amc/J) (Jackson Laboratories, Bar Harbor, ME) (Hayashi and McMahon 2002). SMCs harvested from aortas of *Nampt*$^{flox/flox}$ Cre-ERT2 mice were subjected to hydroxyl-tamoxifen or sunflower oil vehicle for 24 hours.

2.2.2 NAD^+ measurement

Mouse aortic medial NAD^+ levels were determined in freshly harvested aorta after removing the adventitial layer by dissection and denuding the endothelial layer by scraping. NAD^+ content in the mouse aortic media was determined using a colorimetric kit (BioVision Research Products, Mountain View, CA, USA) and expressed relative to total protein content.

2.2.3 Laser capture microdissection and RNA isolation of mouse aortas

Laser capture was undertaken on 10 μm-thick frozen sections of the mouse descending thoracic aorta that had been embedded in OCT compound (Tissue-Tek). The medial layer was micro-dissected (Arcturus 704 Veritas LCM System, Harlow Scientific,

Arlington, VA) from 20 sections of an individual aorta and RNA extracted using TRIzol (Life Technologies) with the addition of linearized polyacrylamide (2 mg/ml, Sigma) following phase separation.

2.2.4 Drug Delivery in Mice

Mini-osmotic pumps (Alzet Model 2004, Durect Corp., Cupertino, CA) were implanted subcutaneously in the right flank for infusion with either saline or Ang II (1.44 mg/kg/day) for 7 or 28 days. Implantation was performed after inducing anesthesia with 3% isofluorane in 100% oxygen at a flow rate of 1 L/min. In a subset of mice, phenylephrine (Sigma, 30 mg/kg/day) was infused via mini-pump for 14 days, with implantation of an Ang II-infusing pump (1.44 mg/kg/day) on the opposite flank on day 7, such that both phenylephrine and Ang II were infused for seven days. Parp activity was inhibited by twice daily intraperitoneal injections of olaparib (50 mg/kg, AZD2281, Selleckchem, Houston, TX) for eight days, beginning 24 hours prior to implantation of saline or Ang II-loaded minpumps.

2.2.5 Blood pressure measurement

Blood pressure and heart rate were measured by noninvasive tail cuff (CODA, Kent Scientific Corp., Torrington, CT) (Vafaie et al. 2014). Mice were acclimatized by undergoing daily blood pressure recordings for one week prior to data acquisition. For data acquisition, 35 serial blood pressure measurements were performed and the average of the last 30 cycles recorded.

2.2.6 Aortic wall morphometry

Mice were anesthetized with ketamine/xylazine and perfused via the left ventricle with phosphate-buffered saline (PBS) and then paraformaldehyde (4% wt/vol) under physiological pressure for 30-45 minutes. After immersion in 4% paraformaldehyde overnight, two-mm segments from four distinct aortic zones (Owens et al. 2010) were

embedded in paraffin: ascending aorta (1 mm distal to the aortic valve); descending thoracic aorta (5 mm distal to the left subclavian artery); suprarenal abdominal aorta (proximal to the superior mesenteric artery); and infrarenal abdominal aorta (distal to the left renal artery). Five-μm sections were stained with hematoxylin-eosin or Movat's pentachrome and visualized with an Olympus BX51 microscope. Medial area, lumen area, and medial cell number were quantified from 3 sections 200 μm apart, in each of the four aortic regions, avoiding areas with aortic hematoma or dissection, using ImageJ software (NIH, Bethesda, MD). Focal areas of medial cell loss in the descending thoracic region were traced and expressed relative to that of the media. Aortic dissection was defined by the presence of blood in one or more of the aortic medial layers extending contiguously for at least 200 μm.

2.2.7 Immunohistochemistry and apoptosis of mouse aortic tissue

Immunostaining was performed on paraffin-embedded sections (for Nampt, eGFP, 8-oxodG, smooth muscle α-actin, p16, γ-H2AX, and cascapse-3). Primary antibodies were: rabbit polyclonal anti-eGFP (AB3080 1:50; EMD Millipore, Billerica, MA), mouse monoclonal anti-smooth muscle α-actin (Clone 1A4, A5228 1:500, Sigma, Oakville, ON, Canada), rabbit polyclonal anti-Nampt (A300-372A 1:50; Bethyl Laboratory, Montgomery, TX), mouse monoclonal anti-8-oxodG (NWA-MOG020 1:50; Northwest Life Sciences, Vancouver, WA), rabbit polyclonal anti-p16 (sc-28260 1:50; Santa Cruz Biotechnology, Dallas, TX), rabbit monoclonal anti-γ-H2AX (#9718 1:400; Cell Signaling, Danvers, MA), rabbit polyclonal anti-active caspase-3 (ab4051 1:50; Abcam, Cambridge, MA), rabbit monoclonal anti-Ki67 (ab16667 1:100; Abcam, Cambridge, MA), and rabbit polyclonal anti-CD45 (ab10558 1:200; Abcam, Cambridge, MA). Bound primary antibodies against eGFP, Nampt, 8-oxodG, p16, Ki67 and CD45 were detected using goat anti-rabbit or goat anti-mouse biotinylated antibody (Vector Labs, Burlington, ON, Canada) and visualized using an ABC kit and diaminobenzidine (DAB, Vector Labs) and counterstained with

Harris' hematoxylin. Bound primary antibodies against smooth muscle α-actin and γ-H2AX were detected using Alexa Fluor 488-conjugated goat anti-mouse and donkey anti-rabbit secondary antibody, respectively (Molecular Probes; Life Technologies, Burlington, ON, Canada) and nuclei were counterstained with propidium iodide. The proportion of immuno-positive cells in a given aortic zone was ascertained from 3 sections, separated by 200 μm, with a minimum of 500 cells evaluated. Terminal deoxynucleotide transferase-mediated dUTP nick end labeling (TUNEL) was used to assess apoptosis on paraffin-embedded sections (Roche Applied Science).

2.2.8 Senescence associated ß-galactosidase activity

Senescence associated ß-galactosidase (SA ß-gal) activity in the mouse aortas was determined as described (Vafaie et al. 2014) Briefly, anesthetized mice were subjected to antegrade perfusion via the left ventricle of phosphate-buffered saline (PBS) followed SA ß-gal solution (1 mg/ml X-Gal, 5 mmol/l potassium ferrocyanide, 5 mmol/l, potassium ferricyanide, 150 mmol/l NaCl, 2 mmol/l $MgCl_2$, 40 mmol/l citrate (titrated to pH 6.0 with NaH_2PO_4). Aortas were then harvested, incubated in SA-ßGal staining solution at 37°C for 16 h, fixed in 4% paraformaldehyde for 16 hours. Whole aortas were imaged with a Nikon SMZ800 stereomicroscope (Nikon Instruments, Mississauga, ON, Canada). Tissue was then frozen, embedded in OCT, and 10-μm cryosections were imaged microscopically to assess for positively stained blue cells.

2.2.9 Cell culture

Mouse aortic SMCs were isolated from aortas of 8-10-week-old mice via chemical digestion using type III porcine pancreatic elastase (250 μg/ml, Sigma) and type I collagenase (1 μg/ml, Worthington Biochemical Corporation, Lakewood, NJ) (Ray et al. 2001). SMCs were maintained in DMEM with 10% FBS and SMC identity confirmed by immunostaining for smooth muscle a-actin. SMCs harvested from aortas of *Nampt*$^{flox/flox}$

Cre-ERT2+ mice were subjected to 1 μM hydroxy-tamoxifen for 24 hours. In order to control for the effect of tamoxifen, *Nampt*$^{flox/flox}$ Cre-ERT2- (control) SMCs were also subjected to 1 μM hydroxy-tamoxifen for 24 hours. Rat aortic SMCs were isolated as previously described (Small and Pickering 2009) and maintained in DMEM with 10% FBS. All cells were studied within the first 4 subcultures.

2.2.10 Western blot analysis

Western blot analysis was undertaken with chemiluminescent detection as previously described (Frontini et al. 2009). Blots were probed by incubating with primary antibodies reacting to PAR (#528815 1:2,000; Calbiochem/EMD Millipore, Billerica, MA), Parp1 (ab6079 1:400; Abcam, Cambridge, MA), and α-tubulin (clone B-5-1-2 1:10,000, Sigma).

2.2.11 Detection of double-strand DNA breakage

Mouse SMCs subjected to irradiation at a dose rate of 1 Gy/minute for ten minutes (10 Gy) (Faxitron RX-650, Faxitron Bioptics, Tucson, AZ) or incubated with Ang II (10^{-7} mol/L) for 24 hours were fixed in 4% paraformaldehyde for 20 minutes. Cells were permeabilized in 0.5% Triton X-100 and incubated with rabbit antibody to γ-H2AX (#9718 1:300; Cell Signaling, Danvers, MA). Signal was detected by incubating with anti-rabbit Alexa Fluor 488 secondary antibody (Invitrogen, Burlington, ON, Canada) and nuclei were counterstained with 4′,6′-diamidino-2-phenylindole (DAPI, Invitrogen). γ-H2AX foci were quantified from at least 300 cells per condition based on fluorescent pixel density, applying a single background threshold for all images and using ImageJ, as described (Fell and Schild-Poulter 2012).

2.2.12 Detection of global DNA strand breakage by Comet assay

Mouse SMCs incubated with 1 mM H_2O_2 (15 minutes) or 10^{-7} mol/L Ang II (24 hours) were analyzed for DNA strand breaks by single cell alkaline electrophoresis

(CometAssay, Trevigen Gaithersburg, MD). Cells were trypsinized, suspended in 50 µl of low-melting point agar, transferred onto slides, and incubated at 4°C to allow the agar to set. Cells were then lysed in alkaline buffer and electrophoresed for 30 minutes with 300 mAmps of current. Cells were subsequently stained with SYBR-gold DNA stain and imaged (Olympus BX51). The comet tail moment (product of the tail length and fraction of total DNA in the tail) was measured using ImageJ and OpenComet (cometbio.org/index.html).

2.2.13 Time-lapse microscopy response to DNA damage

To evaluate the response to specific DNA damaging agents, *Nampt*$^{flox/flox}$ SMCs, with or without expression of Cre-ERT2, were incubated with 1µM hydroxyl-tamoxifen for 24 hours and cultured for an additional 72 hours to ensure *Nampt* depletion. Cells were incubated with designated concentrations of H_2O_2 or MMS for 1 hour and morphology tracked by video microscopy every 15 minutes for the following 24 hours. Cell death was identified based on either cell rounding with detachment from the plate, or a combination of collapse of the cytoskeleton, dissolution of nuclear structure, and complete cessation of movement. The effect of nicotinamide riboside on MMS-induced DNA damage was assessed by pre-incubating cells with 100 µM nicotinamide riboside (Chromadex, Irvine, CA) for 24 hours in NAD^+ precursor-free modified Eagle's medium (MEM) prior to addition of 600 µM MMS.

2.2.14 Immunocytochemical detection of poly(ADP-ribose)

Mouse SMCs fixed in 4% paraformaldehyde were permeabilized in 0.5% Triton X-100 and incubated with mouse anti-PAR antibody (4335-MC-100, 1:500; Trevigen, Gaithersburg, MD). PAR signal was detected with Alexa Fluor 546-conjugated goat anti-mouse secondary antibody (Molecular Probes; Life Technologies, Burlington, ON, Canada) and nuclei were counterstained with DAPI. PAR signal was quantified from at

least 300 cells per condition based on fluorescent pixel density, applying a single background threshold for all images and using ImageJ, as described (Fell and Schild-Poulter 2012).

2.2.15 Quantitative real-time reverse transcription–polymerase chain reaction

Total RNA was isolated from homogenates of the mouse aorta using TRIzol (Life Technologies) and the Rneasy Mini Kit following the manufacturer's protocol (Qiagen, Valencia, CA). Total RNA was isolated from mouse SMCs using the Rneasy Mini Kit following the manufacturer's protocol. Transcript abundance of *Nampt* and *Gapdh* in microdissected mouse aortas was assessed using TaqMan chemistry-based primer-probe sets (Nampt, Mm00451938_m1; Gapdh, Mm99999915_g1, Applied Biosystems). Transcript abundance of mouse *Nampt*, *Acta2*, *Mmp2*, *Col1a1*, *Timp1*, and 18S were assessed using SYBR-green chemistry-based primer sets (mouse *Nampt:* F-GGCACCACTAATCATCAGACCTG R-AAGGTGGCAGCAACTTGTAGCC; mouse *Acta2*: F-TGCTGACAGAGGCACCACTGAA R-CAGTTGTACGTCCAGAGGCATAG; mouse *Mmp2*: F-GAGACCATGCAGTCAGCTCTAG R-TAGAGCTGCCTCTTGTCTGGT; mouse *Col1a1:* F-CCTCAGGGTATTGCTGGACAAC R-CAGAAGGACCTTGTTTGCCAGG; mouse *Timp1:* F-TCTTGGTTCCCTGGCGTACTCT R-GTGAGTGTCACTCTCCAGTTTGC; mouse 18S F-GTAACCCGTTGAACCCCATT R-CCATCCAATCGGTAGTAGCG). Quantitative real-time RT-PCR was performed using an ABI Prism (model 7900HT) and Sequence Detection System software (Life Technologies; Applied Biosystems). For mouse aortas and SMCs, relative mRNA abundance was quantified based on critical threshold (CT) using the comparative CT formula, 2-ΔΔCT, with *Gapdh* or 18S mRNA as an internal control.

2.2.16 Statistical analyses

Values are expressed as mean±standard error of the mean. Statistical analyses were performed using GraphPad Prism software (GraphPad, La Jolla, CA, USA). Mean data were compared using Student's t-test or one- or two-way ANOVA with Holm-Sidak post hoc testing. The prevalence of aortic dissection and of in vivo SA ß-gal activity were compared among groups by chi-squared analyses.

2.3 Results

2.3.1 Generation of mice with SMC *Nampt* gene ablation

To determine if Nampt within SMCs plays a role in aortic health, I generated mice with targeted deletion of *Nampt* in SMCs, using the *smMHC*-Cre/eGFP expressing mouse line(Xin et al. 2002) and *Nampt*$^{flox/flox}$ mice (Rongvaux et al. 2008). Evaluation of eGFP in *smMHC*-Cre/eGFP mice confirmed Cre recombinase in the aorta, as assessed by whole organ microscopy and immunostaining (Fig. 2.1). Analysis of over 200 offspring from a two-step breeding protocol revealed close to expected Mendelian ratios for the predicted genotypes: 26.7% WT, 29.1% SMC-specific *Nampt* heterozygous, 20.6% *Nampt* heterozygous, and 23.5% SMC-*Nampt* KO.

Laser capture microdissection and quantitative RT-PCR revealed that *Nampt* transcript abundance in thoracic aortic media of SMC-*Nampt* KO mice was reduced to 13.5% that of control mice (Fig. 2.2a). Immunostaining revealed nuclear and extra-nuclear Nampt protein in medial SMCs of control aortas, with the nuclear signal being stronger (Fig. 2.2b). Nampt was undetectable in the aortic media of SMC-*Nampt* KO mice in all but rare cells but still detectable in endothelial cells and adventitial cells (Fig. 2.2b). I also determined aortic NAD^+ content, using an NAD^+ cycling assay. This revealed a 43.2% reduction in NAD^+ content in SMC-Nampt compared to control mice (Fig. 2.2c). Thus,

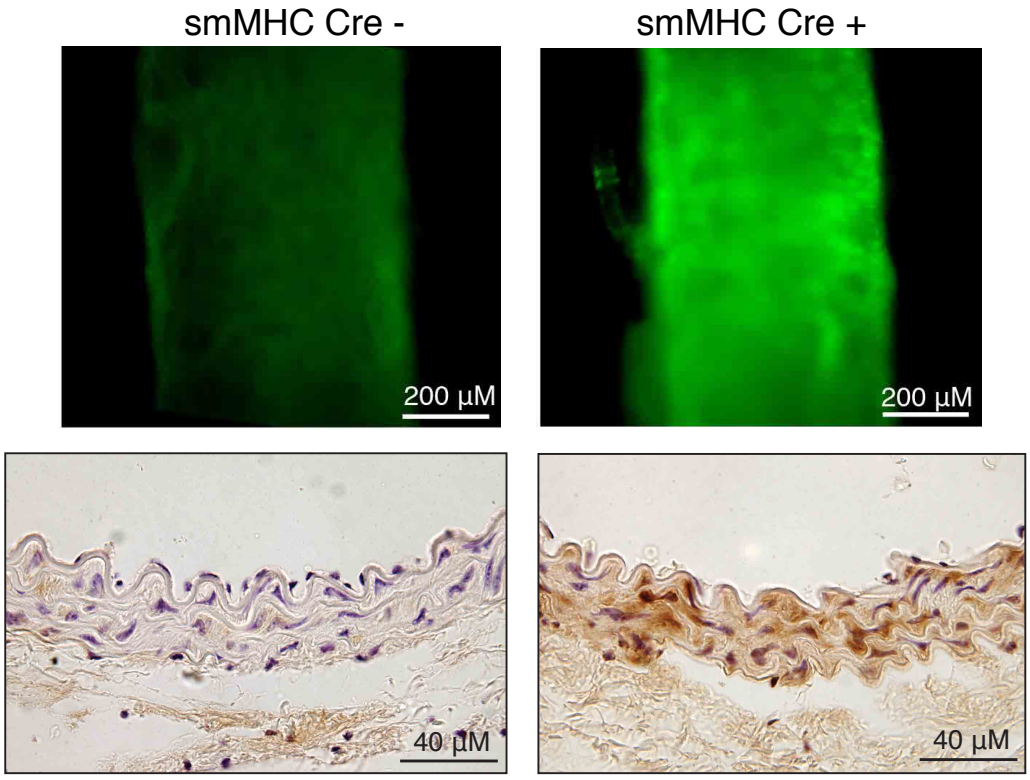

Figure 2.1 eGFP expression in aorta of smMHC-Cre-eGFP+ mice

Fluorescent stereomicroscopy images of whole thoracic aortas (top) and paraformaldehyde-fixed sections of thoracic aorta (bottom), immunostained for eGFP signal in 8-week-old smMHC-Cre-eGFP+ mice.

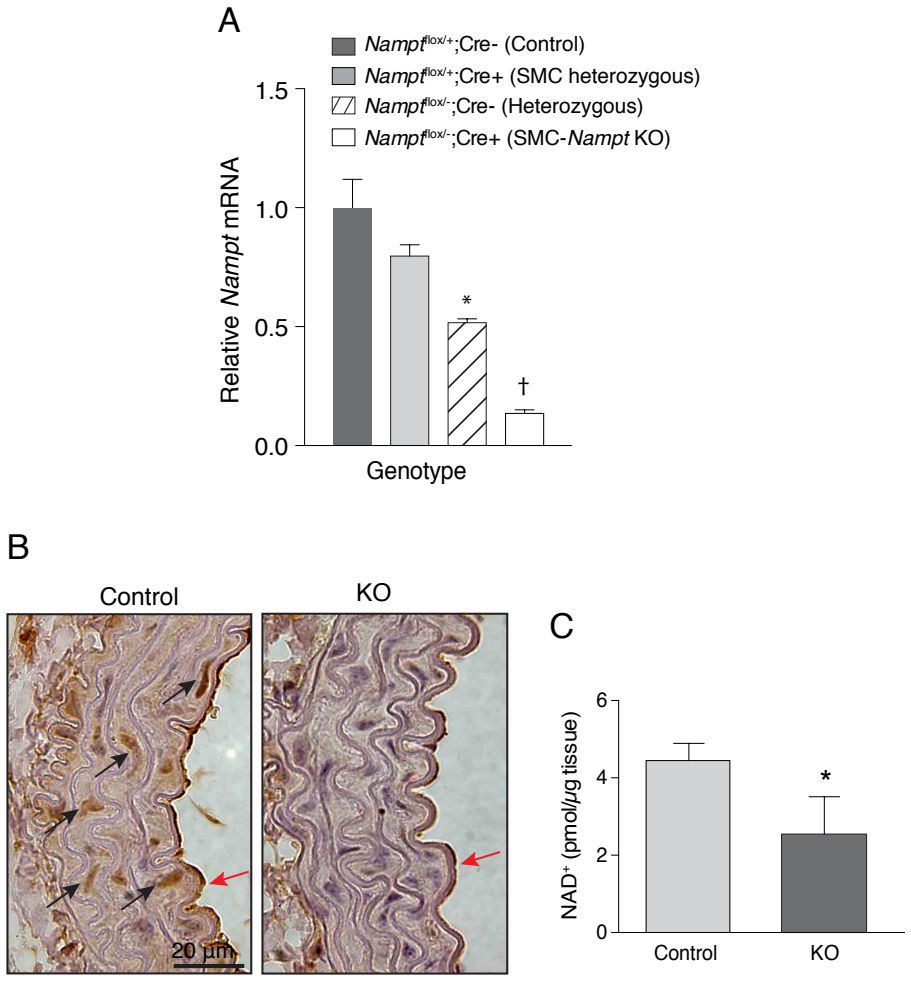

Figure 2.2 Generation of mice with Nampt-deficient aortas

A. Graph depicting *Nampt* transcript abundance in the mouse aortic media harvested using laser capture microdissection, measured by quantitative RT-PCR, and normalized to *18S* expression. Medial tissues from 3 mice for each genotype were studied. *P=0.0034 vs Control, †P<0.0001 vs Control, by 1-way Anova. **B.** Photomicrographs of thoracic aortic sections from control and SMC-*Nampt* KO mice, immunostained for Nampt. Black arrows depict Nampt expression in SMCs, red arrows depict Nampt expression in endothelial cells. **C.** Graph of NAD^+ content in acidic extracts of endothelium-denuded aortas of control and SMC-*Nampt* KO mice. *P=0.024 vs control, by Student's T-test.

Nampt is expressed in SMCs of the mouse aortic media and its depletion in SMCs, obtained using a Cre-lox approach, compromised aortic NAD^+ homeostasis.

2.3.2 Mice with SMC Nampt deletion have modestly dilated thoracic aortas

SMC-*Nampt* KO mice were viable and displayed no gross evidence of vascular anomalies. The average mean arterial pressure and heart rate of 8-week old SMC-*Nampt* KO mice were not significantly different than those of control mice (Fig. 2.3a). Immunostaining revealed abundant smooth muscle α-actin in medial SMCs, a normal number of lamellar units throughout the aorta, and unaltered medial SMC content (Fig. 2.3b-c). Quantification of lumen area of aortas fixed at physiologic pressure did however reveal modest dilatation of the ascending and descending thoracic aortic regions (by 16.7% and 12.4%, Fig. 2.3d). As well, the aortic medial areas of SMC-*Nampt* KO mice were mildly reduced in the ascending, descending thoracic, and suprarenal regions (by 13.2, 17.0, 24.5%, respectively, Fig. 2.3e). Transcript analysis revealed a modest (27.2%) decrease in mRNA abundance of SM-a-actin (P=0.001) and a 1.4-fold increase in *Mmp2* expression (P=0.005) with no change in *Timp1* expression (P=0.010).

2.3.3 Mice with SMC *Nampt* deletion are susceptible to Ang II-induced aortic dissection

To ascertain the response of the Nampt-deficient aorta to disease-associated stress, mice were subjected to continuous delivery of Ang II (1.44 mg/kg/day) by subcutaneous mini-pump. Interestingly, this was associated with a 54% decrease in aortic *Nampt* transcript abundance (P=0.009) and a concordant trend for NAD^+ content (P=0.063, Fig. 2.4a,b). Mean arterial blood pressure increased at 7 days, with no significant differences among the groups (25.3±4.3, 16.5±18.0, and 34.5±22.3 mm Hg for WT control, *Nampt* heterozygous control, and SMC-*Nampt* KO, respectively, p=0.285). However, there was striking aortic hemorrhage in SMC-*Nampt* KO mice, evident microscopically and grossly. Half of the mice displayed aortic hematomas after 7 days and this increased to 62.5% on

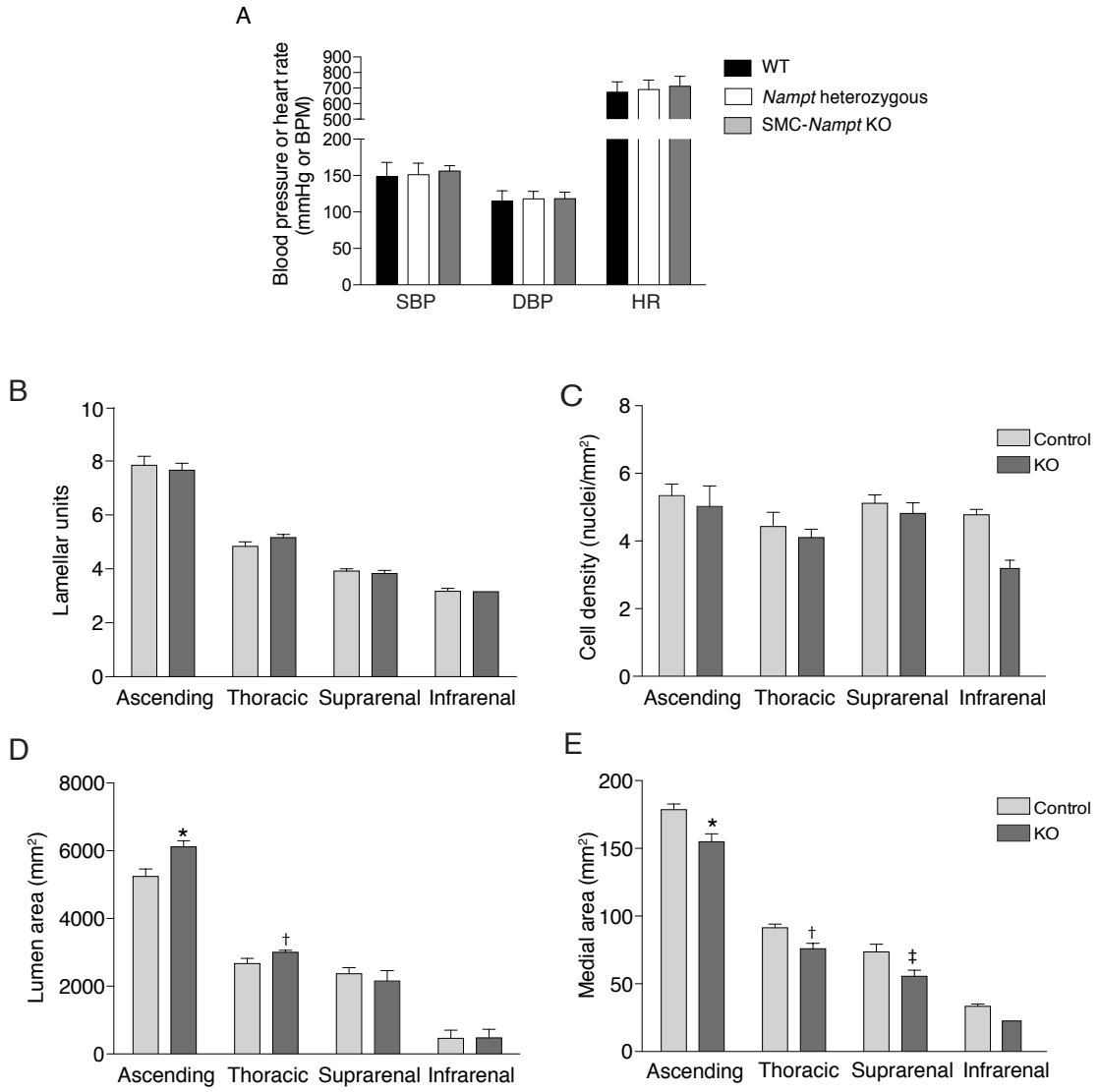

Figure 2.3 Deletion of *Nampt* in SMCs in mice yields modest aortic dilatation

A. Blood pressure and heart rate measurements of wild-type, *Nampt* heterozygous, and SMC-*Nampt* knockout mice were obtained weekly for 6 weeks for each mouse and averaged. Values depict mean data from 10-12 mice per genotype. **B-E.** Graphs showing the number of elastic lamellae per regional cross section (E), medial cell density (F), regional aortic lumen area (G) and medial area (H). **P*=0.023 and †*P*=0.029 vs. respective lumen area control, **P*=0.029, †*P*=0.004, and ‡*P*=0.027 vs. respective medial area control. N=5-6 mice per group.

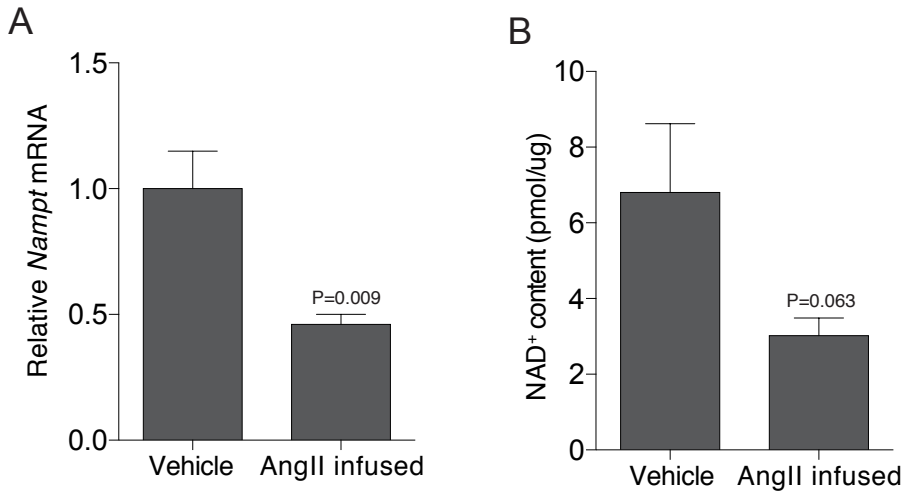

Figure 2.4 Angiotensin II decreases *Nampt* expression and NAD^+ content in mSMCs and mouse aortas

A. Graph depicting *Nampt* transcript abundance as normalized to *18S* transcript abundance in the media of the thoracic aorta of C57Bl/6 mice infused with Ang II (1.44mg/kg/day) or vehicle for 7 days, measured by quantitative RT-PCR (n=3 mice per group) **B.** Graph of NAD^+ content in acidic extracts of aortic media of vehicle- or Ang II-infused mice (n=4 mice per group).

day 28. The hemorrhage typically was within the outer one or two medial layers and could be extensive, with local elastin breakage (Fig. 2.5a). The hematomas did not rupture into the adventitia, as typically seen in Ang II-infused atherosclerotic mice, but instead could be found at multiple sites and dissecting along the length of the aortic media. In contrast, there was no grossly detectable hemorrhage in control mice subjected to Ang II, although microscopic hemorrhage in the ascending aorta was found in 24% of mice. These small bleeds, also noted in other reports (Rateri et al. 2014), had resolved by 28 days of Ang II delivery (Table 2.1). A similar profile was observed for *Nampt* heterozygous mice (14% microscopic hemorrhage in the ascending aorta). Transcript analysis of whole aortas revealed that SM-a-actin expression was 22.2% lower in Ang II-infused SMC-*Nampt* KO than Ang II-infused control mice (P=0.0001) and expression of *Col1a1* was 37.4% lower (P=0.002). However, the *Mmp2/Timp1* ratio did not increase and in fact reduced somewhat (20.9% P=0.002). Immunostaining for CD45 showed no differences between control and SMC-KO mice before or after Ang II infusion (data not shown).

Because of a trend toward greater Ang II-induced blood pressure response in SMC-*Nampt* KO mice, I determined if blood pressure elevation, in and of itself, might be responsible for the more striking aortic disruption. For this, control mice were subjected to double infusion of phenylephrine and Ang II, which elevated the mean arterial pressure by 37.2±16.4 mmHg. This increase was associated with only localized hemorrhage confined to the ascending aorta in 25% of mice (n=8), a profile not different than that of control mice. Collectively, these findings reveal that aortas in SMC-*Nampt* KO mice are prone to Ang II-induced disruption by hematoma and dissection, with minor changes in expression of SM-α-actin and type I collagen chains. Furthermore, whereas control mice adapted to the disrupting potential of Ang II over 28 days, SMC-*Nampt* KO mice remained vulnerable.

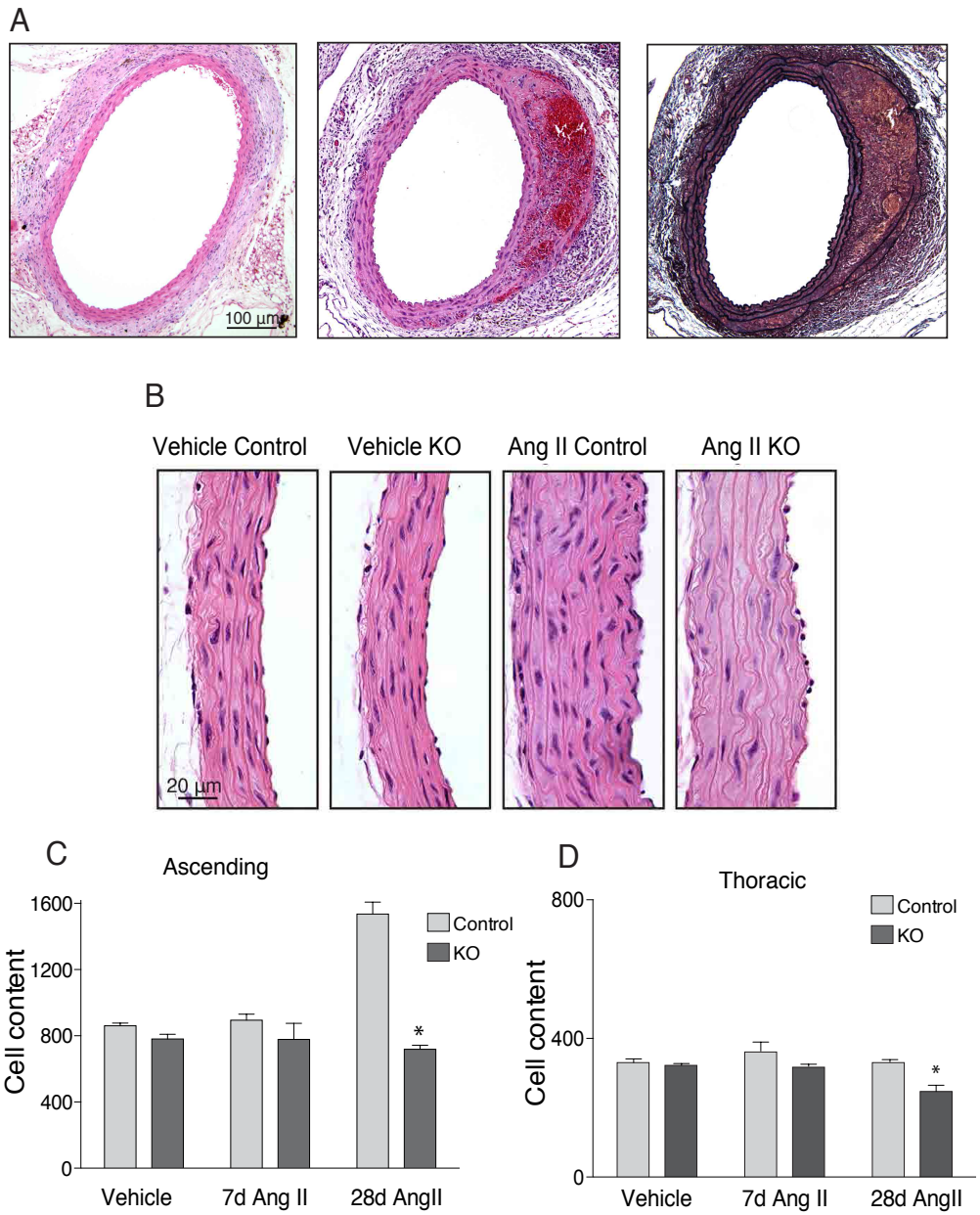

Figure 2.5 SMC-*Nampt* KO mice are susceptible to aortic wall degeneration and dissection

A. Light micrographs of sections of the descending thoracic aorta of a control (left) and SMC-*Nampt* KO (middle) mouse following 28 days of infusion with Ang II, stained with hematoxylin and eosin. The right panel depicts an adjacent section of the KO aorta stained with elastin trichrome, showing confinement of hemorrhage to the aortic media. **B.** Photomicrographs of sections of the ascending aorta stained with hematoxylin and eosin from vehicle- and Ang II-infused (28 days) control and SMC-*Nampt* KO mice. **C. D.** Graphs depicting cell content of the media cross-section after Ang II infusion in ascending (C), **P*<0.0001 vs control, and descending thoracic (D) aortas **P*=0.002 vs. control.

Table 2-1 Angiotensin II-induced aortic medial hemorrhage in mice

	WT		***Nampt* Heterozygous**		**SMC-*Nampt* KO**	
	Ang II (7 days) (*n=17*)	Ang II (28 days) (*n=10*)	Ang II (7 days) (*n=7*)	Ang II (28 days) (*n=7*)	Ang II (7 days)* (*n=14*)	Ang II (28 days)† (*n=8*)
Ascending	4 (23%)	0	1 (14%)	1 (14%)	6 (43%)	1 (13%)
Thoracic	0	0	0	0	1 (7%)	1 (13%)
Suprarenal	0	0	0	0	2 (14%)	4 (50%)
Infrarenal	0	0	0	0	0	0
Total (all regions)	4 (5.9%)	0	1 (3.6%)	1 (3.6%)	9 (16%)	6 (18.7%)
Total (all mice)	4 (23%)	0	1 (14%)	1 (14%)	7 (50%)	5 (62.5%)

*P=0.0002 vs 7-day WT distributions, P=0.0068 vs 7 day *Nampt* Heterozygous distributions
†P=0.0106 vs. 28-day WT distributions, P=0.0328 vs 28-day *Nampt* Heterozygous distributions

2.3.4 Ang II-induced cell loss in mice with SMC-*Nampt* KO mice

Twenty-eight days of Ang II infusion in control mice resulted in a 1.8-fold increase in medial SMC content in the ascending aorta (Fig. 2.5b,c) but no change in SMC content in the descending thoracic aorta, confirming a site-specific response that has been previously noted (Owens et al. 2010) In contrast, in SMC-*Nampt* KO mice medial SMC content in the ascending aorta did not increase in response to Ang II and in the descending thoracic aorta SMC content actually fell by 25.2% (Fig. 2.5d). These aberrant responses occurred despite evidence for residual SMC proliferation in Ang II-infused SMC-*Nampt* KO mice, as indicated by Ki67 immunostaining (Fig. 2.6a,b), supporting a turnover profile skewed toward cell loss. This loss of SMCs was evident both as scattered SMC dropout and cell-free foci of proteoglycan-rich matrix (Fig. 2.6c). Cell-poor zones were occasionally observed in control aortas subjected to Ang II but were 70% larger in aortas of SMC-*Nampt* KO mice (Fig 2.6d). Thus Nampt-depleted SMCs failed to adaptively fortify the ascending aorta and repopulate damaged regions in the descending aorta.

2.3.5 SMCs within the aorta of SMC-*Nampt* KO mice are susceptible to stress-induced premature senescence

To determine if the aberrant SMC responses to Ang II were due to induction of apoptosis, aortas were evaluated using TUNEL and active caspase-3 immunostaining. Surprisingly, although Ang II-induced apoptosis was evident in adventitial cells, I did not identify apoptosis signals in the ascending or descending thoracic aortic media of either control or Nampt-deficient mice (Fig. 2.7a,b). I next asked if SMCs instead developed features of senescence, recognizing that in vitro studies have implicated Nampt in slowing SMC aging (van der Veer et al. 2007). Intravenous infusion and ex vivo immersion in X-Gal solution (Vafaie et al. 2014) revealed no SA ß-gal activity in the aorta of control mice

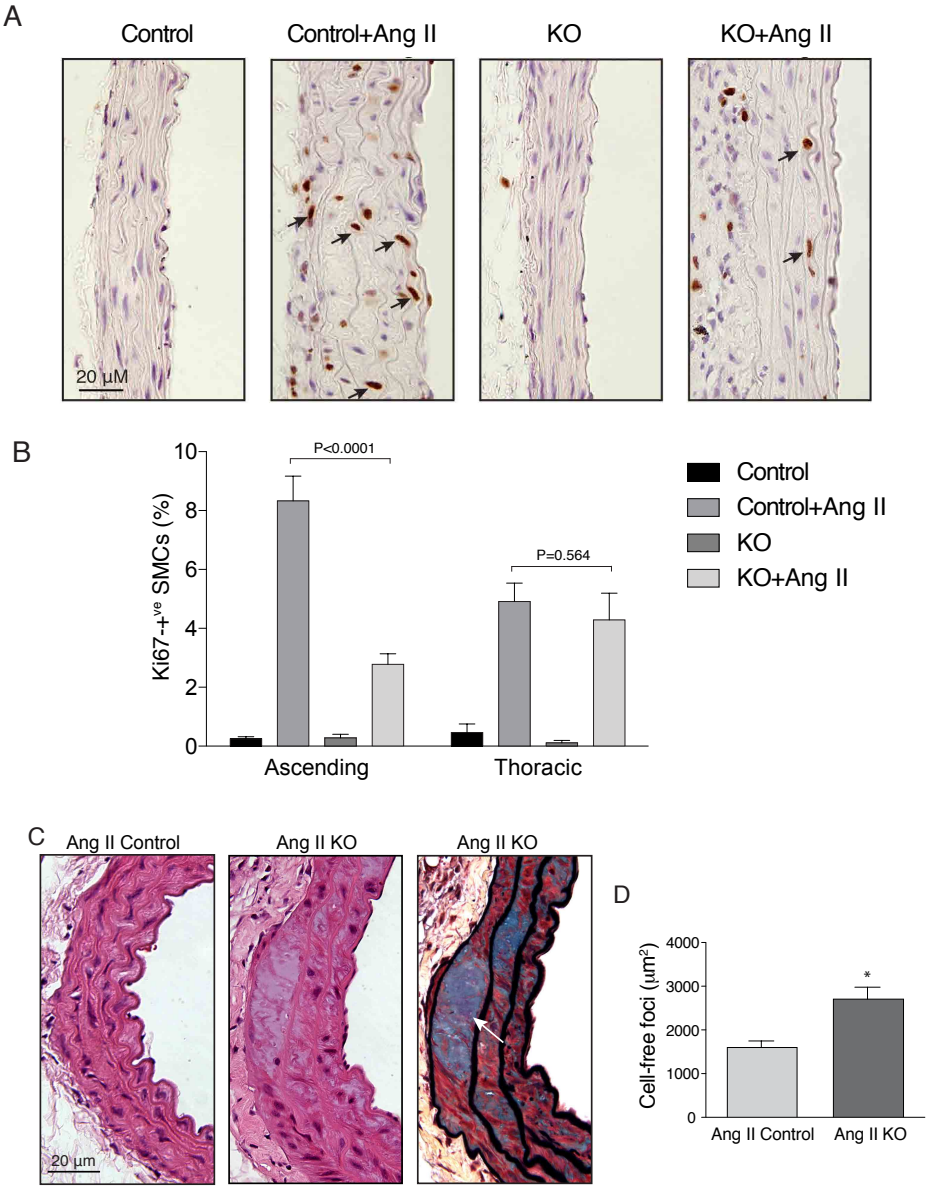

Figure 2.6 Aortas of SMC-*Nampt* KO mice are not proliferative and have areas of cell-free zones

A. Mouse aortic medial SMC proliferation as determined by immunostaining for Ki67. Micrographs of mouse ascending aorta 7 days after infusion with vehicle or Ang II (1.44 mg/kg/day), depicting Ki-67 immunoreactivity in control and SMC-*Nampt* KO mice (arrows). N=4 mice per group. **B**. Quantitative data for both ascending and descending thoracic aorta sections are shown in the graph. **C**. Sections of descending thoracic aorta from control (left) and SMC-*Nampt* KO (middle, right) mice following 28 days of infusion with Ang II illustrating focal cell loss. The right panel is an adjacent section to that in the middle and stained with Movat's pentachrome. Arrow depicts proteoglycan-rich cell-poor zone. **D.** Graph depicts the area of focal zones of SMC loss in the thoracic aorta, **P*=0.0003 vs. control. N=5 mice per group.

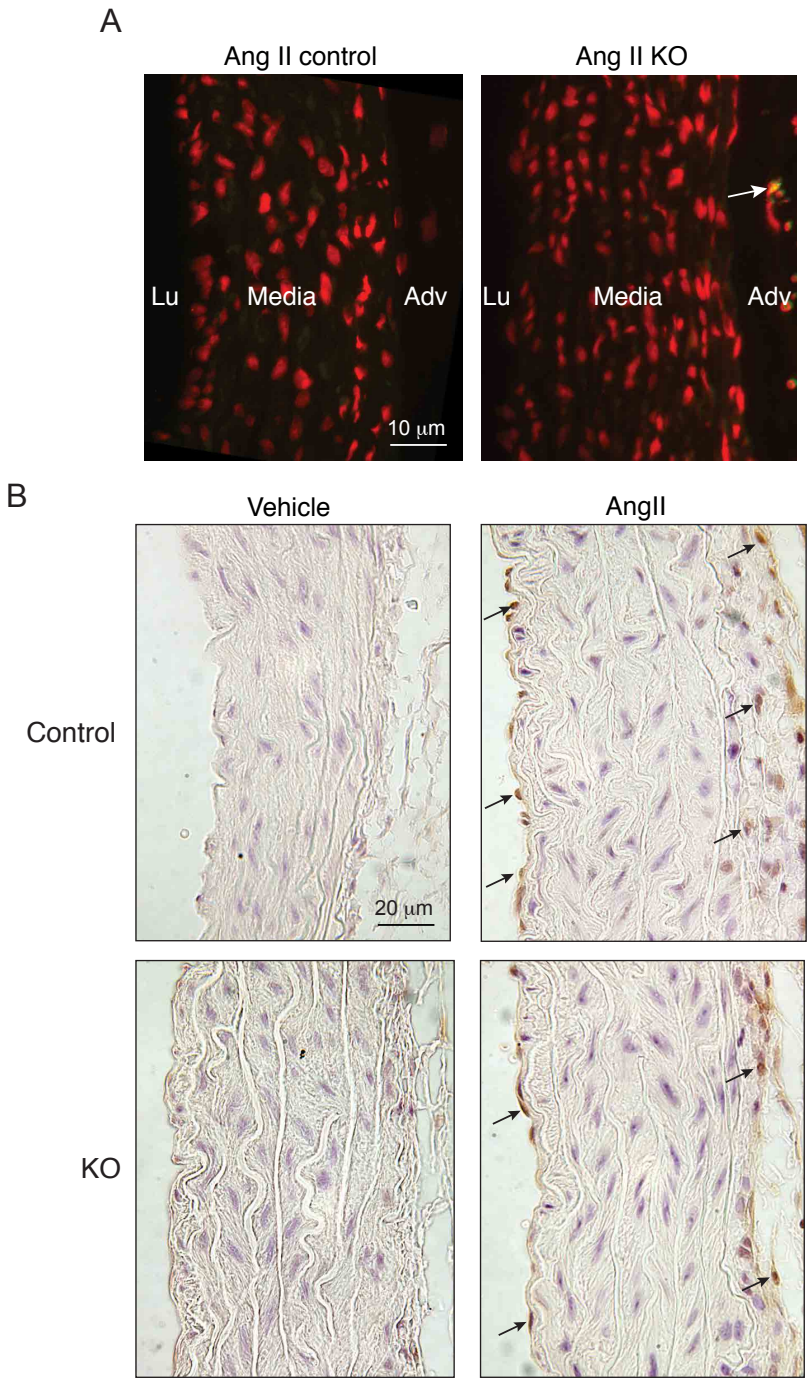

Figure 2.7 Assessment of apoptosis in aortas by TUNEL and active caspase-3 expression

A. Fluorescent photomicrographs of ascending aorta of mice infused with Ang II for 7 days stained using TUNEL (green). Nuclei were counter-stained with propidium iodide (red). Arrow indicates a TUNEL-positive nucleus in the adventitia. Lu, lumen; Adv, adventitia **B.** Ascending aorta sections of mice infused with vehicle or Ang II for 7 days and immunostained for active caspase-3 and counterstained with hematoxylin. Arrows indicate active caspase-3 positive endothelial cell and adventitial cell nuclei

subjected to Ang II. Remarkably however, in SMC-Nampt deficient mice there was SA ß-gal activity throughout the ascending aorta, arch, and proximal descending thoracic aorta after 7 days of Ang II infusion (Fig. 2.8a). Microscopy established that SA ß-gal activity was confined to the medial layers of the aorta and particularly the outer medial layers (Fig 2.8b).

As an additional test for cell senescence, I immunostained aortic sections for the cell cycle inhibitor, $p16^{INK4a}$. This revealed a 6.1-fold increase in the abundance of p16-expressing cells in the media of the ascending aorta of Ang II-infused SMC-*Nampt* KO mice relative to Ang II-infused control mice and a 4.7-fold increase in the thoracic aorta (Fig 2.8e). Therefore, Nampt deficiency impacts the fate of SMCs in the aorta, whereby Ang II sends them into a state of premature senescence.

2.3.6 Nampt-deficient SMCs accumulate oxidized DNA lesions and single-stranded DNA breaks

To explore why *Nampt*-ablated SMCs were prone to senescence I assessed for DNA integrity. I first immunostained for the oxidized nucleoside, 8-oxo-2'-deoxyguanosine (8-oxodG), recognizing that ROS can drive cell senescence (Yin and Pickering 2016). The proportion of ascending aorta medial SMCs with oxidized DNA was 3-fold higher in SMC-*Nampt* KO mice than in control mice. After a 7-day infusion of Ang II, DNA oxidation in SMC-*Nampt* KO aortas was even more prevalent and was 2.5-fold greater than in Ang II-infused control mice (Fig 2.9a,b). The oxidized DNA profile for SMCs in the thoracic aorta was similar although less striking (Fig. 2.9b).

I next asked if Nampt-deficient SMCs accumulated overt breaks in the DNA. For this, I established a culture system that enabled us to time the ablation of *Nampt* and evaluate different DNA break pressures. SMCs were cultured from aortas of $Nampt^{flox/flox}$ mice expressing Cre recombinase under the control of a tamoxifen-inducible promoter

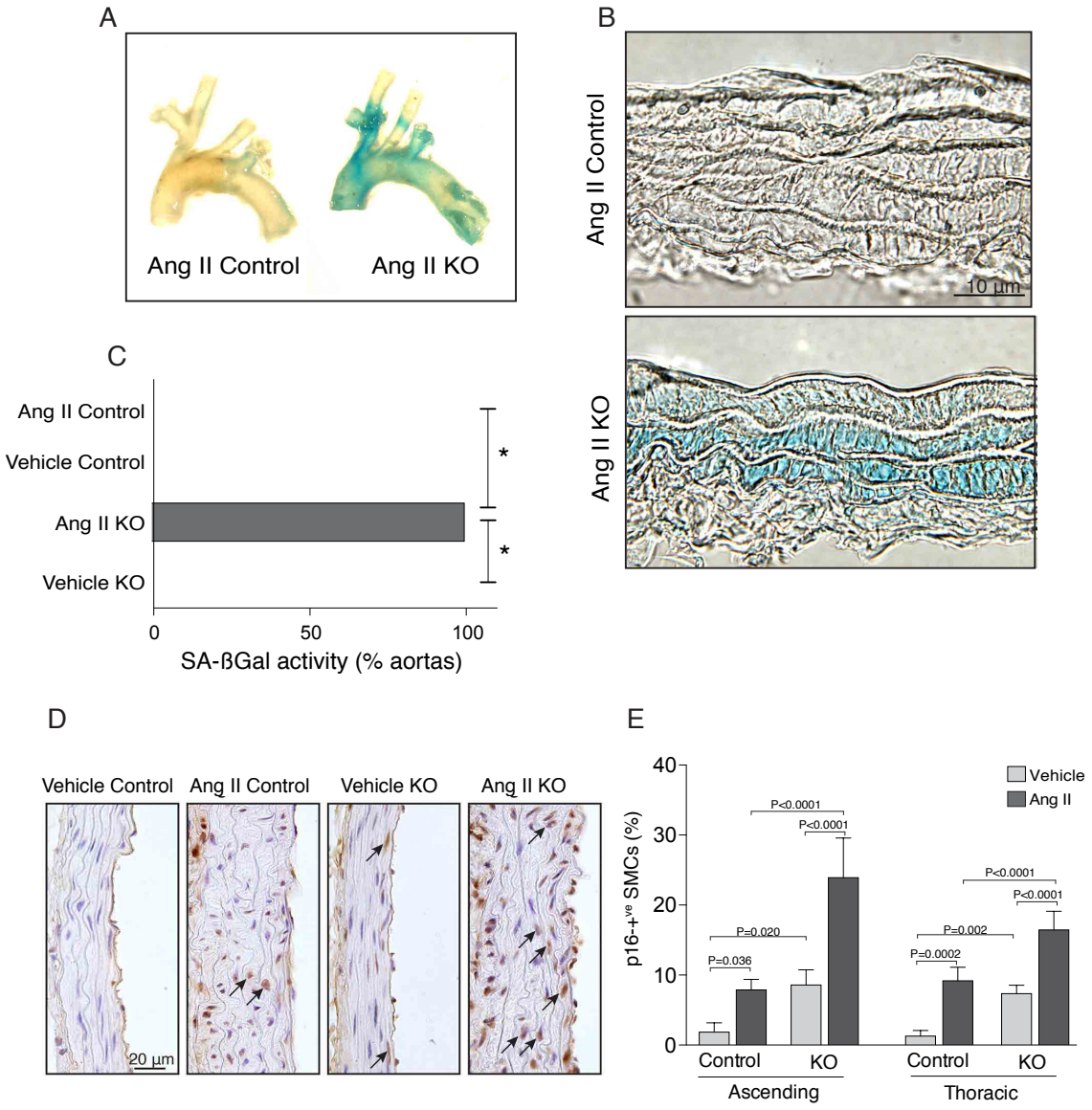

Figure 2.8 Nampt-deficient SMCs within the aorta undergo cellular senescence in response to Ang II infusion

A. Whole mount images of ascending, arch, and proximal descending thoracic aortas harvested after 7 days of Ang II infusion and stained for senescence-associated β-galactosidase (SA-ßGal) activity (blue). **B.** Cryosections of the ascending aorta depicting SA-ßGal activity localized to the aortic media. **C.** Chart showing proportion of aortas (n=16) with SA-ßGal activity. **P*=0.0011 **D**. Micrographs of ascending aorta subjected to 7 days of vehicle or Ang II infusion and immunostained for p16. Arrows depict p16-postive nuclei. **E**. Graph depicting prevalence of p16-positive nuclei.

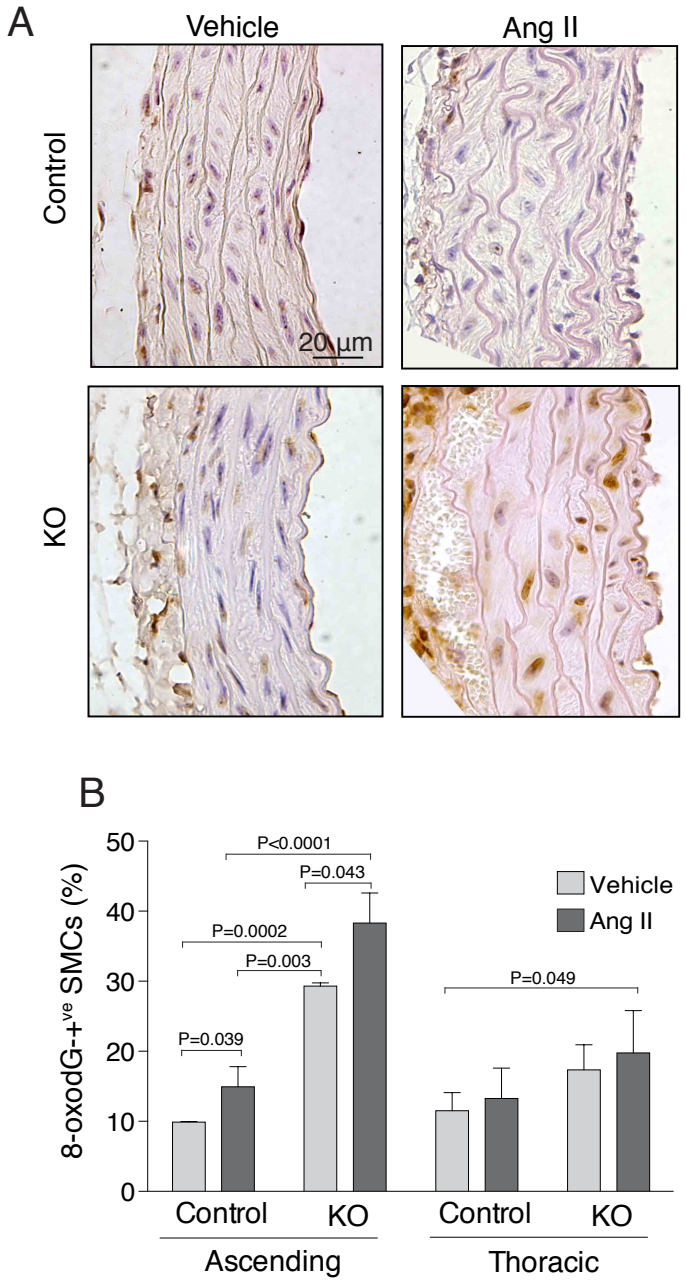

Figure 2.9 Nampt deficient aortas are susceptible to oxidative DNA damage

A. Micrographs of ascending aorta 7 days after infusion with Ang II, depicting oxidative DNA lesions as indicated by 8-oxo-2'-deoxyguanosine (8-oxodG) immunoreactivity. **B**. Graph showing the percentage of 8-oxodG-positive cells in the ascending and descending thoracic aortas. N=4 mice per group.

(Cre-ERT2). I then evaluated electrophoretic migration of cleaved DNA out of harvested nucleoids ("Comet" assay) after delivery of vehicle or hydroxy-tamoxifen. That latter induced robust *Nampt* knockdown (Fig. 2.10a). Interestingly, there was evidence for cleaved DNA in *Nampt*-ablated SMCs under baseline culture conditions (Fig. 10b,c). Incubation with H_2O_2, (100 μM, 1 h) to induce single strand DNA breaks yielded more striking DNA fragment tails and these were substantially more prominent in *Nampt*-ablated SMCs. Incubation with Ang II (10^{-7} mol/L, 24 h) yielded a modest DNA fragment signal that was significantly greater in *Nampt*-ablated SMCs (Fig 2.10b,c).

To further assess the response to DNA break-inducing agents, SMCs were tracked by video microscopy. This revealed a striking death response in Nampt-depleted SMCs, with cell rounding, anoikis, and cessation of cell membrane activity (Fig. 2.11a,b). Incubating SMCs with MMS, another single-strand DNA breaking reagent, led to similarly worse survival for *Nampt*-ablated SMCs (Fig. 2.11a,c). Notably, incubating SMCs with nicotinamide riboside prior to MMS inhibited the death response (Fig. 2.11d). Together, these studies reveal that Nampt protects SMCs from accumulating both oxidized DNA lesions and a toxic burden of single-strand DNA breaks.

2.3.7 Nampt-deficient SMCs have impaired double-strand DNA break repair

Double-strand DNA breaks are a particularly stressful form of DNA damage and potent driver of cell senescence (d'Adda di Fagagna 2008). Using the above culture system, I assessed the potential for accumulating double-strand breaks by subjecting SMCs to irradiation (10 Gy) and immunostaining for phosphorylated histone (γ-H2AX). Interestingly, DNA damage foci were found in low abundance in *Nampt*-ablated SMCs prior to irradiation. Upon irradiation, damage foci accumulated and were significantly more abundant in *Nampt*-ablated SMCs. This difference was evident after 15 minutes but also after 24 hours, at which time control SMCs showed near-complete resolution of the

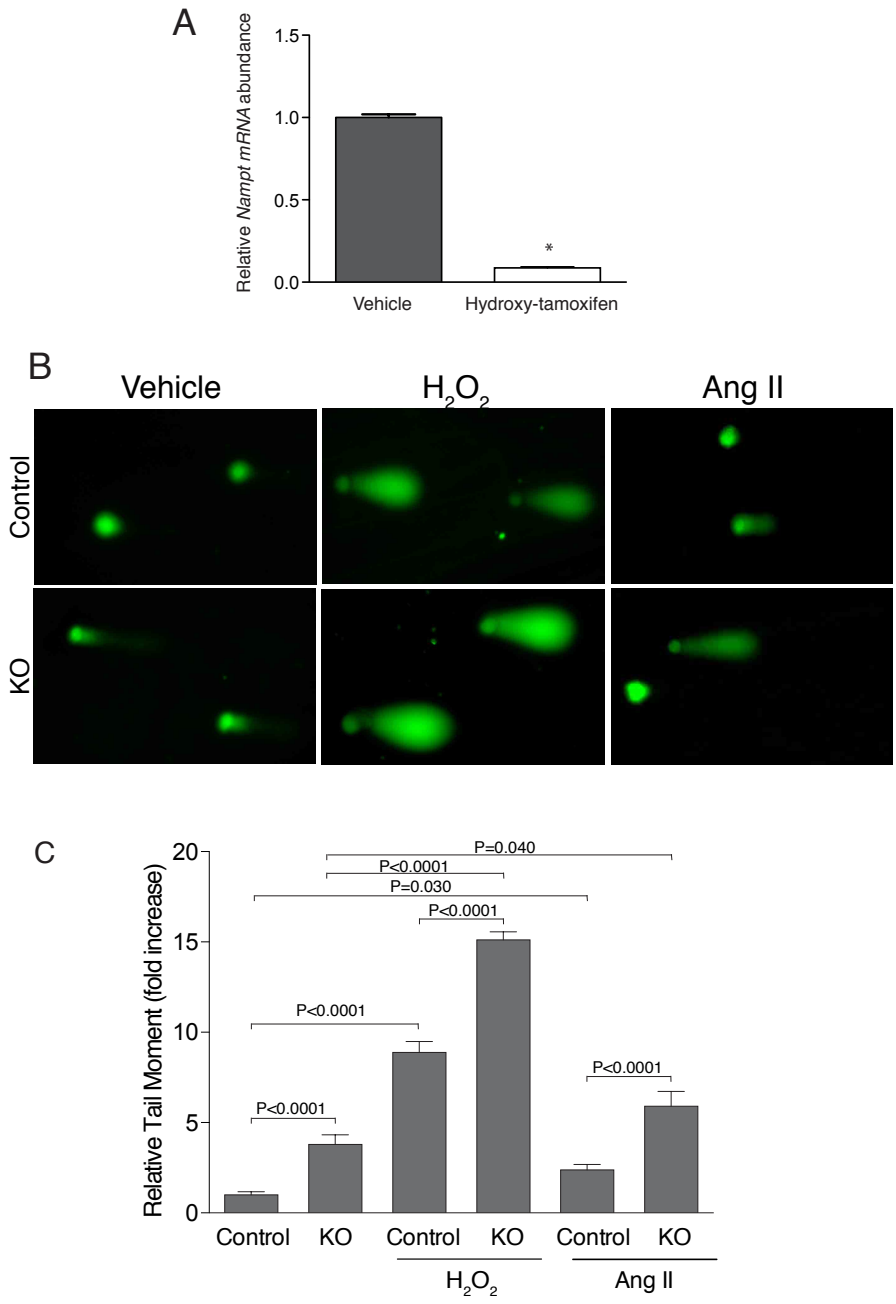

Figure 2.10 Nampt deficiency and susceptibility to oxidative DNA damage

A. Conditional deletion of *Nampt* in mouse aortic smooth muscle cells: SMCs were harvested and cultured from aortas of *Nampt*$^{flox/flox}$; CreERT2+ mice and incubated with vehicle or hydroxy-tamoxifen for 24 hours. Abundance of *Nampt* mRNA was evaluated by RT q-PCR and normalized to expression of *Gapdh* mRNA. *P<0.0001 **B.** Fluorescent micrographs of fragmented DNA "comet" tails from mouse aortic SMCs subjected to vehicle, 100 μM H_2O_2 (1 h), and 10^{-7} mol/L Ang II (24 h). **C.** Graph depicting mean±SEM SMC comet tail moments, relative to controls SMCs incubated with vehicle. **P*=<0.0001

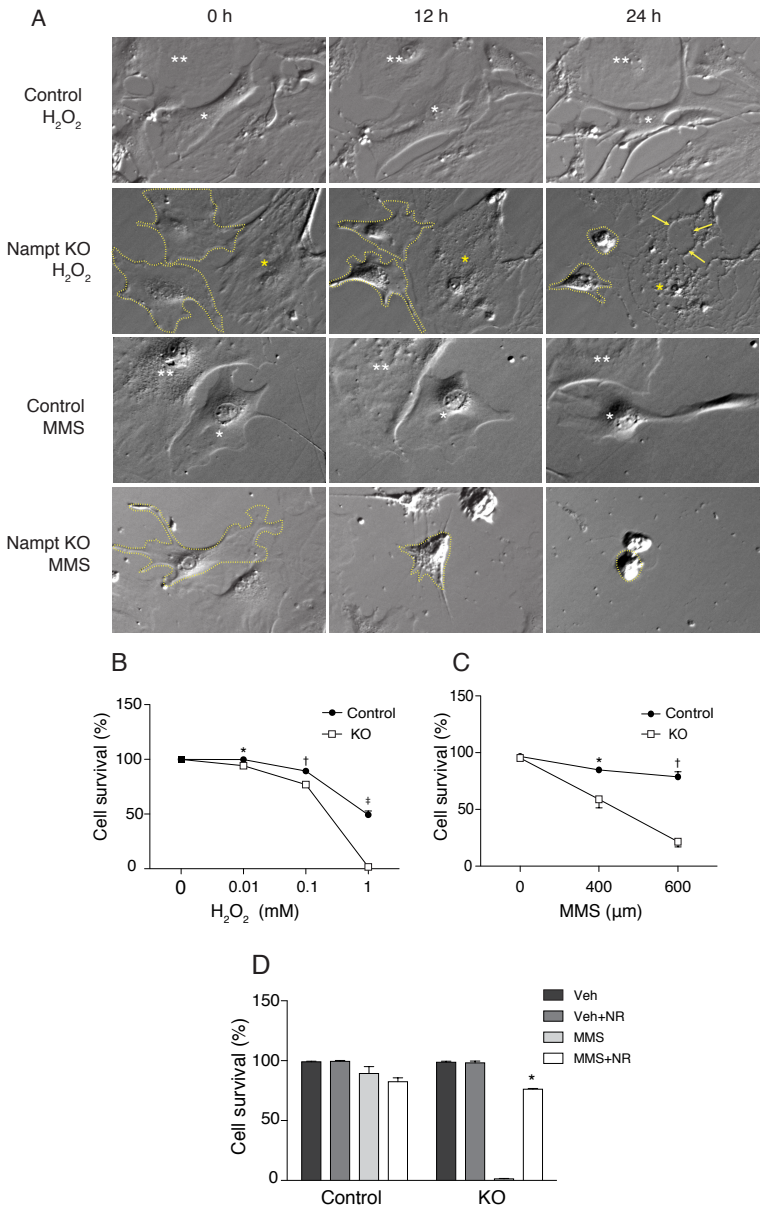

Figure 2.11 Nampt-depleted mouse SMCs are susceptible to death following exposure to H_2O_2 and MMS

A. Time-lapse video images of control (vehicle-treated) and *Nampt*-deleted (hydroxy-tamoxifen-treated) aortic SMCs harvested from *Nampt*$^{flox/flox}$; CreERT2+ mice. SMCs were incubated for one hour with H2O2 (1 mM), methyl methanesulfonate (MMS, 600 µM), or respective vehicles, and tracked for 24 hours. Asterisks and cell tracings depict individual cells over the 24 h time course, with tracings denoting cells undergoing anoiksis. Arrows depict a zone of cell content disintegration. **B, C**. Graphs depicting survival of mouse aortic SMCs, 24 hours after incubation with H_2O_2 (**P*=0.012, †*P*=0.014, ‡*P*=0.0001) or MMS (**P*=0.009, †*P*<0.0001). *N*=3 experimental replicates **E.** Graph depicting the survival of mouse aortic SMCs, 24 hours after incubation with 600 µM MMS, with and without the addition of 100 µM nicotinamide riboside (NR), **P*=<0.0001. *N*=3 experimental replicates

breaks (Fig. 2.12a,b). Incubation of *Nampt*-ablated SMCs with Ang II (24 h) also increased double-strand DNA damage foci and this effect was still evident 24 h after Ang II washout (Fig. 2.12c).

I next assessed if this form of DNA damage could be found in vivo. There were no γ-H2AX-positive SMCs in the aortic media of mice subjected to vehicle infusion. Rare (<0.5%) γ-H2AX-positive cells were found in control mice subjected to Ang II infusion (Fig. 2.13a,b). In contrast, γ-H2AX-positive-SMCs were consistently detected in both ascending (4.0%) and descending (3.8%) thoracic aortas of Ang II-infused SMC-*Nampt* KO mice (Fig. 2.13b).

2.3.8 Parp activity is impaired in Nampt-deficient SMCs and its inhibition in vivo promotes aortic SMC DNA damage and senescence

Parp1 has roles in repairing multiple types of DNA damage (Dantzer et al. 2006). To determine if Parp1 activity was impacted by the disrupted NAD^+ metabolism, I assessed PAR assembly by Western blot analysis following irradiation of rat aortic SMCs. Irradiation-induced PAR formation was markedly suppressed in SMCs incubated with the Nampt inhibitor, FK866 (100 nM, Fig. 2.14a). The abundance of PARP1 itself did not change upon Nampt inhibition. I also immunostained mouse aortic SMCs for PAR. Abundant nuclear PAR signal emerged 15 minutes after control SMCs were exposed to H_2O_2. However, there was barely detectable nuclear PAR in *Nampt*-ablated SMCs subjected to H_2O_2 (Fig. 2.14b,c). In the presence of nicotinamide riboside, PAR assembly in irradiated *Nampt*-ablated SMCs was restored. Nuclear PAR also accumulated upon 24 h of Ang II exposure. As seen with H_2O_2, the Ang II-induced PAR response was not evident in *Nampt*-ablated SMCs, but was restored in the presence of nicotinamide riboside (Fig. 2.14d).

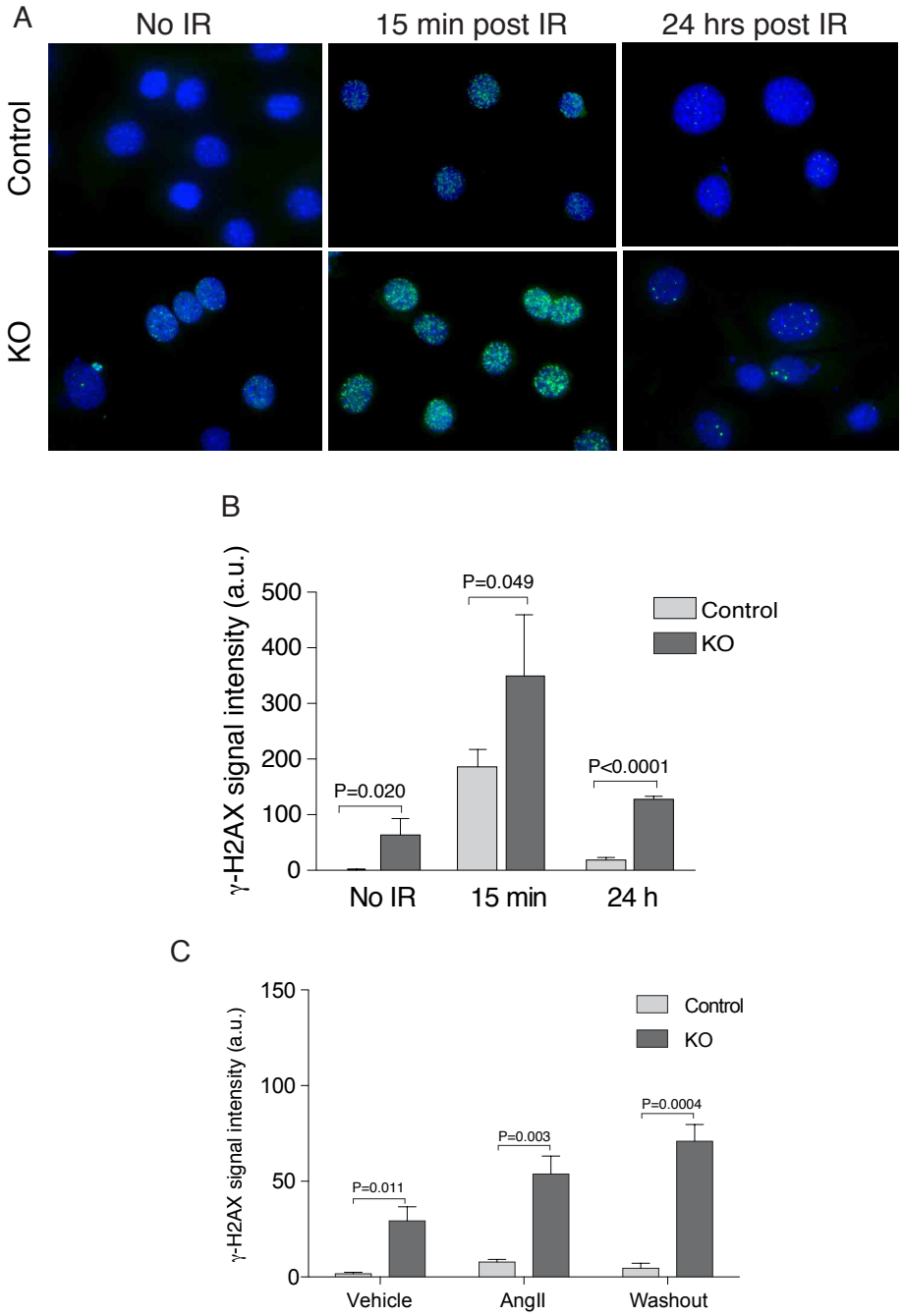

Figure 2.12 Reduced Nampt and doubled-stranded DNA damage in mouse SMCs

A. Fluorescent micrographs depicting the response of mouse aortic SMCs to irradiation (10 Gy). Cells were immunostained for γ-H2AX (green) and nuclei were labeled with Hoechst 33258 dye (blue). **B**. Graph showing the cumulative pixel intensity per cell of γ-H2AX signal. **C**. γ-H2AX signal in control and *Nampt*-ablated mouse aortic SMCs incubated with vehicle or 10-7M Ang II for 24 hours, and 24 hours after Ang II washout.

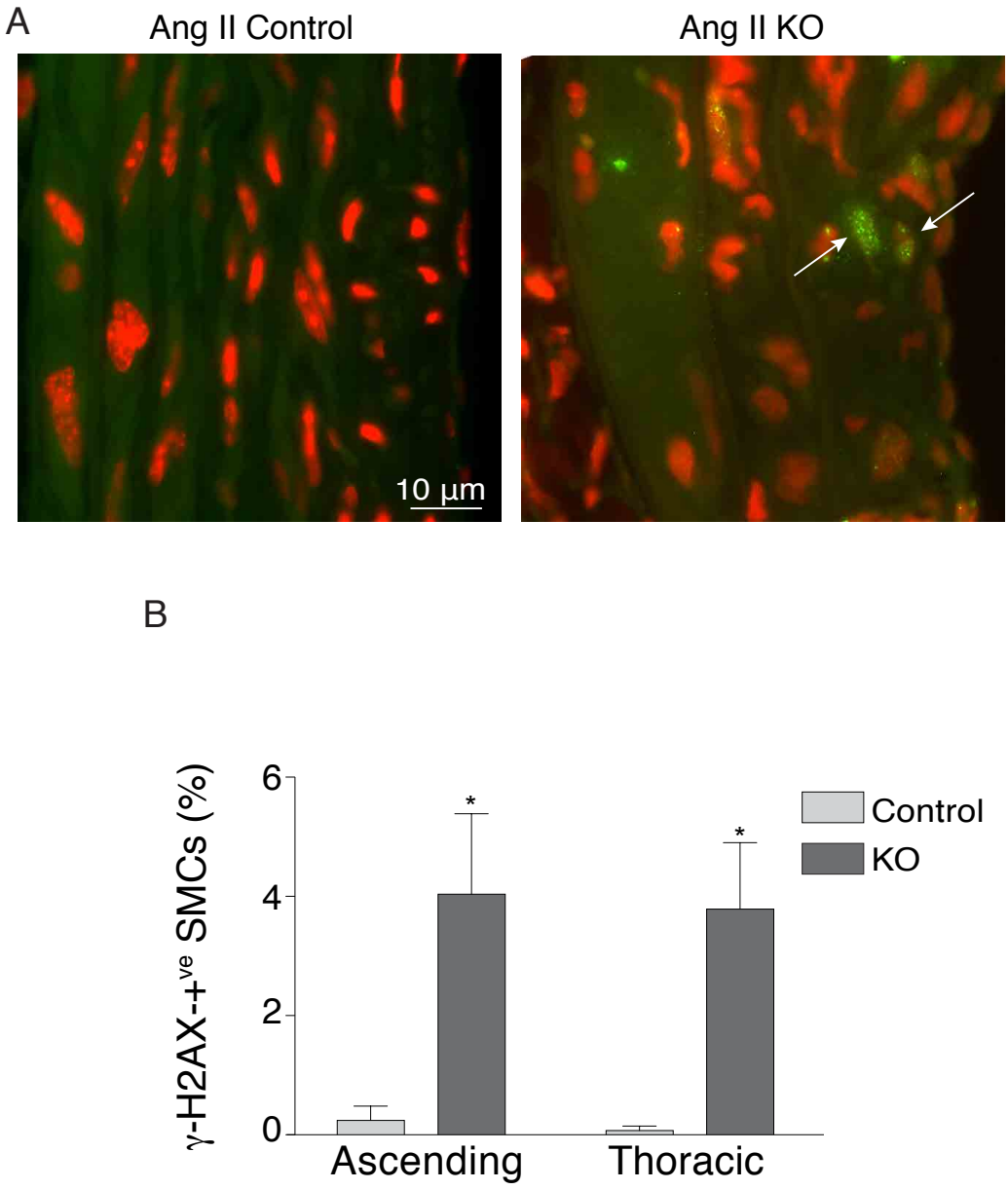

Figure 2.13 Reduced Nampt and double-stranded DNA damage in mouse aortas

A. Micrographs showing γ-H2AX-positive foci (green) in nuclei in the aortic media of mice subjected to a 7-day infusion of Ang II. Nuclei were counterstained with propidium iodide (red). **B.** Graph depicting the proportion of γ-H2AX-positive cells in the aortic media of mice subjected to a 7-day infusion of Ang II, **P*=0.044 vs. Control, ascending aorta; **P*=0.022 vs. Control, thoracic aorta.

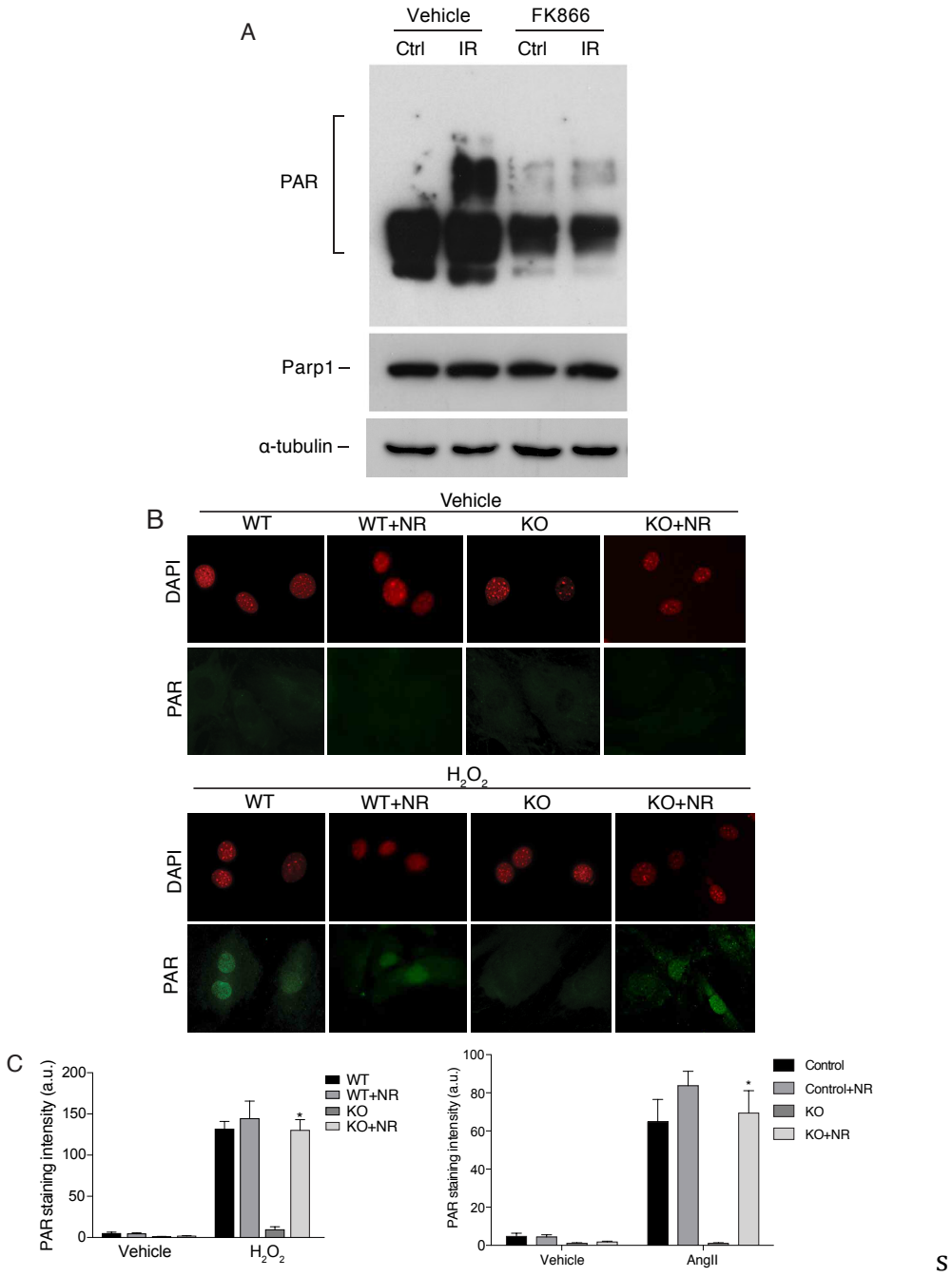

Figure 2.14 Parp inactivation in Nampt-depleted SMCs

A. Western blots depicting poly(ADP-ribose) (PAR) moieties, Parp1, and tubulin content in rat aortic smooth muscle cells incubated with FK866 (24 h) and subjected to irradiation (50 Gy). **B.** Immunofluorescence images showing the presence of PAR moieties (green) in control and *Nampt*-KO SMCs subjected to 1 mM H_2O_2 for 15 minutes. Nuclei were counterstained with DAPI (red). **C**. Graph depicting cumulative pixel intensity per cell of PAR signal, **P*<0.0001 vs. KO. **D.** Nuclear PAR signal, assessed by immunofluoresence, in mouse aortic SMCs subjected to 10^{-7}M Ang II or 24 hours, with and without the addition of 100 μM nicotinamide riboside (NR) *P<0.0001 vs. KO.

In addition, in vivo inhibition of Parp by IP injections of olaparib produced SMC defects in control mice subjected to Ang II that were similar to those in Ang II-infused SMC-*Nampt* KO mice. The proportion of p16-expressing medial SMCs increased by 2.7-fold and 3.7-fold in the ascending and descending thoracic aorta, respectively (p=0.002, p=0.023) and the proportion of SMCs positive for 8-oxodG increased by 2.2-fold and 1.9-fold (p=0.0003, p=0.003, Fig. 15a,b). As well, γ-H2AX-positive SMCs were identified in the media of Ang II-infused mice that received olaparib, and in a range similar to that of Ang II-infused SMC-*Nampt* KO mice (Fig. 2.15c).

Collectively, these data indicate the presence of a NAD^+-PARP1-DNA repair axis in aortic SMCs and the dependence of this cascade on Nampt.

2.4 Discussion

This study reveals that aortic integrity depends on an intrinsic NAD^+ generating system within SMCs. By evaluating the consequences of *Nampt* knockout in these new mouse models, I demonstrate that: i) ablation of *Nampt* in SMCs reduces NAD^+ content in the aortic wall and renders it vulnerable to dissection; ii) Ang II sends Nampt-depleted SMCs in the aorta into a state of premature senescence; and iii) Nampt-deficient SMCs are prone to accumulating a range of DNA lesions and are susceptible to exhaustion of Parp activity.

The finding that SMC-*Nampt* KO mice have reduced aortic medial NAD^+ content is important given the multiple routes for synthesizing NAD^+. There are at least five dietary precursors to NAD^+, four of which do not require Nampt. As well, NAD^+ itself may be directly delivered to cells from nearby cellular sources and an extracellular supply of Nampt has been characterized (eNampt) (Revollo et al. 2007, Nikiforov et al. 2015). However, the 43% drop in NAD^+ in the aortic media revealed that none of these potential alternative pathways circumvented the local loss of Nampt in SMCs. Given the resulting

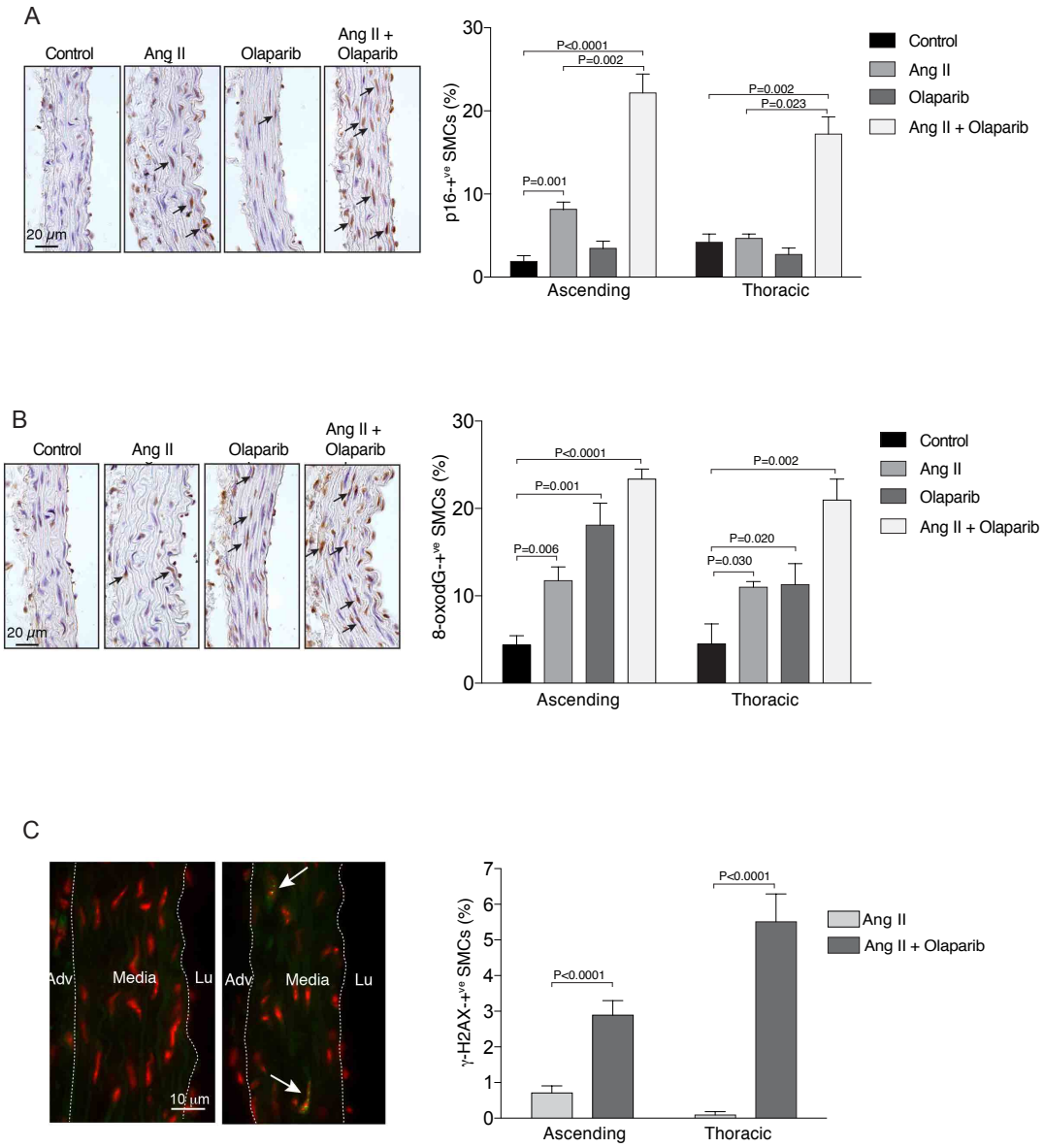

Figure 2.15 Effect of Parp inhibition on aortic SMC senescence and susceptibility to oxidative DNA damage

A. Micrographs of ascending aorta sections 7 days after infusion with Ang II (1.44 mg/kg/day) as well as daily i.p. injections of the Parp inhibitor, olaparib (50 mg/kg). Sections were immunostained for p16 (arrows). Graph depicting the prevalence of p16-positive nuclei in the ascending and descending thoracic aorta is shown on the right. **B.** Sections of ascending aorta depicting oxidative DNA lesions, as indicated by 8-oxo-2'-deoxyguanosine (8-oxodG) immunoreactivity. Graph on the right depicts the abundance of 8-oxodG-positive SMCs. **C.** Micrographs showing γ-H2AX-positive foci (green) in nuclei in the aortic media of mice subjected to Ang II infusion and PARP inhibition with olaparib. Nuclei were counterstained with DAPI (pseudocoloured red). Lu, lumen; Adv, adentitia. Data on the right depict the proportion of γ-H2AX-positive cells in the ascending and descending thoracic aortic media.

aortic compromise, and our prior studies showing no evidence for secretion of Nampt by SMCs (van der Veer et al. 2005), the current data indicate that an autonomous, Nampt-dependent NAD^+ production cascade in SMCs serves as a vital metabolic hub for the aorta.

The observed drop in aortic medial NAD^+ was sufficient to lead to mild dilation, but more striking consequences became apparent with the stress of Ang II. Rather than adapt to this stress, the Nampt-deficient aortic wall degenerated, with abrogated SMC hyperplasia, overt SMC dropout, and medial hematomas and dissections. The latter had similar distributions to that of other models of aortic disruption (Rateri et al. 2014), suggesting that the reduced Nampt acted on a background of prevailing aortic susceptibilities. The additional finding of widespread SMC senescence provides an intriguing mechanistic basis for the Nampt-driven maladaptive response to Ang II. Ang II has been found to induce SMC senescence in vitro and in atherosclerotic arteries (Kunieda et al. 2006, Matthews et al. 2006) and the current data thus expand the in vivo contexts for SMC senescence. Several attributes of senescent or otherwise aged SMCs could adversely impact aortic stability including the relative inability to replicate, perturbed contractility, and an altered secretory profile that favours a pro-degeneration phenotype (Liu et al. 2013, Yin and Pickering 2016).

The inability to maintain genomic integrity is a hallmark of accelerated aging and a key stimulus for cellular senescence. The range of DNA lesions that I identified places Nampt as an important guardian of genomic health. The presence of oxidized guanine residues in SMCs reflects a persistent ROS burden that could promote senescence through several mechanisms, including lipid oxidation and interference with cellular metabolism (Yin and Pickering 2016). In addition, 8-oxodG DNA lesions themselves have been found to be pathological and their continuous clearance is required to prevent the cell from entering a senescent cascade (Rai et al. 2009). Single-strand DNA breaks, readily detected in aortic SMCs depleted of Nampt, is also linked to cellular senescence, either directly or

by predisposing to double-strand DNA breakage (Kuzminov 2001, Nassour et al. 2016). Double-strand DNA breakage in turn is a well established driver of cellular senescence (d'Adda di Fagagna 2008). Taken together, the findings establish that compromised NAD^+ constitutes an intracellular milieu that is hazardous for DNA integrity.

Although several upstream defects may contribute to the observed DNA lesions, these findings point to incapacitation of Parp1 as an important mechanism. One of the best-understood roles of Parp1 is the sensing and repair of single-strand DNA breaks, effectively serving as the first line of defense to this common DNA assault (Dantzer et al. 2006). More recent evidence has established that protein PARylation, mediated in part by Parp1, also functions in double-strand break repair (Wang et al. 2006, Beck et al. 2014). As well, Parp1 participates in clearance of oxidized nucleotides through binding to 8-oxoguanine-DNA glycolase, an enzyme fundamental to removing 8-oxodG base lesions (Fisher et al. 2007, Noren Hooten et al. 2011, Beck et al. 2014). The possibility cannot be excluded that molecular perturbations arising from NAD^+ depletion other than Parp incapacitation may have contributed to aortic wall degeneration. In this regard, Sirt1 activity in SMCs has been shown to depend on a Nampt-mediated supply of NAD^+ (Ho et al. 2009) and Sirt1 has been found to protect against aortic disruption in response to Ang II (Fry et al. 2015, Chen et al. 2016) As well, substantially reduced NAD^+ can lead to critical ATP depletion and energetic stress, which has been found to cause muscle degeneration in skeletal muscle-specific *Nampt*-knock out mice (Frederick et al. 2016). However, the threshold NAD^+ level below which ATP production becomes compromised in the aorta remains to be elucidated.

In summary, I demonstrate that Nampt within SMCs protects the aorta from degenerating. My findings indicate that low Nampt, while not necessarily an inciting event, can substantially compromise the manner in which the aorta responds to stress. I speculate that an "NAD^+ fatigue" phenomenon may underlie progression in aortopathy

(Fig. 2.16). Nampt fuels a critical DNA repair system in the medial aortic layer and resists premature cellular senescence. These findings raise the possibility that disturbed local NAD^+ metabolism renders the aortic tissue susceptible to forces that lead to disruption.

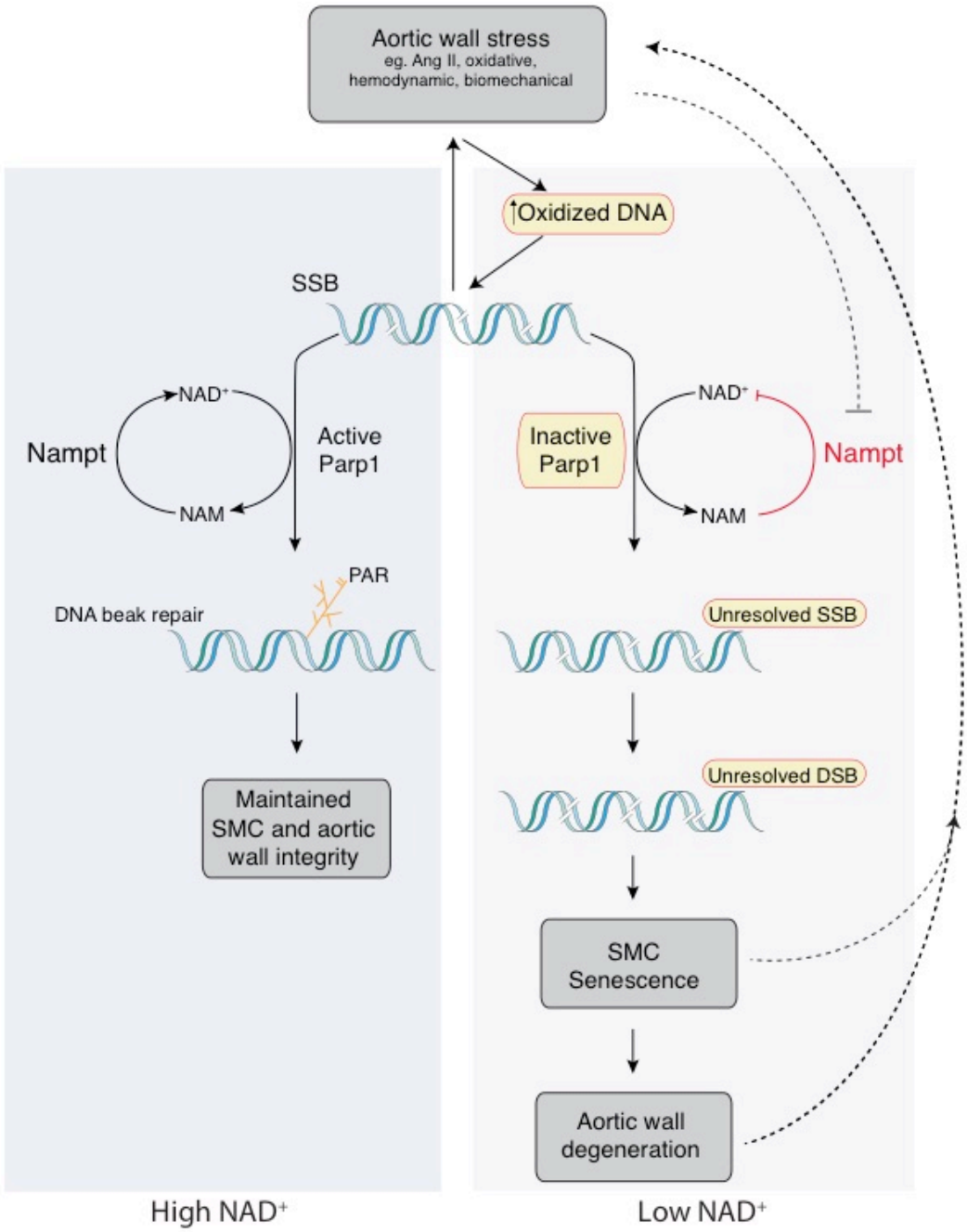

Figure 2.16 Schematic depicting aortic wall consequences of reduced SMC Nampt

In the setting of aortic wall insults and compromised NAD^+ (right), SMC DNA damage accumulates and is inadequately repaired. This can lead to accelerated SMC aging and destabilization of the aortic wall. Deleterious DNA events that can be exacerbated by low Nampt are outlined in red. A proposed route to decreasing Nampt and a self-sustaining damage cycle are noted by the dashed lines. SSB, single strand break; DSB, double strand break; PAR, poly(ADP ribose).

2.5 References

Beck, C., Robert, I., Reina-San-Martin, B., Schreiber, V., & Dantzer, F. (2014). Poly(ADP-ribose) polymerases in double-strand break repair: focus on PARP1, PARP2 and PARP3. *Exp Cell Res, 329*(1), 18-25

Canto, C., Menzies, K. J., & Auwerx, J. (2015). NAD(+) Metabolism and the Control of Energy Homeostasis: A Balancing Act between Mitochondria and the Nucleus. *Cell Metab, 22*(1), 31-53

Chen, H. Z., Wang, F., Gao, P., Pei, J. F., Liu, Y., Xu, T. T., Tang, X., Fu, W. Y., Lu, J., Yan, Y. F., Wang, X. M., Han, L., Zhang, Z. Q., Zhang, R., Zou, M. H., & Liu, D. P. (2016). Age-Associated Sirtuin 1 Reduction in Vascular Smooth Muscle Links Vascular Senescence and Inflammation to Abdominal Aortic Aneurysm. *Circ Res, 119*(10), 1076-1088

d'Adda di Fagagna, F. (2008). Living on a break: cellular senescence as a DNA-damage response. *Nat Rev Cancer, 8*(7), 512-522

Dantzer, F., Amé, J.-C., Schreiber, V., Nakamura, J., Ménissier-de Murcia, J., & de Murcia, G. (2006). Poly(ADP-ribose) polymerase-1 activation during DNA damage and repair. *Meth Enzymol, 409*, 493-510

de Lange, W. J., Halabi, C. M., Beyer, A. M., & Sigmund, C. D. (2008). Germ line activation of the Tie2 and SMMHC promoters causes noncell-specific deletion of floxed alleles. *Physiol Genomics, 35*(1), 1-4

de Picciotto, N. E., Gano, L. B., Johnson, L. C., Martens, C. R., Sindler, A. L., Mills, K. F., Imai, S., & Seals, D. R. (2016). Nicotinamide mononucleotide supplementation reverses vascular dysfunction and oxidative stress with aging in mice. *Aging Cell, 15*(3), 522-530

Fell, V. L., & Schild-Poulter, C. (2012). Ku regulates signaling to DNA damage response pathways through the Ku70 von Willebrand A domain. *Mol Cell Biol, 32*(1), 76-87

Fisher, A. E., Hochegger, H., Takeda, S., & Caldecott, K. W. (2007). Poly(ADP-ribose) polymerase 1 accelerates single-strand break repair in concert with poly(ADP-ribose) glycohydrolase. *Mol Cell Biol, 27*(15), 5597-5605

Frederick, D. W., Loro, E., Liu, L., Davila, A., Jr., Chellappa, K., Silverman, I. M., Quinn, W. J., 3rd, Gosai, S. J., Tichy, E. D., Davis, J. G., Mourkioti, F., Gregory, B. D., Dellinger, R. W., Redpath, P., Migaud, M. E., Nakamaru-Ogiso, E., Rabinowitz, J. D., Khurana, T. S., & Baur, J. A. (2016). Loss of NAD Homeostasis Leads to Progressive and Reversible Degeneration of Skeletal Muscle. *Cell Metab, 24*(2), 269-282

Frontini, M. J., O'Neil, C., Sawyez, C., Chan, B. M., Huff, M. W., & Pickering, J. G. (2009). Lipid incorporation inhibits Src-dependent assembly of fibronectin and type I collagen by vascular smooth muscle cells. *Circ Res, 104*(7), 832-841

Fry, J. L., Shiraishi, Y., Turcotte, R., Yu, X., Gao, Y. Z., Akiki, R., Bachschmid, M., Zhang, Y., Morgan, K. G., Cohen, R. A., & Seta, F. (2015). Vascular Smooth Muscle Sirtuin-1 Protects Against Aortic Dissection During Angiotensin II-Induced Hypertension. *J Am Heart Assoc, 4*(9), e002384

Halushka, M. K., Angelini, A., Bartoloni, G., Basso, C., Batoroeva, L., Bruneval, P., Buja, L. M., Butany, J., d'Amati, G., Fallon, J. T., Gallagher, P. J., Gittenberger-de Groot, A. C., Gouveia, R. H., Kholova, I., Kelly, K. L., Leone, O., Litovsky, S. H., Maleszewski, J. J., Miller, D. V., Mitchell, R. N., Preston, S. D., Pucci, A., Radio, S. J., Rodriguez, E. R., Sheppard, M. N., Stone, J. R., Suvarna, S. K., Tan, C. D., Thiene, G., Veinot, J. P., & van der Wal, A. C. (2016). Consensus statement on surgical pathology of the aorta from the Society for Cardiovascular Pathology and the Association For European Cardiovascular Pathology: II. Noninflammatory degenerative diseases - nomenclature and diagnostic criteria. *Cardiovasc Pathol, 25*(3), 247-257

Hayashi, S., & McMahon, A. P. (2002). Efficient recombination in diverse tissues by a tamoxifen-inducible form of Cre: a tool for temporally regulated gene activation/inactivation in the mouse. *Dev Biol, 244*(2), 305-318

Ho, C., van der Veer, E., Akawi, O., & Pickering, J. G. (2009). SIRT1 markedly extends replicative lifespan if the NAD+ salvage pathway is enhanced. *FEBS Lett, 583*(18), 3081-3085

Howard, D. P., Banerjee, A., Fairhead, J. F., Perkins, J., Silver, L. E., Rothwell, P. M., & Oxford Vascular, S. (2013). Population-based study of incidence and outcome of

acute aortic dissection and premorbid risk factor control: 10-year results from the Oxford Vascular Study. *Circulation, 127*(20), 2031-2037

Humphrey, J. D., Milewicz, D. M., Tellides, G., & Schwartz, M. A. (2014). Cell biology. Dysfunctional mechanosensing in aneurysms. *Science, 344*(6183), 477-479

Kunieda, T., Minamino, T., Nishi, J., Tateno, K., Oyama, T., Katsuno, T., Miyauchi, H., Orimo, M., Okada, S., Takamura, M., Nagai, T., Kaneko, S., & Komuro, I. (2006). Angiotensin II induces premature senescence of vascular smooth muscle cells and accelerates the development of atherosclerosis via a p21-dependent pathway. *Circulation, 114*(9), 953-960

Kuzminov, A. (2001). Single-strand interruptions in replicating chromosomes cause double-strand breaks. *Proc Natl Acad Sci U S A, 98*(15), 8241-8246

Li, S., Van Den Diepstraten, C., D'Souza, S. J., Chan, B. M., & Pickering, J. G. (2003). Vascular smooth muscle cells orchestrate the assembly of type I collagen via alpha2beta1 integrin, RhoA, and fibronectin polymerization. *Am J Pathol, 163*(3), 1045-1056

Liu, Y., Drozdov, I., Shroff, R., Beltran, L. E., & Shanahan, C. M. (2013). Prelamin A accelerates vascular calcification via activation of the DNA damage response and senescence-associated secretory phenotype in vascular smooth muscle cells. *Circ Res, 112*(10), e99-109

Matthews, C., Gorenne, I., Scott, S., Figg, N., Kirkpatrick, P., Ritchie, A., Goddard, M., & Bennett, M. (2006). Vascular smooth muscle cells undergo telomere-based senescence in human atherosclerosis: effects of telomerase and oxidative stress. *Circ Res, 99*(2), 156-164

Milewicz, D. M., Guo, D. C., Tran-Fadulu, V., Lafont, A. L., Papke, C. L., Inamoto, S., Kwartler, C. S., & Pannu, H. (2008). Genetic basis of thoracic aortic aneurysms and dissections: focus on smooth muscle cell contractile dysfunction. *Annu Rev Genomics Hum Genet, 9*, 283-302

Nassour, J., Martien, S., Martin, N., Deruy, E., Tomellini, E., Malaquin, N., Bouali, F., Sabatier, L., Wernert, N., Pinte, S., Gilson, E., Pourtier, A., Pluquet, O., & Abbadie, C. (2016). Defective DNA single-strand break repair is responsible for senescence and neoplastic escape of epithelial cells. *Nat Commun, 7*, 10399

Nikiforov, A., Kulikova, V., & Ziegler, M. (2015). The human NAD metabolome: Functions, metabolism and compartmentalization. *Crit Rev Biochem Mol Biol, 50*(4), 284-297

Noren Hooten, N., Kompaniez, K., Barnes, J., Lohani, A., & Evans, M. K. (2011). Poly(ADP-ribose) polymerase 1 (PARP-1) binds to 8-oxoguanine-DNA glycosylase (OGG1). *J Biol Chem, 286*(52), 44679-44690

Owens, A. P., 3rd, Subramanian, V., Moorleghen, J. J., Guo, Z., McNamara, C. A., Cassis, L. A., & Daugherty, A. (2010). Angiotensin II induces a region-specific hyperplasia of the ascending aorta through regulation of inhibitor of differentiation 3. *Circ Res, 106*(3), 611-619

Rai, P., Onder, T. T., Young, J. J., McFaline, J. L., Pang, B., Dedon, P. C., & Weinberg, R. A. (2009). Continuous elimination of oxidized nucleotides is necessary to prevent rapid onset of cellular senescence. *Proc Natl Acad Sci U S A, 106*(1), 169-174

Rateri, D. L., Davis, F. M., Balakrishnan, A., Howatt, D. A., Moorleghen, J. J., O'Connor, W. N., Charnigo, R., Cassis, L. A., & Daugherty, A. (2014). Angiotensin II induces region-specific medial disruption during evolution of ascending aortic aneurysms. *Am J Pathol, 184*(9), 2586-2595

Ray, J. L., Leach, R., Herbert, J. M., & Benson, M. (2001). Isolation of vascular smooth muscle cells from a single murine aorta. *Methods Cell Sci, 23*(4), 185-188

Revollo, J. R., Korner, A., Mills, K. F., Satoh, A., Wang, T., Garten, A., Dasgupta, B., Sasaki, Y., Wolberger, C., Townsend, R. R., Milbrandt, J., Kiess, W., & Imai, S. (2007). Nampt/PBEF/Visfatin regulates insulin secretion in beta cells as a systemic NAD biosynthetic enzyme. *Cell Metab, 6*(5), 363-375

Rongvaux, A., Galli, M., Denanglaire, S., Van Gool, F., Dreze, P. L., Szpirer, C., Bureau, F., Andris, F., & Leo, O. (2008). Nicotinamide phosphoribosyl transferase/pre-B cell colony-enhancing factor/visfatin is required for lymphocyte development and cellular resistance to genotoxic stress. *J Immunol, 181*(7), 4685-4695

Rongvaux, A., Shea, R. J., Mulks, M. H., Gigot, D., Urbain, J., Leo, O., & Andris, F. (2002). Pre-B-cell colony-enhancing factor, whose expression is up-regulated in activated lymphocytes, is a nicotinamide phosphoribosyltransferase, a cytosolic enzyme involved in NAD biosynthesis. *Eur J Immunol, 32*(11), 3225-3234

Ruiz-Torres, A., Gimeno, A., Melon, J., Mendez, L., Munoz, F. J., & Macia, M. (1999). Age-related loss of proliferative activity of human vascular smooth muscle cells in culture. *Mech Ageing Dev, 110*(1-2), 49-55

Schlatmann, T. J., & Becker, A. E. (1977). Histologic changes in the normal aging aorta: implications for dissecting aortic aneurysm. *Am J Cardiol, 39*(1), 13-20

Small, T. W., & Pickering, J. G. (2009). Nuclear degradation of Wilms tumor 1-associating protein and survivin splice variant switching underlie IGF-1-mediated survival. *J Biol Chem, 284*(37), 24684-24695

Stein, L. R., & Imai, S. (2014). Specific ablation of Nampt in adult neural stem cells recapitulates their functional defects during aging. *EMBO J, 33*(12), 1321-1340

Vafaie, F., Yin, H., O'Neil, C., Nong, Z., Watson, A., Arpino, J. M., Chu, M. W., Wayne Holdsworth, D., Gros, R., & Pickering, J. G. (2014). Collagenase-resistant collagen promotes mouse aging and vascular cell senescence. *Aging Cell, 13*(1), 121-130

van der Veer, E., Ho, C., O'Neil, C., Barbosa, N., Scott, R., Cregan, S. P., & Pickering, J. G. (2007). Extension of human cell lifespan by nicotinamide phosphoribosyltransferase. *J Biol Chem, 282*(15), 10841-10845

van der Veer, E., Nong, Z., O'Neil, C., Urquhart, B., Freeman, D., & Pickering, J. G. (2005). Pre-B-cell colony-enhancing factor regulates NAD+-dependent protein deacetylase activity and promotes vascular smooth muscle cell maturation. *Circ Res, 97*(1), 25-34

Wang, M., Wu, W., Wu, W., Rosidi, B., Zhang, L., Wang, H., & Iliakis, G. (2006). PARP-1 and Ku compete for repair of DNA double strand breaks by distinct NHEJ pathways. *Nucleic Acids Res, 34*(21), 6170-6182

Wang, P., Li, W. L., Liu, J. M., & Miao, C. Y. (2016). NAMPT and NAMPT-controlled NAD Metabolism in Vascular Repair. *J Cardiovasc Pharmacol, 67*(6), 474-481

Wang, P., Xu, T. Y., Guan, Y. F., Su, D. F., Fan, G. R., & Miao, C. Y. (2009). Perivascular adipose tissue-derived visfatin is a vascular smooth muscle cell growth factor: role of nicotinamide mononucleotide. *Cardiovasc Res, 81*(2), 370-380

Xin, H. B., Deng, K. Y., Rishniw, M., Ji, G., & Kotlikoff, M. I. (2002). Smooth muscle expression of Cre recombinase and eGFP in transgenic mice. *Physiol Genomics, 10*(3), 211-215

Yin, H., & Pickering, J. G. (2016). Cellular Senescence and Vascular Disease: Novel Routes to Better Understanding and Therapy. *Can J Cardiol, 32*(5), 612-623

Yin, H., van der Veer, E., Frontini, M. J., Thibert, V., O'Neil, C., Watson, A., Szasz, P., Chu, M. W., & Pickering, J. G. (2012). Intrinsic directionality of migrating vascular smooth muscle cells is regulated by NAD(+) biosynthesis. *J Cell Sci, 125*(Pt 23), 5770-5780

Zhou, C. C., Yang, X., Hua, X., Liu, J., Fan, M. B., Li, G. Q., Song, J., Xu, T. Y., Li, Z. Y., Guan, Y. F., Wang, P., & Miao, C. Y. (2016). Hepatic NAD(+) deficiency as a therapeutic target for non-alcoholic fatty liver disease in ageing. *Br J Pharmacol, 173*(15), 2352-2368

CHAPTER 3 - NICOTINAMIDE PHOSPHORIBOSYLTRANSFERASE IN SMOOTH MUSCLE CELLS IS SUPPRESSED IN HUMAN THORACIC AORTIC ANEURYSM DISEASE

3.1 Introduction

The aorta is a highly important conduit vessel that collects oxygenated blood from the heart and delivers it to the branching and peripheral vessels supplying every organ and tissue in the body. Failure of this vessel is often catastrophic. As outlined in previous chapters, the aorta is structurally designed to withstand stress; however, it can nevertheless degenerate over time when subjected to hypertension, atherosclerosis, or the effect of genetic mutations (Schlatmann and Becker 1977, Howard et al. 2013)

Thoracic aortic diseases (TAD) encompass dilation as well as aneurysms and dissections of the ascending or descending thoracic aorta (Ramanath et al. 2009). Population-based studies estimate an annual incidence of 6-16 cases per 100,000, and aortic dissection is the most devastating complication of TAD (Kuzmik et al. 2012, Andelfinger et al. 2016). Clinical studies have suggested that a familial predisposition exists for TADs: up to 20% of individuals who do not have features of Marfan syndrome, vascular Ehlers Danlos syndrome, or Loeys-Dietz syndrome have a familial history of TAD (Milewicz and Regalado 1993, Biddinger et al. 1997). In these individuals there is at least one genetic cause. To date, there are a number of causative genes identified, including those associated with extracellular matrix regulation, cytoskeleton, and the TGF-β signalling pathway (Coady et al. 1999, Zhang et al. 2013, Zhang and Wang 2016).

It has recently become evident that Nampt is a determinant of SMC health and longevity. Nicotinamide phosphoribosyltransferase (Nampt) is the rate-limiting enzyme for the NAD^+ salvage pathway, converting nicotinamide to nicotinamide mononucleotide (van der Veer et al. 2005). As outlined in previous chapters, nicotinamide adenine dinucleotide (NAD^+) is an essential dinucleotide that serves as a cofactor for the oxidation-reduction

events of cellular nutrient metabolism. NAD^+ can also serve as a signaling nucleotide that regulates gene expression, genome integrity, and mitochondrial function. I have previously shown that Nampt is crucial to the aortic resistance of hemodynamic stress in a mouse model of SMC Nampt depletion (Watson et al. 2017). In this model, SMC Nampt depletion led to an absence of Parp1 activity (the activity of which depends on the requisite bioavailability of NAD^+) and an accumulation of DNA damage. This accumulation was associated with an increase in aortic dissection events.

I have studied the expression of NAMPT in the aortic media of patients with life-threatening thoracic aortic dilation disease. The findings reveal that the expression of NAMPT is in the aortic media of human aotopathy patients is negatively correlated with aortic diameter. Additionally, low levels of NAMPT expression in dilated human aortopathy samples are associated with the presence of double-strand DNA breaks in aortic smooth muscle cells. The findings also shed new light on the epigenetic mechanisms that may underlie vulnerability in NAD^+ homeostasis in human thoracic aortopathy.

3.2 Methods

3.2.1 Human aorta material

Human ascending aortic tissue was obtained from patients undergoing ascending aortic replacement, coronary bypass surgery, or cardiac transplantation, as approved by the institutional review board of Western University Research Ethics Committee. Maximum aortic diameter was determined from contrast-enhanced CT scan or echocardiogram obtained prior to surgery. NAMPT levels were assessed by histology of the aortopathy material, performed on the maximally dilated region of the ascending aorta. *NAMPT* transcript abundance was assessed in human aortic medial tissue from which the adventitial and intimal layers were dissected away. RNA was isolated using TRIzol (Life Technologies) and the RNeasy Mini Kit following the manufacturer's protocol (Qiagen,

Valencia, CA). Human aortic SMCs were isolated by explant outgrowth as previously described (Vafaie et al. 2014).

3.2.2 Immunohistochemistry of human aortic tissue

NAMPT immunostaining was performed on paraformaldehyde-fixed, paraffin-embedded sections as above. NAMPT staining was quantified in 5 equally spaced fields of view (x40 objective) across the specimen, avoiding regions of inflammatory cell infiltration and vascularization to restrict analyses to medial SMCs. Signal was quantified using ImageJ software (NIH) with a DAB Deconvolution Plugin that separates the hematoxylin from the DAB signal. Background signal was ascertained in each tissue by capitalizing on the normal presence of interlamellar regions that do not contain SMCs. An area of at least 300 μm^2 was utilized for this. The SMC NAMPT signal was determined as the cumulative signal intensity and expressed relative to the number of nuclei in the field of view.

Sections were also double-stained for NAMPT and γ-H2AX (ab26350, 1:100; Abcam, Cambridge, MA). Bound primary antibodies were visualized with Alexa Fluor 488-conjugated donkey anti-rabbit secondary antibody and Alex Fluor 546-conjugated anti-mouse secondary antibody, respectively (Molecular Probes). Nuclei were counterstained with DAPI. NAMPT and γ-H2AX signal intensities were determined a cell-by-cell basis (total of 524 cells) using ImageJ.

3.2.3 Quantitative real-time reverse transcription–polymerase chain reaction

Total RNA was isolated from homogenates of aortic media using TRIzol (Life Technologies) and the RNeasy Mini Kit following the manufacturer's protocol (Qiagen, Valencia, CA). Total RNA was isolated from human SMCs using the RNeasy Mini Kit following the manufacturer's protocol. Transcript abundance of *NAMPT* and 18S were assessed using SYBR-green chemistry-based primer sets (human *NAMPT* F-AGGGTTACAAGTTGCTGCCACC R-CTCCACCAGAACCGAAGGCAAT; human 18S

F-ACCCGTTGAACCCCATTCGTGA R-GCCTCACTAAACCATCCAATCGG). Quantitative real-time RT-PCR was performed using an ABI Prism (model 7900HT) and Sequence Detection System software (Life Technologies; Applied Biosystems). For human aortic medial tissue and human primary SMCs, mRNA abundance was quantified based on the standard curve method, with 18S mRNA as an internal reference control, and expressed as relative units (r.u.)

3.2.4 Analysis of DNA methylation

Human aortic media was isolated by laser capture microdissection of 10 μm-thick frozen sections. Genomic DNA was harvested from this tissue and from cultured human SMCs using the DNeasy Blood and Tissue Kit (Qiagen). DNA was subjected to selective digestion-based PCR to quantify methylation status using the Epitect Methyl DNA Restriction Kit (Qiagen) and the pre-designed Epitect qPCR Methyl Promoter Primer set (335002 EPHS113392-1A). The amount of input DNA that was methylated was determined using the manufacturer-supplied algorithm.

3.2.5 Statistical analyses

Values are expressed as mean±standard error of the mean. Statistical analyses were performed using GraphPad Prism software (GraphPad, La Jolla, CA, USA). Mean data were compared using Student's t-test or one- or two-way ANOVA with Holm-Sidak *post hoc* testing. The relationship between NAMPT content and human aortic dilatation was determined using linear regression analysis (SPSS, IBM Corp. Armonk, NY). To assess the single-cell relationship between NAMPT and g-H2AX signal, within-patient cellular NAMPT content was segregated into tertiles.

3.3 Results

3.3.1 Medial SMCs in dilated human thoracic aortas have reduced NAMPT

To determine if NAMPT is expressed in SMCs of the human aorta, I evaluated ascending aortas surgically harvested from patients with dilated ascending aortopathy (n=20, mean age 58.4±16.4) and compared the findings with those of non-dilated ascending aorta harvested from individuals undergoing heart transplantation or coronary artery bypass surgery (n=16, mean age 68.7±14.1). The mean aortic diameter of diseased ascending aortas measured at the maximally dilated point was 54.3±9.5 mm. The mean aortic diameter of control ascending aortas was 31.1±2.8 mm (P<0.0001). Individual patient demographic data, aortic diameter, and aortic valve configuration and function are presented in Table 3.1.

Immunostaining revealed widespread NAMPT expression in medial SMCs of the normal calibre aortas, with signal in both cytoplasm and nucleus (Fig. 3.1a). Medial cell NAMPT expression was also evident in dilated aortas. However, the NAMPT signal was more heterogeneous, and largely absent from the nucleus (Fig.3.1 b-c) DAB intensity analysis revealed that the NAMPT staining signal was 34% lower in dilated aortas (Fig. 3.2a). Reduced NAMPT expression in the media of dilated aortas was also observed at the transcript level (Fig. 3.2b). Interestingly, there was an inverse relationship between aortic medial NAMPT content and the maximal diameter of the ascending aorta (R^2=0.44, P<0.0001). This inverse relationship existed for both the entire patient cohort as well as only those patients with ascending aortopathy (R^2=0.31, P=0.009, Fig. 3.2c), and persisted after adjusting for patient age (P=0.016). These findings implicate a NAMPT-based NAD^+ biosynthesis pathway within SMCs of the human aorta. Moreover, they suggest that this local biosynthetic machinery is related to aortic medial integrity.

Table 3-1 Demographic and clinical characteristics of study subjects

Age	Sex	Aortic valve configuration	Aortic Valve Dysfunction	Maximum diameter of ascending aorta (mm)
64	Female	Bicuspid	Severe AR	54
82	Male	Tricuspid	Moderate AR	57
37	Male	Bicuspid	None	57
44	Male	Bicuspid	Severe AR	68
73	Male	Bicuspid	Moderate AR/AS	55
55	Male	Tricuspid	Severe AR*	77
59	Male	Bicuspid	Severe AS	42
40	Male	Bicuspid	Severe AR/AS	57
64	Male	Bicuspid	Severe AS	43
80	Female	Tricuspid	Moderate AR	56
79	Male	Bicuspid	None	56
75	Female	Tricuspid	None	63
52	Male	Bicuspid	Moderate AR	61
56	Male	Bicuspid	None	53
32	Male	Bicuspid	Severe AR	40
62	Male	Tricuspid	Moderate AR	60
61	Male	Bicuspid	Severe AS	43
49	Female	Bicuspid	Severe AS	41
30	Female	Tricuspid	Mild AR*	50
75	Male	Bicuspid	Moderate AR	54
83	Male	Tricuspid	None (CAD)	35
53	Male	Tricuspid	None (CAD)	30
85	Female	Tricuspid	None (CAD)	33
ND	ND	ND	None (Transplant donor)	ND
70	Female	Tricuspid	None (Transplant recipient)	24
39	Female	Tricuspid	None (Transplant recipient)	29
70	Male	Tricuspid	None (CAD)	34
78	Male	Tricuspid	None (CAD)	32
79	Female	Tricuspid	Moderate AS	28
86	Female	Tricuspid	None (CAD)	33
78	Male	Tricuspid	None (Mitral valve insufficiency)	31
50	Male	Tricuspid	None (CAD)	31
68	Female	Tricuspid	None (CAD)	29
72	Male	Tricuspid	None (CAD)	32
66	Male	Tricuspid	None (CAD)	34
54	Male	Tricuspid	None (CAD)	32

***Marfan syndrome; AR-Aortic Regurgitation; AS-Aortic Stenosis; CAD-coronary artery disease**

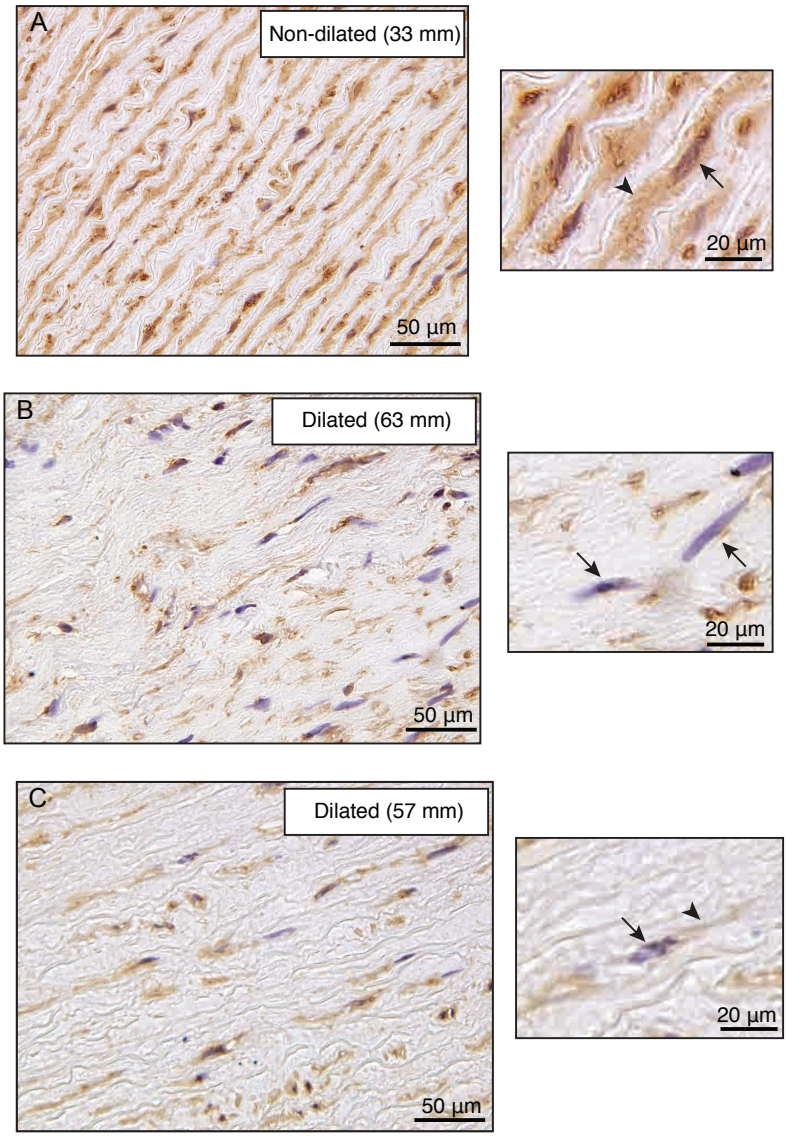

Figure 3.1 NAMPT is present in the nucleus and cytoplasm of SMCs in the media of human aortic media

Photomicrographs of paraformaldehyde-fixed non-dilated (**A**) and dilated (**B, C**) human aorta sections immunostained for NAMPT and counterstained with hematoxylin. Arrow in zoomed image of A depicts nuclear signal and arrowhead depicts cytoplasmic signal. Arrows in zoomed image of **B** indicate NAMPT-negative cells. Arrow in zoomed image of **C** indicates absent nuclear signal and arrowhead depicts weak cytoplasmic signal.

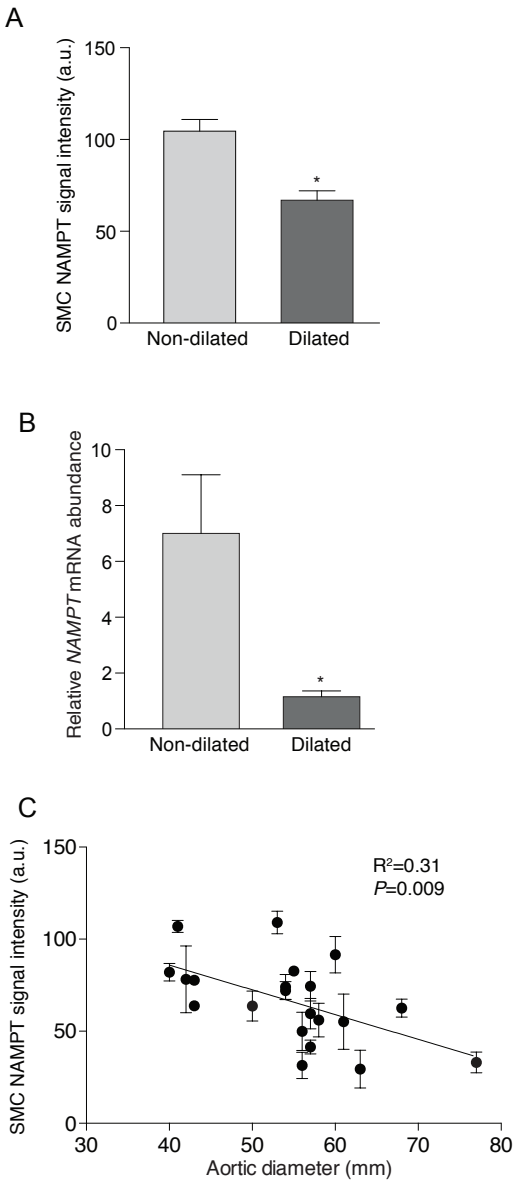

Figure 3.2 Human ascending aortic dilation is associated with reduced NAMPT

A. Graph depicting NAMPT content – immunostaining signal per cell - in aortas from patients with control, non-dilated aortas (n=16) and dilated aortas (n=20). **P*<0.0001 **B**. Graph depicting *NAMPT* mRNA abundance in control (n=6) and dilated (n=6) aortas. *P*=0.038 *NAMPT* mRNA abundance was normalized to *18S* mRNA abundance **C**. Inverse relationship between NAMPT content in dilated aortas and aortic diameter; n=20.

3.3.2 The media of dilated human thoracic aortas is populated by SMCs with DNA strand breaks and low NAMPT

Given my previous work demonstrating compromised genomic integrity in the mouse models (Watson et al. 2017), I asked if DNA integrity was compromised in SMCs within the human ascending aorta. This was of interest because although double-strand DNA breaks have been found in atherosclerotic lesions (Gray et al. 2015), the media of the non-atherosclerotic aorta is considered a more quiescent vascular setting. Remarkably, γ-H2AX-immunostaining revealed that 25% of normal caliber aortas contained unrepaired DNA strand breaks in the medial layer cells. On average, 2.4% of medial cells displayed DNA damage foci (range 0-10.1%). Even more striking was that 90% of aortopathy samples had evidence of unrepaired DNA strand breaks, with an average of 28.7% SMCs with DNA damage foci (range 7.3-60.0% of cells, Fig. 3.3a). To more precisely define the relationship between NAMPT expression and unrepaired DNA damage, I double-immunolabeled aortas for NAMPT and γ-H2AX (Fig. 3.3b). NAMPT content was then quantified in a total of 524 individual SMCs, which were separated into tertiles based on NAMPT expression. SMCs in the lowest tertile had more than 5-fold greater DNA damage signal than those in the mid and highest NAMPT tertiles (Fig. 3.3c).

3.3.3 Hypermethylation of the NAMPT promoter in dilated human thoracic aortas

Given the linkages between low NAMPT and DNA damage, I assessed what might underlie the low NAMPT in human thoracic aortopathy. Epigenetic control of genes relevant to aortopathy has recently been described (Gomez et al. 2013). To determine if this might be the case for *NAMPT*, I first assessed if the expression profile of *NAMPT* in human aortic SMCs was preserved between in vivo and culture environments. This revealed that *NAMPT* transcript abundance in early passage SMCs correlated with NAMPT abundance in the corresponding aortic media (R^2=0.72, P=0.004, Fig. 3.4a). Furthermore, *NAMPT* transcript abundance in SMCs derived from both normal and dilated aortas was stable over

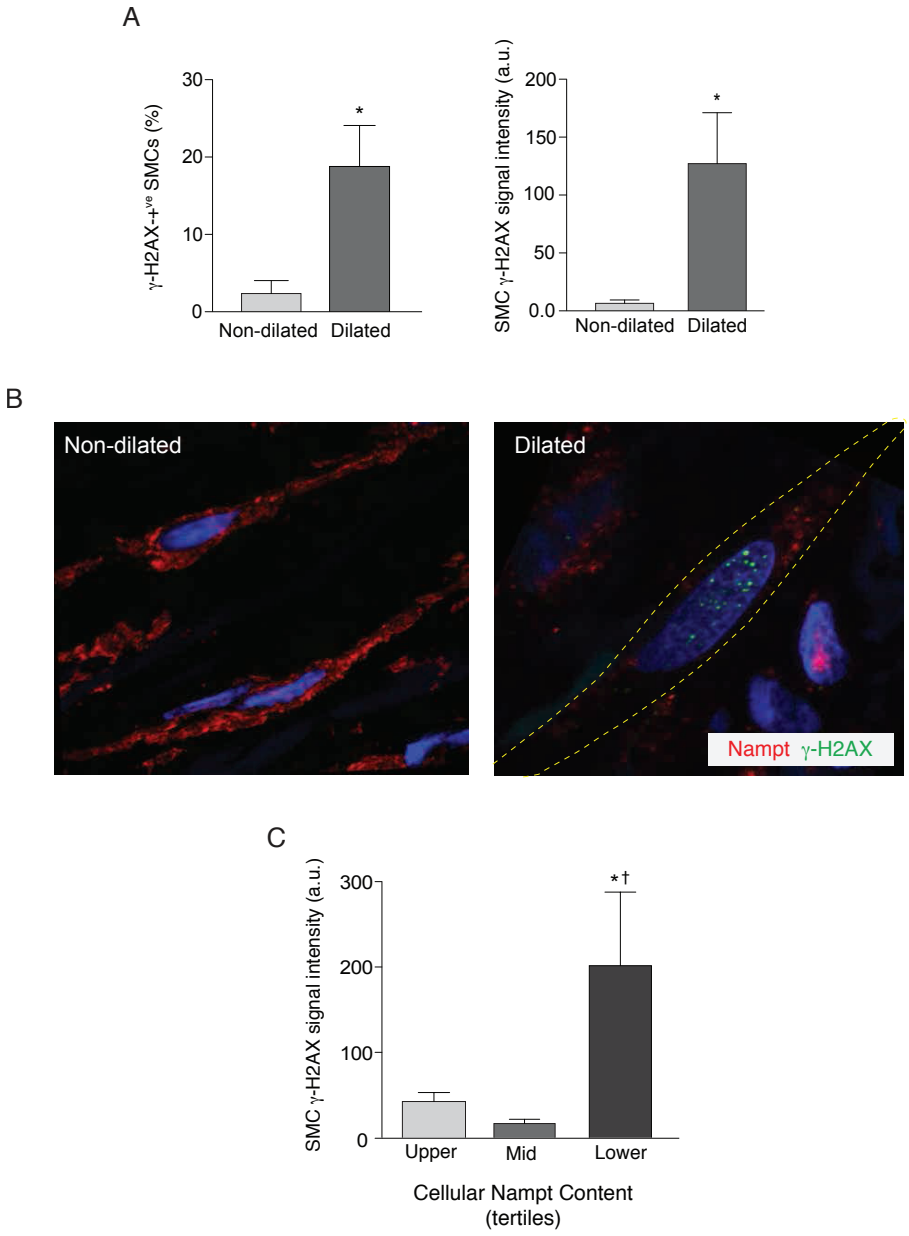

Figure 3.3 Correlation of double-strand DNA damage with reduced NAMPT in human aortic SMCs

A. Prevalence of medial SMCs in aortas with γ-H2AX signal (Right, **P*=0.047) and intensity of γ-H2AX signal (Left, **P*=0.021). **B**. Confocal photomicrographs illustrating reciprocal relationship between NAMPT (green) and γ-H2AX-positivity (red) in human ascending aorta. Nuclei were counterstained with DAPI. **C**. Cellular DNA damage signal, stratified by cellular NAMPT content in 524 independent cells. **P*=0.034 vs. upper NAMPT tertile, †*P*=0.013 vs. mid NAMPT tertile.

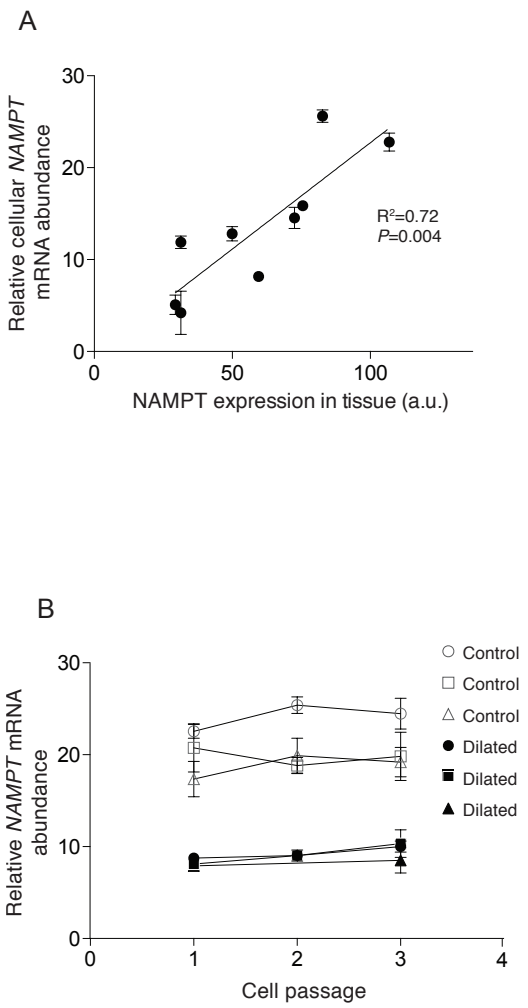

Figure 3.4 Cultured SMCs from patients with dilated ascending aortopathy express *NAMPT*

A. Relationship between *NAMPT* transcript abundance in human SMCs cultured from the ascending aorta and NAMPT content in situ in the corresponding aortic media, as assessed by immunostaining. **B**. *NAMPT* transcript abundance in early passage human SMCs derived from control and dilated patients measured over early serial cell subcultures, showing stability.

3 serial subcultures and differences between patient SMCs were maintained (Fig. 3.4b). To determine if there was potential for epigenetic control by DNA methylation, I performed a bioinformatic assessment (http://genome.ucsc.edu/) of the *NAMPT* gene locus. Bioinformatic tools provided by the UCSC genome browser predicted a ~1000-base CpG island surrounding the *NAMPT* transcriptional start site (Fig. 3.5). CpG islands are regions with a high frequency of CpG sites. Methylation of cytosine residues in the region of the transcriptional start site (in the context of CpG dinucleotides) could serve as an epigenetic repression of gene transcription (Jones 2012). Methylation analysis using selective digestion-based PCR revealed little to no methylation of *NAMPT* promoter DNA from non-dilated human aortas. However, 13.0±4.1% of input DNA from dilated aortas was methylated (P=0.044, Fig. 3.6a). Furthermore, in SMCs cultured from the ascending aorta, the level of promoter methylation inversely correlated with *NAMPT* mRNA abundance in the corresponding SMCs (R^2=0.028, P=0.024). This also revealed that the *NAMPT* promoter in SMCs from patients with dilated aortas was hypermethylated relative to that of SMCs cultured from control aortas (P=0.004, Fig. 3.6b,c).

3.4 Discussion

By evaluating human aortopathy material, I demonstrate that: i) NAMPT is reduced in the aortic media of patients with aneurysmal thoracic aortic disease, ii) SMCs with low NAMPT and unrepaired DNA damage constitute a previously unrecognized SMC phenotype in human aortopathy, and iii) low NAMPT levels in human aortopathy are associated with hypermethylation of the *NAMPT* promoter.

The possibility that the functional linkage between low SMC Nampt and aortic degeneration in mice translates to human aortopathy was supported by several findings. SMC NAMPT content was lower in dilated human aortas that in non-dilated aortas. Moreover, there was an inverse relationship between the aortic diameter and medial SMC

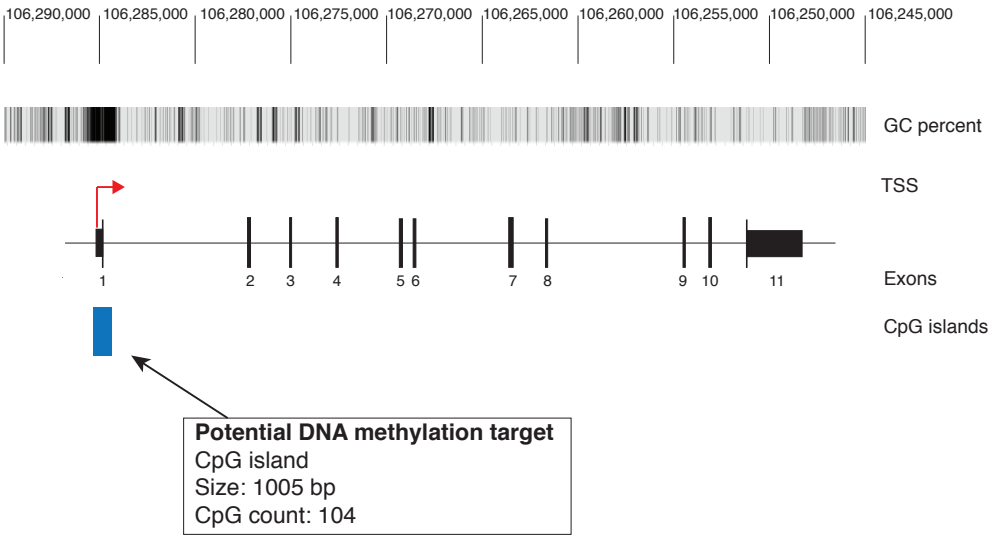

Figure 3.5 The promoter region of *NAMPT* is associated with a potential CpG locus

Scale diagrammatic representation of the *NAMPT* gene locus including the genome base position (Top row), the percentage of G (guanine) and C (cytosine) bases in 5-base windows (Second row; low to high GC content is expressed by light to very dark colour), the transcription start site of *NAMPT* (TSS, third row), *NAMPT* exon position (Fourth row), and the putative location of a CpG island (Fifth row).

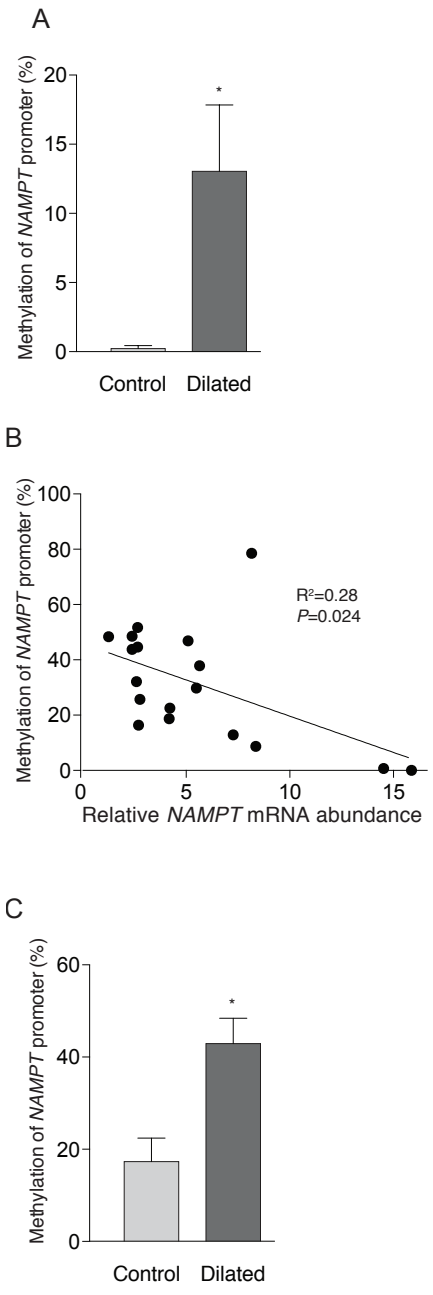

Figure 3.6 Hypermethylation of the *NAMPT* promoter in the aortic media and cultured SMCs of patients with dilated ascending aortopathy

A. Methylation of the *NAMPT* promoter in the media of control, non-dilated (n=3) and dilated (n=6) aortas, *P=0.044 vs. control. **B**. Relationship between methylation of the *NAMPT* promoter in primary early passage (1-4) human SMCs and *NAMPT* transcript abundance in the respective SMCs. **C**. Methylation of the *NAMPT* promoter in early passage human SMCs derived from the ascending aorta of patients with non-dilated (n=8) and dilated (n=10) aortas, *P=0.004 vs. control.

NAMPT content. This fits an emerging pattern of reduced Nampt in aged or compromised tissues (Yoshino et al. 2011, Stein and Imai 2014), and the current study may be the first to identify such a relationship in human diseased tissue. It is noted that aortic medial dissection, prominent in the previous mouse model work, was not represented in the patient series. Nonetheless, ascending aortic diameter is a strong predictor of dissection risk in patients (Hiratzka et al. 2010). Also remarkable was the discovery of unrepaired DNA breaks in aortic medial SMCs in situ and the relatively high prevalence of this genome pathology in the aorta of individuals with aortopathy. Although the data do not prove causation, the single-cell relationship between low NAMPT and unresolved DNA strand breaks strengthens the potential for a mechanistic relationship. Moreover, the combination of unresolved DNA breaks and low Nampt can be considered to denote a SMC phenotype of substantially declined cellular vitality.

The findings indicate that low Nampt, while not necessarily an inciting event, can substantially compromise the manner in which the aorta responds to stress independent of the primary cause of the aortopathy. Low aortic NAMPT was observed not only the dilated aortas of patients with a bicuspid aortic valve but also those with a tricuspid aortic valve and Marfan syndrome. A larger series would be required to determine if there are aortic disease-specific differences in NAD^+ control and also if NAD^+ homeostasis in SMCs is relevant to atherosclerotic abdominal aortic aneurysms. The chronic nature of aortic dilation disease is such that a suboptimal NAD^+ regenerating system could both potentiate and sustain aortic wall degeneration.

In summary, I demonstrate that low Nampt within medial SMCs is associated with a degenerative aortic phenotype; findings that raise the possibility that disturbed local NAD^+ metabolism underlies the progression of degenerative aortic disease.

3.5 References

Andelfinger, G., Loeys, B., & Dietz, H. (2016). A Decade of Discovery in the Genetic Understanding of Thoracic Aortic Disease. *Can J Cardiol, 32*(1), 13-25

Biddinger, A., Rocklin, M., Coselli, J., & Milewicz, D. M. (1997). Familial thoracic aortic dilatations and dissections: a case control study. *J Vasc Surg, 25*(3), 506-511

Coady, M. A., Davies, R. R., Roberts, M., Goldstein, L. J., Rogalski, M. J., Rizzo, J. A., Hammond, G. L., Kopf, G. S., & Elefteriades, J. A. (1999). Familial patterns of thoracic aortic aneurysms. *Arch Surg, 134*(4), 361-367

Gomez, D., Kessler, K., Michel, J. B., & Vranckx, R. (2013). Modifications of chromatin dynamics control Smad2 pathway activation in aneurysmal smooth muscle cells. *Circ Res, 113*(7), 881-890

Gray, K., Kumar, S., Figg, N., Harrison, J., Baker, L., Mercer, J., Littlewood, T., & Bennett, M. (2015). Effects of DNA damage in smooth muscle cells in atherosclerosis. *Circ Res, 116*(5), 816-826

Hiratzka, L. F., Bakris, G. L., Beckman, J. A., Bersin, R. M., Carr, V. F., Casey, D. E., Jr., Eagle, K. A., Hermann, L. K., Isselbacher, E. M., Kazerooni, E. A., Kouchoukos, N. T., Lytle, B. W., Milewicz, D. M., Reich, D. L., Sen, S., Shinn, J. A., Svensson, L. G., Williams, D. M., (2010). 2010 Guidelines for the diagnosis and management of patients with Thoracic Aortic Disease: a report of the American College of Cardiology Foundation/American Heart Association Task Force on Practice Guidelines, American Association for Thoracic Surgery, American College of Radiology, American Stroke Association, Society of Cardiovascular Anesthesiologists, Society for Cardiovascular Angiography and Interventions, Society of Interventional Radiology, Society of Thoracic Surgeons, and Society for Vascular Medicine. *Circulation, 121*(13), e266-369

Howard, D. P., Banerjee, A., Fairhead, J. F., Perkins, J., Silver, L. E., Rothwell, P. M., & Oxford Vascular, S. (2013). Population-based study of incidence and outcome of acute aortic dissection and premorbid risk factor control: 10-year results from the Oxford Vascular Study. *Circulation, 127*(20), 2031-2037

Jones, P. A. (2012). Functions of DNA methylation: islands, start sites, gene bodies and beyond. *Nat Rev Genet, 13*(7), 484-492

Kuzmik, G. A., Sang, A. X., & Elefteriades, J. A. (2012). Natural history of thoracic aortic aneurysms. *J Vasc Surg, 56*(2), 565-571

Milewicz, D. M., & Regalado, E. (1993). Heritable Thoracic Aortic Disease Overview. In R. A. Pagon, M. P. Adam, H. H. Ardinger, S. E. Wallace, A. Amemiya, L. J. H. Bean, T. D. Bird, N. Ledbetter, H. C. Mefford, R. J. H. Smith, & K. Stephens (Eds.), *GeneReviews(R)*. Seattle (WA).

Ramanath, V. S., Oh, J. K., Sundt, T. M., 3rd, & Eagle, K. A. (2009). Acute aortic syndromes and thoracic aortic aneurysm. *Mayo Clin Proc, 84*(5), 465-481

Schlatmann, T. J., & Becker, A. E. (1977). Histologic changes in the normal aging aorta: implications for dissecting aortic aneurysm. *Am J Cardiol, 39*(1), 13-20

Stein, L. R., & Imai, S. (2014). Specific ablation of Nampt in adult neural stem cells recapitulates their functional defects during aging. *EMBO J, 33*(12), 1321-1340

Vafaie, F., Yin, H., O'Neil, C., Nong, Z., Watson, A., Arpino, J. M., Chu, M. W., Wayne Holdsworth, D., Gros, R., & Pickering, J. G. (2014). Collagenase-resistant collagen promotes mouse aging and vascular cell senescence. *Aging Cell, 13*(1), 121-130

van der Veer, E., Nong, Z., O'Neil, C., Urquhart, B., Freeman, D., & Pickering, J. G. (2005). Pre-B-cell colony-enhancing factor regulates NAD+-dependent protein deacetylase activity and promotes vascular smooth muscle cell maturation. *Circ Res, 97*(1), 25-34

Watson, A., Nong, Z., Yin, H., O'Neil, C., Fox, S., Balint, B., Guo, L., Leo, O., Chu, M. W. A., Gros, R., & Pickering, J. G. (2017). Nicotinamide Phosphoribosyltransferase in Smooth Muscle Cells Maintains Genome Integrity, Resists Aortic Medial Degeneration, and Is Suppressed in Human Thoracic Aortic Aneurysm Disease. *Circ Res, 120*(12), 1889-1902

Yoshino, J., Mills, K. F., Yoon, M. J., & Imai, S. (2011). Nicotinamide mononucleotide, a key NAD(+) intermediate, treats the pathophysiology of diet- and age-induced diabetes in mice. *Cell Metab, 14*(4), 528-536

Zhang, L., & Wang, H. H. (2016). The genetics and pathogenesis of thoracic aortic aneurysm disorder and dissections. *Clin Genet, 89*(6), 639-646

Zhang, P., Zhang, E., Fan, J., & Gu, J. (2013). Non-syndromic thoracic aortic aneurysms and dissections--a genetic review. *Front Biosci (Landmark Ed), 18*, 305-311

CHAPTER 4 - NAMPT IN SMOOTH MUSCLE CELLS REGULATES EXTRACELLULAR MATRIX GENE EXPRESSION HOMEOSTASIS

4.1 Introduction

Vascular smooth muscle cells (SMCs) perform a number of functions that are relevant to withstanding hemodynamic stress, including contraction and the synthesis and assembly of extracellular matrix (ECM) components (Li et al. 2003, Humphrey et al. 2014). The aorta is an elastic artery of which the main structural components, outside of smooth muscle cells, are elastin, collagen fibres, and a proteoglycan-rich ground substance. In most instances of thoracic aortic disease, regardless of etiology, there is a disruption in the extracellular matrix (Ishii and Asuwa 2000, Koullias et al. 2004, Borges et al. 2009). The underlying molecular mechanisms that control how SMCs in the aorta tightly regulate ECM production during environmental stress remains poorly understood.

My work in previous chapters has shown that the regeneration of nicotinamide adenine dinucleotide (NAD^+) by Nampt in SMCs is essential to maintaining an aorta that is resistant to hemodynamic stress. Nampt is expressed in cultured SMCs and its content and activity decline during advanced SMC aging (van der Veer et al. 2005, van der Veer et al. 2007). As well, Nampt has been found to regulate in vitro SMC longevity and migratory behavior (van der Veer et al. 2007, Yin et al. 2012). I have shown that NAMPT content is decreased in aortic samples from aortopathy patients and that this decrease is correlated with an increase in DNA lesions and SMC senescence (Watson et al. 2017). However, it is unclear if there is a direct link between a decrease in Nampt in the aorta and the integrity of the ECM.

To elucidate relationships between expression of Nampt in SMCs and gene expression profiles, I have undertaken genome-wide assessment of mouse aortic SMCs. I report that when *Nampt* is ablated in SMCs, there is a striking change in overall gene

transcription. Importantly, this includes the expression of transcripts associated with collagen and proteoglycan expression and assembly. I further report that there is a decrease in fibrillar collagen in SMC-*Nampt* KO mouse aortas and an increase in proteoglycan accumulation. Bioinformatic analysis suggested that these changes are potentially mediated by an upstream shift in the transcription regulator Smad7.

4.2 Methods

4.2.1 Generation of Nampt-deficient smooth muscle cells in vitro

Mouse experiments followed protocols approved by the Western University Animal Use Committee. All mice were on a C57Bl/6 background. We generated mice in which *Nampt* could be globally and inducibly deleted. *Nampt*$^{flox/flox}$ mice (Rongvaux et al. 2008) were bred with mice expressing Cre recombinase fused to the mutated ligand binding domain of the human estrogen receptor (ER) under the control of a chimeric cytomegalovirus immediate-early enhancer/chicken ß-actin promoter (*B6.Cg-Tg(CAG-Cre/Esr1)5Amc/J*) (Jackson Laboratories, Bar Harbor, ME) (Hayashi and McMahon 2002). Aortas were harvested from 8-10-week-old mice anesthetized mice in one piece, and placed in sterile PBS. The adventitial layer was removed, and the endothelial layer scraped away. Aortas were minced into 3-4 mm pieces and mouse aortic SMCs were isolated via digestion using type III porcine pancreatic elastase (250 μg/ml, Sigma) and type I collagenase (1 μg/ml, Worthington Biochemical Corporation, Lakewood, NJ) (Ray et al. 2001). Aortic tissue was digested at 37°C with agitation for 1-4 hours. SMCs were maintained in DMEM-F12 with addition of a SMC-specific bullet kit: smGM-2 BulletKit (Lonza, Allendale, NJ). SMC identity was confirmed by immunostaining for smooth muscle α-actin. SMCs harvested from aortas of *Nampt*$^{flox/flox}$ Cre-ERT2+ mice were subjected to 1 μM hydroxy-tamoxifen for 24 hours. In order to control for the effect of tamoxifen, *Nampt*$^{flox/flox}$ Cre-ERT2- (control) SMCs were also subjected to 1 μM hydroxy-

tamoxifen for 24 hours. SMCs underwent a maximum of five subcultures, and experiments were performed with cells from the third or fourth subculture.

4.2.2 Generation of SMC-Nampt deficient mice

We generated mice with a SMC-specific knockout of *Nampt* as previously described (Watson et al. 2017). Briefly, an initial cross was undertaken between female mice harbouring loxP sites flanking exons 5 and 6 of *Nampt* (*Nampt*$^{flox/flox}$) (Rongvaux et al. 2008) and male transgenic mice expressing Cre recombinase and eGFP under the control of the SMC-specific myosin heavy chain promoter (smMHC-Cre/eGFP, Jackson Laboratories, Bar Harbor, ME) (Xin et al. 2002). In a second round of breeding, the male SMC-targeted *Nampt* heterozygotes (*Nampt*$^{flox/+}$; smMHC-Cre+) were bred with female *Nampt*$^{flox/flox}$ mice to generate *Nampt*$^{flox/+}$; smMHC-Cre- (control) and *Nampt*$^{flox/flox}$; smMHC-Cre+ (SMC-*Nampt* KO) mice.

4.2.3 RNA isolation, quality assessment, probe preparation and GeneChip hybridization

Total RNA was prepared from three independent cell cultures of control mouse aortic smooth muscle cells, and three independent cell cultures of mouse aortic smooth muscle cells wherein *Nampt* had been knocked out (*Nampt*-KO SMCs). All six independent cells cultures were harvested at passage three. Cell monolayers were harvested using trypsin and lysed with QIAshredder columns (Qiagen). Total RNA was isolated using an RNeasy Mini Kit (Qiagen), and eluted with nuclease-free water.

All subsequent sample handling, labeling, and GeneChip (Human Gene 1.0 ST arrays) processing was performed at the London Regional Genomics Center (Robarts Research Institute, London, Ontario, Canada; http://www.lrgc.ca). RNA quality was assessed using an Agilent 2100 Bioanalyzer (Agilent Technologies Inc., Palo Alto, CA) and the RNA 6000 Nano kit (Caliper Life Sciences, Mountain View, CA). Single stranded

complimentary DNA was prepared from 100 ng of total RNA as per the Affymetrix GeneChip WT PLUS Reagent Kit (Affymetrix, Santa Clara, CA). Total RNA was first converted to cDNA, followed by in vitro transcription to make cRNA. 5.5 μg of single stranded cDNA was synthesized, end labeled and hybridized, for 16 h at 45 °C, to Mouse Gene 2.0 ST arrays (Affymetrix). All liquid handling steps were performed by a GeneChip Fluidics Station 450 and GeneChips were scanned with the GeneChip Scanner 3000 7G (Affymetrix) using Command Console v3.2.4.

4.2.4 Statistical analyses of changes in global gene expression

All microarray data complies with MIAME guidelines. Probe level (.CEL file) data was generated using Affymetrix Command Console v3.2.4. Probes were summarized to gene level data in Partek Genomics Suite v6.6 (Partek) using the robust multi-array average (RMA) algorithm (Irizarry et al. 2003). Partek was used to determine gene level ANOVA *P*-values and fold changes. A filtered gene list was generated for expression changes of least 1.5 fold and having a *P*-value of less than 0.05. A Fisher's exact test was used to create *P*-values for GO and KEGG Pathway enrichment. Gene ontology (GO) and KEGG pathway analysis was performed using the online resource DAVID (available at https://david.ncifcrf.gov) (Huang da et al. 2009, Huang da et al. 2009). Upstream Regulators were generated through the use of QIAGEN's Ingenuity Pathway Analysis (IPA®) and the Biological Processes and QIAGEN's Ingenuity® iReport (QIAGEN Redwood City, www.qiagen.com/ingenuity).

4.2.5 NAD^+ measurement

Mouse aortic SMC NAD^+ levels were determined in freshly harvested cells. NAD^+ content in the mouse aortic media was determined using a colorimetric kit (BioVision Research Products, Mountain View, CA, USA) and expressed relative to total protein content.

4.2.6 Real time quantitative PCR

Changes in the expression of selected genes were independently assessed by real time quantitative PCR (qRT-PCR). cDNA was synthesized from RNA samples from control and *Nampt*-KO SMCs (isolated as noted above), in addition to total RNA isolated from homogenates of de-endothelialized mouse aortas using TRIzol (Life Technologies) and the RNeasy Mini Kit following the manufacturer's protocol (Qiagen, Valencia, CA), using a High Capacity RNA-to-cDNA kit (Applied Biosystems). Transcript abundance of mouse *Nampt*, *Mmp2*, *Mmp9*, *Mmp13*, *Col1a1*, Fibronectin, Tenascin C, Decorin, Perlecan, Biglycan, Versican, N-cadherin, and *18S*, were assessed using SYBR-green chemistry-based primer sets (*Nampt:* F-GGCACCACTAATCATCAGACCTG R-AAGGTGGCAGCAACTTGTAGCC; *Mmp2*: F-GAGACCATGCAGTCAGCTCTAG R-TAGAGCTGCCTCTTGTCTGGT; *Mmp9*: F-GCTGACTACGATAAGGACGGCA R-TAGTGGTGCAGGCAGAGTAGGA; *Mmp13*: F- GATGACCTGTCTGAGGAAGACC R-GCATTTCTCGGAGCCTGTCAAC; *Col1a1:* F-CCTCAGGGTATTGCTGGACAAC R-CAGAAGGACCTTGTTTGCCAGG; *Fn1*: F-CCCTATCTCTGATACCGTTGTCC R-TGCCGCAACTACTGTGATTCGG; *Tnc*: F-GAGACCTGACACGGAGTATGAG R-CTCCAAGGTGATGCTGTTGTCTG; *Dcn*: F-ACTCTCCAGGAACTTCGTGTCC R-AGTCCCTGGAAGGCTCCGTTTT; *Hspg2*: F-CATTCAGGTGGTCGTCCTCTCA R-AGGTCAAGCGTCTGTCCTTCAG; *Bgn*: F-TGAACCAGGAGCCTTTGATGGC R-GTCCTCCAACTCAATAGCCTGG; *Vcan*: F-GGACCAAGTTCCACCCTGACAT R-CTTCACTGCAAGGTTCCTCTTCT; *Cdh2*: F-CCTCCAGAGTTTACTGCCATGAC R-CCACCACTGATTCTGTATGCCG; *18S*: F-GTAACCCGTTGAACCCCATT R-CCATCCAATCGGTAGTAGCG). Quantitative real-time RT-PCR was performed using an ABI Prism (model 7900HT) and Sequence Detection System software (Life Technologies; Applied Biosystems). Relative mRNA abundance was quantified based on

critical threshold (CT) using the comparative CT formula, $2^{-\Delta\Delta CT}$, with 18S mRNA as an internal control.

4.2.7 Assessment of collagen fibrils by circular polarization microscopy

Paraformaldehyde-fixed aortic sections were stained with Picrosirius red using a commercially available kit from Polysciences, Inc (Warrington, PA). Briefly, deparaffinized sections were incubated with 0.1% Sirius red F3BA in saturated picric acid for 30 minutes and rinsing twice with 0.01 mol/L HCl. Collagen organization was assessed using circular polarization microscopy. Picrosirius red–stained sections of aorta were visualized as described (Nong et al, 2011). Briefly, measurements were obtained using an Olympus BX51 microscope (Olympus Canada, Inc., Richmond Hill, ON, Canada) with polarizer-interference filters, a liquid crystal compensator, a charge-coupled device video camera, and Abrio software (Abrio LC-PolScope; Cambridge Research and Instrumentation, Inc., Hopkinton, MA). This system enabled measurement of light retardation by collagen, in absolute terms (nanometers), in defined fields of view. Mean collagen birefringence was assessed in the medial layers of n=5 mice: the full medial field of view (objective, ×60) yielding the sum of retardation signals (in nanometers) for all pixels in the images. Mean collagen fiber width was determined by measuring a minimum of 20 equidistant widths of per-elastic collagen fibers in one field of view, from a minimum of n=5 mice.

4.2.8 Glycosaminoglycan assessment of aortas by Movat's staining

Paraformaldehyde-fixed aortic sections were stained according to Movat's pentachrome protocol. Briefly, sections were first deparaffinized and incubated with Alcian blue in order to stain acid polysaccharides. They are then stained with Verhoeff hematoxylin, crocein scarlet combined with acidic fuchsine and saffron. The percentage of area occupied by blue-stained proteoglycan was quantified from 3 sections

200 μm apart, in the ascending and descending thoracic aorta regions, avoiding areas with aortic hematoma or dissection, using ImageJ software (NIH, Bethesda, MD).

4.2.9 Statistical analyses

Values are expressed as mean ± standard error of the mean. Statistical analyses were performed using GraphPad Prism software (GraphPad, La Jolla, CA, USA). Mean data were compared using Student's t-test or one- or two-way ANOVA with Holm-Sidak *post hoc* testing.

4.3 Results

4.3.1 Nampt knockout elicits a change in the gene expression pattern in aortic SMCs.

I previously demonstrated that Nampt in smooth muscle cells is required to maintain vascular integrity by maintaining genomic integrity. Here, I sought to determine whether there were other processes impacted by Nampt that may contribute to vascular integrity. To address this question, I generated mice wherein *Nampt* could be conditionally deleted with the use of the CreER recombinase/LoxP system. Mouse aortic smooth muscle cells were isolated from the aortas of 3 *Nampt*$^{flox/flox}$;CreERT2+ and 3 *Nampt*$^{flox/flox}$;CreERT2- (control) mice and subjected to 1 μm 4-hydroxytamoxifen for 24 hours in order to induce *Nampt* deletion in culture. Seventy-two hours following *Nampt* ablation, *Nampt* mRNA transcript level in KO mSMCs was decreased by 86.5% (P<0.0001, Fig. 4.1a). Additionally, NAD^+ levels measured in these cells were decreased by 84.9% (P<0.0001, Fig. 4.1b).

To explore how Nampt reduction in SMCs might impact vascular associated processes, I undertook a global, unbiased comparison of gene expression in control and *Nampt*-KO SMCs using Affymetrix high-density microarray analyses. Gene expression microarray analysis was performed using RNA isolated from 3 independent primary

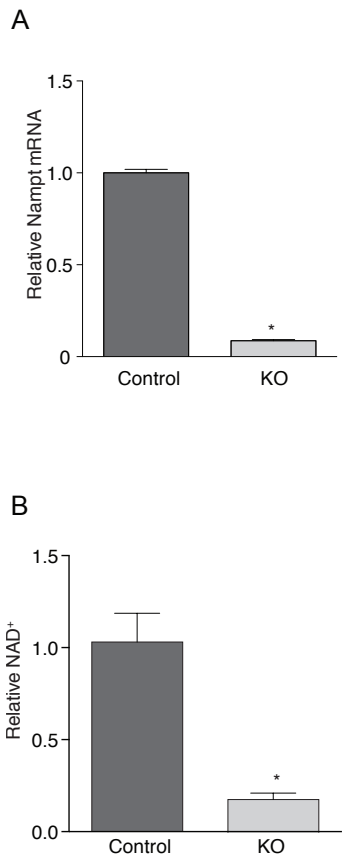

Figure 4.1 *Nampt* knockout in SMCs leads to decreased NAD^+ levels

A. Smooth muscle cells were harvested and cultured from aortas of *Nampt*$^{flox/flox}$;CreERT2+ mice and incubated with vehicle or hydroxy-tamoxifen for 24 hours. Abundance of *Nampt* mRNA was evaluated by RT q-PCR and normalized to expression of Gapdh mRNA (n=3 mice per condition, **P*<0.0001) **B**. Nampt-depleted cells were harvested 72 hours following *Nampt* knockdown. Graph of NAD^+ content in acidic extracts of control and Nampt-depleted smooth muscle cells (SMCs). (n=3 independent cultures per condition, **P*=0.024).

cultures of *Nampt*-KO SMCs and WT control SMCs. As illustrated by Volcano plot, *Nampt* knockout evoked a transcriptional response in SMCs, with balance of statistically significantly up-regulated and down-regulated genes (Fig. 4.2). Lists of differentially expressed genes in response to Nampt depletion were generated using the criteria of 1.5-fold change in expression level with $P<0.05$. Within 72 hours of Nampt disruption in SMCs 856 genes were upregulated and 633 genes were downregulated (as illustrated by heatmap in Fig. 4.3).

4.3.2 Transcriptome alteration in Nampt-deficient aortic SMCs indicates a defect in extracellular matrix

To determine what gene expression patterns were changed in *Nampt*-KO SMCs, I utilized DAVID Bioinformatics Resources (available at https://david.ncifcrf.gov) and analyzed Gene Ontology (GO) and Kegg Pathway terms that were statistically overrepresented in the lists of up- and down-regulated genes ($P<0.05$). The most overrepresented down-regulated genes in the Biological Process and Cellular Compartment GO categories were those belonging to the Extracellular Matrix categories (Fig. 4.4a). Additionally, analysis of genes in Kegg Pathway categories showed that the most overrepresented down-regulated genes belong to the ECM-receptor interaction group (Fig. 4.4b). The most significant GO terms for Biological Processes and Kegg Pathway categories corresponding to genes upregulated in *Nampt*-KO SMCs were those relating to RNA, specifically Poly(A) RNA Binding and Ribosome Biogenesis in Eukaryotes (Fig. 4.5a,b). Interestingly, the most significant GO terms for Cellular Compartments category corresponding to genes upregulated in *Nampt*-KO SMCs also corresponded to Extracellular Matrix.

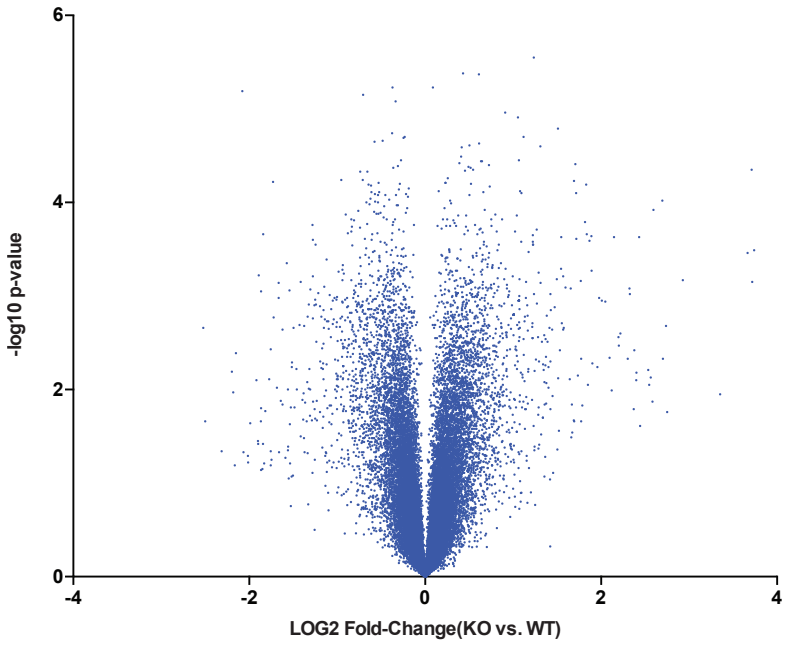

Figure 4.2 *Nampt* knockout in SMCs induces global transcriptome changes

Volcano plot depicting differences in gene expression between SMCs with or without *Nampt* ablation. The x-axis represents the log-transformed fold-change (log2 fold change) of transcript abundance between the two groups. The y-axis represents the negative log transformed p value (-log10 p value).

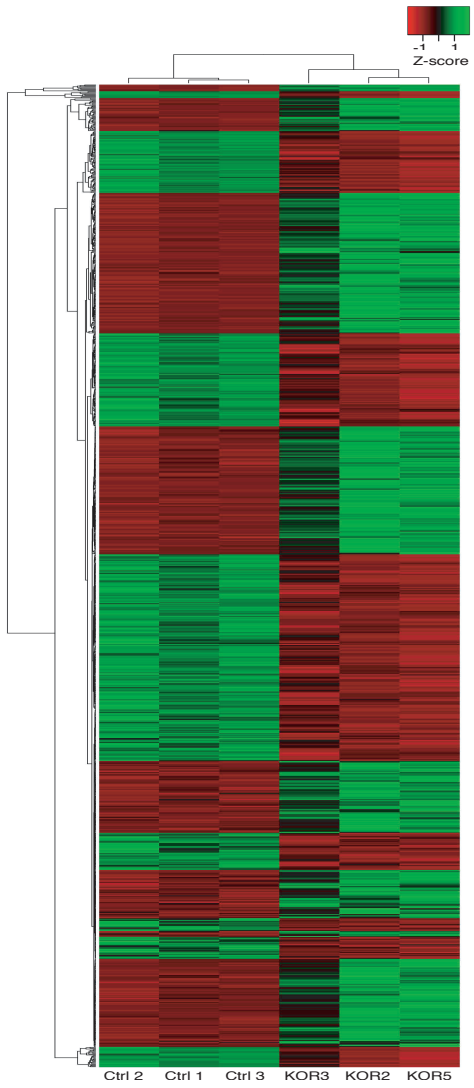

Figure 4.3 *Nampt* knockout in SMCs and gene expression changes

Heatmap depicting the microarray analysis of differentially expressed genes (greater than 1.5-fold change, $P \leq 0.05$) between 3 independent cultures of control, vehicle-treated SMCs and 3 independent cultures of *Nampt*-ablated SMCs. Each column represents one independent SMC culture and each row represents one mRNA transcript. Transcript abundance across the 6 independent cultures was normalized and the *Z*-score is depicted; **Green** indicates relative higher expression, **Red** indicates relative lower expression. Rows and columns were ordered by hierarchical clustering according to the similarity of expression patterns.

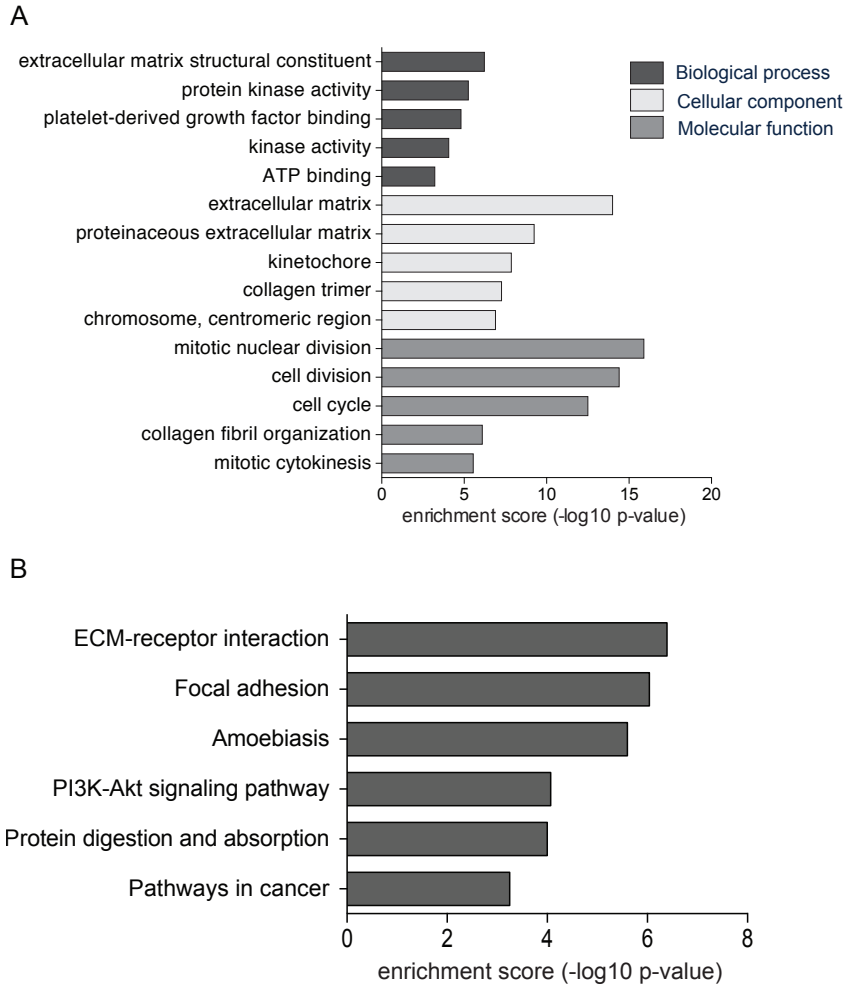

Figure 4.4 GO and KEGG pathways most significantly over-represented in the transcripts downregulated in SMCs after *Nampt* ablation

A. Bar graphs depicting the top 5 overrepresented GO categories from each of the GO classifications: Biological Processes, Cellular Components, and Molecular Functions. **B**. Graph depicting the top overrepresented KEGG pathways as determined by DAVID analysis.

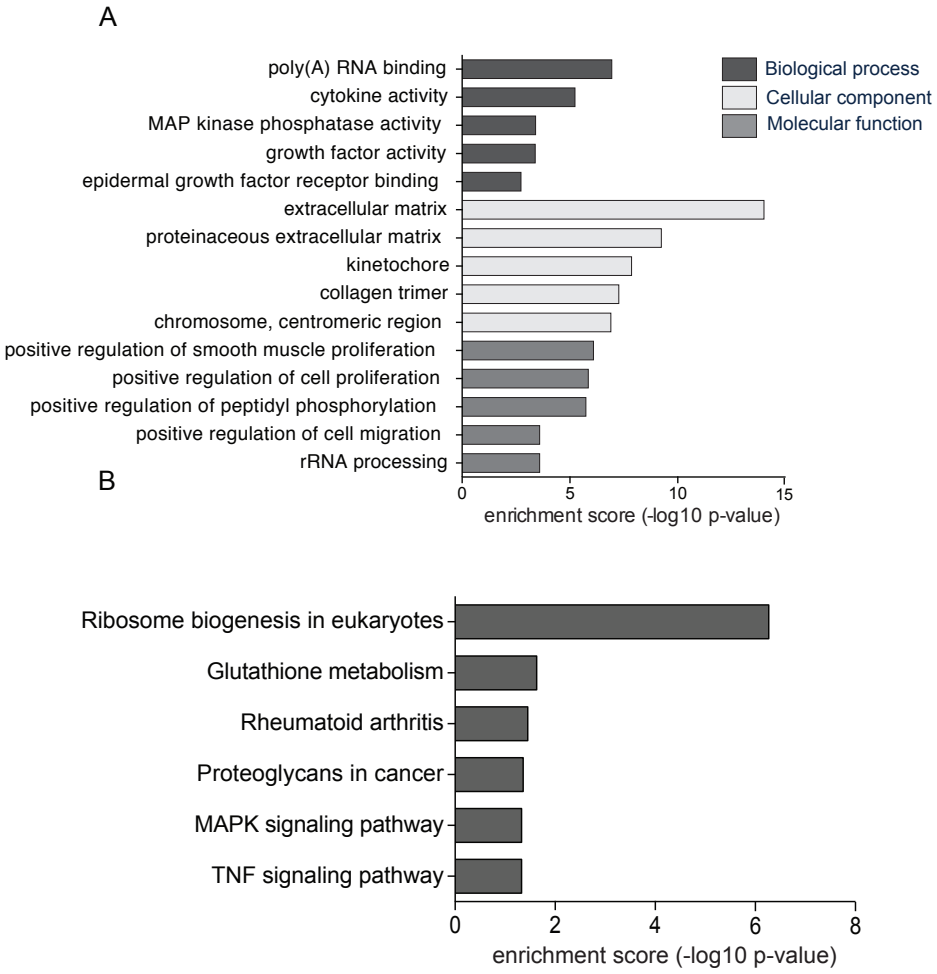

Figure 4.5 GO and KEGG pathways most significantly over-represented in the transcripts upregulated in SMCs after *Nampt* ablation

A. Bar graphs depicting the top 5 overrepresented GO categories from each of the GO classifications: Biological Processes, Cellular Components, and Molecular Functions. **B**. Graph depicting the top overrepresented KEGG pathways as determined by DAVID analysis.

4.3.3 Transcripts associated with collagen and proteoglycan equilibrium are altered in Nampt-deficient SMCS.

To further define the changes in ECM as a consequence of *Nampt* ablation in SMCs, I curated the differentially expressed transcripts for genes known to be associated with pathology of the vascular ECM. I identified a number of transcripts among the overrepresented genes in the ECM categories that were associated with the production or degradation of extracellular collagen (Table 4.1). Notably, there was a 3.65-fold decrease in the expression of *col3a1* (P=0.022), a 1.75-fold decrease in the expression of *col1a1* (P=0.021), and a 4.97-fold decrease in *col14a1* (P=0.046). Matrix metalloproteinase 13 (*Mmp13*) was significantly upregulated in *Nampt*-KO SMCs, which also may contribute to a disturbed collagen balance in the extracellular environment of these SMCs.

As a corollary to this collagen depletion phenotype, I identified a number of transcripts in the lists of overrepresented genes in the ECM categories that were associated with the production of vascular proteoglycans (Table 4.2). These include a 1.54-fold increase in versican (P=0.006), and an increase in the enzymes that synthesize the glycosaminoglycan hyaluronan (or, hyaluronic acid): hyaluronan synthases 1 and 2 (1.99-fold and 1.57-fold, P=0.001 and 0.034, respectively).

I next confirmed differential expression of ECM components including MMPs, collagens, fibronectin, and proteoglycans in *Nampt*-KO SMCs, by quantitative RT-PCR. Expression of MMPs 2, 9, and 13 were all significantly upregulated by 1.78-, 10.40-, and 3.90-fold, respectively (P=0.0001, <0.0001, and <0.0001, respectively, Fig. 4.6). The expression of *col1a1* was decreased by 57.9% (P=0.021) while the expression of fibronectin increased 1.85-fold (P<0.0001). Interestingly, the expression of various proteoglycans associated with the vascular space was increased. Versican was upregulated

Table 4-1 Microarray analysis identifies that *Nampt* ablation in SMCs changes expression of genes associated with collagen production and assembly

Gene name	Function	GenBank accession number	*P*-value	Fold change
Collagen, Type III, Alpha 1	Member of group I collagen (fibrillar forming collagen)	NM_009930	0.022	-3.65
Collagen, Type XXVIII, Alpha 1	May act as a cell-binding protein	NM_001037865	0.017	-3.53
Matrix Metalloproteinase 13	Overexpressed by smooth muscle cells in abdominal aortic aneurysm. Role in the degradation of ECM including fibrillar collagen, fibronectin, TNC and ACAN	NM_008607	0.001	2.97
Lysyl Oxidase	Necessary for the formation of covalent cross-links in collagen and elastic fibers	NM_001286181	0.013	-1.77
Collagen, Type IV, Alpha 2	Major structural component of glomerular basement membranes.	NM_009932	0.007	-1.99
Collagen, Type XII, Alpha 1	Basement membrane protein that forms anchoring fibrils which may contribute to epithelial basement membrane organization and adherence by interacting with extracellular matrix (ECM)	NM_001290308	0.003	-1.91
Lysyl Oxidase-Like 1	Active on elastin and collagen substrates	NM_010729	0.026	-1.62
Collagen, Type IV, Alpha 1	Major structural component of glomerular basement membranes.	NM_009931	0.022	-1.83
Collagen, Type V, Alpha 2	Fibrillar forming collgen; a minor connective tissue component of nearly ubiquitous distribution. Binds to DNA, heparan sulfate, thrombospondin, heparin, and insulin. Key determinant in the assembly of tissue-specific matrices	NM_007737	0.002	-2.69
Collagen, Type XIV, Alpha 1	Plays an adhesive role by integrating collagen bundles.	NM_181277	0.046	-4.97
Collagen, Type I, Alpha 2	Type I collagen is a member of group I collagen (fibrillar forming collagen)	NM_007743	0.006	-1.86
Procollagen-Lysine, 2-Oxoglutarate 5-Dioxygenase 2	Forms hydroxylysine residues in collagens that serve as sites of attachment for carbohydrate units and are essential for the stability of the intermolecular collagen cross-links	NM_001142916	0.003	-1.73
ADAM Metallopeptidase With Thrombospondin Type 1 Motif, 2	Cleaves the propeptides of type I and II collagen prior to fibril assembly.	NM_001277305	0.033	-2.60
Collagen, Type I, Alpha 1	Type I collagen is a member of group I collagen (fibrillar forming collagen)	NM_007742	0.0002	-1.75
Collagen, Type XI, Alpha 1	May play an important role in fibrillogenesis by controlling lateral growth of collagen II fibrils	NM_007729	0.00005	-1.58
Collagen, Type IV, Alpha 5	Major structural component of glomerular basement membranes.	NM_001163155	0.001	-1.64
Collagen, Type VIII, Alpha 1	Macromolecular component of the subendothelium. Necessary for migration and proliferation of vascular smooth muscle cells and thus, has a potential role in the maintenance of vessel wall integrity and structure.	NM_007739	0.019	-2.48
Matrix Metallopeptidase 3	Can degrade fibronectin, laminin, gelatins of type I, III, IV, and V; collagens III, IV, X, and IX, and cartilage proteoglycans. Activates procollagenase	NM_010809	0.0001	-3.32
Collagen, Type V, Alpha 1	Fibrillar formaing collgen; it is a minor connective tissue component of nearly ubiquitous distribution. Type V collagen binds to DNA, heparan sulfate, thrombospondin, heparin, and insulin.	NM_015734	0.001	-1.64

Table 4-2 Microarray analysis identifies that *Nampt* ablation in SMCs changes expression of genes associated with proteoglycan production and assembly

Gene name	Function	GenBank accession number	*P*-value	Fold change
Hyaluronan Synthase 2	Essential to hyaluronan synthesis a major component of most extracellular matrices that has a structural role in tissues architectures and regulates cell adhesion, migration and differentiation.	NM_008216	0.034	1.57
Hyaluronan Synthase 1	Essential to hyaluronan synthesis a major component of most extracellular matrices that has a structural role in tissues architectures and regulates cell adhesion, migration and differentiation.	NM_008215	0.001	1.99
UDP-Gal:BetaGlcNAc Beta 1,4-Galactosyltransferase, Polypeptide 1	The cell surface form functions as a recognition molecule during a variety of cell to cell and cell to matrix interactions.	NM_022305	0.006	-1.61
Podocalyxin-Like	Involved in the regulation of both adhesion and cell morphology and cancer progression.	NM_013723	0.043	1.98
Chondroitin Sulfate Proteoglycan 4	Proteoglycan playing a role in cell proliferation and migration.	NM_139001	0.003	1.55
Versican	May play a role in intercellular signaling and in connecting cells with the extracellular matrix. May take part in the regulation of cell motility, growth and differentiation. Binds hyaluronic acid	NM_001081249	0.006	1.54
Syndecan 4	Cooperating with integrins in a Rho dependent manner in the assembly of focal adhesion and actin stress fibers. Cell surface proteoglycan that bears heparan sulfate	NM_011521	0.019	-1.53
Cell Migration Inducing Protein, Hyaluronan Binding	Random hydrolysis of (1->4)-linkages between N-acetyl-beta-D-glucosamine and D-glucuronate residues in hyaluronate.	NM_030728	0.008	-3.78
Hyaluronoglucosaminidase	Random hydrolysis of (1->4)-linkages between N-acetyl-beta-D-glucosamine and D-glucuronate residues in hyaluronate. Hyaluronan synthase activity	NM_008317	0.002	-1.67
Proline/Arginine-Rich End Leucine-Rich Repeat Protein	May anchor basement membranes to the underlying connective tissue	NM_054077	0.032	-2.67

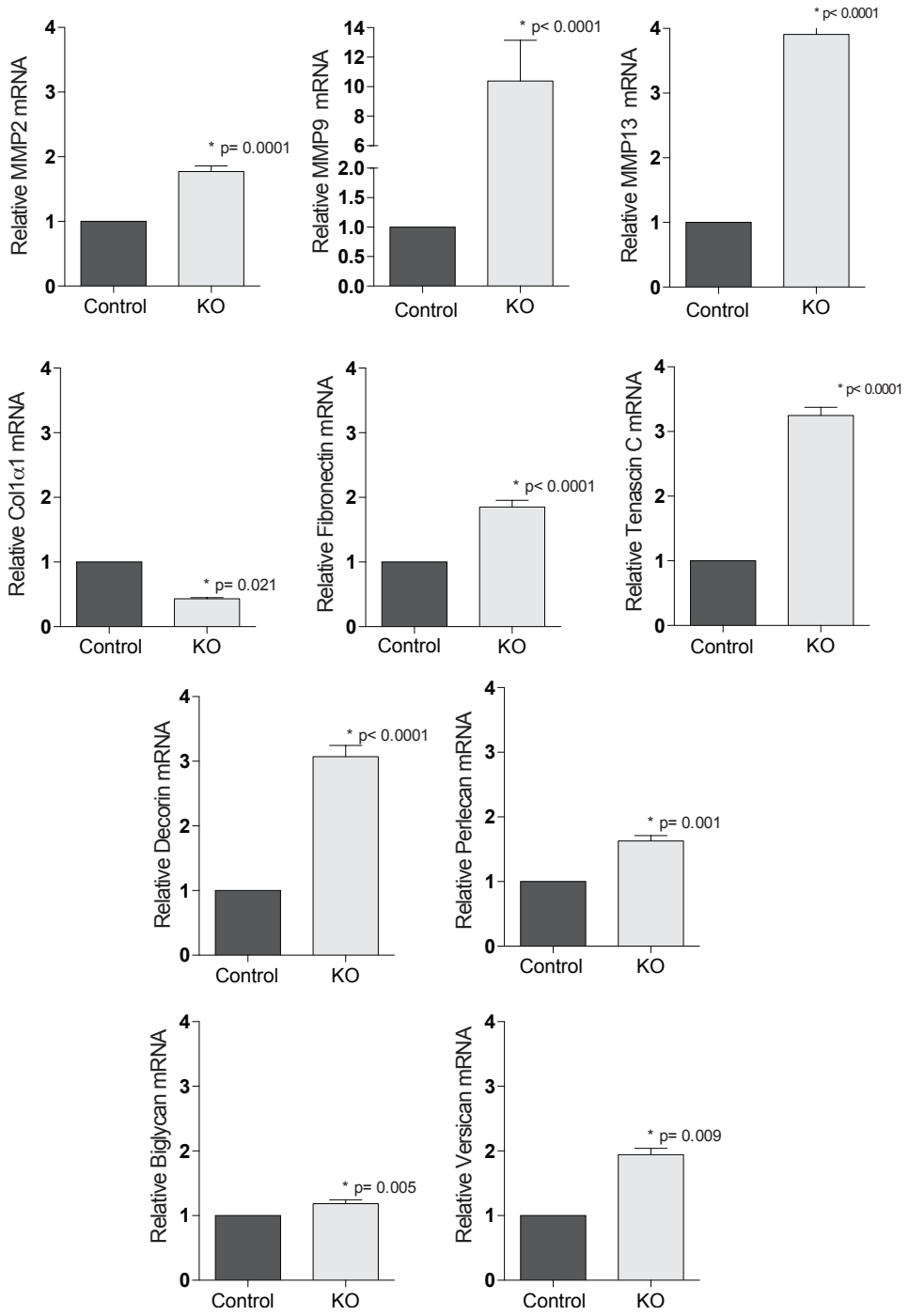

Figure 4.6 *Nampt* ablation in SMCs changes expression of ECM transcripts

Graphs depicting the relative transcript abundance of **A**) *Mmp2*, **B**) *Mmp9*, **C**) *Mmp13*, **D**) *Col1a1*, **E**) Fibronectin, **F**) Tenascin C, **G**) Decorin, **H**) Perlecan, **I**) Biglycan, and **J**) Versican, in control and in SMCs after *Nampt* ablation, as assessed by quantitative RT-PCR. mRNA data are expressed as ΔΔCT (n=3 independent cultures per condition, transcript abundance of 18s was used as an internal normalizing reference).

1.96-fold (P=0.009), decorin was upregulated 3.07-fold (P<0.0001) and perlecan was upregulated 1.63-fold (P=0.001) (Fig. 4.7). Additionally, the expression of the glycoprotein tenascin C was increased by 3.24-fold (P<0.0001), Taken together, these transcriptional data are evidence for a disruption in the SMC ECM environment when *Nampt* is ablated.

4.3.4 Collagen deposition and organization is abrogated in SMC-Nampt deficient aortas at baseline and following Ang II infusion

We have previously shown that mice with *Nampt* ablated in their smooth muscle cells were prone to Ang II-induced aortic disruption. Because of our evidence that collagen expression is suppressed in *Nampt*-KO SMCs in culture, I next determined whether the collagen component of the aorta was compromised in SMC-Nampt deficient mouse aortas. It has been shown that aortic fibrosis, caused by increased collagen content, is detectable in the mouse aorta as early as 7 days after initiation of Ang II infusion (Xu et al. 2011). Therefore, I infused *Nampt*$^{flox/flox}$;*smMHC*-Cre+ (SMC-*Nampt* KO) mice and *Nampt*$^{flox/+}$;*smMHC*-Cre- (control) mice Ang II for 7 or 28 days (1.44 mg/kg/day). Following Ang II infusion the aortas were perfusion-fixed and sectioned. Fibrillar collagen content and organization was assessed using circular polarization images of picrosirius red-stained aortic cross sections (Fig. 4.7a). This revealed that, consistent with previous studies, control mice substantially increased the fibrillar collagen content in response to Ang II at both 7 and 28 days. These changes were evident in both the ascending and descending thoracic aortic segments. Strikingly, this fibrillar response was completely absent in the aortas of SMC-*Nampt* KO mice (Fig. 4.7b).

To further evaluate the impact of *Nampt* knockout on the architecture of the collagen fibers, and the possibility that this might predispose to medial dissection, we resolved the collagen fibers into two distinct components: 1) tracks of collagen that were closely opposed to either side of each elastic lamella (Fig. 4.7c); and 2) collagen fibers that

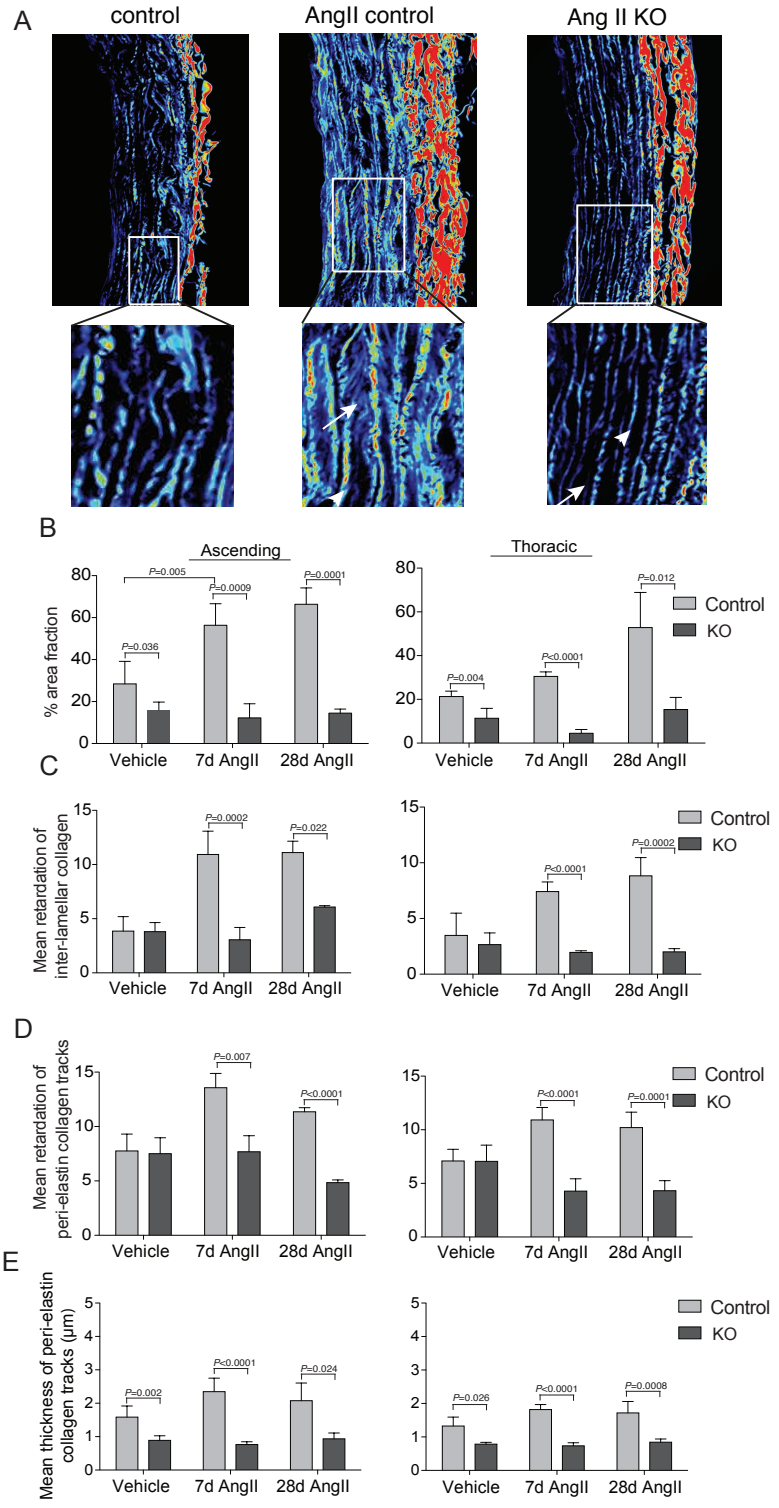
A
control
AngII control
Ang II KO
B
Ascending
Thoracic
% area fraction
P=0.005
P=0.0009
P=0.0001
P=0.036
P=0.004
P<0.0001
P=0.012
Control
KO
Vehicle
7d AngII
28d AngII
C
Mean retardation of inter-lamellar collagen
P=0.0002
P=0.022
P<0.0001
P=0.0002
D
Mean retardation of peri-elastin collagen tracks
P=0.007
P<0.0001
P<0.0001
P=0.0001
E
Mean thickness of peri-elastin collagen tracks (µm)
P=0.002
P<0.0001
P=0.024
P=0.026
P<0.0001
P=0.0008

Figure 4.7 Collagen deposition and organization in response to Ang II is abrogated in the aortas of SMC-***Nampt*** KO **mice**

Control and SMC-*Nampt* KO mice were infused with Ang II (1.44mg/kg/day) or vehicle (PBS) for 7 or 28 days. Following infusion, paraformaldehyde-perfusion fixed ascending and descending thoracic aortas were harvested and stained with picrosirius red (PSR). Micrographs depict digitally acquired light retardation images of the ascending aortas, imaged with polarized light and liquid crystal compensation. The resulting retardation images are independent of illumination intensity, such that images can be directly compared; **A**. Representative images of control and SMC-*Nampt* KO ascending aortas infused with Ang II for 7 days; **B**. Quantification of the area fraction of birefringent collagen in the media of the ascending and thoracic aortas; **C**. Graph depicting the mean retardation values (a measure of collagen deposition and organization) of the inter-lamellar spaces (white arrows) in the ascending and thoracic aortas of KO mice; **D**. Graph depicting the mean retardation values of peri-elastin lamellae collagen tracks (white arrowheads); **E**. Graph depicting the thickness of the inter-lamellar tracks of collagen, (n = 4-5 mice per group).

existed between elastic lamellae and oriented primarily orthogonal to the peri-elastic collagen fibers (Fig. 4.7d). Notably, both collagen components in *Nampt* KO aortic media were attenuated at baseline, and not responsive to Ang II stimulation. Interestingly, the mean thickness of the peri-elastic collagen tracks in SMC-*Nampt* KO mice was also less than that of control mice, even before Ang II stimulation. In control mice, the mean thickness of the peri-elastic collagen tracks increased with Ang II stimulation. However, no increase was noted in SMC-Nampt deficient aortas (Fig. 4.7e). Taken together, these findings suggest an inability of Nampt-deficient SMCs to produce and/or assemble collagen fibrils at both baseline and under Ang II-induced biochemical and biomechanical stress.

4.3.5 Glycosaminoglycan elaboration is increased in SMC-Nampt deficient aortas at baseline and following Ang II infusion

I next sought to determine if the ECM elaboration response to Ang II in SMC-Nampt deficient aortas shifted to other, non-collagen ECM components. Quantitative transcript analysis by RT-PCR of aortas infused with Ang II for 7 days revealed that *Col1a1* expression in SMC-*Nampt* KO aortas was 27.3% lower than that in control aortas infused with Ang II (P=0.0002, Fig. 4.8a). Surprisingly, fibronectin expression was also lower in Ang II-infused SMC-*Nampt* KO aortas than infused control aortas (42.5%, P=0.0004, Fig. 4.8b). Additionally, N-cadherin, important in maintaining SMC adhesion, was also 43.4% lower in Ang II-infused aortas as compared to control infused aortas (P=0.002, Fig. 4.8c). In contrast, expression of the small leucine-rich repeat proteoglycan biglycan was higher in SMC-*Nampt* KO aortas than control aortas infused with Ang II (1.91-fold, P=0.002, Fig. 4.8d).

To further determine whether proteoglycan moieties were accumulating in the Ang II-infused SMC-*Nampt* KO mouse aortas, I stained paraformaldehyde-fixed sections of aorta with Movat's petachrome stain (Fig. 4.8e). This stain contains alcian blue, which

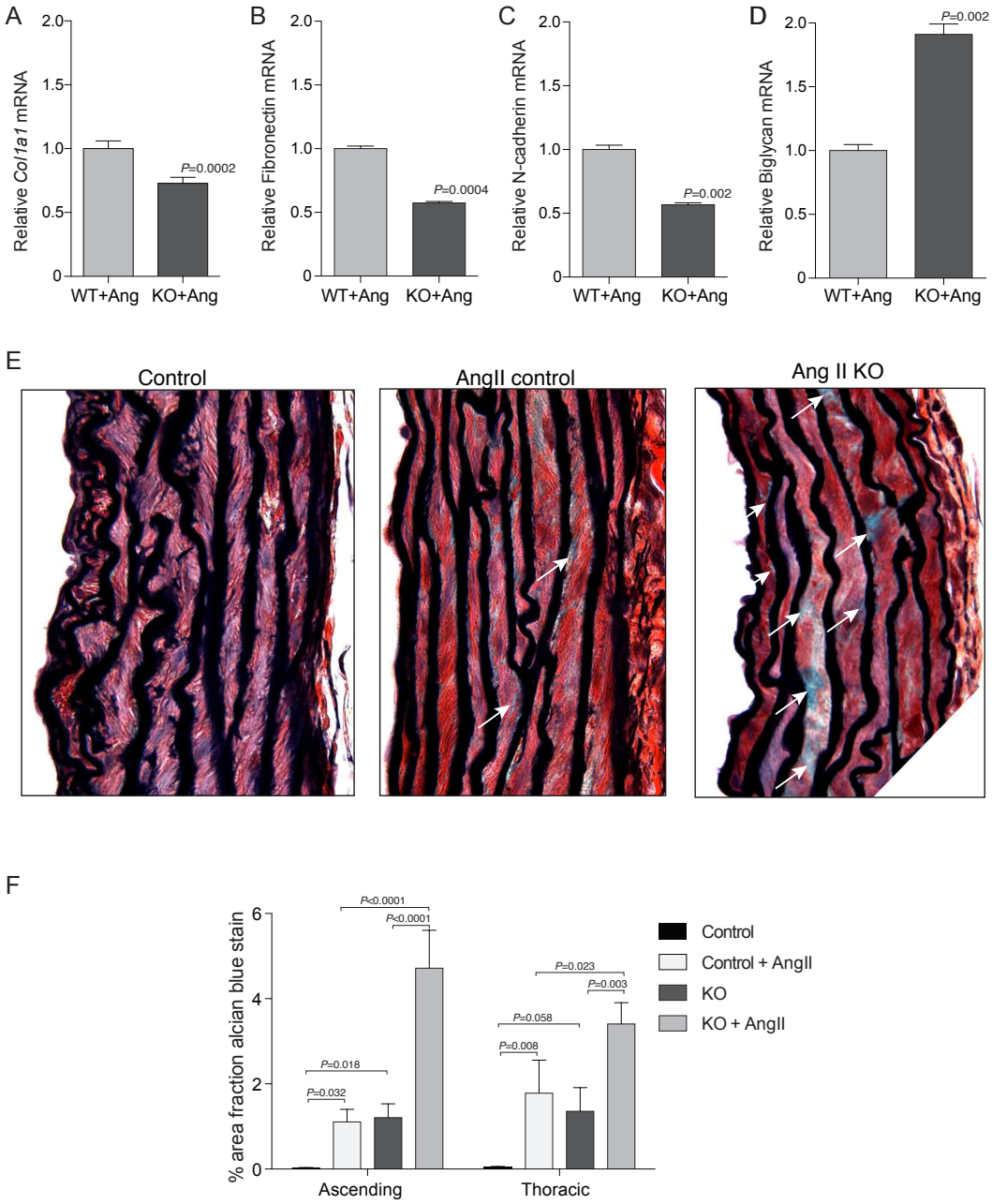

Figure 4.8 ECM expression in response to Ang II is perturbed in the aortas of SMC-*Nampt* KO mice

Graphs depicting the relative transcript abundance (ΔΔCT) of **A**) *Col1a1*, **B**) Fibronectin, **C**) N-Cadherin, and **D**) Biglycan, in control and *Nampt*-KO mouse aortic medias, as assessed by quantitative RT-PCR (n=3 independent cultures per condition, transcript abundance of 18s was used as an internal reference). **E**. Representative images of control and SMC-*Nampt* KO ascending aortas infused with Ang II, 1.44 mg/kg/day for 7 days, and stained with Movat's pentachrome stain. Areas of blue stain are predominantly enriched with GAG (white arrowhead). **F**. Quantification of blue GAG stain expressed as the percentage of the medial area of both the ascending and thoracic aorta (n = 4-5 per group, by one-way ANOVA with Holm-Sidak post hoc testing).

binds to acidic polysaccharides such as glycosaminoglycans (GAGs) – the side chains that together with a core protein make up a proteoglycan. Interestingly, even without Ang II infusion, SMC-*Nampt* KO aortas have a detectable amount of GAG accumulation while GAG accumulation in control aortas was virtually undetectable, both in the ascending and thoracic regions (P=0.03 and P=0.007, respectively, Fig. 4.8f). Following 7 days of Ang II infusion the area fraction of GAG accumulation was 4.2-fold higher in SMC-*Nampt* KO ascending aortas (P<0.0001) than that of Ang II-infused control ascending aortas. Similarly, both KO and control thoracic aortas had an increase in the area fraction of proteoglycan present in response to Ang II (P=0.02). This evidence of proteoglycan accumulation, along with reduction in the more structurally resistant ECM components (e.g. collagen), points to a vascular structural weakening in response to *Nampt* ablation.

4.3.6 Smad7 is a potential upstream regulator of Nampt-dependent changes in the ECM equilibrium

To screen for potential drivers of the gene-expression phenotypes related to *Nampt*-ablation in the SMCs, I performed Ingenuity Pathway Analysis (IPA) on the up- and down-regulated genes revealed by the microarray analysis data. Specifically, I evaluated the data set using the Upstream Regulator Analytic. Transcription regulators potentially affected by SMC-Nampt depletion were identified based on the number of up- and down-regulated genes that were statistically overrepresented in the potential downstream target gene set (Fig. 4.9a). The transcription factor predicted to be most significantly impacted by *Nampt* ablation was Smad7 (P=5.52x10^{-14}), and it was predicted to be activated (activation Z-score=2.27). Smad7 was followed by Jun, Myc, Foxm1 and Nupr1. Interestingly, the putative downstream targets of Smad7, as predicted by the IPA platform, include a number of ECM components that were differentially expressed in Nampt depleted SMCs (Fig. 4.9b). Although the involvement of Smad7 remains to be validated, it may represent a key node through which Nampt regulates the ECM environment of SMCs.

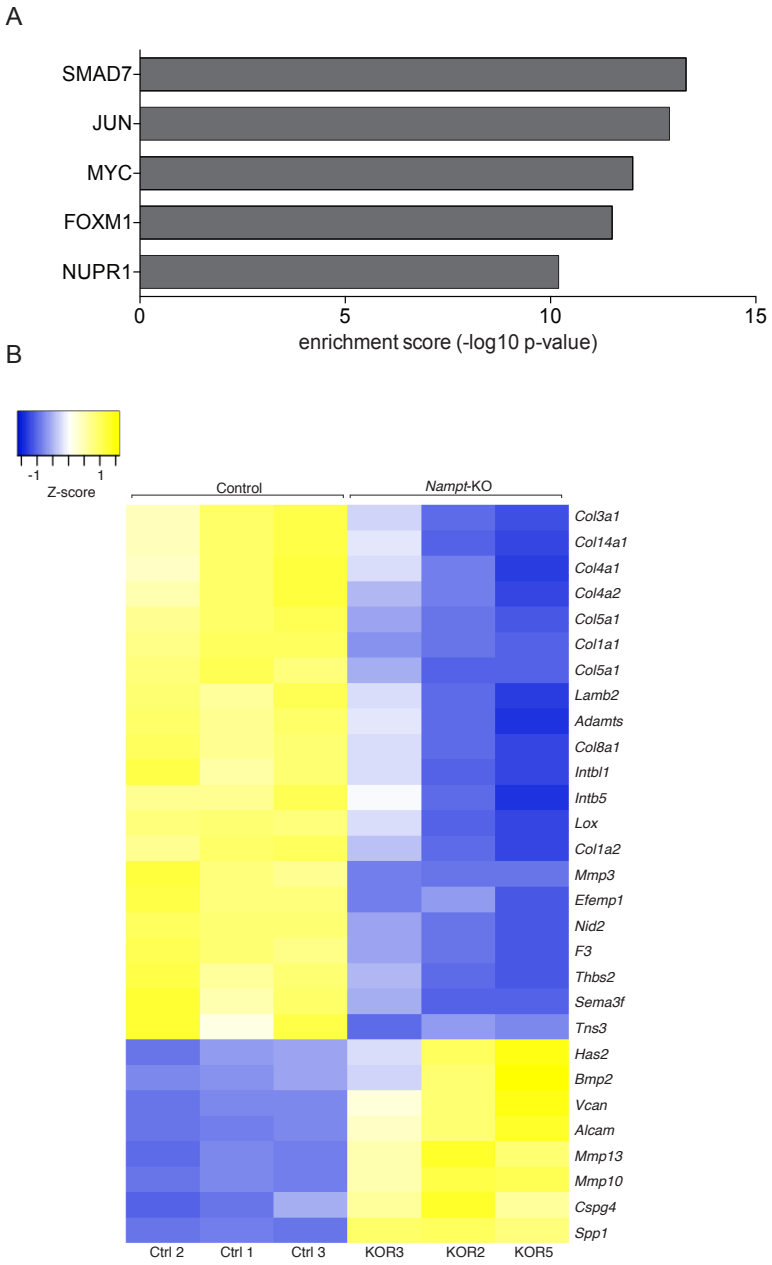

Figure 4.7 Predicted transcription factors mediating transcript changes by loss of Nampt

A. The 5 upstream transcription regulators most strongly predicted to be impacted by *Nampt* depletion in SMCs as identified by Ingenuity Pathway Analysis of SMC-*Nampt* knockout microarray data. **B**. Heatmap of specific ECM transcripts downstream of Smad7, as identified by IPA, which are also differentially expressed (greater than 1.5-fold change, $P<0.05$) in *Nampt*-KO SMCs. Each column represents one independent SMC culture and each row represents one mRNA transcript. mRNA Transcript expression across the 6 independent cultures was normalized and the *Z*-score is depicted; **Yellow** indicates relative high expression, **Blue** indicates relative low expression.

4.4 Discussion

This study reveals that ECM homeostasis in the aortic media depends on a NAD^+ fueling system. By evaluating changes in *Nampt*-KO SMCs and in SMC Nampt-deficient aortas we show that: 1) *Nampt* knockdown in SMCs profoundly changes the expression pattern of SMC gene transcripts, 2) there were reciprocal shifts in the expression of transcripts associated with collagen synthesis and assembly, and proteoglycan synthesis, 3) Nampt-deficient mouse aortas displayed decreased content and organization of fibrillar collagen at baseline and following infusion with Ang II, 4) Nampt-deficient mouse aortas had increased proteoglycan accumulation at baseline, and following Ang II infusion, and 5) the Smad7 signaling pathway may be altered in response to Nampt knockdown in SMCs.

Nampt was originally identified as a putative cytokine, pre-B enhancing colony factor (PBEF) (Samal et al. 1994, Rongvaux et al. 2002), and subsequently as a putative insulin-mimetic hormone, Visfatin (Fukuhara et al. 2005). Evidence for the former is inconclusive, and the index report for the latter has been retracted (Fukuhara et al. 2007). Our previous work has established Nampt as a phosphoribosyltransferase, impacting the ability of SMCs in vitro to withstand the effects of replicative stress in culture (van der Veer et al. 2007). Additionally, my recent findings have revealed the importance of an autonomous, Nampt-dependent NAD^+ production cascade in SMCs that serves as a vital metabolic hub for the aorta. The current findings highlight the magnitude of transcript control exerted by this hub. Two major NAD^+-dependent enzyme families are likely central to this transcript program, Parps and Sirtuins. Parp's actions include ADP-ribosylation of histones (Verdone et al. 2015). Sirtuins couple NAD^+ breakdown to the deacetylation and/or ADP-ribosylation of target proteins. Numerous target proteins, including histones and a variety of transcription factors, have been reported for sirtuins (Dai and Faller 2008, Imai 2009). Major gene expression changes have been found in mouse fibroblasts with

increased Nampt, which is at least partly due to augmenting the transcriptional regulatory activity of Sirt1 by increasing NAD^+ bioavailability (Revollo et al. 2004). The current data shed light on the converse paradigm, i.e. decreased Nampt content depressed total cellular NAD^+ and re-wired gene expression in SMCs.

Remarkably, both the Gene Ontology (GO) terms and KEGG pathways that were most particularly enriched by altered *Nampt*-KO SMC transcripts are those associated with extracellular matrix production and assembly. In particular, this revealed an abundance of genes associated with the synthesis and assembly of collagens, with a profile suggesting a collagen depletion phenotype. Consistent with this, I found that aortas of SMC-*Nampt* KO mice had reduced collagen content and organization. Ang II has been found to directly contribute to vascular smooth muscle cell growth and vessel remodeling, including an upregulation of collagen synthesis (Intengan and Schiffrin 2001, Sparks et al. 2011), and this was also impaired in the SMC-*Nampt* KO mice. It has been reported that the deacetylation activity of Sirt1 increases the expression of collagen type I (*Col1a2*) transcription in vascular SMCs by directly antagonizing the *Col1a2* repressor, RFX5 (Xia et al. 2012). As well, Y. Wang et al. have reported that the inhibition of Parp1 prevented fibrosis in response to Ang II (Wang et al. 2013). Under baseline conditions, Parp1 associates in the nucleus with the transcription factor Smad3. When activated by DNA damage, Parp1 poly-ADP-ribosylates target histones, but also undergoes auto-poly-ADP-ribosylation. This modification caused it to dissociate from Smad3, and Smad3 was able to bind to the promoter of its target genes: including *Col1a1* and *Col11a1*, thus increasing collagen production by vSMCs (Huang et al. 2011). These findings, together with my data, support that idea that the reduced collagen in the aortas of KO mice may be due to decreased Sirt1 and Parp1 activity.

The observed decrease in collagen production, both at baseline and in response to Ang II, was accompanied by an increase in proteoglycan transcripts. The molecular basis of this reciprocal relationship is unclear, however the end-result is associated with both structural weakness of the aorta and the pathology of human aortopathy (Lakatta et al. 2009, Humphrey 2013, Roccabianca et al. 2014).

The statistical determination that Smad7 is an upstream transcription factor that drives the expression profile is noteworthy. NAD^+-dependent Sirt1-mediated deacetylation of Smad7 has been documented. Deacetylation of Smad7 targets it for degradation, and inhibition of Smad7 deacetylation leads to greater Smad7 stability and activity (Kume et al. 2007). Smad7 is a key negative regulator of TGF-β signalling (Yan and Chen 2011, Beppu 2013). In the vascular compartment TGF-β has been implicated in matrix deposition and in matrix degradation, positioning it as a critical regulator of the vascular ECM (Jones and Ikonomidis 2010). In particular, TGF-β can enhance collagen and fibronectin synthesis and deposition (Ignotz and Massague 1986), increase elastin expression (Kucich et al. 2002), and repress MMPs (Yan and Boyd 2007). TGF-β signalling also can increase the size of glycosaminoglycan chains on both bigylcan and decorin (Schonherr et al. 1993, Dadlani et al. 2008). A Nampt-regulated shift in TGF-β signalling due increased Smad7 stability could well be responsible for unbalancing the homeostasis of the aortic extracellular environment, leaving the aorta vulnerable to disruption.

In summary, I demonstrate that a SMC-autonomous supply of NAD^+ generated Nampt is necessary for vascular SMCs to synthesize maintain a physiologic balance of collagen versus proteoglycans. Upsetting this Nampt-regulated balance may weaken the aorta and increase its susceptibility to dissection.

4.5 References

Beppu, H. (2013). Smad7-modified alleles by various gene-targeting strategies. *J Biochem, 153*(5), 399-401

Borges, L. F., Touat, Z., Leclercq, A., Zen, A. A., Jondeau, G., Franc, B., Philippe, M., Meilhac, O., Gutierrez, P. S., & Michel, J. B. (2009). Tissue diffusion and retention of metalloproteinases in ascending aortic aneurysms and dissections. *Hum Pathol, 40*(3), 306-313

Dadlani, H., Ballinger, M. L., Osman, N., Getachew, R., & Little, P. J. (2008). Smad and p38 MAP kinase-mediated signaling of proteoglycan synthesis in vascular smooth muscle. *J Biol Chem, 283*(12), 7844-7852

Dai, Y., & Faller, D. V. (2008). Transcription Regulation by Class III Histone Deacetylases (HDACs)-Sirtuins. *Transl Oncogenomics, 3*, 53-65

Fukuhara, A., Matsuda, M., Nishizawa, M., Segawa, K., Tanaka, M., Kishimoto, K., Matsuki, Y., Murakami, M., Ichisaka, T., Murakami, H., Watanabe, E., Takagi, T., Akiyoshi, M., Ohtsubo, T., Kihara, S., Yamashita, S., Makishima, M., Funahashi, T., Yamanaka, S., Hiramatsu, R., Matsuzawa, Y., & Shimomura, I. (2005). Visfatin: a protein secreted by visceral fat that mimics the effects of insulin. *Science, 307*(5708), 426-430

Fukuhara, A., Matsuda, M., Nishizawa, M., Segawa, K., Tanaka, M., Kishimoto, K., Matsuki, Y., Murakami, M., Ichisaka, T., Murakami, H., Watanabe, E., Takagi, T., Akiyoshi, M., Ohtsubo, T., Kihara, S., Yamashita, S., Makishima, M., Funahashi, T., Yamanaka, S., Hiramatsu, R., Matsuzawa, Y., & Shimomura, I. (2007). Retraction. *Science, 318*(5850), 565

Hayashi, S., & McMahon, A. P. (2002). Efficient recombination in diverse tissues by a tamoxifen-inducible form of Cre: a tool for temporally regulated gene activation/inactivation in the mouse. *Dev Biol, 244*(2), 305-318

Huang, D., Wang, Y., Wang, L., Zhang, F., Deng, S., Wang, R., Zhang, Y., & Huang, K. (2011). Poly(ADP-ribose) polymerase 1 is indispensable for transforming growth factor-beta Induced Smad3 activation in vascular smooth muscle cell. *PLOS ONE, 6*(10), e27123

Huang da, W., Sherman, B. T., & Lempicki, R. A. (2009a). Bioinformatics enrichment tools: paths toward the comprehensive functional analysis of large gene lists. *Nucleic Acids Res, 37*(1), 1-13

Huang da, W., Sherman, B. T., & Lempicki, R. A. (2009b). Systematic and integrative analysis of large gene lists using DAVID bioinformatics resources. *Nat Protoc, 4*(1), 44-57

Humphrey, J. D. (2013). Possible mechanical roles of glycosaminoglycans in thoracic aortic dissection and associations with dysregulated transforming growth factor-beta. *J Vasc Res, 50*(1), 1-10

Humphrey, J. D., Milewicz, D. M., Tellides, G., & Schwartz, M. A. (2014). Cell biology. Dysfunctional mechanosensing in aneurysms. *Science, 344*(6183), 477-479

Ignotz, R. A., & Massague, J. (1986). Transforming growth factor-beta stimulates the expression of fibronectin and collagen and their incorporation into the extracellular matrix. *J Biol Chem, 261*(9), 4337-4345

Imai, S. (2009). The NAD World: a new systemic regulatory network for metabolism and aging--Sirt1, systemic NAD biosynthesis, and their importance. *Cell Biochem Biophys, 53*(2), 65-74

Intengan, H. D., & Schiffrin, E. L. (2001). Vascular remodeling in hypertension: roles of apoptosis, inflammation, and fibrosis. *Hypertension, 38*(3 Pt 2), 581-587

Irizarry, R. A., Bolstad, B. M., Collin, F., Cope, L. M., Hobbs, B., & Speed, T. P. (2003). Summaries of Affymetrix GeneChip probe level data. *Nucleic Acids Res, 31*(4), e15

Ishii, T., & Asuwa, N. (2000). Collagen and elastin degradation by matrix metalloproteinases and tissue inhibitors of matrix metalloproteinase in aortic dissection. *Hum Pathol, 31*(6), 640-646

Jones, J. A., & Ikonomidis, J. S. (2010). The pathogenesis of aortopathy in Marfan syndrome and related diseases. *Curr Cardiol Rep, 12*(2), 99-107

Koullias, G. J., Ravichandran, P., Korkolis, D. P., Rimm, D. L., & Elefteriades, J. A. (2004). Increased tissue microarray matrix metalloproteinase expression favors proteolysis in thoracic aortic aneurysms and dissections. *Ann Thorac Surg, 78*(6), 2106-2110; discussion 2110-2101

Kucich, U., Rosenbloom, J. C., Abrams, W. R., & Rosenbloom, J. (2002). Transforming growth factor-beta stabilizes elastin mRNA by a pathway requiring active Smads, protein kinase C-delta, and p38. *Am J Respir Cell Mol Biol, 26*(2), 183-188

Kume, S., Haneda, M., Kanasaki, K., Sugimoto, T., Araki, S., Isshiki, K., Isono, M., Uzu, T., Guarente, L., Kashiwagi, A., & Koya, D. (2007). SIRT1 inhibits transforming growth factor beta-induced apoptosis in glomerular mesangial cells via Smad7 deacetylation. *J Biol Chem, 282*(1), 151-158

Lakatta, E. G., Wang, M., & Najjar, S. S. (2009). Arterial aging and subclinical arterial disease are fundamentally intertwined at macroscopic and molecular levels. *Med Clin North Am, 93*(3), 583-604, Table of Contents

Li, S., Van Den Diepstraten, C., D'Souza, S. J., Chan, B. M., & Pickering, J. G. (2003). Vascular smooth muscle cells orchestrate the assembly of type I collagen via alpha2beta1 integrin, RhoA, and fibronectin polymerization. *Am J Pathol, 163*(3), 1045-1056

Ray, J. L., Leach, R., Herbert, J. M., & Benson, M. (2001). Isolation of vascular smooth muscle cells from a single murine aorta. *Methods Cell Sci, 23*(4), 185-188

Revollo, J. R., Grimm, A. A., & Imai, S. (2004). The NAD biosynthesis pathway mediated by nicotinamide phosphoribosyltransferase regulates Sir2 activity in mammalian cells. *J Biol Chem, 279*(49), 50754-50763

Roccabianca, S., Bellini, C., & Humphrey, J. D. (2014). Computational modelling suggests good, bad and ugly roles of glycosaminoglycans in arterial wall mechanics and mechanobiology. *J R Soc Interface, 11*(97), 20140397

Rongvaux, A., Galli, M., Denanglaire, S., Van Gool, F., Dreze, P. L., Szpirer, C., Bureau, F., Andris, F., & Leo, O. (2008). Nicotinamide phosphoribosyl transferase/pre-B cell colony-enhancing factor/visfatin is required for lymphocyte development and cellular resistance to genotoxic stress. *J Immunol, 181*(7), 4685-4695

Rongvaux, A., Shea, R. J., Mulks, M. H., Gigot, D., Urbain, J., Leo, O., & Andris, F. (2002). Pre-B-cell colony-enhancing factor, whose expression is up-regulated in activated lymphocytes, is a nicotinamide phosphoribosyltransferase, a cytosolic enzyme involved in NAD biosynthesis. *Eur J Immunol, 32*(11), 3225-3234

Samal, B., Sun, Y., Stearns, G., Xie, C., Suggs, S., & McNiece, I. (1994). Cloning and characterization of the cDNA encoding a novel human pre-B-cell colony-enhancing factor. *Mol Cell Biol, 14*(2), 1431-1437

Schonherr, E., Jarvelainen, H. T., Kinsella, M. G., Sandell, L. J., & Wight, T. N. (1993). Platelet-derived growth factor and transforming growth factor-beta 1 differentially affect the synthesis of biglycan and decorin by monkey arterial smooth muscle cells. *Arterioscler Thromb, 13*(7), 1026-1036

Sparks, M. A., Parsons, K. K., Stegbauer, J., Gurley, S. B., Vivekanandan-Giri, A., Fortner, C. N., Snouwaert, J., Raasch, E. W., Griffiths, R. C., Haystead, T. A., Le, T. H., Pennathur, S., Koller, B., & Coffman, T. M. (2011). Angiotensin II type 1A receptors in vascular smooth muscle cells do not influence aortic remodeling in hypertension. *Hypertension, 57*(3), 577-585

van der Veer, E., Ho, C., O'Neil, C., Barbosa, N., Scott, R., Cregan, S. P., & Pickering, J. G. (2007). Extension of human cell lifespan by nicotinamide phosphoribosyltransferase. *J Biol Chem, 282*(15), 10841-10845

van der Veer, E., Nong, Z., O'Neil, C., Urquhart, B., Freeman, D., & Pickering, J. G. (2005). Pre-B-cell colony-enhancing factor regulates NAD+-dependent protein deacetylase activity and promotes vascular smooth muscle cell maturation. *Circ Res, 97*(1), 25-34

Verdone, L., La Fortezza, M., Ciccarone, F., Caiafa, P., Zampieri, M., & Caserta, M. (2015). Poly(ADP-Ribosyl)ation Affects Histone Acetylation and Transcription. *PLOS ONE, 10*(12), e0144287

Wang, Y., Wang, L., Zhang, F., Zhang, C., Deng, S., Wang, R., Zhang, Y., Huang, D., & Huang, K. (2013). Inhibition of PARP prevents angiotensin II-induced aortic fibrosis in rats. *Int J Cardiol, 167*(5), 2285-2293

Watson, A., Nong, Z., Yin, H., O'Neil, C., Fox, S., Balint, B., Guo, L., Leo, O., Chu, M. W. A., Gros, R., & Pickering, J. G. (2017). Nicotinamide Phosphoribosyltransferase in Smooth Muscle Cells Maintains Genome Integrity, Resists Aortic Medial Degeneration, and Is Suppressed in Human Thoracic Aortic Aneurysm Disease. *Circ Res, 120*(12), 1889-1902

Xia, J., Wu, X., Yang, Y., Zhao, Y., Fang, M., Xie, W., Wang, H., & Xu, Y. (2012). SIRT1 deacetylates RFX5 and antagonizes repression of collagen type I (COL1A2) transcription in smooth muscle cells. *Biochem Biophys Res Commun, 428*(2), 264-270

Xin, H. B., Deng, K. Y., Rishniw, M., Ji, G., & Kotlikoff, M. I. (2002). Smooth muscle expression of Cre recombinase and eGFP in transgenic mice. *Physiol Genomics, 10*(3), 211-215

Xu, S., Zhi, H., Hou, X., Cohen, R. A., & Jiang, B. (2011). IkappaBbeta attenuates angiotensin II-induced cardiovascular inflammation and fibrosis in mice. *Hypertension, 58*(2), 310-316

Yan, C., & Boyd, D. D. (2007). Regulation of matrix metalloproteinase gene expression. *J Cell Physiol, 211*(1), 19-26

Yan, X., & Chen, Y. G. (2011). Smad7: not only a regulator, but also a cross-talk mediator of TGF-beta signalling. *Biochem J, 434*(1), 1-10

Yin, H., van der Veer, E., Frontini, M. J., Thibert, V., O'Neil, C., Watson, A., Szasz, P., Chu, M. W., & Pickering, J. G. (2012). Intrinsic directionality of migrating vascular smooth muscle cells is regulated by NAD(+) biosynthesis. *J Cell Sci, 125*(Pt 23), 5770-5780

CHAPTER 5 - NICOTINAMIDE PHOSPHORIBOSYLTRANSFERASE IS ESSENTIAL FOR ADULT MICE SURVIVAL

5.1 Introduction

Nampt is required for the regeneration of NAD^+ when NAD^+ has been depleted by NAD^+-consuming reactions, including the ADP ribosylation of proteins, protein deacetylation, and the production of cyclic ADP ribose (Sauve and Schramm 2004, Lee 2012, Luo and Kraus 2012). Several studies have reported Nampt to be highly expressed in lung, liver, kidney, heart, adipose, and skeletal muscle, with much lower expression in brain and pancreas (Samal et al. 1994, Revollo et al. 2007).

Tissue-specific gene targeting strategies in mice have revealed a pattern of degenerative or aging-related tissue dysfunction when Nampt is perturbed in skeletal muscle, adipose tissue, and brain (Stein and Imai 2014, Frederick et al. 2016, Stromsdorfer et al. 2016, Zhou et al. 2016), in addition to the data presented in earlier chapters outlining the degenerative consequences of *Nampt* knockout in SMCs.

Mice lacking Nampt in forebrain excitatory neurons showed hippocampal and cortical atrophy, astrogliosis, microgliosis, and abnormal CA1 dendritic morphology by 2–3 months of age (Stein et al. 2014). Ablation of *Nampt* in adult neural stem cells also causes signs of accelerated aging in this neural cell population (Stein and Imai 2014). Knockout of *Nampt* in skeletal muscle contributed to an aging phenotype-related loss mass and contractile function (Frederick et al. 2016). Adipocyte-specific *Nampt* knockout mice had severe insulin resistance in adipose tissue, liver, and skeletal muscle, and adipose tissue dysfunction, manifested by increased plasma free fatty acid concentrations and decreased plasma concentrations of a major insulin-sensitizing adipokine, adiponectin (Stromsdorfer et al. 2016). Additionally, Nampt is critically required for the development of both T and B lymphocytes (Rongvaux et al. 2008). Interestingly, this dysfunction was shown to be at

least partially ameliorated in some cell types by the exogenous delivery of NAD^+ precursors, such as nicotinamide (NAM) or nicotinamide riboside (NR). However, due to the variability of the limited tissue-specific *Nampt* knockout data available, it is unclear which may be the most vulnerable systems.

Nampt has been understood to be an essential enzyme for embryo development based on reports that the development of the mouse embryo cannot proceed past e10.5 without Nampt (Revollo et al. 2007). A very recent report has emerged in which this finding is confirmed. Nampt begins to be expressed at e8.5 in mouse development, and Nampt deficient embryos cannot develop past e10.5 (Zhang et al. 2017). The essentiality of Nampt was further confirmed in the adult mouse when knocked out using tamoxifen-regulated Cre activity. These mice did not survive longer than 10 days post *Nampt* knockout. The authors report severe atrophy of the villi of the gastrointestinal tract, an increase in serum triglyceride levels, and a catastrophic decrease in abdominal adipose stores (Zhang et al. 2017). However, their findings were limited, as they did not present data on any other tissues that may have been affected by *Nampt* knockout. Additionally, although these pathologies are attributed to liver dysfunction caused by liver Nampt depletion, the model of *Nampt* knockout they used for their studies only yielded 20% decrease in *Nampt* expression in the liver.

Here, I investigate the role of global expression of *Nampt* in a mouse model by inducing knockout in an adult mouse, thus circumventing the embryonic lethality. My findings reveal that *Nampt* is an essential gene necessary to sustain life. The findings also reveal the different tissues are seemingly more resistant to the depletion of *Nampt*. Additionally, I was able to extend the lifespan of *Nampt* KO mice by supplying the mice with NR, an exogenous NAD^+ precursor. These findings shed new light on the tissue-specific requirements for Nampt.

5.2 Methods

5.2.1 Generation of Nampt-deficient mouse model

Mouse experiments followed protocols approved by the Western University Animal Use Committee. All mice were on a C57Bl/6 background. I generated mice in which *Nampt* could be globally and inducibly deleted. *Nampt*$^{flox/flox}$ mice were bred with mice expressing Cre recombinase fused to the mutated ligand binding domain of the human estrogen receptor (ER) under the control of a chimeric cytomegalovirus immediate-early enhancer/chicken ß-actin promoter (B6.Cg-Tg(CAG-Cre/Esr1)5Amc/J) (Jackson Laboratories, Bar Harbor, ME) (Hayashi and McMahon 2002). To induce *Nampt*$^{flox/flox}$ recombination and excision by Cre recombinase, 8-10 week old *Nampt*$^{flox/flox}$;Cre-ERT2(+) mice (denoted as Nampt KO) were i.p. injected with (1 mg/kg/day) tamoxifen (Tmx) in sunflower oil vehicle, for five consecutive days. *Nampt*$^{flox/flox}$;Cre-ERT2(-) (denoted as WT control) were also injected concomitantly with Tmx in sunflower oil to control for any effects due to Tmx toxicity. For NR studies, mice were given a daily single dose (1000 mg/kg body weight) by i.p. injection. Initial necropsy studies were performed by the CMHD Pathology Core at the Toronto Centre for Phenogenomics (Toronto, Ontario, Canada).

5.2.2 Serum collection and analysis

Serum was collected using an approved standard protocol. Briefly, mice were anaesthetized and blood was immediately collected by cardiac puncture. Blood was allowed to clot for 20-30 minutes and then centrifuged for 10 mins at 1,500g to separate the clotted material from the serum. Serum was then flash frozen and stored at -80°C for future analysis. Clinical chemistry parameters were measured by standard protocols by Charles River Laboratories (Wilmington, MA). Plasma insulin was determined by mouse-specific

ELISA as per manufacturer's instructions (ALPCO Diagnostics, Salem, NH: mouse ultrasensitive ELISA #80-NSMSU-E01).

5.2.3 Histology and immunohistochemistry of mouse tissues

Mouse tissues were collected and fixed intact (with the exception of the intestinal tract which was split open and rolled in order to survey the entire organ) overnight in 4%-paraformaldehyde and embedded in paraffin. 10 mm-thick sections were stained with hematoxylin and eosin (H&E) to broadly evaluate tissue architecture. Immunostaining was performed on paraffin-embedded sections for Nampt using a rabbit polyclonal anti-Nampt (A300-372A 1:50; Bethyl Laboratory, Montgomery, TX). Bound primary antibodies against Nampt were detected using goat anti-rabbit biotinylated antibody (Vector Labs, Burlington, ON, Canada) and visualized using an ABC kit and diaminobenzidine (DAB, Vector Labs) and counterstained with Harris' hematoxylin.

5.2.4 Morphology of esophagus and intestine

Mouse esophagus was removed intact 4%-paraformaldehyde fixed and paraffin embedded sections were stained with H&E and visualized with an Olympus BX51 microscope. Epithelial structure thickness was quantified from an average of 10 equidistant measurements around 3 sections 200 μm apart using ImageJ software (NIH, Bethesda, MD). Mouse intestine was dissected and prepared with the adapted Swiss roll technique to visualize the entire organ (Williams et al. 2016). Abnormal mucosal architecture was evaluated in 3 regions of the jejunum 200 μm apart by measuring irregular crypts, and crypt and villous blunting (Erben et al. 2014).

5.2.5 Laser capture microdissection and RNA isolation of pancreatic islets and acinar cells.

Laser capture was undertaken on 10 μm-thick frozen sections of WT control and Nampt KO pancreas (15 days after initiation of Tmx injections) that had been embedded in

OCT compound (Tissue-Tek). Islet cells and acinar cells were micro-dissected (Arcturus 704 Veritas LCM System, Harlow Scientific, Arlington, VA) from 10 pancreas sections and RNA extracted using TRIzol (Life Technologies) with the addition of linearized polyacrylamide (2 mg/ml, Sigma) following phase separation.

5.2.6 Quantitative real-time reverse transcription–polymerase chain reaction

Total RNA was isolated from homogenates of the mouse aorta using TRIzol (Life Technologies) and the RNeasy Mini Kit following the manufacturer's protocol (Qiagen, Valencia, CA). Total RNA was isolated from mouse and human SMCs using the RNeasy Mini Kit following the manufacturer's protocol. Transcript abundance of mouse *Nampt*, *Nrk1,* and 18S were assessed using SYBR-green chemistry-based primer sets (*Nampt:* F-GGCACCACTAATCATCAGACCTG R-AAGGTGGCAGCAACTTGTAGCC; *Nrk1*: F-AGAGCTTGCAGAAGCACCTTCC R-CATCCAACAGGAAACTGCTGACA; 18S F-GTAACCCGTTGAACCCCATT R-CCATCCAATCGGTAGTAGCG). Quantitative real-time RT-PCR was performed using an ABI Prism (model 7900HT) and Sequence Detection System software (Life Technologies; Applied Biosystems). For *Nampt* expression in LCM islet and acinar cell samples, relative mRNA abundance was quantified based on critical threshold (CT) using the comparative CT formula, 2-ΔΔCT, with 18S mRNA as an internal control. For *Nampt* and *Nrk1* expression in whole tissues, mRNA abundance was quantified based on the standard curve method, with 18S mRNA as an internal reference control, and expressed as relative units (r.u.)

5.2.7 Statistical analyses

Values are expressed as mean±standard error of the mean. Statistical analyses were performed using GraphPad Prism software (GraphPad, La Jolla, CA, USA). Mean data were compared using Student's t-test or one-ANOVA with Holm-Sidak post hoc testing.

Kaplan–Meier survival analysis was used to assess mouse longevity, and data were compared using log-rank (Mantel-Cox) testing.

5.3 Results

5.3.1 Nampt knockout specifically in adult mice is lethal

To determine whether Nampt expression is a requisite necessity for survival, I generated a mouse in which *Nampt* could be globally deleted in the adult. Because *Nampt* knockout is embryonically lethal before e10.5 (Revollo et al. 2007, Zhang et al. 2017), the deletion needed to be inducible in an adult animal and therefore *Nampt*$^{flox/flox}$;Cre-ERT2(+) mice were generated. Mice (8-10 weeks old) were injected with tamoxifen (Tmx) for five days to induce recombination and excision of the *Nampt*$^{flox/flox}$ allele. To determine the amount of *Nampt* depletion I evaluated the expression of *Nampt* mRNA in peri-mortem *Nampt*$^{flox/flox}$;Cre-ERT2 (*Nampt* KO) mice by quantitative PCR. *Nampt* expression was reduced in the heart (93.1%, $P<0.0001$, Fig. 1a), skeletal muscle (94.8%, $P=0.0003$, Fig. 5.1b), kidney (75.0%, $P=0.004$, Fig. 5.1c), brain (78.0%, $P<0.0001$, Fig. 5.1d), and intestine (77.7%, $P=0.003$, Fig. 5.1e). There was no significant change in *Nampt* expression in the liver ($P=0.790$, Fig. 5.1f)

Median survival time of *Nampt* KO mice was 16 days and no mouse survived past 20 days following the initiation of Tmx injection (n=12, $P=0.003$, Fig. 5.2a). An onset of rapid weight loss began five days after Tmx injections were initiated and *Nampt* KO mice had a 13.2 ± 5.44% decrease in body weight at time of death ($P=0.001$, Fig. 5.2b).

5.3.2 *Nampt* knockout is accompanied by gross pathological changes in the intestine and pancreas

To help determine cause of death following *Nampt* knockout, a gross pathological analysis of peri-mortem mice was undertaken. In addition to the weight loss described above, *Nampt* KO peri-mortem mice were slow to move and were hunched (Fig. 5.2c).

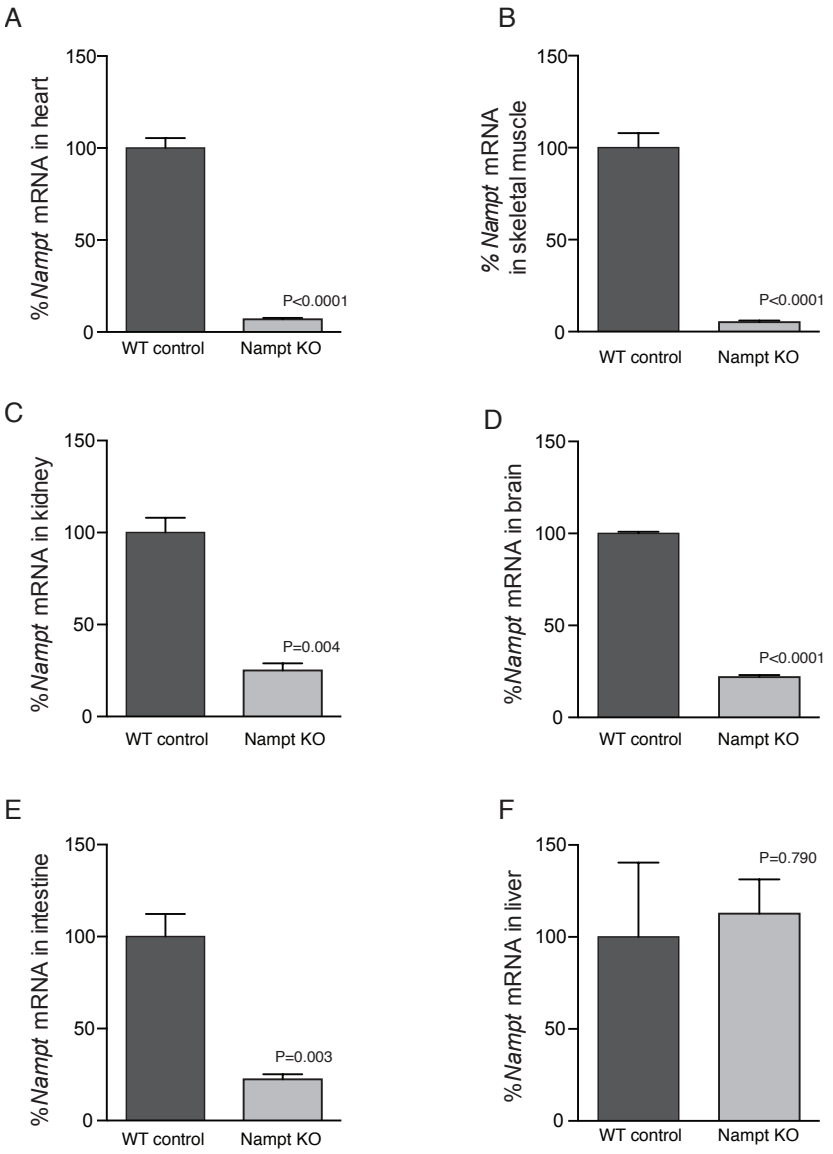

Figure 5.1 *Nampt* expression is decreased in heart, skeletal muscle, kidney, brain and small intestine in *Nampt* KO mice

Graphs depicting the amount of *Nampt* expression in the **A**) heart, **B**) skeletal muscle, **C**) kidney, **D**), brain, **E**) intestine, and **F**) liver of *Nampt* KO mice as compared to WT control mice, as measured by quantitative RT-PCR. *Nampt* expression was normalized to the internal *18S* expression. Tissues were harvested in peri-mortem mice, on average 15 days following the initiation of Tmx injections (n=3-4 per group, Student's T-test).

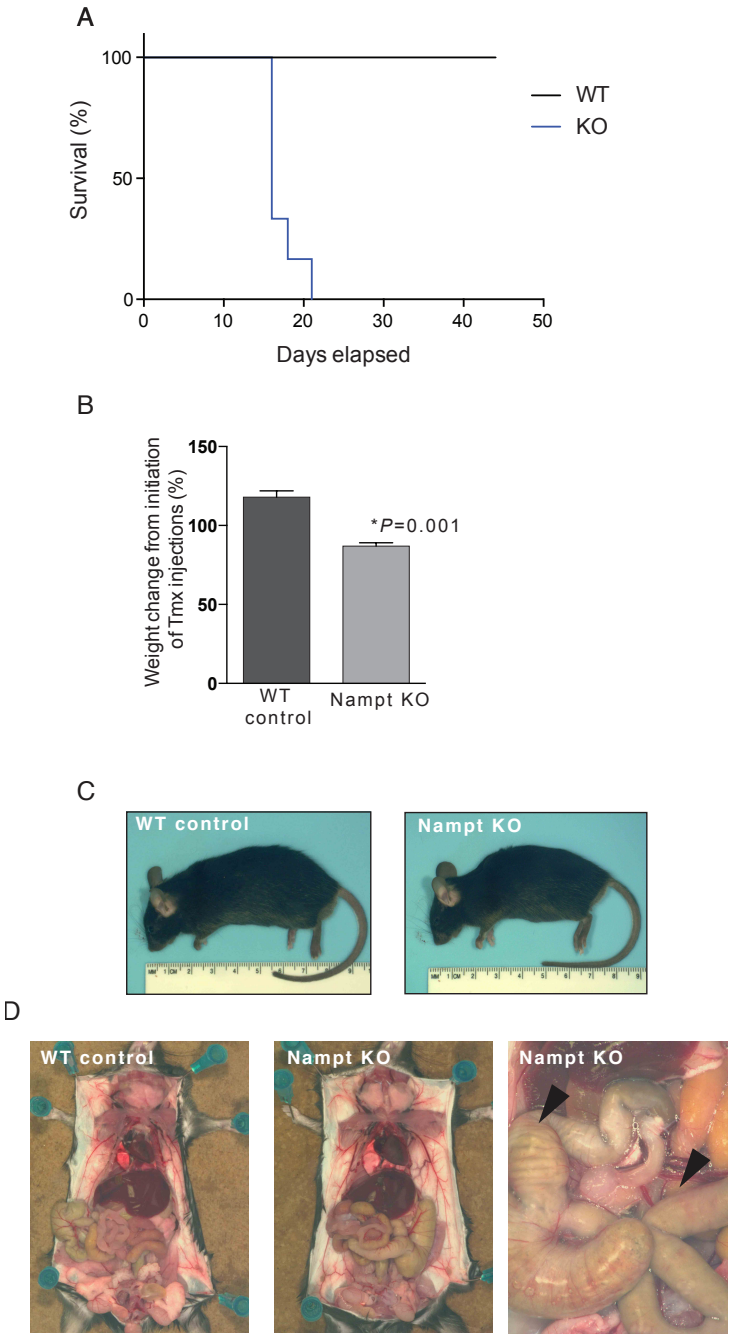

Figure 5.2 *Nampt* knockout is lethal in adult mice

A) Kaplan-Meier survival curve of WT and *Nampt* KO mice following tamoxifen injection for 5 days (n=8 per group, **P*<0.002, Log-rank (Mantel-Cox) test). **B**) Graph depicts change in weight at the end of lifespan as compared to the animal's individual starting weight. **C**) Images of WT control and peri-mortem *Nampt* KO mice at time of death. **D**) Gross dissection of abdominal cavity of WT control and peri-mortem *Nampt* KO mice. Third panel demonstrates gross evidence of intestinal distension (black arrowheads).

These observations consistently preceded death within 24 hours. Upon abdominal dissection, it was apparent that the esophagus, stomach, and the small and large intestine were distended with food materials (Fig. 5.2d). In addition, there was gross evidence of a loss of pancreatic parenchymal integrity and enlarged lymph nodes. Examination of the kidney, heart, skeletal muscle, brain, and liver revealed no gross pathology (Table 5.1).

5.3.3 *Nampt* knockout changes liver serum chemistry parameters

To further characterize the decline of *Nampt* KO mice, the serum chemistry of a subset of mice was analysed. Serum was collected 5 days, 10 days, and 15 days following initiation of Tmx injection (n=3 per group). Five days after initiation of Tmx injection serum parameters were not significantly different from the range of expected values. However, ten days after initiation of Tmx injections there was a significant change in levels of alanine aminotransferase (8.3-fold increase, P=0.02, Fig. 5.3), aspartate aminotransferase (27.6-fold increase, P=0.04, Fig. 5.3), alkaline phosphatase (2.9-fold increase, P=0.01, Fig. 5.3), and glucose (55.9% decrease, P=0.03, Fig. 5.3). Interestingly, 15 days after Tmx injections these levels returned to the range of expected values, except for aspartate aminotransferase. These serum chemistry changes indicate a possible early disruption in liver processes.

5.3.4 *Nampt* knockout affects the epithelial layers of the gastrointestinal tissues

To determine which tissues are affected by the knockout of Nampt, I evaluated histological sections of the *Nampt* KO mice. There was no evidence of histological changes in the heart, liver, kidney, or skeletal muscle of *Nampt* KO mice (Fig. 5.4). Surprisingly, while there was gross appearance of dysfunction in the gastrointestinal tract (i.e. distension of the esophagus, small intestine and colon), there was limited evidence for cellular disruption. Villus height was variable; villi were midly, but not significantly, blunted in the intestine (21.2% decrease 15 days after Tmx, P=0.080, Fig. 5.5a,b) with

Table 5-1 The number of *Nampt* KO mice with tissue-specific gross pathology 5 days, 10 days, and 15 days following injection of tamoxifen and induction of *Nampt* knockout

Tissue	**Pathology finding (if present)**	5 days post Tmx *(n=3)*	10 days post Tmx *(n=3)*	15 days post Tmx *(n=8)*
Pancreas	Loss of parenchymal integrity	3	3	8
Esophagus	Abnormal esophagus morphology, dilated with food (partially digested)	1	1	6
Stomach	Dilated stomach filled with food materials	0	2	7
Jejunum	Dilated with thickened wall filled fully with liquid and green fecal material,	0	3	8
Ileum	Enlarged, dilated with thickened wall filled fully with liquid and green fecal material	0	3	8
Colon	Abnormal colon morphology, dilated with thicken wall, and filled fully with liquid and green fecal material	0	3	8
Cecum	Enlarged cecum	0	3	8
Kidney	Small kidney	0	0	2
Testis	Seminal vesicles are smaller. Small testis	0	0	2
Lymph nodes	Enlarged lymph nodes	0	0	2
Adrenal gland	Small adrenal glands	0	0	2
Heart	None	0	0	0
Skeletal muscle	None	0	0	0
Liver	None	0	0	0

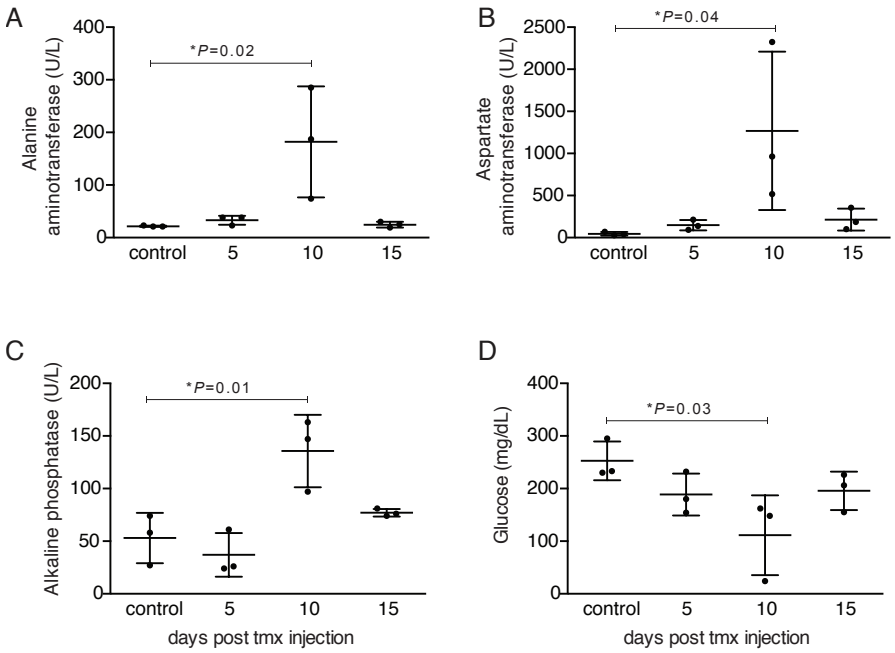

Figure 5.3 *Nampt* knockout increases serum levels of aspartate aminotransferase, alanine aminotransferase, and alanine phosphatase, and decreases circulating glucose levels

Serum was collected from WT control and *Nampt* KO mice by cardiac puncture 5 days, 10 days, and 15 days following the initiation of tamoxifen injections (1000ng/mg/ml). Basic serum clinical chemistry was measured for **A**) alanine aminotransferase, **B**) aspartate aminotransferase, **C**) alkaline phosphatase, **D**) glucose. N=3 mice at each time point. Graph depicts data points in addition to mean ± standard deviation, by one-way ANOVA with Holm-Sidak post hoc testing

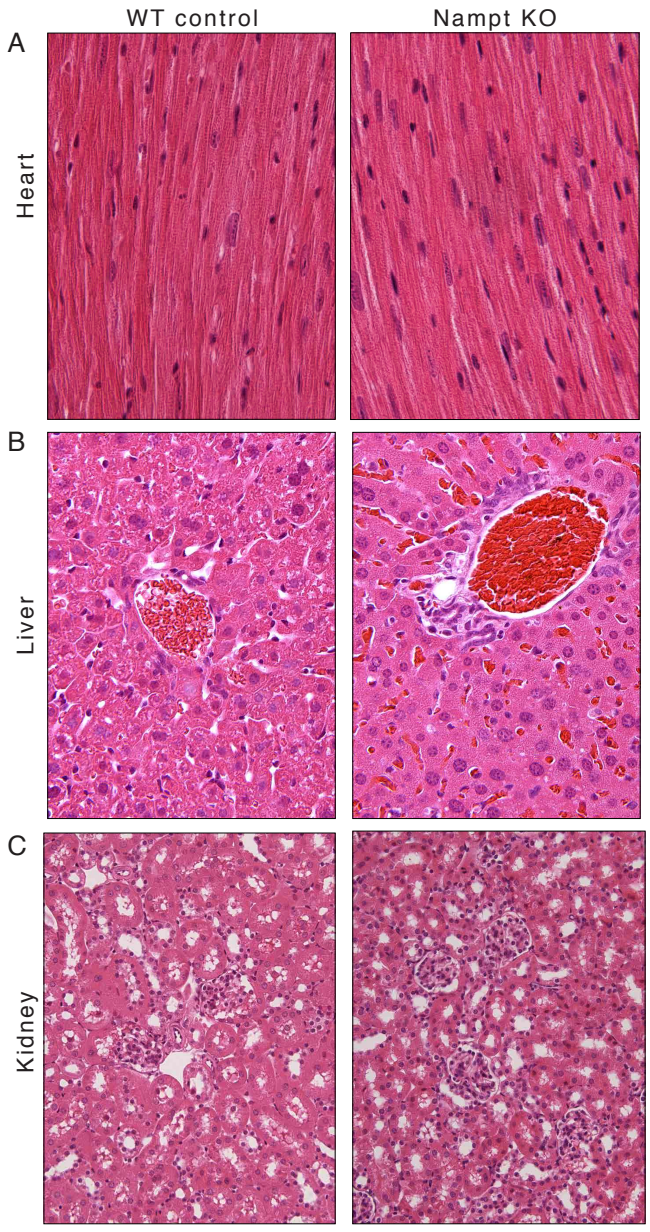

Figure 5.4 *Nampt* knockout does not have an effect on the histological appearance of the heart, liver, or kidney

Micrographs of H&E-stained WT control and *Nampt* KO **A**) heart (cardiac myocytes), **B**) liver, and **C**) kidney depicting no apparent differences.

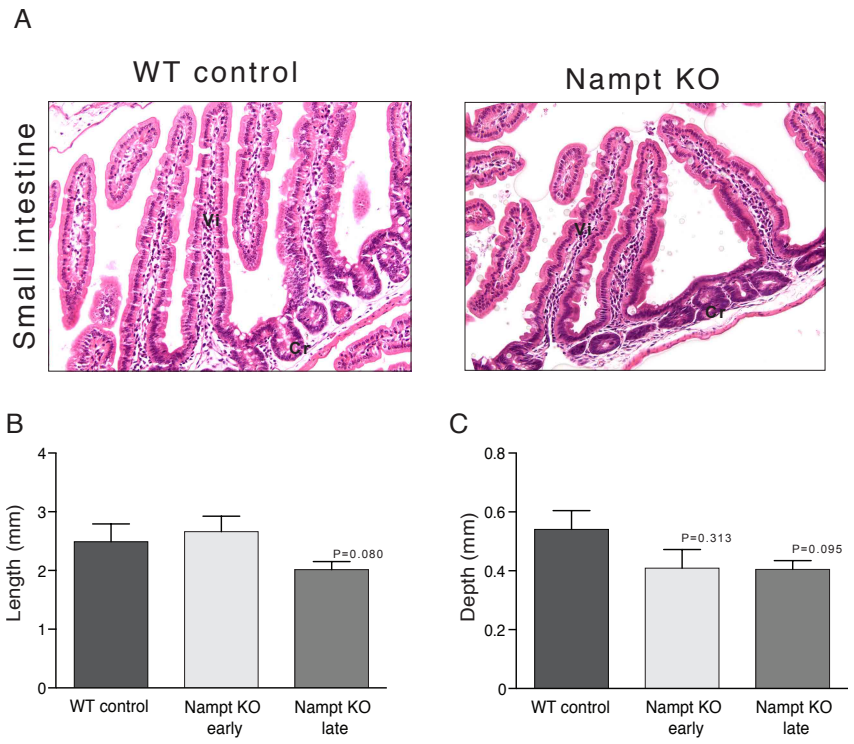

Figure 5.5 *Nampt* knockout is associated with a blunted villus and crypt architecture in the small intestine

A) Micrographs of H&E-stained sections of WT control and *Nampt* KO small intestine. The effect that *Nampt* KO had on the tissue was heterogenous; some villi (Vi) and crypts (Cr) were slightly blunted (panel 2), others were significantly blunted (panel 3). **B**) Average length of villi in the small intestine (WT control n=3, early (5 day) n=3, late (10-15 day) n=6, one-way ANOVA with Holm-Sidak post hoc testing). **C**) Average depth of crypts in the small intestine (WT control n=3, early (5 day) n=3, late (10-15 day) n=6, one-way ANOVA with Holm-Sidak post hoc testing).

some evidence of villus loss in patchy areas. There was also crypt architecture that appeared mildly, but not significantly, compressed 5 days after the initiation of Tmx injections (26.2% decrease in crypt depth, P=0.313, Fig. 5.5a,c), and persisted through the decline of the mice to day 15 (26.9% decrease in crypt depth 15 days after Tmx injection, *P*=0.090, Fig. 5.5a,c). Additionally, there was a thinning of the epithelial layer of the esophagus (Fig. 5.6a,b). Specifically, there was a 52.9% decrease in the average thickness of the epithelial layer starting 5 days after the initiation of Tmx injections (*P*=0.0002, Fig. 5.6d).

5.3.5 *Nampt* knockout affects integrity of the pancreas

Evaluation of the pancreas as early as five days following the initiation of Tmx injection, I observed evidence of multifocal to coalescing pancreatic acinar atrophy and islet hyperplasia. Throughout the organ, there is histological evidence that localized acinar cells have been replaced by ductal cells (acinar-to-ductal metaplasia Fig. 5.7a) and the islet areas appear enlarged due to increased number of cells (3.1 ± 0.78-fold increase, *P*=0.03). I also observed an appearance of interstitial stellate cells, which are often activated upon injury. Additionally, there was an observed 89.5% decrease in serum insulin levels in peri-mortem *Nampt* KO mice (Fig. 5.7b); evidence of a dysfunction of islet cells.

This adverse pancreatic affect was particularly surprising as the baseline expression of *Nampt* in the pancreas is reportedly very low to non-existent, particularly in comparison to *Nampt* expression in other tissues (Fig. 5.7c) (Samal et al. 1994, Revollo et al. 2007). I sought to confirm the result in the pancreas using both immunohistochemistry (Fig. 5.7c) and also the more stringent approach of isolating pancreatic RNA specifically from islet cells versus acinar cells by laser-capture microdissection. The results revealed that at baseline *Nampt* is expressed only in islet cells of the pancreas (Fig. 5.7d,e). There is no expression detected either by qPCR or immunohistochemistry in acinar cells.

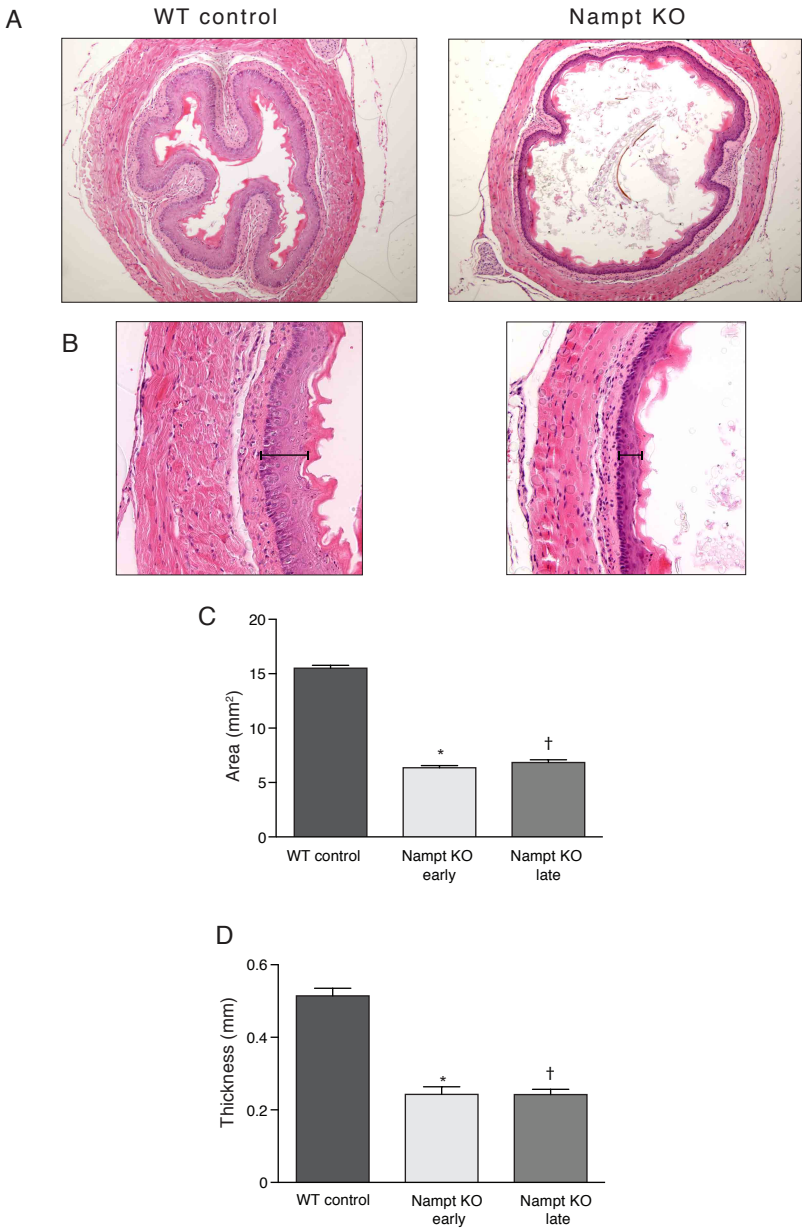

Figure 5.6 *Nampt* knockout is associated with a thinning of the epithelial layer of the esophagus

A) Micrographs depicting cross-sections of the dilated *Nampt* KO esophagus, still containing remnants of mouse chow (second panel). **B**) Higher magnification view of the *Nampt* KO esophagus, depicting the thin epithelial layer (black line). **C**) Graph depicting the average area occupied by the epithelial layer in a cross section of the esophagus (WT control n=3, early (5 day) n=3, late (10-15 day) n=6, **P*<0.0001 vs. WT control, †*P*<0.0001 vs. WT control, by one-way ANOVA with Holm-Sidak post hoc testing). D) Graph depicting the average thickness of the epithelial layer in a cross section of the esophagus (WT control n=3, early (5 day) n=3, late (10-15 day) n=6, **P*<0.0001 vs. WT control, †*P*<0.0001 vs. WT control, by one-way ANOVA with Holm-Sidak post hoc testing).

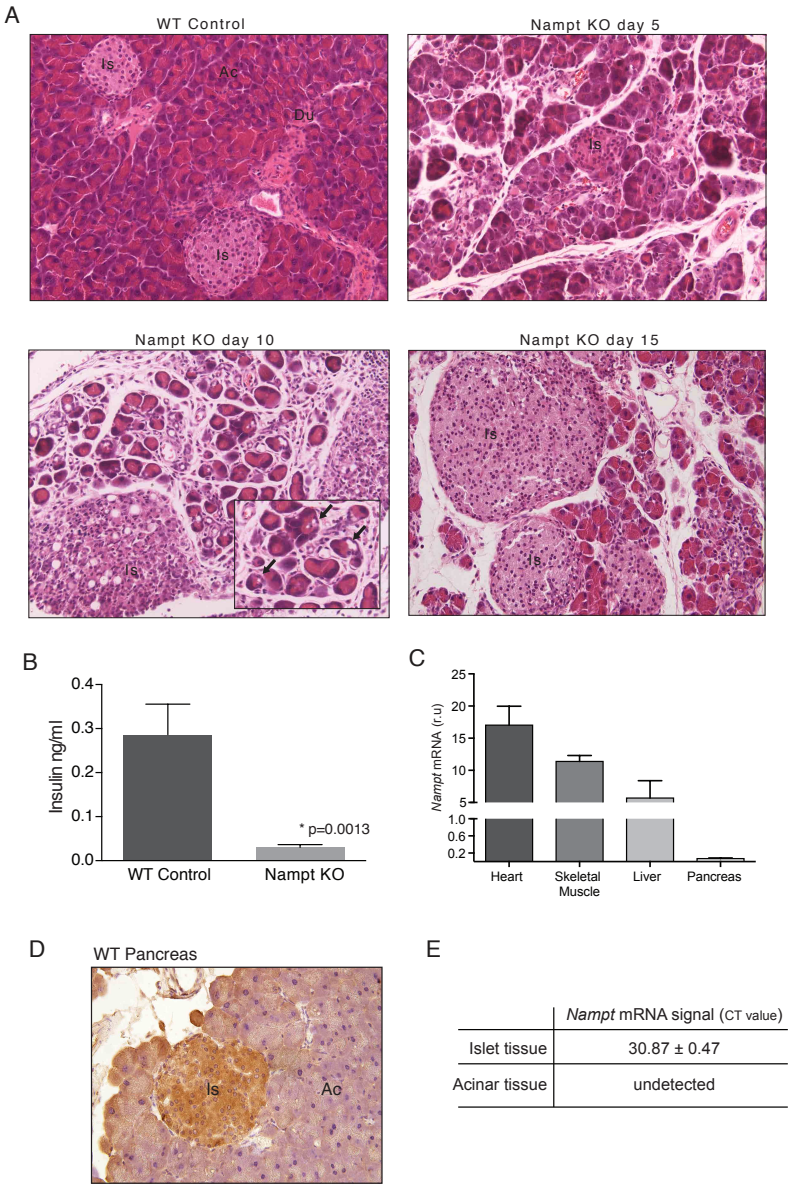

Figure 5.7 *Nampt* knockout affects the integrity of the pancreas

A) Representative micrographs of the multifocal to coalescing pancreatic acinar atrophy and islet cell hyperplasia throughout the pancreas at 5, 10 and 15 days following the initiation of Tmx injections. Is: Islet cells, Ac; Acinar cells, Du: Ductal cells. Black arrows in inset indicate examples of acinar-to-ductal metaplasia. **B**) Serum insulin levels measured in peri-mortem *Nampt* KO mice (WT control n=5, Nampt KO n=7) **C)** Graph depicting *Nampt* mRNA as measured by RT-PCR and normalized to *18S* expression in WT Control mouse tissues (n=3 mice) **D**) Representative micrographs of immunohistochemistry for Nampt expression in WT control pancreas harvested from peri-mortem mice (Is: islet cells; Ac: acinar cells). **E**) *Nampt* mRNA signal detected by RT-PCR and expressed as absolute CT values in islet cells and acinar cells isolated by laser-capture microdissection. Pancreatic tissue from a minimum of 10 sections from 2 mice was evaluated.

5.3.6 Nicotinamide riboside delays the decline of *Nampt* KO mice, but is unable to ultimately prevent death.

To determine whether delivery of NR, an exogenous precursor to NAD^+, would be sufficient to compensate for the loss of the NAD^+-regenerating activity of Nampt, I first measured the expression of *Nrk1*. Nrk1 is the enzyme that converts NR to NAD^+. The natural source of oral NR (and other NAD^+ precursors NAM and NA) is largely in the food we eat as broken down by digestion and the microbiome (Bogan and Brenner 2008, Canto et al. 2015) Interestingly, it was recently shown that the human cytosolic 5′-nucleotidase CD73 can catalyse the conversion of NMN into NR and that at least some cells are able to release this nucleoside precursor of NAD^+ (Kulikova et al. 2015), suggesting that NR is in available in the circulation. *Nrk1* expression was assessed by qPCR in the heart, skeletal muscle, liver, and pancreas of control and *Nampt* KO mice, both at baseline and also in mice that had been supplemented with daily i.p. injections of NR. In *Nampt* KO mice supplemented with NR there was an increase in *Nrk1* expression in the liver as compared to the WT control (2.80-fold, P=0.043, Fig. 5.8a) and a trend towards increase in the heart, although the data were not significant (1.25-fold, Fig. 5.8b). Interestingly, in the pancreas of *Nampt* KO mice, both with and without NR supplementation, there was an increase of *Nrk1* expression (4.48-fold, P=0.182 and 4.82-fold, P=0.009, respectively, Fig. 5.8d). This suggests a pancreatic dependence on a bio-available source of NAD^+, or a precursor to NAD^+.

It was also of interest to deduce whether NR supplementation would be sufficient to overcome decline and death due to Nampt knockout. I was able to demonstrate that administration of NR can prolong the survival of *Nampt* KO mice, doubling the median survival time from 16 to 34 days (P=0.001, Fig. 5.9a). Interestingly, at 20 days following Tmx injection (the point at which all *Nampt* KO mice had died) *Nampt* KO mice supplemented with NR began to regain weight, although this was not sustained (Fig. 5.9b).

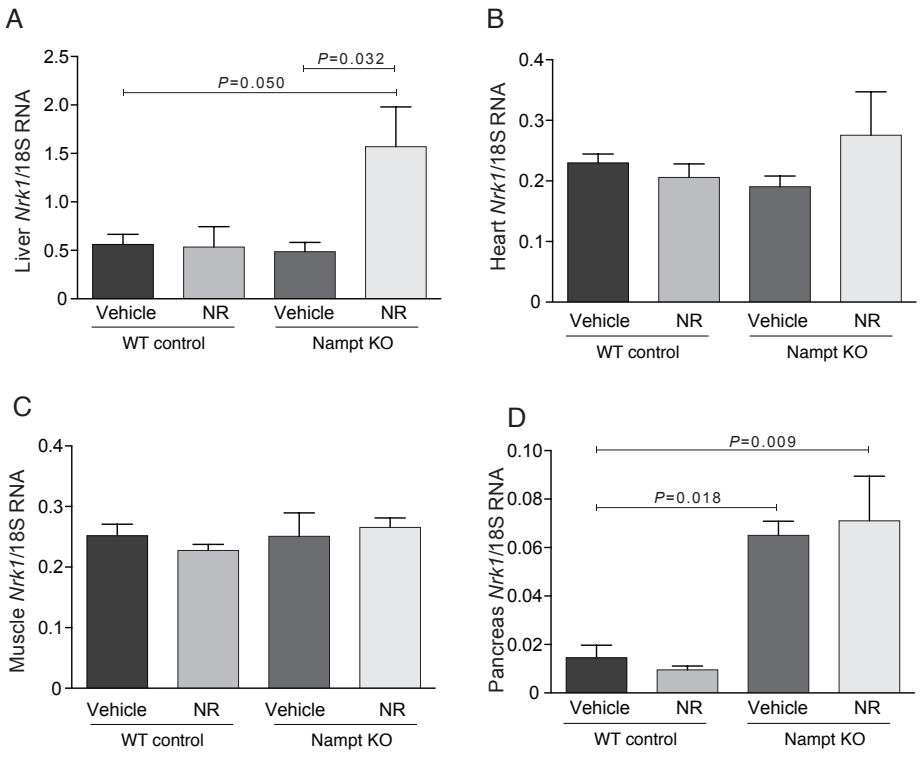

Figure 5.8 Expression of *Nrk1* is increased in the liver and the pancreas of *Nampt* KO mice

Graphs depicting the expression of *Nrk1* in the **A**) liver, **B**) heart, **C**) skeletal muscle, and **D**) pancreas of WT control and *Nampt* KO mice, both at baseline or supplemented with daily i.p. injections of NR (1000 mg/kg/day). *Nrk1* expression was normalized to the internal expression of *18s*. N=4 mice per group, one-ANOVA with Holm-Sidak post hoc testing.

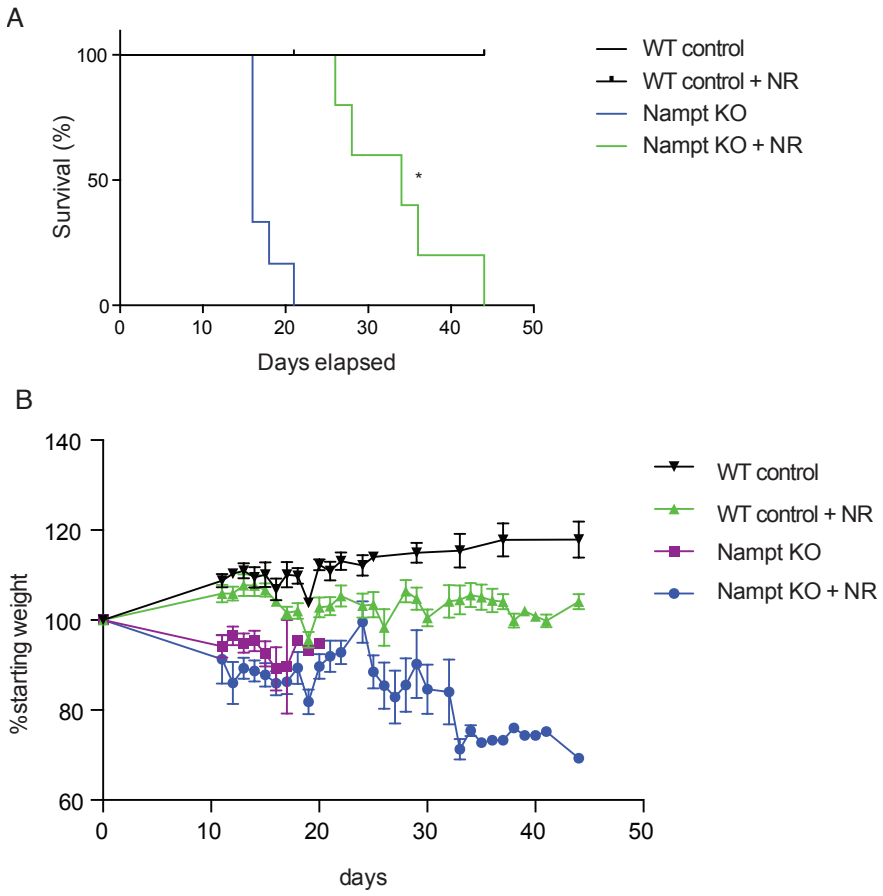

Figure 5.9 Global loss of Nampt-mediated NAD^+ biosynthesis in the adult mouse in lethal and is partially rescued by administration of nicotinamide riboside (NR)

A) Kaplan-Meier survival curve of WT and *Nampt* KO mice. NR (1000 mg/kg/day) was i.p. injected daily until day of death (n=8 per group, **P*=0.001 vs. *Nampt* KO, by log-rank [Mantel-Cox] testing). **B**) Graph depicting weights of mice until time of death (n=8 per group).

5.4 Discussion

This study is one of the first reports on the essentiality of Nampt expression. *Nampt* KO mice i) did not survive longer than 20 days without Nampt expression; ii) underwent extreme pancreatic atrophy; iii) died with a GI tract filled with food materials; iv) had their lifespans doubled by supplementing them with NR, but ultimately succumbed to the Nampt deficiency.

The finding that global *Nampt* KO is quickly lethal in an adult animal is noteworthy. Previous reports have mentioned as an observation that *Nampt* knockout is lethal in the developing embryo prior to e10.5 (Rongvaux et al. 2002, Fukuhara et al. 2005, Revollo et al. 2007). Our previous findings have demonstrated that knocking out *Nampt* specifically in smooth muscle cells does not lead to the complete failure of SMC-rich vessels and organs. However, there is a propensity to DNA damage, abnormal expression of matrix components and senescence in vascular smooth muscle cells along with a dysfunction, albeit not complete failure, of bladder and intestinal smooth muscle (Watson et al. 2017). Other reports have indicated that *Nampt* ablation in the liver, skeletal muscle, and brain does not lead to the failure of these organs, but it does predispose to a pattern of aging or degenerative tissue disorder (Stein and Imai 2014, Frederick et al. 2016, Zhou et al. 2016). Concordantly, our initial expectation was that a global *Nampt* knockout would lead to an aging or degenerative phenotype. These results were unexpected; however, my findings of quick decline and death corroborate the very recent report of a global inducible *Nampt* knockout in an adult animal (Zhang et al. 2017).

Nampt-depleted mice demonstrated a striking atrophy of the exocrine pancreas. This was first observed in peri-mortem *Nampt* KO mice, but upon further examination this atrophy began as early as five days after the initiation of Tmx injection. This atrophy was accompanied by acinar nuclear dysplasia, fibrosis, some necrotic cells, and a striking

occurrence of acinar-to-ductal metaplasia (ADM). Notably, there was a lack of inflammatory cells, even with the appearance of a few necrotic cells. ADM is thought to be a response to pancreatic injury, and has been observed in several conditions including pancreatitis, chemically induced carcinogenesis, duct ligation, pancreatectomy, chronic hyperglycemia and animal models of diabetes (reviewed in (Storz 2017)). It was shown that exocrine cells might also trans-differentiate into ß cells (Minami et al. 2005). Although there was little evidence for local *Nampt* expression in the pancreas there was strong evidence of organ-wide dysfunction, pointing to the requisite need for a source of Nampt or bioavailable NAD^+. This source could, in theory, be i) supplied locally even with Nampt expression in islet cells, ii) delivered from circulating extracellular Nampt, or iii) circulating nucleoside NAD^+ precursors, such as NR. It has not been established whether or not the pancreas can use distal sources of Nampt or NAD^+ precursors. However, paradigm of dependence on a distal supply of Nampt has been reported in the case of hippocampal cells requiring Nampt secreted from adipose tissue (Yoon et al. 2015).

Nampt KO mice had a dilated and chow-filled alimentary canal - from the esophagus to the colon. There was a thinning of the structure composed of epithelial cells in these tissues, which may suggest that cell types with high turnover rates are more dependent on a bioavailable source of NAD^+. Dilation and chow arrest may have stemmed from a malfunctioning exocrine pancreas as reduced secretion of pancreatic enzymes may result in an increase of undigested food material in the intestines and an increase in water content due to compensatory osmotic reactions. However, reduced pancreatic enzyme availability, as seen in cases of pancreatic insufficiency, is often associated with cases of diarrheal steatorrhea, and not cessation of motility (DiMagno et al. 1973, Pongprasobchai 2013), although these conditions do not have to be exclusive. It is also possible that an altered motility of the alimentary system affects the propulsion of the content. One mechanism could be an altered electrical activity of the smooth muscle or altered

neuro/hormonal regulation of motility. Motility disorders, including diabetic enteropathy, slow-transit constipation, and ageing-associated motility disorders are linked, directly or indirectly, to defects in the neural control of the GI tract (Bassotti and Villanacci 2006, Camilleri et al. 2008, Lomax et al. 2010). An important component of enteric inhibitory neurotransmission is mediated by a purine neurotransmitter binding to purinoreceptors (Wood 2006, Gallego et al. 2008, Grasa et al. 2009). NAD^+ is a purine substance (ß-NAD^+) released by nerve stimulation in vascular and visceral smooth muscles and neuro-secretory cells (Smyth et al. 2004, Smyth et al. 2006, Mutafova-Yambolieva et al. 2007, Yamboliev et al. 2009), raising the possibility that NAD^+ could be playing an important role in the control of gut motility at the neural level.

NAD^+ is made available to the cell through more than one pathway. There are at least five dietary precursors to NAD^+, four of which do not require Nampt and NAD^+ itself may be directly delivered to cells from nearby cellular sources (Revollo et al. 2007, Nikiforov et al. 2015). The last aim of this study was to determine whether supplying *Nampt* KO mice with NR, an exogenous precursor that is metabolized to NAD^+ via a Nampt-independent pathway (i.e. Nrk1), could overcome decline and death. Work in our lab and in others has shown that NR supplementation can increase cellular NAD^+ levels. This NR-derived increase in NAD^+ has been protective against various environment-induced pathologies including noise-induced hearing loss (Brown et al. 2014), high fat diet-induced obesity (Canto et al. 2012), and age-induced muscle dysfunction (Frederick et al. 2016). Supplementing with NR was able to double the lifespan of *Nampt* KO mice, suggesting that NR can bolster the effects of the local loss of bioavailable NAD^+. However, NR supplementation was only successful for a time. NR supplemented *Nampt* KO mice eventually succumbed to decline and death.

By evaluating the consequences of *Nampt* KO in the newly developed inducible mouse model I am able to propose that i) Nampt expression is essential on a global level, ii) *Nampt* expression is variable from tissue to tissue, and even tissues that don't normally markedly express Nampt may be susceptible to a global Nampt depletion, iii) exogenous supplementation of a Nampt-independent NAD^+ precursor is not sufficient to completely compensate for the global loss of Nampt expression; however, lifespan is doubled when NR is administered. In summary, these data demonstrate that loss of Nampt in the adult is catastrophic. While the exact pathway of death on a cellular level may still be yet to be elucidated, it is clear that supplementation with an exogenous NAD^+ precursor is powerful, but cannot overcome the need for a local NAD^+-regeneration system.

5.5 References

Bassotti, G., & Villanacci, V. (2006). Slow transit constipation: a functional disorder becomes an enteric neuropathy. *World J Gastroenterol, 12*(29), 4609-4613

Bogan, K. L., & Brenner, C. (2008). Nicotinic acid, nicotinamide, and nicotinamide riboside: a molecular evaluation of NAD+ precursor vitamins in human nutrition. *Annu Rev Nutr, 28*, 115-130

Brown, K. D., Maqsood, S., Huang, J. Y., Pan, Y., Harkcom, W., Li, W., Sauve, A., Verdin, E., & Jaffrey, S. R. (2014). Activation of SIRT3 by the NAD(+) precursor nicotinamide riboside protects from noise-induced hearing loss. *Cell Metab, 20*(6), 1059-1068

Camilleri, M., Cowen, T., & Koch, T. R. (2008). Enteric neurodegeneration in ageing. *Neurogastroenterol Motil, 20*(4), 418-429

Canto, C., Houtkooper, R. H., Pirinen, E., Youn, D. Y., Oosterveer, M. H., Cen, Y., Fernandez-Marcos, P. J., Yamamoto, H., Andreux, P. A., Cettour-Rose, P., Gademann, K., Rinsch, C., Schoonjans, K., Sauve, A. A., & Auwerx, J. (2012). The NAD(+) precursor nicotinamide riboside enhances oxidative metabolism and protects against high-fat diet-induced obesity. *Cell Metab, 15*(6), 838-847

Canto, C., Menzies, K. J., & Auwerx, J. (2015). NAD(+) Metabolism and the Control of Energy Homeostasis: A Balancing Act between Mitochondria and the Nucleus. *Cell Metab, 22*(1), 31-53

DiMagno, E. P., Go, V. L., & Summerskill, W. H. (1973). Relations between pancreatic enzyme outputs and malabsorption in severe pancreatic insufficiency. *N Engl J Med, 288*(16), 813-815

Erben, U., Loddenkemper, C., Doerfel, K., Spieckermann, S., Haller, D., Heimesaat, M. M., Zeitz, M., Siegmund, B., & Kuhl, A. A. (2014). A guide to histomorphological evaluation of intestinal inflammation in mouse models. *Int J Clin Exp Pathol, 7*(8), 4557-4576

Frederick, D. W., Loro, E., Liu, L., Davila, A., Jr., Chellappa, K., Silverman, I. M., Quinn, W. J., 3rd, Gosai, S. J., Tichy, E. D., Davis, J. G., Mourkioti, F., Gregory, B. D., Dellinger, R. W., Redpath, P., Migaud, M. E., Nakamaru-Ogiso, E., Rabinowitz, J.

D., Khurana, T. S., & Baur, J. A. (2016). Loss of NAD Homeostasis Leads to Progressive and Reversible Degeneration of Skeletal Muscle. *Cell Metab, 24*(2), 269-282

Fukuhara, A., Matsuda, M., Nishizawa, M., Segawa, K., Tanaka, M., Kishimoto, K., Matsuki, Y., Murakami, M., Ichisaka, T., Murakami, H., Watanabe, E., Takagi, T., Akiyoshi, M., Ohtsubo, T., Kihara, S., Yamashita, S., Makishima, M., Funahashi, T., Yamanaka, S., Hiramatsu, R., Matsuzawa, Y., & Shimomura, I. (2005). Visfatin: a protein secreted by visceral fat that mimics the effects of insulin. *Science, 307*(5708), 426-430

Gallego, D., Gil, V., Aleu, J., Auli, M., Clave, P., & Jimenez, M. (2008). Purinergic and nitrergic junction potential in the human colon. *Am J Physiol Gastrointest Liver Physiol, 295*(3), G522-533

Grasa, L., Gil, V., Gallego, D., Martin, M. T., & Jimenez, M. (2009). P2Y(1) receptors mediate inhibitory neuromuscular transmission in the rat colon. *Br J Pharmacol, 158*(6), 1641-1652

Hayashi, S., & McMahon, A. P. (2002). Efficient recombination in diverse tissues by a tamoxifen-inducible form of Cre: a tool for temporally regulated gene activation/inactivation in the mouse. *Dev Biol, 244*(2), 305-318

Kulikova, V., Shabalin, K., Nerinovski, K., Dolle, C., Niere, M., Yakimov, A., Redpath, P., Khodorkovskiy, M., Migaud, M. E., Ziegler, M., & Nikiforov, A. (2015). Generation, Release, and Uptake of the NAD Precursor Nicotinic Acid Riboside by Human Cells. *J Biol Chem, 290*(45), 27124-27137

Lee, H. C. (2012). Cyclic ADP-ribose and nicotinic acid adenine dinucleotide phosphate (NAADP) as messengers for calcium mobilization. *J Biol Chem, 287*(38), 31633-31640

Lomax, A. E., Sharkey, K. A., & Furness, J. B. (2010). The participation of the sympathetic innervation of the gastrointestinal tract in disease states. *Neurogastroenterol Motil, 22*(1), 7-18

Luo, X., & Kraus, W. L. (2012). On PAR with PARP: cellular stress signaling through poly(ADP-ribose) and PARP-1. *Genes Dev, 26*(5), 417-432

Minami, K., Okuno, M., Miyawaki, K., Okumachi, A., Ishizaki, K., Oyama, K., Kawaguchi, M., Ishizuka, N., Iwanaga, T., & Seino, S. (2005). Lineage tracing and characterization of insulin-secreting cells generated from adult pancreatic acinar cells. *Proc Natl Acad Sci U S A, 102*(42), 15116-15121

Mutafova-Yambolieva, V. N., Hwang, S. J., Hao, X., Chen, H., Zhu, M. X., Wood, J. D., Ward, S. M., & Sanders, K. M. (2007). Beta-nicotinamide adenine dinucleotide is an inhibitory neurotransmitter in visceral smooth muscle. *Proc Natl Acad Sci U S A, 104*(41), 16359-16364

Nikiforov, A., Kulikova, V., & Ziegler, M. (2015). The human NAD metabolome: Functions, metabolism and compartmentalization. *Crit Rev Biochem Mol Biol, 50*(4), 284-297

Pongprasobchai, S. (2013). Maldigestion from pancreatic exocrine insufficiency. *J Gastroenterol Hepatol, 28 Suppl 4*, 99-102

Revollo, J. R., Korner, A., Mills, K. F., Satoh, A., Wang, T., Garten, A., Dasgupta, B., Sasaki, Y., Wolberger, C., Townsend, R. R., Milbrandt, J., Kiess, W., & Imai, S. (2007). Nampt/PBEF/Visfatin regulates insulin secretion in beta cells as a systemic NAD biosynthetic enzyme. *Cell Metab, 6*(5), 363-375

Rongvaux, A., Galli, M., Denanglaire, S., Van Gool, F., Dreze, P. L., Szpirer, C., Bureau, F., Andris, F., & Leo, O. (2008). Nicotinamide phosphoribosyl transferase/pre-B cell colony-enhancing factor/visfatin is required for lymphocyte development and cellular resistance to genotoxic stress. *J Immunol, 181*(7), 4685-4695

Rongvaux, A., Shea, R. J., Mulks, M. H., Gigot, D., Urbain, J., Leo, O., & Andris, F. (2002). Pre-B-cell colony-enhancing factor, whose expression is up-regulated in activated lymphocytes, is a nicotinamide phosphoribosyltransferase, a cytosolic enzyme involved in NAD biosynthesis. *Eur J Immunol, 32*(11), 3225-3234

Samal, B., Sun, Y., Stearns, G., Xie, C., Suggs, S., & McNiece, I. (1994). Cloning and characterization of the cDNA encoding a novel human pre-B-cell colony-enhancing factor. *Mol Cell Biol, 14*(2), 1431-1437

Sauve, A. A., & Schramm, V. L. (2004). SIR2: the biochemical mechanism of NAD(+)-dependent protein deacetylation and ADP-ribosyl enzyme intermediates. *Curr Med Chem, 11*(7), 807-826

Smyth, L. M., Bobalova, J., Mendoza, M. G., Lew, C., & Mutafova-Yambolieva, V. N. (2004). Release of beta-nicotinamide adenine dinucleotide upon stimulation of postganglionic nerve terminals in blood vessels and urinary bladder. *J Biol Chem, 279*(47), 48893-48903

Smyth, L. M., Breen, L. T., & Mutafova-Yambolieva, V. N. (2006). Nicotinamide adenine dinucleotide is released from sympathetic nerve terminals via a botulinum neurotoxin A-mediated mechanism in canine mesenteric artery. *Am J Physiol Heart Circ Physiol, 290*(5), H1818-1825

Stein, L. R., & Imai, S. (2014). Specific ablation of Nampt in adult neural stem cells recapitulates their functional defects during aging. *EMBO J, 33*(12), 1321-1340

Stein, L. R., Wozniak, D. F., Dearborn, J. T., Kubota, S., Apte, R. S., Izumi, Y., Zorumski, C. F., & Imai, S. (2014). Expression of Nampt in hippocampal and cortical excitatory neurons is critical for cognitive function. *J Neurosci, 34*(17), 5800-5815

Storz, P. (2017). Acinar cell plasticity and development of pancreatic ductal adenocarcinoma. *Nat Rev Gastroenterol Hepatol, 14*(5), 296-304

Stromsdorfer, K. L., Yamaguchi, S., Yoon, M. J., Moseley, A. C., Franczyk, M. P., Kelly, S. C., Qi, N., Imai, S., & Yoshino, J. (2016). NAMPT-Mediated NAD(+) Biosynthesis in Adipocytes Regulates Adipose Tissue Function and Multi-organ Insulin Sensitivity in Mice. *Cell Rep, 16*(7), 1851-1860

Watson, A., Nong, Z., Yin, H., O'Neil, C., Fox, S., Balint, B., Guo, L., Leo, O., Chu, M. W. A., Gros, R., & Pickering, J. G. (2017). Nicotinamide Phosphoribosyltransferase in Smooth Muscle Cells Maintains Genome Integrity, Resists Aortic Medial Degeneration, and Is Suppressed in Human Thoracic Aortic Aneurysm Disease. *Circ Res, 120*(12), 1889-1902

Williams, J. M., Duckworth, C. A., Vowell, K., Burkitt, M. D., & Pritchard, D. M. (2016). Intestinal Preparation Techniques for Histological Analysis in the Mouse. *Curr Protoc Mouse Biol, 6*(2), 148-168

Wood, J. D. (2006). The enteric purinergic P2Y1 receptor. *Curr Opin Pharmacol, 6*(6), 564-570

Yamboliev, I. A., Smyth, L. M., Durnin, L., Dai, Y., & Mutafova-Yambolieva, V. N. (2009). Storage and secretion of beta-NAD, ATP and dopamine in NGF-differentiated rat pheochromocytoma PC12 cells. *Eur J Neurosci, 30*(5), 756-768

Yoon, M. J., Yoshida, M., Johnson, S., Takikawa, A., Usui, I., Tobe, K., Nakagawa, T., Yoshino, J., & Imai, S. (2015). SIRT1-Mediated eNAMPT Secretion from Adipose Tissue Regulates Hypothalamic NAD+ and Function in Mice. *Cell Metab, 21*(5), 706-717

Zhang, L. Q., Van Haandel, L., Xiong, M., Huang, P., Heruth, D. P., Bi, C., Gaedigk, R., Jiang, X., Li, D. Y., Wyckoff, G., Grigoryev, D. N., Gao, L., Li, L., Wu, M., Leeder, J. S., & Ye, S. Q. (2017). Metabolic and molecular insights into an essential role of nicotinamide phosphoribosyltransferase. *Cell Death Dis, 8*(3), e2705

Zhou, C. C., Yang, X., Hua, X., Liu, J., Fan, M. B., Li, G. Q., Song, J., Xu, T. Y., Li, Z. Y., Guan, Y. F., Wang, P., & Miao, C. Y. (2016). Hepatic NAD(+) deficiency as a therapeutic target for non-alcoholic fatty liver disease in ageing. *Br J Pharmacol, 173*(15), 2352-2368

CHAPTER 6 - DISCUSSION

Maintaining SMC health and vitality is crucial to protecting vascular stability in the face of hemodynamic and environmental insults. This is particularly true as these insults increase and accumulate over time and with age. Expanding our understanding of how SMCs resist stress is critical to developing strategies that enable a well-functioning vascular system over a long period of time.

The novel findings presented in this thesis contribute to understanding how the NAD^+-regenerating enzyme, Nampt, enables SMCs in vivo to resist key stresses that are exacerbated with aging. First, I developed a novel mouse knockout model wherein *Nampt* was knocked out in SMCs. The aortas of these knockout mice were susceptible to stress-induced dissections, and the *Nampt*-KO aortic SMCs were compromised. These SMCs accumulated a range of DNA lesions that, I propose, pushed the cells to a fate of early cell senescence and cell loss. Second, I determined that the paradigm of low NAMPT expression correlating with a higher occurrence of DNA damage also exists in human aortic tissue obtained from patients with dilated aortas. Remarkably, the pattern of *NAMPT* expression in these aortas was associated with changes in the methylation status of the *NAMPT* promoter region, suggesting epigenetic control over *NAMPT* expression. Third, I determined that ablating *Nampt* expression in SMCs leads to a global shift in gene expression involving the downregulation of genes that produce collagens and the upregulation of genes that favour the production and assembly of certain proteoglycans. Fourth, I have demonstrated that *Nampt* is an essential gene in the adult mouse, and the knockout of *Nampt* is fatal within 20 days. Interestingly, I also determined that delivering NR to the knockout animal (NR is available as a dietary supplement) was sufficient to double its lifespan. Collectively, these findings reveal new functions for Nampt in the context of supporting SMC health and longevity.

6.1 *Nampt* knockout in SMCs

Previous work done in Dr. Pickering's lab established that Nampt is a phosphoribosyltransferase and that it plays a role in vitro in extending the lifespan of SMCs. However, the role of Nampt in SMCs in vivo had not been established. My finding that *Nampt*-KO SMCs were part of a vasculature that developed largely normally was somewhat surprising. This is because prior reports indicated that global *Nampt* knockout was embryonic lethal (Revollo et al. 2007). Additionally, specific knockout of *Nampt* in T and B cells led to a near complete loss of these cells in mice (Rongvaux et al. 2008).

Recently, additional cell-specific *Nampt* knockouts have been reported. *Nampt* knockout in forebrain excitatory neurons lead to hippocampal and cortical atrophy, astrogliosis, microgliosis, and abnormal dendritic morphology by 2-3 months of age (Stein et al. 2014). Adipose-specific *Nampt* KO mice were found to have severe insulin resistance in adipose tissue, liver, and skeletal muscle, as well as adipose tissue dysfunction (Stromsdorfer et al. 2016). The deletion of *Nampt* in mice in both heart and skeletal muscle was embryonically lethal, whereas a skeletal muscle-specific deletion led to exhibited progressive weakness and loss of both endurance and bone structure, along with an increase of senescence markers in the skeletal muscle cells (Frederick et al. 2016). Thus, together with my data, it is becoming clear that different tissues have different requirements for Nampt.

6.2 *Nampt* knockout and SMC DNA

A striking consequence of *Nampt* knockout in SMCs was the accumulation of DNA lesions. These included oxidative damage, as indicated by the presence of 8-oxo-dG, and γ-H2AX foci, an indication of double stranded DNA breaks. Classically, DNA damage in uncovered in the context of tumours. In this regard, it is noteworthy that Nampt is

overexpressed in various cancers, including prostate, pancreatic, ovarian, fibrosarcoma, lung, colon, and myeloid (Hasmann and Schemainda 2003, Beauparlant et al. 2009, Watson et al. 2009, Olesen et al. 2010, Wang et al. 2011, O'Brien et al. 2013, Xiao et al. 2013, Chan et al. 2014, Chini et al. 2014), and that the inhibition of Nampt is studied as tumour therapy. Inhibition of Nampt in some cancer cells can induce apoptosis, inhibit glycoloysis and nucleotide metabolism, decrease carbon flux through the TCA cycle, and suppress ATP synthesis (Tan et al. 2013, Tolstikov et al. 2014). Cell death follows a >90% reduction in ATP (Watson et al. 2009, Tan et al. 2013, Chan et al. 2014, Del Nagro et al. 2014). However, with less catastrophic ATP depletion, inhibition of Nampt has been found to sensitize tumour cells to oxidative stress and DNA-damaging agents (Hasmann and Schemainda 2003, Yang et al. 2007, Watson et al. 2009, Bi et al. 2011, Wang et al. 2011). Importantly, the work presented in Chapter 2 is the first report in non-cancerous, well-differentiated cells of the association of Nampt depletion with a susceptibility to DNA damage.

6.3 *Nampt* knockout and senescence

Widespread evidence of senescence in the aortic media of SMC-*Nampt* KO mice infused with Ang II was another striking finding. Previous studies in Dr. Pickering's lab demonstrated that inhibiting Nampt in SMCs in culture led to premature senescence, while overexpressing Nampt protected SMCs from undergoing replicative senescence (van der Veer et al. 2007). Additionally, it has been demonstrated that infusion of Ang II in vivo has been associated with an increase of SA β–gal activity the media of C57Bl/6 mice (Chen et al. 2016). Ang II has also been shown to induce SA β–gal activity in that aortic media of Sirt1 KO mice, aged mice, and aged *Col1a1*-/- mice (Vafaie et al. 2014, Chen et al. 2016). Interestingly, although I found senescence markers to be more abundant following Ang II infusion, I also detected evidence of senescence in the aortas of SMC-knockout mice at

baseline. Baseline senescence was not observed in Sirt1 KO mice (Chen et al. 2016), suggesting that the senescence-promoting effects of *Nampt* knockout are not exclusively mediated via a decrease in Sirt1 activity, but also involve the activity of other NAD^+-dependent processes.

6.4 *Nampt* knockout and Parp1 activity

It is well established that knocking down Nampt activity can lead to a depletion of bioavailable NAD^+(Revollo et al. 2004). As Parp1 requires NAD^+ to function, a depletion could compromise the PAR-moiety forming activity of Parp1. I observed this paradigm in SMC-*Nampt* KO mouse aortas, as detailed in Chapter 2. Notably, levels of Parp1 were unchanged, but the ability to form poly-ADP-ribose moieties was abrogated. This was associated with impaired repair of damaged DNA, consistent with the body of evidence of Parp1's involvement in multiple DNA damage repair pathways (Ray Chaudhuri and Nussenzweig 2017). Upon supplying the *Nampt* KO SMCs with NR, a precursor to NAD+, I was able to restore the ability of the cells to form PAR moieties; the hypothesis being that Parp1 retained its catalytic capacity, but the building blocks required to form PAR moieties (i.e. NAD^+, acting as cosubstrate) were unavailable.

Recently there has been evidence that low bioavailable NAD^+ not only limits the PAR-synthetic activity of Parp1, but directly promotes the protein-protein interaction of Parp1 and its inhibitor DBC1. NAD^+ interacts with DBC1 via nudix homology domains (NDHs) (Li et al. 2017). NDHs have been considered protein homology domains of previously unknown function that have recently been discovered to be NAD^+ binding domains that regulate protein-protein interactions (Srouji et al. 2017). A decline in NAD^+ promotes the binding of DBC1 to Parp1, which inhibits Parp1's ability to mediate DNA repair (Li et al. 2017). It is speculated that this function allows a cell to adapt to fluctuations in NAD^+ abundance without degrading it, and to serve as a negative-feedback

loop to prevent Parp1 from depleting NAD^+ down to lethal levels during DNA damage (Yang et al. 2007). It is possible that this paradigm explains the predisposition to DNA damage in SMC-*Nampt* KO mice, without widespread medial cell death.

6.5 SMC *Nampt* knockout and future directions

The studies carried out in Chapter 2 provide insight into the role Nampt plays in vivo in SMCs. Using a mouse model of SMC-specific *Nampt* knockout I uncovered that Nampt deficient SMCs developed into a close-to normal aorta. However, when this vasculature was subjected to hemodynamic stress of Ang II, the Nampt-deficient aortas were prone to dissection. These dissections were associated with an increased burden of cells with DNA damage and senescent cells.

The main phenotype uncovered in the SMC-*Nampt* KO aortas was related to a deficiency in Parp1 activity, activity very much dependent on the bioavailability of NAD^+. It would be interesting to determine whether supplying an exogenous source of NAD^+ to the animal would regenerate Parp1 activity. I have demonstrated in vivo that delivering the NAD^+ precursor, NR, to *Nampt*-KO SMCs in vitro restored Parp1 activity. Thus, undertaking Ang II-infusion experiments in SMC-*Nampt* KO mice, while supplementing the animal with NAD^+ precursors, either NR or NMN, would be important. NR may be of particular interest as it can be obtained in a dietary fashion. As Nampt levels have been shown to decrease in aged tissues (Stein and Imai 2014), along with concomitant drops in NAD^+ levels, it is of particular interest to know if a dietary supplement could offset the effects of this drop.

Furthermore, the bulk of my studies were restricted to the largest vessel, the aorta. While the failure of this vessel occurs often in an acute and catastrophic fashion, compromised function of smaller arteries can have important long-term effects on blood

pressure and flow. Therefore, it would be interesting to characterize the consequences of *Nampt* knockout in the more distal vasculature this mouse model.

6.6 Nampt expression in human aortopathy

The correlation between low Nampt in mouse aortic SMCs and susceptibility to aortic dissection and hemorrhage caused me to consider whether this correlation exists in human aortic pathologies. As presented in Chapter 3, I uncovered that NAMPT content was lower in dilated human aortas that in non-dilated aortas, with an inverse relationship between the aortic diameter and medial SMC NAMPT content. This fits an emerging pattern of reduced Nampt in aged or compromised tissues (Yoshino et al. 2011, Stein and Imai 2014). The current study may be the first to identify such a relationship in human diseased tissue. It is interesting to note that a downregulation of the NAD^+-dependent enzyme Sirt1 has been associated with aortic aneurysms in humans (Chen et al. 2016), and decreased Sirt1 activity has been found in the dysfunctional vasculature of aged mice (de Picciotto et al. 2016). As Sirt1 activity is dependent on the bioavailability of NAD^+, the described Sirt1 effects could depend, at least in part, on the NAD^+-regenerating activity of Nampt.

6.7 Nampt expression and DNA damage in human aortopathy

A remarkable discovery presented in Chapter 3 was the presence of double-stranded DNA breaks in human aortic medial tissue. While there were rare breaks (indicated by the presence of γ-H2AX foci) detected in the media of normal control tissue, the incidence of γ-H2AX foci was significantly increased in tissue obtained from patients with dilated aortas. This is the first in situ evidence for double-stranded DNA lesions in non-atherosclerotic human aortic media (Gray et al. 2015). Cells in which these foci were detected also demonstrated low Nampt expression. Although the data do not prove

causation, the single-cell relationship between low NAMPT and unresolved DNA strand breaks strengthens the potential for a mechanistic relationship.

Although the activity of DNA damage repair enzymes was not evaluated in the human aortopathy samples, I propose that the persistence of DNA breaks was due to a deficiency of repair mechanisms. There has been uncertainty as to whether DNA damage occurs in "post-mitotic" tissues, and if it does occur, whether repair of DNA breaks occurs in post-mitotic tissues. However, studies of post-mitotic neural tissue have found that these tissues do endure DNA damage, and also have the capability to repair DNA damage (Chow and Herrup 2015). Much of the damage is attributable to radiation or reactive oxygen species, but also to gene transcription that generates DNA damage through topoisomerase I cleavage complexes (Katyal et al. 2014). Additionally, even in post-mitotic cells, DNA damage repair processes such as base excision repair, single-strand break repair, and non-homologous end joining have been detected (Iyama and Wilson 2013). Importantly, the activities of a number of NAD^+-dependent enzymes have been associated with these repair pathways, including Parp1, Sirt1, and Sirt6, thus strengthening the case for a potential mechanistic relationship with Nampt (Mostoslavsky et al. 2006, Mao et al. 2011, Dobbin et al. 2013, Ray Chaudhuri and Nussenzweig 2017).

6.8 Epigenetic control of Nampt expression

The discovery that *NAMPT* expression varied from patient to patient prompted an investigation into what could potentially be regulating *NAMPT* expression. To date it has been understood that Nampt expression was regulated by the binding of the circadian transcription factors Bmal1 and Clock (Nakahata et al. 2009). Expression of Clock:Bmal1 is in turn mediated by Sirt1 activity (Nakahata et al. 2008), and thus Nampt expression is regulated by its own NAD^+-regenerating activity.

To facilitate transcription, the Clock:Bmal1 complex binds to enhancer-box (E-box) sites in the *Nampt* promoter region. My analysis of the *Nampt* promoter region also revealed CpG islands; regions that are susceptible to DNA hypermethylation, which interferes with gene transcription. Accordingly, patient samples with low levels of Nampt expression in their aortic media had higher levels of DNA methylation in the *Nampt* promoter region. There is a growing body of evidence that local CpG islands undergo DNA hypermethylation with aging (Jones et al. 2015). Hypermethylation of the *Nampt* promoter region during aging could be part of the sequence of events driving cells to a low NAD^+-state, and perpetuating an aging or frailty phenotype.

6.9 Future directions for human aortic Nampt studies

The data presented in Chapter 3 represented predominantly bicuspid aortic valve patients. However, low aortic NAMPT was observed not only the dilated aortas of patients with a bicuspid aortic valve but also those with a tricuspid aortic valve and Marfan syndrome. A larger series would be required to determine if there are aortic disease-specific differences in *NAMPT* expression and also if *NAMPT* expression in SMCs is relevant to atherosclerotic abdominal aortic aneurysms. It would also be beneficial to attempt to correlate *NAMPT* expression with NAD^+ levels in the aortic media, although this could require larger pieces of human aorta to be harvested.

DNA methylation is a heritable epigenetic mark involving the covalent transfer of a methyl group to the C-5 position of the cytosine ring of DNA by DNA methyltransferases (DNMTs) (Chen and Li 2006). It would be interesting to evaluate the expression or activity status of DNMTs, particularly DNMT1 (responsible for maintaining DNA methylation patterns) and DNMT3a or 3b (which are responsible for de novo methylation of DNA), in the aortic media of patients with dilated aortas (Robert et al. 2003, Hino et al. 2009, Daniel et al. 2011).

6.10 SMC Nampt and extracellular matrix

Studies in Chapter 2 revealed that SMC-Nampt depletion conveyed a vulnerability to the aorta and a susceptibility to SMC dropout. Thoracic aortic aneurysm and dissection disease (TAAD) is classically associated with SMC dropout, but also damaged elastic fibers, compromised smooth muscle function, pooled mucoid material, and remodeled collagen fibers (Humphrey et al. 2015).

The studies in Chapter 4 involved transcriptome profiling of *Nampt*-knockout SMCs. RNA expression array analysis revealed a notable change in the transcriptome. The expression of genes related to collagen production and assembly was significantly depressed and the expression of genes related to mucoid/proteoglycan material was significantly increased. This is consistent with an aortic wall environment seen in aged tissues, and in TAAD tissues (Humphrey et al. 2015). Loss of collagen fiber integrity decreases mechanical strength, which can render the aortic wall vulnerable to rupture (Wenstrup et al. 2006). Proteoglycans that can accumulate and pool in localized areas with aging and as part of the pathology in TAADs contribute to the risk of dissection (Roccabianca et al. 2014).

6.11 SMC *Nampt* knockout and SMAD signalling

Identifying a mechanistic link between Nampt knockdown and ECM transcriptome changes was outside the scope of the work presented in Chapter 4. However, I was able to identify Smad7 as a potential upstream driver of these changes using a prediction algorithm built into the Upstream Analysis tool from IPA. Smad7 is an inhibitor of TGF-β signaling by preventing formation of Smad2/3:Smad4 complexes that initiate the TGF-β signalling (Shi and Massague 2003). TGF-β signaling is associated with enhanced collagen and fibronectin synthesis and deposition (Ignotz and Massague 1986), increased elastin

expression (Kucich et al. 2002), and direct repression of MMPs (Yan and Boyd 2007). TGF-β signaling also increases the size of glycosaminoglycan chains on both bigylcan and decorin (Schonherr et al. 1993, Dadlani et al. 2008). Interestingly, NAD^+-dependent Sirt1-mediated deacetylation of Smad7 has been documented. Deacetylation of Smad7 targets it for degradation, and inhibition of Smad7 deacetylation leads to greater Smad7 stability and activity (Kume et al. 2007). This may be significant as disruptions in TGF-β signalling have been identified in aortic pathologies such as Marfan syndrome and in Loeys-Dietz syndrome (Loeys and Dietz 1993, Jones and Ikonomidis 2010). TGF-β signaling has been implicated not only in matrix deposition, but also in matrix degradation, positioning it as a critical mediator of the balance of structure and composition of the vascular ECM (Jones and Ikonomidis 2010). Accordingly, my data raise the possibility of a Nampt-Smad7 dependency that is relevant to health and disease.

6.12 Future directions for the link between Nampt expression and the control of ECM transcription.

The NAD^+-dependent activity of Sirt1 has been found to regulate the stability of Smad7 by deacetylation (Kume et al. 2007). Therefore a depletion of Nampt-generated NAD^+ in the cell could, consistent with my hypothesis, have an effect on the stability of Smad7. It would be important to evaluate the acetylation status of Smad7 and consequent Smad7 protein levels in WT and *Nampt* KO SMCs. Loss-of-function and overexpression of Smad7 and measuring the expression of key ECM proteins would help to illuminate its role. A change in the phosphorylation status of Smad2/3 would also indicate functionally a change in Smad7 activity, as Smad7 is a key regulator of the TGF-β signalling pathway (Yan and Chen 2011, Beppu 2013).

6.13 Global *Nampt* knockout

Studies presented in Chapters 2, 3, and 4 all focus on the role of Nampt specifically in SMCs. Chapter 5 explored the role Nampt plays in all other organs, and how the need for Nampt in SMCs can compare to the requirements of different tissues. Reports to date have indicated that *Nampt* knockout is embryonically lethal prior to e10.5 (Revollo et al. 2007). Therefore I developed a mouse model wherein *Nampt* could be conditionally deleted at a post-natal time-point. *Nampt* KO mice did not survive longer than 20 days the acute knockout event. Interestingly, this early death was not due to vascular SMC abnormalities but was associated with rapid degeneration of the exocrine pancreas, gut epithelial abnormalities, and halted gastrointestinal transit of undigested food. It is interesting to note that soon after these studies had been undertaken, reports of a similar knockout model were published (Zhang et al. 2017). A similar time-course of decline was reported; rapid weight loss after the induction of the knockout with death occurring within 5-10 days of knockout. The authors report severe atrophy of the villi of the gastrointestinal tract, an increase in serum triglyceride levels, and a catastrophic decrease in abdominal adipose stores (Zhang et al. 2017). These results were attributed to liver dysfunction caused by liver Nampt depletion, however, the model of *Nampt* knockout they used for their studies only yielded 20% decrease in *Nampt* expression in the liver. Also, mice that are subjected to calorie restriction for any reason can reduce their body fat stores remarkably quickly – i.e. up to 20% within 72 hours (Tang et al. 2017). Their findings were limited, as they did not present data on any other tissues that may have been affected by *Nampt* knockout.

The results of my *Nampt* knockout study suggest that some tissues are more quickly vulnerable to knockout than others, indicating cell differences in their requirement for NAD^+ bioavailability. In tissue-specific knockout of *Nampt*, mice lacking Nampt in

forebrain excitatory neurons showed abnormal morphology and accelerated aging (Stein et al. 2014). Ablation of *Nampt* in adult neural stem cells also causes signs of accelerated aging in this neural cell population (Stein and Imai 2014). Knockout of *Nampt* in skeletal muscle contributed to an aging phenotype-related loss mass and contractile function (Frederick et al. 2016). Adipocyte-specific *Nampt* knockout mice had severe insulin resistance in adipose tissue, as well as liver, and skeletal muscle, and adipose tissue dysfunction (Stromsdorfer et al. 2016). In my model of global *Nampt* knockout, none of these tissues were grossly abnormal, save for the loss of most of the adipose tissue stores. In contrast, the pancreas seems to be profoundly affected. Remarkably, there doesn't seem to be strong, local, baseline expression of Nampt in the pancreas, therefore it may be dependent on distal sources of Nampt-generated NAD^+. This would agree with the concept that some tissues are "NAD^+-frail"; i.e. they aren't autonomously able to regenerate the NAD^+ they need to function. This is ascribed namely to the pancreas and brain, as there is little evidence of Nampt expression (Revollo et al. 2007), yet there is dependence on NAD^+ availability (Ramsey et al. 2008, Yoon et al. 2015). It is of particular interest to note, however, that the concept of the pancreas being "NAD^+-frail" is in relation to the NAD^+ requirement of the β islet cells of the pancreas for glucose-stimulated insulin secretion (Imai 2016). And yet in my model of global *Nampt* knockout it was the exocrine pancreas that experienced a more robust failure.

6.14 Supplementation of the NAD^+ supply pathway

Evidence is accumulating that a lack of bioavailable NAD^+ may underline a number of pathologies associated with aging. As such, strategies to prevent or overcome this metabolic decline could have therapeutic benefit. During the course of my experiments I observed an upregulation in the expression of Nrk1, the enzyme responsible for converting NR to NAD^+, in the pancreas and liver of *Nampt* KO mice. This increase was also seen in

the aorta and brain of *Nampt* KO mice during previous work in our lab measuring Nrk1 expression. NR is a naturally occurring precursor to NAD^+ that is easy to obtain and deliver. I attempted to circumvent the lethality of *Nampt* knockout with NR supplementation. NR did not ultimately succeed in eliminating the lethal effects of *Nampt* knockout. However, it did strikingly double the lifespan of the *Nampt* knockout mouse. This was particularly impressive given the otherwise rapid decline in mouse health. The reason why the beneficial effect of NR supplementation was not sustained is unclear. Regardless, the ability of NR to slow and transiently reverse the decline in mouse health, in the setting of profound, widespread impairment of NAD^+ synthesis, holds promise for conditions of less severely impaired NAD^+ metabolism.

6.15 Future directions of *Nampt* knockout and NAD^+ supplementation therapy

NR is a molecule found in dietary sources, and such would be a nutrient supplement. My findings thus constitute a novel example of a defect in an essential gene that can be reversed, at least partially, with a nutritional supplement. Most examples of genetic disorders treated by diet involve the omission of a nutrient that might be problematic. For example, phenylketonuria is the absence or deficiency in phenylalanine hydroxylase, an enzyme involved in metabolizing or converting phenylalanine into tyrosine, and patients are managed by following a diet that limits phenylalanine (found in foods that contain protein). Future studies to determine which tissues are most able to withstand *Nampt* knockout when supplemented with NR would be an important step to then designing therapeutic trials.

6.16 Summary

As described in this thesis, the NAD^+-regenerating enzyme Nampt is critical to the resistance of hemodynamic and oxidative stress insults that are experienced by SMCs in

the aortic media. Depletion of Nampt in SMCs leads to an overwhelming increase in the burden of DNA lesions, which may push these cells to a senescent phenotype. Nampt depletion is also associated with a decrease of collagen production and assembly, along with an increase in proteoglycan deposition, further leading the instability of the aorta. In the face of a life-long accumulation of stresses that may serve to shift Nampt expression and NAD^+ levels to pathologically low levels, strategies of supplementation with exogenous NAD^+ precursors may help to buffer against the consequences. However, the need for a local Nampt-dependent regeneration of NAD^+ may never be overcome in certain tissues, and disturbed NAD^+ metabolism may be the nexus on which the fate of a cell hinges. Collectively, my findings reveal new processes by which SMCs stay healthy and functional, with important implications for mitigating the consequences of the accumulation of the stresses that push blood vessels, and other organs, to catastrophic failure.

6.17 References

Beauparlant, P., Bedard, D., Bernier, C., Chan, H., Gilbert, K., Goulet, D., Gratton, M. O., Lavoie, M., Roulston, A., Turcotte, E., & Watson, M. (2009). Preclinical development of the nicotinamide phosphoribosyl transferase inhibitor prodrug GMX1777. *Anticancer Drugs, 20*(5), 346-354

Beppu, H. (2013). Smad7-modified alleles by various gene-targeting strategies. *J Biochem, 153*(5), 399-401

Bi, T. Q., Che, X. M., Liao, X. H., Zhang, D. J., Long, H. L., Li, H. J., & Zhao, W. (2011). Overexpression of Nampt in gastric cancer and chemopotentiating effects of the Nampt inhibitor FK866 in combination with fluorouracil. *Oncol Rep, 26*(5), 1251-1257

Chan, M., Gravel, M., Bramoulle, A., Bridon, G., Avizonis, D., Shore, G. C., & Roulston, A. (2014). Synergy between the NAMPT inhibitor GMX1777(8) and pemetrexed in non-small cell lung cancer cells is mediated by PARP activation and enhanced NAD consumption. *Cancer Res, 74*(21), 5948-5954

Chen, H. Z., Wang, F., Gao, P., Pei, J. F., Liu, Y., Xu, T. T., Tang, X., Fu, W. Y., Lu, J., Yan, Y. F., Wang, X. M., Han, L., Zhang, Z. Q., Zhang, R., Zou, M. H., & Liu, D. P. (2016). Age-Associated Sirtuin 1 Reduction in Vascular Smooth Muscle Links Vascular Senescence and Inflammation to Abdominal Aortic Aneurysm. *Circ Res, 119*(10), 1076-1088

Chen, T., & Li, E. (2006). Establishment and maintenance of DNA methylation patterns in mammals. *Curr Top Microbiol Immunol, 301*, 179-201

Chini, C. C., Guerrico, A. M., Nin, V., Camacho-Pereira, J., Escande, C., Barbosa, M. T., & Chini, E. N. (2014). Targeting of NAD metabolism in pancreatic cancer cells: potential novel therapy for pancreatic tumors. *Clin Cancer Res, 20*(1), 120-130

Chow, H. M., & Herrup, K. (2015). Genomic integrity and the ageing brain. *Nat Rev Neurosci, 16*(11), 672-684

Dadlani, H., Ballinger, M. L., Osman, N., Getachew, R., & Little, P. J. (2008). Smad and p38 MAP kinase-mediated signaling of proteoglycan synthesis in vascular smooth muscle. *J Biol Chem, 283*(12), 7844-7852

Daniel, F. I., Cherubini, K., Yurgel, L. S., de Figueiredo, M. A., & Salum, F. G. (2011). The role of epigenetic transcription repression and DNA methyltransferases in cancer. *Cancer, 117*(4), 677-687

de Picciotto, N. E., Gano, L. B., Johnson, L. C., Martens, C. R., Sindler, A. L., Mills, K. F., Imai, S., & Seals, D. R. (2016). Nicotinamide mononucleotide supplementation reverses vascular dysfunction and oxidative stress with aging in mice. *Aging Cell, 15*(3), 522-530

Del Nagro, C., Xiao, Y., Rangell, L., Reichelt, M., & O'Brien, T. (2014). Depletion of the central metabolite NAD leads to oncosis-mediated cell death. *J Biol Chem, 289*(51), 35182-35192

Dobbin, M. M., Madabhushi, R., Pan, L., Chen, Y., Kim, D., Gao, J., Ahanonu, B., Pao, P. C., Qiu, Y., Zhao, Y., & Tsai, L. H. (2013). SIRT1 collaborates with ATM and HDAC1 to maintain genomic stability in neurons. *Nat Neurosci, 16*(8), 1008-1015

Frederick, D. W., Loro, E., Liu, L., Davila, A., Jr., Chellappa, K., Silverman, I. M., Quinn, W. J., 3rd, Gosai, S. J., Tichy, E. D., Davis, J. G., Mourkioti, F., Gregory, B. D., Dellinger, R. W., Redpath, P., Migaud, M. E., Nakamaru-Ogiso, E., Rabinowitz, J. D., Khurana, T. S., & Baur, J. A. (2016). Loss of NAD Homeostasis Leads to Progressive and Reversible Degeneration of Skeletal Muscle. *Cell Metab, 24*(2), 269-282

Gray, K., Kumar, S., Figg, N., Harrison, J., Baker, L., Mercer, J., Littlewood, T., & Bennett, M. (2015). Effects of DNA damage in smooth muscle cells in atherosclerosis. *Circ Res, 116*(5), 816-826

Hasmann, M., & Schemainda, I. (2003). FK866, a highly specific noncompetitive inhibitor of nicotinamide phosphoribosyltransferase, represents a novel mechanism for induction of tumor cell apoptosis. *Cancer Res, 63*(21), 7436-7442

Hino, R., Uozaki, H., Murakami, N., Ushiku, T., Shinozaki, A., Ishikawa, S., Morikawa, T., Nakaya, T., Sakatani, T., Takada, K., & Fukayama, M. (2009). Activation of DNA methyltransferase 1 by EBV latent membrane protein 2A leads to promoter hypermethylation of PTEN gene in gastric carcinoma. *Cancer Res, 69*(7), 2766-2774

Humphrey, J. D., Schwartz, M. A., Tellides, G., & Milewicz, D. M. (2015). Role of mechanotransduction in vascular biology: focus on thoracic aortic aneurysms and dissections. *Circ Res, 116*(8), 1448-1461

Ignotz, R. A., & Massague, J. (1986). Transforming growth factor-beta stimulates the expression of fibronectin and collagen and their incorporation into the extracellular matrix. *J Biol Chem, 261*(9), 4337-4345

Imai, S. I. (2016). The NAD World 2.0: the importance of the inter-tissue communication mediated by NAMPT/NAD+/SIRT1 in mammalian aging and longevity control. *NPJ Syst Biol Appl, 2*, 16018

Iyama, T., & Wilson, D. M., 3rd. (2013). DNA repair mechanisms in dividing and non-dividing cells. *DNA Repair (Amst), 12*(8), 620-636

Jones, J. A., & Ikonomidis, J. S. (2010). The pathogenesis of aortopathy in Marfan syndrome and related diseases. *Curr Cardiol Rep, 12*(2), 99-107

Jones, M. J., Goodman, S. J., & Kobor, M. S. (2015). DNA methylation and healthy human aging. *Aging Cell, 14*(6), 924-932

Katyal, S., Lee, Y., Nitiss, K. C., Downing, S. M., Li, Y., Shimada, M., Zhao, J., Russell, H. R., Petrini, J. H., Nitiss, J. L., & McKinnon, P. J. (2014). Aberrant topoisomerase-1 DNA lesions are pathogenic in neurodegenerative genome instability syndromes. *Nat Neurosci, 17*(6), 813-821

Kucich, U., Rosenbloom, J. C., Abrams, W. R., & Rosenbloom, J. (2002). Transforming growth factor-beta stabilizes elastin mRNA by a pathway requiring active Smads, protein kinase C-delta, and p38. *Am J Respir Cell Mol Biol, 26*(2), 183-188

Kume, S., Haneda, M., Kanasaki, K., Sugimoto, T., Araki, S., Isshiki, K., Isono, M., Uzu, T., Guarente, L., Kashiwagi, A., & Koya, D. (2007). SIRT1 inhibits transforming growth factor beta-induced apoptosis in glomerular mesangial cells via Smad7 deacetylation. *J Biol Chem, 282*(1), 151-158

Li, J., Bonkowski, M. S., Moniot, S., Zhang, D., Hubbard, B. P., Ling, A. J., Rajman, L. A., Qin, B., Lou, Z., Gorbunova, V., Aravind, L., Steegborn, C., & Sinclair, D. A. (2017). A conserved NAD+ binding pocket that regulates protein-protein interactions during aging. *Science, 355*(6331), 1312-1317

Loeys, B. L., & Dietz, H. C. (1993). Loeys-Dietz Syndrome. In R. A. Pagon, M. P. Adam, H. H. Ardinger, S. E. Wallace, A. Amemiya, L. J. H. Bean, T. D. Bird, N. Ledbetter, H. C. Mefford, R. J. H. Smith, & K. Stephens (Eds.), *GeneReviews(R)*. Seattle (WA).

Mao, Z., Hine, C., Tian, X., Van Meter, M., Au, M., Vaidya, A., Seluanov, A., & Gorbunova, V. (2011). SIRT6 promotes DNA repair under stress by activating PARP1. *Science, 332*(6036), 1443-1446

Mostoslavsky, R., Chua, K. F., Lombard, D. B., Pang, W. W., Fischer, M. R., Gellon, L., Liu, P., Mostoslavsky, G., Franco, S., Murphy, M. M., Mills, K. D., Patel, P., Hsu, J. T., Hong, A. L., Ford, E., Cheng, H. L., Kennedy, C., Nunez, N., Bronson, R., Frendewey, D., Auerbach, W., Valenzuela, D., Karow, M., Hottiger, M. O., Hursting, S., Barrett, J. C., Guarente, L., Mulligan, R., Demple, B., Yancopoulos, G. D., & Alt, F. W. (2006). Genomic instability and aging-like phenotype in the absence of mammalian SIRT6. *Cell, 124*(2), 315-329

Nakahata, Y., Kaluzova, M., Grimaldi, B., Sahar, S., Hirayama, J., Chen, D., Guarente, L. P., & Sassone-Corsi, P. (2008). The NAD+-dependent deacetylase SIRT1 modulates CLOCK-mediated chromatin remodeling and circadian control. *Cell, 134*(2), 329-340

Nakahata, Y., Sahar, S., Astarita, G., Kaluzova, M., & Sassone-Corsi, P. (2009). Circadian control of the NAD+ salvage pathway by CLOCK-SIRT1. *Science, 324*(5927), 654-657

O'Brien, T., Oeh, J., Xiao, Y., Liang, X., Vanderbilt, A., Qin, A., Yang, L., Lee, L. B., Ly, J., Cosino, E., LaCap, J. A., Ogasawara, A., Williams, S., Nannini, M., Liederer, B. M., Jackson, P., Dragovich, P. S., & Sampath, D. (2013). Supplementation of nicotinic acid with NAMPT inhibitors results in loss of in vivo efficacy in NAPRT1-deficient tumor models. *Neoplasia, 15*(12), 1314-1329

Olesen, U. H., Thougaard, A. V., Jensen, P. B., & Sehested, M. (2010). A preclinical study on the rescue of normal tissue by nicotinic acid in high-dose treatment with APO866, a specific nicotinamide phosphoribosyltransferase inhibitor. *Mol Cancer Ther, 9*(6), 1609-1617

Ramsey, K. M., Mills, K. F., Satoh, A., & Imai, S. (2008). Age-associated loss of Sirt1-mediated enhancement of glucose-stimulated insulin secretion in beta cell-specific Sirt1-overexpressing (BESTO) mice. *Aging Cell, 7*(1), 78-88

Ray Chaudhuri, A., & Nussenzweig, A. (2017). The multifaceted roles of PARP1 in DNA repair and chromatin remodelling. *Nat Rev Mol Cell Biol*

Revollo, J. R., Grimm, A. A., & Imai, S. (2004). The NAD biosynthesis pathway mediated by nicotinamide phosphoribosyltransferase regulates Sir2 activity in mammalian cells. *J Biol Chem, 279*(49), 50754-50763

Revollo, J. R., Korner, A., Mills, K. F., Satoh, A., Wang, T., Garten, A., Dasgupta, B., Sasaki, Y., Wolberger, C., Townsend, R. R., Milbrandt, J., Kiess, W., & Imai, S. (2007). Nampt/PBEF/Visfatin regulates insulin secretion in beta cells as a systemic NAD biosynthetic enzyme. *Cell Metab, 6*(5), 363-375

Robert, M. F., Morin, S., Beaulieu, N., Gauthier, F., Chute, I. C., Barsalou, A., & MacLeod, A. R. (2003). DNMT1 is required to maintain CpG methylation and aberrant gene silencing in human cancer cells. *Nat Genet, 33*(1), 61-65

Roccabianca, S., Bellini, C., & Humphrey, J. D. (2014). Computational modelling suggests good, bad and ugly roles of glycosaminoglycans in arterial wall mechanics and mechanobiology. *J R Soc Interface, 11*(97), 20140397

Rongvaux, A., Galli, M., Denanglaire, S., Van Gool, F., Dreze, P. L., Szpirer, C., Bureau, F., Andris, F., & Leo, O. (2008). Nicotinamide phosphoribosyl transferase/pre-B cell colony-enhancing factor/visfatin is required for lymphocyte development and cellular resistance to genotoxic stress. *J Immunol, 181*(7), 4685-4695

Schonherr, E., Jarvelainen, H. T., Kinsella, M. G., Sandell, L. J., & Wight, T. N. (1993). Platelet-derived growth factor and transforming growth factor-beta 1 differentially affect the synthesis of biglycan and decorin by monkey arterial smooth muscle cells. *Arterioscler Thromb, 13*(7), 1026-1036

Shi, Y., & Massague, J. (2003). Mechanisms of TGF-beta signaling from cell membrane to the nucleus. *Cell, 113*(6), 685-700

Srouji, J. R., Xu, A., Park, A., Kirsch, J. F., & Brenner, S. E. (2017). The evolution of function within the Nudix homology clan. *Proteins, 85*(5), 775-811

Stein, L. R., & Imai, S. (2014). Specific ablation of Nampt in adult neural stem cells recapitulates their functional defects during aging. *EMBO J, 33*(12), 1321-1340

Stein, L. R., Wozniak, D. F., Dearborn, J. T., Kubota, S., Apte, R. S., Izumi, Y., Zorumski, C. F., & Imai, S. (2014). Expression of Nampt in hippocampal and cortical excitatory neurons is critical for cognitive function. *J Neurosci, 34*(17), 5800-5815

Stromsdorfer, K. L., Yamaguchi, S., Yoon, M. J., Moseley, A. C., Franczyk, M. P., Kelly, S. C., Qi, N., Imai, S., & Yoshino, J. (2016). NAMPT-Mediated NAD(+) Biosynthesis in Adipocytes Regulates Adipose Tissue Function and Multi-organ Insulin Sensitivity in Mice. *Cell Rep, 16*(7), 1851-1860

Tan, B., Young, D. A., Lu, Z. H., Wang, T., Meier, T. I., Shepard, R. L., Roth, K., Zhai, Y., Huss, K., Kuo, M. S., Gillig, J., Parthasarathy, S., Burkholder, T. P., Smith, M. C., Geeganage, S., & Zhao, G. (2013). Pharmacological inhibition of nicotinamide phosphoribosyltransferase (NAMPT), an enzyme essential for NAD+ biosynthesis, in human cancer cells: metabolic basis and potential clinical implications. *J Biol Chem, 288*(5), 3500-3511

Tang, H. N., Tang, C. Y., Man, X. F., Tan, S. W., Guo, Y., Tang, J., Zhou, C. L., & Zhou, H. D. (2017). Plasticity of adipose tissue in response to fasting and refeeding in male mice. *Nutr Metab (Lond), 14*, 3

Tolstikov, V., Nikolayev, A., Dong, S., Zhao, G., & Kuo, M. S. (2014). Metabolomics analysis of metabolic effects of nicotinamide phosphoribosyltransferase (NAMPT) inhibition on human cancer cells. *PLOS ONE, 9*(12), e114019

Vafaie, F., Yin, H., O'Neil, C., Nong, Z., Watson, A., Arpino, J. M., Chu, M. W., Wayne Holdsworth, D., Gros, R., & Pickering, J. G. (2014). Collagenase-resistant collagen promotes mouse aging and vascular cell senescence. *Aging Cell, 13*(1), 121-130

van der Veer, E., Ho, C., O'Neil, C., Barbosa, N., Scott, R., Cregan, S. P., & Pickering, J. G. (2007). Extension of human cell lifespan by nicotinamide phosphoribosyltransferase. *J Biol Chem, 282*(15), 10841-10845

Wang, B., Hasan, M. K., Alvarado, E., Yuan, H., Wu, H., & Chen, W. Y. (2011). NAMPT overexpression in prostate cancer and its contribution to tumor cell survival and stress response. *Oncogene, 30*(8), 907-921

Watson, M., Roulston, A., Belec, L., Billot, X., Marcellus, R., Bedard, D., Bernier, C., Branchaud, S., Chan, H., Dairi, K., Gilbert, K., Goulet, D., Gratton, M. O., Isakau, H., Jang, A., Khadir, A., Koch, E., Lavoie, M., Lawless, M., Nguyen, M., Paquette, D., Turcotte, E., Berger, A., Mitchell, M., Shore, G. C., & Beauparlant, P. (2009). The small molecule GMX1778 is a potent inhibitor of NAD+ biosynthesis: strategy for enhanced therapy in nicotinic acid phosphoribosyltransferase 1-deficient tumors. *Mol Cell Biol, 29*(21), 5872-5888

Wenstrup, R. J., Florer, J. B., Davidson, J. M., Phillips, C. L., Pfeiffer, B. J., Menezes, D. W., Chervoneva, I., & Birk, D. E. (2006). Murine model of the Ehlers-Danlos syndrome. col5a1 haploinsufficiency disrupts collagen fibril assembly at multiple stages. *J Biol Chem, 281*(18), 12888-12895

Xiao, Y., Elkins, K., Durieux, J. K., Lee, L., Oeh, J., Yang, L. X., Liang, X., DelNagro, C., Tremayne, J., Kwong, M., Liederer, B. M., Jackson, P. K., Belmont, L. D., Sampath, D., & O'Brien, T. (2013). Dependence of tumor cell lines and patient-derived tumors on the NAD salvage pathway renders them sensitive to NAMPT inhibition with GNE-618. *Neoplasia, 15*(10), 1151-1160

Yan, C., & Boyd, D. D. (2007). Regulation of matrix metalloproteinase gene expression. *J Cell Physiol, 211*(1), 19-26

Yan, X., & Chen, Y. G. (2011). Smad7: not only a regulator, but also a cross-talk mediator of TGF-beta signalling. *Biochem J, 434*(1), 1-10

Yang, H., Yang, T., Baur, J. A., Perez, E., Matsui, T., Carmona, J. J., Lamming, D. W., Souza-Pinto, N. C., Bohr, V. A., Rosenzweig, A., de Cabo, R., Sauve, A. A., & Sinclair, D. A. (2007). Nutrient-sensitive mitochondrial NAD+ levels dictate cell survival. *Cell, 130*(6), 1095-1107

Yoon, M. J., Yoshida, M., Johnson, S., Takikawa, A., Usui, I., Tobe, K., Nakagawa, T., Yoshino, J., & Imai, S. (2015). SIRT1-Mediated eNAMPT Secretion from Adipose Tissue Regulates Hypothalamic NAD+ and Function in Mice. *Cell Metab, 21*(5), 706-717

Yoshino, J., Mills, K. F., Yoon, M. J., & Imai, S. (2011). Nicotinamide mononucleotide, a key NAD(+) intermediate, treats the pathophysiology of diet- and age-induced diabetes in mice. *Cell Metab, 14*(4), 528-536

Zhang, L. Q., Van Haandel, L., Xiong, M., Huang, P., Heruth, D. P., Bi, C., Gaedigk, R., Jiang, X., Li, D. Y., Wyckoff, G., Grigoryev, D. N., Gao, L., Li, L., Wu, M., Leeder, J. S., & Ye, S. Q. (2017). Metabolic and molecular insights into an essential role of nicotinamide phosphoribosyltransferase. *Cell Death Dis, 8*(3), e2705

APPENDIX I - GENE WRITING CONVENTIONS

	Human	Mouse
DNA	*NAMPT*	*Nampt*
cDNA	*NAMPT*	*Nampt*
Genotypes*		*Nampt*
mRNA	*NAMPT*	*Nampt*
Protein	NAMPT	Nampt

* Gene symbols are italicized when published, as are allele symbols. Transgenes, which are not part of the native genome, are not italicized (from JAX)

For reference, see:
http://www.jci.org/kiosk/publish/genestyle
http://www.biosciencewriters.com/Guidelines-for-Formatting-Gene-and-Protein-Names.aspx
http://www.informatics.jax.org/mgihome/nomen/gene.shtml#gaas
http://www.genenames.org/about/guidelines#Appendix1

APPENDIX II - COPYRIGHT CLEARANCE

RightsLink®

Home | Create Account | Help

Title: Nicotinamide Phosphoribosyltransferase in Smooth Muscle Cells Maintains Genome Integrity, Resists Aortic Medial Degeneration, and Is Suppressed in Human Thoracic Aortic Aneurysm DiseaseNovelty and Significance

Author: Alanna Watson,Zengxuan Nong,Hao Yin,Caroline O'Neil,Stephanie Fox,Brittany Balint,Linrui Guo,Oberdan Leo,Michael W.A. Chu,Robert Gros,J. Geoffrey Pickering

Publication: Circulation Research

Publisher: Wolters Kluwer Health, Inc.

Date: Jun 9, 2017

LOGIN

If you're a copyright.com user, you can login to RightsLink using your copyright.com credentials. Already **a RightsLink user** or want to learn more?

License Not Required

This request is granted gratis and no formal license is required from Wolters Kluwer. Please note that modifications are not permitted. Please use the following citation format: author(s), title of article, title of journal, volume number, issue number, inclusive pages and website URL to the journal page.

BACK CLOSE WINDOW

APPENDIX III - ANIMAL USE ETHICS APPROVAL

AUP Number: 2010-244
PI Name: Pickering, Geoffrey
AUP Title: Smooth Muscle Cells and Vascular Disease

The YEARLY RENEWAL to Animal Use Protocol (AUP) 2010-244 has been approved.

1. This AUP number must be indicated when ordering animals for this project.
2. Animals for other projects may not be ordered under this AUP number.
3. Purchases of animals other than through this system must be cleared through the ACVS office.
   Health certificates will be required.

REQUIREMENTS/COMMENTS
Please ensure that individual(s) performing procedures on live animals, as described in this protocol, are familiar with the contents of this document.

The holder of this Animal Use Protocol is responsible to ensure that all associated safety components (biosafety, radiation safety, general laboratory safety) comply with institutional safety standards and have received all necessary approvals. Please consult directly with your institutional safety officers.

Submitted by: Thompson, Sharla H
on behalf of the Animal Use Subcommittee

APPENDIX IV - HUMAN RESEARCH ETHICS APPROVAL

Western Research

Research Ethics

Western University Health Science Research Ethics Board
HSREB Annual Continuing Ethics Approval Notice

Date: July 19, 2017
Principal Investigator: Dr. Geoffrey Pickering
Department & Institution: Science\Biochemistry,London Health Sciences Centre

Review Type: Delegated
HSREB File Number: 5512
Study Title: Identifying the relationship between molecular determinants and age-related disorders in the human population 15405E

HSREB Renewal Due Date & HSREB Expiry Date:
Renewal Due -2018/07/31
Expiry Date -2018/08/13

The Western University Health Science Research Ethics Board (HSREB) has reviewed the Continuing Ethics Review (CER) Form and is re-issuing approval for the above noted study.

The Western University HSREB operates in compliance with the Tri-Council Policy Statement Ethical Conduct for Research Involving Humans (TCPS2), the International Conference on Harmonization of Technical Requirements for Registration of Pharmaceuticals for Human Use Guideline for Good Clinical Practice (ICH E6 R1), the Ontario Freedom of Information and Protection of Privacy Act (FIPPA, 1990), the Ontario Personal Health Information Protection Act (PHIPA, 2004), Part 4 of the Natural Health Product Regulations, Health Canada Medical Device Regulations and Part C, Division 5, of the Food and Drug Regulations of Health Canada.

Members of the HSREB who are named as Investigators in research studies do not participate in discussions related to, nor vote on such studies when they are presented to the REB.

The HSREB is registered with the U.S. Department of Health & Human Services under the IRB registration number IRB 00000940.

CURRICULUM VITAE

EDUCATION

MSc: Microbiology and Immunology, The University of Western Ontario, 2007

BSc Hons: Microbiology and Immunology, The University of Western Ontario, 2003

HONOURS AND AWARDS

2013-2014 Queen Elizabeth II Graduate Scholarship in Science and Technology (QEIIGSST)

2012-2013 Queen Elizabeth II Graduate Scholarship in Science and Technology (QEIIGSST)

2012 Trainee Research Award – Basic Science, Runner up. Canadian Cardiovascular Society

2011 Travel award, Canadian Hypertension Congress

2010-2012 CIHR Strategic Training Program in Vascular Research Fellowship

2010 Outstanding Presentation Award – Ontario Hypertension Congress

2007 Poster presentation award – Infection and Immunity Research Forum, University of Western Ontario.

PUBLICATIONS

Watson A, Nong Z, Yin H, O'Neil C, Fox S, Balint B, Guo L, Leo O, Chu MWA, Gros R, Pickering JG. Nicotinamide Phosphoribosyltransferase in Smooth Muscle Cells Maintains Genome Integrity, Resists Aortic Medial Degeneration, and Is Suppressed in Human Thoracic Aortic Aneurysm Disease. Circ Res. 2017. 120(12):1889-1902

Vafaie F, Yin H, O'Neil C, Nong Z, **Watson A**, Arpino JM, Chu MW, Wayne Holdsworth D, Gros R, Pickering JG. Collagenase-resistant collagen promotes mouse aging and vascular cell senescence. Aging Cell. 2014. 13(1):121-30.

Yin H, van der Veer E, Frontini MJ, Thibert V, O'Neil C, **Watson A**, Szasz P, Chu MW, Pickering JG. Intrinsic directionality of migrating vascular smooth muscle cells is regulated by NAD(+) biosynthesis. J Cell Sci. 2012. 125(Pt 23):5770-80.

Nong Z, O'Neil C, Lei M, Gros R, **Watson A**, Rizkalla A, Mequanint K, Li S, Frontini MJ, Feng Q, Pickering JG. Type I collagen cleavage is essential for effective fibrotic repair after myocardial infarction. American Journal of Pathology. 2011. 179(5): 2189-2198

Borradaille NM, **Watson AR**, Pickering JG. Regeneration and Aging: Regulation by Sirtuins and the NAD+ Salvage Pathway. In *Regenerative Nephrology*. Goligorsky, M.S., Ed. Elsevier: San Diego, 2010. Chapter 26.

Watson A, Morris VL, Chan BMC. Coordinated integrin and growth factor regulation of primary keratinocyte migration mediated through extracellular signal regulated kinase and phosphoinositide 3-kinase. Arch Dermatol Res. 2009. 301(4): 307-17

PRESENTATIONS

Watson A*, Nong Z, O'Neil C, Pickering JG. NAD+ regeneration in smooth muscle cells is required to maintain aortic integrity. 19th International Vascular Biology Meeting. October 30 – November 3, 2016; Boston, MA, USA.

Watson A*, Nong Z, Gros R, Leo O, Pickering JG. NAD^+ regeneration in smooth muscle cells is required to maintain vascular integrity during angiotensin II-mediated stress. London Health Sciences Research Day. March 18th, 2013. London, ON, Canada.

Watson A*, Nong Z, Gros R, Leo O, Pickering JG. NAD^+ regeneration in smooth muscle cells is required to maintain vascular integrity during angiotensin II-mediated stress. 2012 Canadian Cardiovascular Congress. October 27 – 31, 2012. Toronto, ON, Canada.

Watson A*, Nong Z, Xu Y, Pickering JG. Expression of Nampt, and NAD+ regenerating enzyme, in the developing adult and vasculature. 51st annual conference of The American Society of Cell Biology. December 2011; Denver, CO, USA.

Watson A*, Nong Z, Xu Y, Pickering JG. Expression of an NAD+ regenerating enzyme in the developing vasculature. 2011 Canadian Hypertension Congress October 2-5, 2011; Alliston, Ontario, Canada.

O'Neil C, Watson A*, Vafaie F, Nong Z, Yin H, Chu M, Holdsworth D, Pickering JG. Collagenase-resistant type I collagen promotes vascular smooth muscle cell senescence. 50th annual conference of The American Society of Cell Biology. December 2010; Philadelphia, PA, USA.

Watson A*, Nong Z, Frontini M, Chen S, O'Neil C, Pickering JG. NAD+ regeneration regulates vascular smooth muscle cell polarity and directed migration. 50th Annual Conference of The American Society of Cell Biology. December 2010; Philadelphia, PA, USA.

Watson A*, Nong Z, Frontini M, Chen S, O'Neil C, Pickering JG. Selective expression of an NAD regenerating enzyme in small and medium sized arteries. The 23rd Scientific

Meeting of the International Society of Hypertension. September 26-30 2010; Vancouver, BC, Canada

Watson A*, Nong Z, Chen S, O'Neil C, Pickering JG. Selective expression of an NAD regenerating enzyme in small and medium sized arteries. Ontario Hypertension Society Meeting May 28-30, 2010; Alliston, ON, Canada.

Vafaie F*, O'Neil C, Watson A, Holdsworth D, Pickering JG. Proteolysis-resistant Collagen Drives Vascular Smooth Muscle Cell Senescence. (2009) Circulation 120:S1082.

Watson AR*, Morris VL, and Chan BC. Regulation of growth factor-stimulated chemotaxis and chemokinesis of primary murine keratinocytes. Infection and Immunity Research Forum 2007. University of Western Ontario.

* = *presenting author*

Experience

Lab Technician, November 2008 – August 2010
Robarts Research Institute, Vascular Biology Group
The University of Western Ontario

Teaching Assistant, September 2003 – January 2005
Second and third-year undergraduate microbiology
The University of Western Ontario

Summer Student, Summer 2003
The University of Western Ontario